THE ROLE OF ADVENTITIA IN PRESSURE-DEPENDENT MYOGENIC TONE

By

SATIRAH ZAINALABIDIN

A thesis submitted in fulfilment of the requirements for the
Degree of Doctor of Philosophy

Strathclyde Institute of Pharmacy and Biomedical Sciences
University of Strathclyde
Glasgow
United Kingdom
2011

This thesis is the result of the author's original research. It has been composed by the author and has not previously submitted for examination, which has led to the award of a degree.

Signed: Date:

AKNOWLEDGEMENTS

It is a pleasure to thank the many people who made this thesis possible.

First and foremost, I would like to offer my greatest gratitude to my supervisors, Dr. Paul Coats and Prof. Roger Wadsworth, for giving me the opportunity to work with them. They have given me the guidance, advice and penetrating criticism throughout my study, which has helped in building my practical and intellectual skill.

My sincere gratitude is also extended to all the research fellows and lab technicians in SIPBS. In particular, I thank the Cardiovascular Group members for their generous support and smile during the long hours in the lab. Also, I would like to thank the Neuroscience, Cell Signalling, Calcium Signalling Lab and Biophotonic groups, especially to Prof. Dr. John McCarron and Mr. Dave Blatchford, for their kind assistance when I was in need of help. Also, I would like to thank fellow colleagues for their kind gesture to proofread my thesis.

I am indebted to the Ministry of Higher Education of Malaysia and Universiti Kebangsaan Malaysia (UKM) for giving me the financial support.

It would be difficult to list my special and close friends one by one here, but I would like to show my appreciation to all of them for the emotional support, laughter, and caring they provided, either from near or far. I feel so blessed to have them as my friends. There are no words that can thank them enough for lending me their shoulders through the difficult times and for making my life so ever colourful.

I wish to thank my extended family for providing the constant moral support and love, particularly sister-cousin, my two brothers, sister-in-laws, uncles and aunties.

Lastly and most importantly, I owe my deepest gratitude to my precious and beloved parents. They have raised me, supported me, loved me and always believed in me. To them, I dedicate this thesis.

ABSTRACT

Introduction: Increasing evidence has demonstrated a potential role for reactive oxygen species (ROS) as a key signalling mediator in the genesis of myogenic tone, and the main source is the adventitial fibroblasts. The aim was to investigate the potential role of adventitial-derived ROS in the development of pressure-dependent and pressure-independent vascular tone. **Methods:** Second-order mesenteric resistance arteries (MRA: diameter 356 ± 11.09 μm) and middle cerebral arteries (MCA: diameter 150 ± 7.81 μm) were isolated from adult male Sprague-Dawley rats (12 weeks, 250-300g). Pressure-dependent responses were studied by pressure-step (40 to 80 to 120 mmHg) using pressure myography. Pharmacological and nervous responses were measure by wire myograph and transmural nerve stimulation (TNS), respectively. Confocal microscopy was used to visualize F-actin staining and to confirm the vascular integrity. Lucigenin-enhanced chemiluminescence was used to measure superoxide (O_2^-) signal. Statistical analysis was measured by two-way ANOVA for repeated measure and paired Student's t-test for two matched groups. Values were presented as mean ± SEM. **Results and discussion:** The effects of antioxidant N-acetylcysteine (NAC, 10 mM), NADPH-oxidase inhibitor diphenyleneiodonium (DPI, 10 μM) and actin polymerization inhibitor Cytochalasin D (Cyto D, 5 μM) were shown to produce significant inhibition on pressure-dependent myogenic tone at 40-80-120 mmHg. NAC and DPI did not have any effect on 60 mM KPSS constriction. Confocal microscopy showed a significant F-actin fluorescence increase in vascular smooth muscle (VSM) at 120 mmHg (171.2 ± 6.4 unit) vs. 40 mmHg (76.3 ± 8.2 unit). Cyto D reduced the fluorescence at 120 mmHg (44.6 ± 9 unit), confirming a dynamic actin polymerization contribution to the pressure-dependent myogenic tone. A technique for isolating adventitial-dependent function in small arteries was developed by dipping in 4% paraformaldehyde for 15 s (-Adv). MCA and MRA showed similar results. Confocal microscopy confirmed that paraformaldehyde had not compromised the underlying VSM and endothelium in -Adv. The vessels were mounted on a four-channel wire myography and the contraction to 60 mM KPSS, endothelium-dependent relaxation to acetylcholine (ACh, 0.1 and 1 μM), endothelium-independent relaxation to sodium

nitroprusside (SNP, 0.1 and 1 μM) showed no significant difference between +Adv and –Adv. The passive mechanical properties by pressure myograph showed no difference between +Adv vs. –Adv too. The significant reduction of perivascular relaxant nicotine (10 μM) in MRA (+Adv 52.84 ± 2.81 vs. –Adv 14.12 ± 2.87 %) and MCA (+Adv 65.21 ± 6.90 vs. -Adv 18.83 ± 8.85 %) by wire myograph; and loss of neurogenic contractile function (+Adv 59.34 ± 3.40 % vs. –Adv 0.05 ± 0.05 %) in MRA by TNS confirmed the ablation of adventitial function. Pressure-mounted arteries showed contraction to 60 mM KPSS was unaffected in –Adv. However, there was a significant reduction in myogenic tone at 80 and 120 mmHg in MCA and MRA, respectively. ANG II-induced O_2^- release in –Adv was also reduced in lucigenin-enhanced chemiluminescence. The mechanistic experiment showed no changes in $[Ca^{2+}]_i$ indicated by Ca^{2+}-sensitive dye Fura-2 AM in both -Adv vs. +Adv. **Conclusion:** Collectively, this thesis has shown the activation of adventitial-derived NADPH oxidase/ ROS and actin polymerization as part of acute pressure-dependent myogenic constriction.

LIST OF FIGURES AND TABLES

ABBREVIATIONS

$[Ca^{2+}]_i$	Intracellular calcium
11,12-EET	11,12-epoxyeicosatrienoic acid
20-HETE	20-hydroxyeicosatetraenoic acid
5HT	5-Hydroxytryptamine (Serotonin)
AA	Arachidonic acid
Abl	Abelson tyrosine kinase
ACh	Acetylcholine
AFM	Atomic Force Microscopy
Akt/PKB	Akt/protein kinase B
ANG II	Angiotensin II
ANOVA	Analysis of varians
Arp2/3	Actin-related protein 2/3
AT_1R	Angiotensin II type I receptor
AT_2R	Angiotensin II type II receptor
ATP	Adenosine triphosphate
BMK1	Big mitogen-activated protein kinase 1
Ca^{2+}	Calcium
$CaCl_2$	Calcium chloride
CaM	Calmodulin
CaR	Calcium-sensing receptor
CAS	Crk-associated substrate
$Ca_V1.2$	L-type voltage operated calcium channel subunit 1.2
CCRC	Cumulative concentration response curve
Cdc42	Cell division control protein 42 homolog
CGRP	Calcitonin gene-related peptide
CICR	Calcium-induced calcium-released
Cl_{Ca}	Calcium-activated chloride channel
CLI	Critical limb ischemia
CSA	Cross sectional area
c-Src	Cellular Src gene

Cu^{2+}	Cuprum
CuZn	Cuprum zinc
CYP450	Cytochrome P450
Cyto D	Cytochalasin D
DAG	Diacylglycerol
DCF	2′,7′-dichlorofluorescin
DETCA	Diethyldithiocarbamate
DHE	Dihydroethidine
DMSO	Dimethyl sulfoxide
DPI	Diphenyleneiodonium
EC	Endothelial cells
ECM	Extracellular matrix
EDHF	Endothelium-derived hyperpolarizing factor
EDNO	Endothelium-dependent nitric oxide
EDRF	Endothelium-derived relaxing factor
EGFR	Epidermal growth factor receptor
EGTA	Ethylene glycol tetraacetic acid
eNOS	Endothelial nitric oxide synthase
ERK1/2	Extracellular signal-regulated kinase 1/2
ET-1	Endothelin-1
EtOH	Ethanol
F actin	Filamentous actin
FAK	Focal adhesion kinase
FITC	Fluorescein isothiocyanate
Fura 2AM	Fura 2-acetoxymethy ester
G actin	Globular actin
Glc	Glucose
GPCR	G-protein-coupled receptor
Grb2	Growth factor receptor-bound protein 2
GSH	Glutathione peroxidise
GSSH	Gluthione reductase
GTP	Guanine triphosphate

GTPase	Guanine triphosphatase
Gua	Guanethidine
H_20_2	Hydrogen peroxide
HB-EGF	Heparin-binding EGF-like growth factor
HC x PL APO	High-grade Corrected Plan Apochromat lens
HeNe	Helium-neon
HEPES	4-(2-hydroxyethyl)-1-piperazineethanesulfonic acid
HSP	Heat-shock protein
Hz	Hertz
ID	Internal diameter
IP	Intraluminal pressure
IP3	Inositol-1,4,5-triphosphate
JNK	c-Jun n-terminal kinase
K^+	Potassium
K_{Ca}	Large-conductance calcium-activated potassium channel
KCa	Calcium-activated potassium channel
KCl	Potassium chloride
KH_2PO_4	Potassium hydrogen phosphate
KPSS	Potassium-modified physiological saline solution
Kv	Voltage-gated potassium channel
LAS AF	Leica Application Suite Advanced Fluorescence
LPS	Lipopolysaccharide
MAP	Mitogen-activated protein
MCA	Middle cerebral artery
$MgSO_4$	Magnesium sulphate
$MgSO_4.7H_2O$	Magnesium sulphate heptahydrate
Mins	Minutes
MLCK	Myosin light chain kinase
MLCP	Myosin light chain phosphatase
MMP	Matrix metalloproteinases
Mn	Manganese

MnTMPyP	Manganese (III) tetrakis (1-methyl-4-pyridyl) porphyrin
MRA	Mesenteric resistance artery
Msecs	Milliseconds
NA	Noradrenaline
N/A	Numerical aperture
Na^+	Sodium
NAC	N-acetylcysteine
NaCl	Sodium chloride
$NADH^+$	β-nicotinamide adenine dinucleotide
NADPH	Reduced nicotinamide adenine dinucleotide phosphate
$NaHCO_3$	Sodium hydrogen carbonate
NANC	Non-adrenergic non-cholinergic
NaOH	Sodium hydroxide
NF-κb	Nuclear factor kappa-light-chain-enhancer of activated B cells
Nic	Nicotine
NO	Nitric oxide
NOS	Nitric oxide synthase
Nox	NADPH oxidase
NRTK	Non-receptor tyrosine kinases
N-WASP	Wiskot-Aldrich Syndrome protein
O_2^-	Superoxide
$ONOO^-$	Peroxynitrate
PAK	p21-activated kinase
PDBu	Phorbol 12,13-dibutyrate
PDGF	Platelet-derived growth factor
PE	Phenylephrine
PI	Propidium iodide
PI3K	Phosphatidylinositosol-3 kinase
PIP_2	Phosphatidylinositosol-(4,5)-biphosphate
PIP3	Phosphatidylinositol (3,4,5)-triphosphate

PKC	Protein kinase C
PKG	Protein kinase G
PLA_2	Phospholipase A_2
PLC	Phospholipase C
Pp	Pages
PSS	Physiological saline solution
RGD	Argine-Glycine-Aspartic acid
RLU/s	Relative light unit per second
ROS	Reactive oxygen species
RyR	Ryanodine receptor
S1P	Sphingosine 1-phosphate
SAC	Stretch-activated cation channel
Secs	Seconds
SEM	Standard error mean
Shc	Src homology complex
SHR	Spontaneously hypertensive rats
Sk1	Sphingosine kinase 1
SNP	Sodium nitroprusside
SOD	Superoxide dismutase
Sos	son-of-sevenless
SR	Sarcoplasmic reticulum
TCS SP-5	True Confocal Scanner for 5-SpectroPhotometer
TGF	Tumor growth factor
TKR	Tyrosine kinases receptor
TNF-α	Tumor necrosis factor-apha
TNS	Transmural nerve stimulation
TRPC	Transient response potential channel
TRPV1	Transient receptor potential cation channel, subfamily V, member 1
VEGF	Vascular endothelial growth factor
VOCC	Voltage-operated calcium channel
VSM	Vascular smooth muscle

WT	Wall thickness
XO	Xanthine oxidase
Zn^{2+}	Zinc

CHAPTER 1:
GENERAL INTRODUCTION
PRESSURE-DEPENDENT MYOGENIC TONE

1.1 AUTOREGULATION IN RESISTANCE ARTERIES

In the cardiovascular system, blood vessel function is related to the structure. Specifically, major arteries of the trunk are the elastic conductance arteries with large diameter and low resistance. On the contrary, distal arteries are muscular arteries of small diameter and high resistance that are critical for blood flow or pressure within the microcirculation system. Under physiological conditions, the viscoelasticity of the large arteries results in pulsatile pressure and flow so that the microvasculature can mediate blood supply steadily. The microvessels proximal to the arterioles with lumen diameter less than 200 μm were defined by Mulvany and Aalkjaer (1990) as the vessels offering the greatest resistance. The resistance value can vary depending for the entire vascular system, for the vascular network in selected organs and for individual vessels (Zweifach 1991), therefore, the size of resistance arteries may vary and be more than 200 μm diameter. Resistance arteries have the ability to alter their diameter independent of neural and hormonal control, in order to keep a relatively constant blood flow. The efficiency of autoregulation varies from tissue to tissue with those organs most vital for survival, e.g. brain, heart, kidney, demonstrating the most marked autoregulatory capacity. A number of local intrinsic control mechanisms have been proposed to account for the homeostatic properties of autoregulation, which are the combination of metabolites such as lactate and adenosine, flow-dependent regulation and myogenic tone (Henrion, 2005, Hill *et al.*, 2006).

Pressure-dependent myogenic tone in small resistance arteries is defined as the intrinsic property of vascular smooth muscle (VSM) cells to respond to changes in transmural pressure. Sir William Bayliss was the first to discover myogenic tone in 1902 when he recorded large increases in the volume of a dog's hind limb following the release of brief aortic occlusion (Bayliss, 1902). Bayliss considered the blood volume increase response too rapid to be mediated by accumulation of metabolites and concluded that a significant component of vascular tone could be modulated by changes in intravascular pressure. Bjorn Folkow (1949) supported Bayliss's theory demonstrating that denervated preparations of blood vessels developed pressure-

dependent vascular tone and autoregulation of blood flow was neurohormonal-independent (Folkow, 1949).

In cardiovascular diseases, these myogenic responses are altered. For example, in critical limb ischaemia (CLI) (Coats, 2010), the disrupted autoregulation in the peripheral limbs microvasculature can cause muscle atrophy, loss of ability to increase vascular resistance in the limb's skeletal muscle, uncontrolled orthostatic-dependent changes and reduced aerobic muscle capacity (Coats and Wadsworth, 2005). However, in spite of more than 100 years of myogenic tone study, the knowledge of the exact primary sensors to the signalling mechanisms that allow changes of intraluminal pressure to be converted accordingly into appropriate arterial diameter, remain incomplete and controversial. This has been a key challenge and a true understanding of the underlying mechanism is important in order to tackle the treatment of the pathological states.

The cerebrovasculature can be extremely mechanosensitive, independent of neurohormones, for example, taking the magnitude of myogenic contractile response in rabbit coronary artery as 1.0, the relative contractile magnitude of rabbit basilar artery would be 6.7 and renal artery 2.1 (Nakayama *et al.,* 2010). Myogenic tone has been shown in many other arteries, such as rat cremaster arteries (Raina *et al.*, 2008), rat skeletal muscle arteries (Kotecha and Hill, 2005), rat mesenteric arteries (Wesselman *et al.*, 2001), rat posterior cerebral arteries (Maneen *et al.*, 2006), rat femoral arteries (Matchkov *et al.*, 2002), human subcutaneous resistance arteries (Coats, 2010) and human cerebral arteries (Zhao *et al.*, 2007). The focal point of study interest in this thesis is the physiological mechanism of pressure-dependent myogenic tone in the species of rat and type of vessel is the middle cerebral arteries. A more comprehensive discussion of the possible mechanism that allows pressure stimulus transduction into pressure-dependent myogenic tone will be discussed in Section 1.4.

1.2 ULTRASTRUCTURE & FUNCTION OF A RESISTANCE ARTERY

The wall of an artery is made up of three layers: the tunica externa, the tunica media and the tunica intima (Figure 1.1). In resistance arteries, the external elastic lamina is typically absent (Lee 1995).

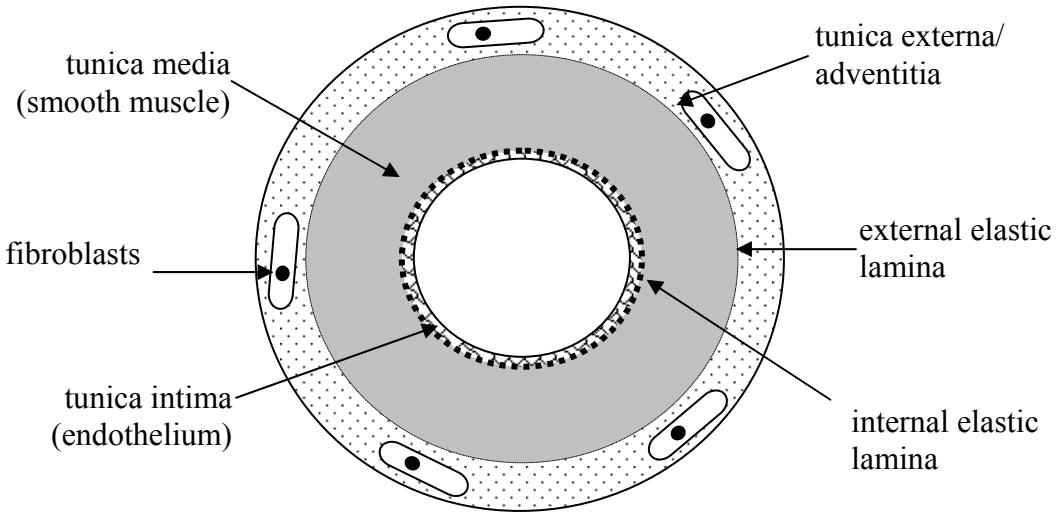

Figure 1.1 General schematic diagram of an artery.

1.2.1 Tunica externa/ adventitia

The tunica adventitia is the outermost layer of the resistance artery and has been known classically to be composed of connective tissue (elastin and collagen), mast cells, macrophages, perivascular nerves and progenitor cells (Lee, 1995, Pagano *et al.*, 1997). The nerves are located mostly in the adventitial-medial border, often with interposing connective tissue and do not penetrate into the muscle layers. The primary cell type in the adventitia is primary fibroblasts, which do not express α–smooth muscle actin (α-actin), myosin or desmin under normal physiological conditions (Kleschyov *et al.*, 1998).

Increasing attention has been given to the adventitia as it has been found to be the major source of superoxide (O_2^-), produced by NADPH oxidase (Nox) in rabbit aorta

(Pagano *et al.*, 1997, An *et al.*, 2007). Adventitial reactive oxygen species (ROS) have been associated with oxidative stress and also in vascular tone function. For instance, the adventitial inducible nitric oxide synthase (iNOS) was shown to produce nitric oxide (NO) in response to lipopolysaccharide (LPS) more than the medial layer (Gibbons *et al.*, 1992, Zhang *et al.*, 2004). In the aorta challenged to LPS exposure, the adventitia produced more NO than the medial layer (Kleschyov et al., 1998). Additionally, angiotensin II (ANG II)-induced O_2^- production inactivated endothelium-derived NO (EDNO), which gave rise to smooth muscle Ca^{2+} influx and spontaneous myogenic contraction (Schiffrin, 2004). Taken together, this evidence demonstrates that the adventitia holds an intriguing role as a centre for biological processes as well as in vascular tone, which is the major interest of study in this thesis. More comprehensive detail regarding adventitial function and microcirculation tone will be discussed in Section 1.5.5.

1.2.2 Tunica media

The tunica media is the middle layer made up of three to six layers of circumferentially-orientated spindle-shaped smooth muscle cells, elastic tissue and the internal elastic lamina (Mulvany & Aalkjaer 1990). Elastin is present as laminae and as an interconnected fibrous meshwork, while collagen is arranged in an irregular network of individual fibrils that forms nests around cells in arteries (Walker-Caprioglio *et al.*, 1991). The external elastic lamina, which borders the adventitia and the VSM, is present in all arteries except for cerebral arteries (Lee, 1995). The volume fraction of smooth muscle cells in the resistance arteries is significantly greater than that found in large arteries (Mulvany & Aalkjaer 1990). The medial layer is about 70% of the total thickness of a small artery, and the smooth muscle cells contain organelles such as sarcoplasmic reticulum (SR) and superficial storage sites for Ca^{2+} underneath the plasma membrane (Mulvany *et al.,* 1978). Between adjacent plasma membranes are the gap junctions with only 2-3 nm diameter and these gap junctions are involved in low resistance electronic signalling and a route for direct diffusion of low molecular weight substances (Lee *et al.,* 1983).

VSM is the biological centre for vasocontraction. Contractions are initiated by sensors such as wall stress, pressure and agonists, that stimulate the increase of

$[Ca^{2+}]_i$ followed by sarcolemma depolarization and release of Ca^{2+} from the sarcoplasmic reticulum (SR). The Ca^{2+}-induced Ca^{2+}-release (CICR) from the SR is from the ryanodine receptor channels. The Ca^{2+} then binds to calmodulin, which then activates the myosin light-chain kinase (MLCK). This enzyme phosphorylates myosin light chains in the presence of ATP, which then allows a cross-bridge to form between the myosin head and the actin filament, and eventually causes vasocontraction. In the cellular process of pressure-dependent myogenic constriction, the classical calmodulin/myosin light chain/actomyosin is not the only pathway involved. The stimulus (wall stress) can activate various factors such as the actin cytoskeleton (Cipolla *et al.,* 2002), Nox (Di Wang *et al.,* 1998, Pagano *et al.,* 1998), different ion channels (Schubert *et al.,* 2008, Sobey *et al.,* 1997), sphingosine kinase (Keller *et al.,* 2006), protein kinases (Eskildsen-Helmond & Mulvany 2003, Wesselman *et al.,* 2001) and many more to cause myogenic constriction. Now it is evident that the VSM is clearly the centre of orchestrated signaling pathways that affect adjacent adventitia and intima either in physiological or pathophysiological states.

1.2.3 Tunica intima/ interna

The tunica intima is the innermost layer; made up of a monolayer of squamous epithelium called endothelium, which adhere to the basement membrane and internal elastic lamina (Mulvany & Aalkjaer 1990).

In the past, there was a general consensus that VSM function was related to vasomotor tone control; and the endothelium as nothing more than non-reactive barrier properties that provides a surface for blood flow. The most significant discovery was in 1980 when Furchgott and Zawadzki showed that endothelial cells had a role in the relaxation of rabbit aorta to acetylcholine (ACh) and related muscarinic agonists (Furchgott and Zawadzki, 1980). The factor responsible for causing the relaxation was called endothelium-derived relaxing factor (EDRF), which was later identified as NO (Ignarro *et al.*, 1987). Also discovered was the production of prostacyclin, an arachidonic acid-derived vasodilator (Ager *et al.*, 1982). The studies have shown that not all relaxation can be fully explained by the

action of prostacyclin or NO, and that there is another substance that hyperpolarizes the VSM cells, subsequently referred to as endothelium-derived hyperpolarizing factor (EDHF) (Lin *et al.*, 1993, Feletou and Vanhoutte, 1996). Besides producing vasodilating factors, the endothelium has been shown to also secrete endothelium-dependent constricting factors such as thromboxane (De Vriese *et al.*, 2000) and endothelin (Kramer *et al.*, 1997).

Disturbed endothelial function plays a role in cardiovascular pathology, most commonly, in atherosclerosis (Hamilton *et al.*, 2004). Injured endothelium is an initiating event for atherosclerosis, where the injury will be followed by lipid accumulation and the adhesion of monocytes and platelets. The aggregation of monocytes within the subendothelium is known as a fatty streak, which will produce and release growth factors and cytokines, leading to the migration and proliferation of VSM cells, the recruitment of additional blood cells, and the accumulation of more lipids. With time, the tissue injury will be aggravated and an atheromatous plaque will be formed. In pulmonary hypertension, endothelin-1 (ET-1) derived from the endothelium is also increased (Yoshibayashi *et al.*, 1991). The endothelium can also produce ROS that reduces NO bioavailability and initiate lesion leading to atherosclerotic plaque within the lumen (Judkins *et al.*, 2010).

Collectively, the three main layers of tunica adventitia, media and intima have unique structural properties that determine their different functions within the vascular wall, and damage or interruption to any of these layers could lead to pathological conditions.

1.3 THE MECHANICS OF RESISTANCE ARTERIES

The resistance (R) presented by a resistance artery to the blood flow can be calculated from a derivation elucidated by a physician Jean Leonard Marie Poiseuille. According to Poiseuille's law, resistance to flow is inversely related to the fourth power of the radius lumen of the vessel. As a result, a small decrease in resistance artery lumen diameter significantly increases resistance (Schmid-Schonbein and Murakami, 1985). Thus, resistance arteries are the significant determinant of peripheral vascular resistance and contribute to systemic blood pressure control (Schmid-Schonbein and Murakami, 1985).

$$R = 8\eta \, . \, L/ \, \pi r^4$$

where η is the viscosity of the perfusing liquid, L is the length of the artery and r is the internal radius.

The wall tension (T) is the sum of active tension in vascular smooth muscle (VSM) and passive tension in the collagen, elastin and smooth muscle in the wall. The wall tension depends on the difference of transmural pressure and the radius.

$$T = \Delta P r$$

where P is transmural pressure (P_{in}-P_{out}).

A pressurized artery is subjected to forces in three dimensions, which allows the arterial wall to be treated as a cylindrical body with all net strains oriented along the circumferential (θ), longitudinal (z), and radial (r) directions. Figure 1.2 shows these three orthogonal axes whereby experimental analysis can be evaluated from.

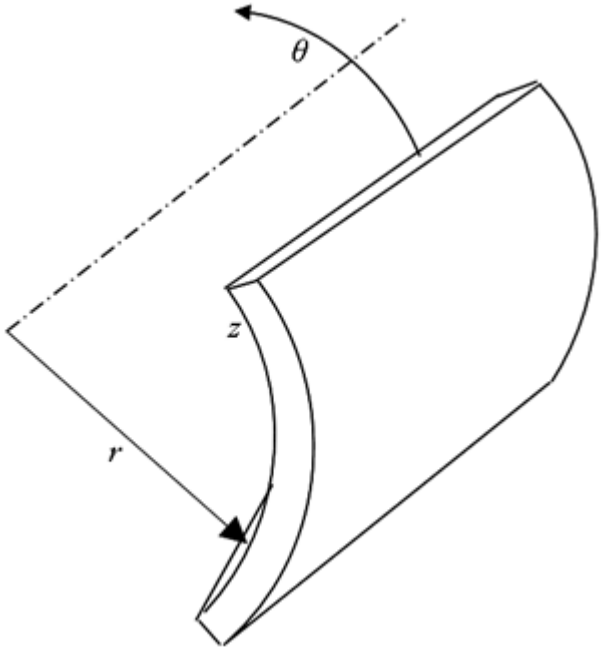

Figure 1.2 Diagram of the orthogonal axes of an artery. *The arterial segment showing the circumferential (θ), longitudinal (z) and radial (r) directions. Strains and stresses in the circumferential and longitudinal directions are tensile because the vessels tend to distend in these directions with pressure. Strains and stresses in the radial direction are compressive as the wall tends to be narrowed with pressure (Dobrin, 1978).*

The mechanical characteristics of blood vessels are determined by passive and active tissue properties. Passive properties provide an understanding of the behaviour of the extracellular matrix (ECM) components such as collagen and elastin, whereas the VSM represents the active element (Rizzoni *et al.*, 2009, van den Akker *et al.*, 2010). In the study of vascular remodelling for example, passive mechanical properties are typically investigated rather than the maximally active VSM, because these two main passive elements (elastin and collagen) are the major contributors to the vascular wall stiffness. Changes in the organization or abundance of elastin and collagen can modify vascular compliance and microvascular regulation (Martinez-Lemus *et al.*, 2009). Elastic fibres of the ECM are comprised of elastin and microfibril-related proteins e.g. fibrillin and fibullin, which give the vessel elasticity; whereas collagen, a much stiffer protein, has a role in limiting vessel distension. The large amount of

elastin and collagen in large arteries decreases in smaller vessels, but they are still considered as abundant in terms of occupied volume (Gonzalez *et al.*, 2005). Gonzalez's group has studied intensively the mechanical properties of resistance arteries and their relation to haemodynamics (Briones *et al.*, 2003, Gonzalez *et al.*, 2005, Jimenez-Altayo *et al.*, 2007). They have observed that cerebral arteries show less elasticity, fenestrae size and elastin content compared to mesenteric arteries, despite their similar diameter measurement, which could be due to their different physiological roles and haemodynamic response. The cerebral arteries are able to control the blood flow by their ability to constrict in response to distending intramural pressure with the VSM found to be the major determinant in the diameter dimensions (Brekke *et al.*, 2002, Coulson *et al.*, 2002). On the contrary, mesenteric arteries exhibit a lower degree of myogenic constriction (Sun *et al.,* 1992) whereby its passive properties might play a key role in regulating vessel diameter. Middle cerebral arteries are adhered to surrounding tissue within the intracranial and therefore lower degree of movement freedom, while mesenteric arteries require a larger degree of elasticity because they irrigate the continuous movement of the intestines. Therefore, differences in myogenic tone of different vessel diameter and type of tissue might be related to the different physiological roles and responses to haemodynamic stimuli of cerebral and mesenteric arteries.

Blood vessels are not static entities and they are able to change structure, i.e. to remodel. Vascular remodelling may be considered as an adaptive process in response to the haemodynamic environment to maintain relatively constant tensile and shear stress (Mulvany *et al.*, 1996, Martinez-Lemus *et al.*, 2004, VanBavel *et al.*, 2006, Rizzoni *et al.*, 2009, Folkow, 2010). Mulvany *et al.* (1996) has represented a now widely-used graphic of the remodelling types on the basis of lumen change (inward or outward), and wall cross sectional area (CSA) area (hypertrophic, hypotrophic or eutrophic). It is widely accepted that abnormal structural changes and reorganization of the wall components in vascular remodeling are associated with diseases. For instance, transient cerebral ischaemia in a normotensive model showed an increase of fenestrae, distensibility with reduced myogenic tone as a result of short-term remodeling and compensation to ensure cerebral flow (Coulson *et al.*, 2002,

Jimenez-Altayo *et al.*, 2007). Interestingly in the same model, the adventitial cells showed an increase in number, hence causing adventitial hypertrophy after ischaemia-reperfusion (Jimenez-Altayo *et al.*, 2007). On the other hand, the hypertensive model post cerebral ischaemia showed hypertrophic inward remodeling with decreased CSA but no change in distensibility in spite of increased fenestrae. The myogenic tone was unaltered eventually due to loss of compensatory mechanism, resulted in low blood supply and eventually ischeamic infarct tissue (Jimenez-Altayo *et al.*, 2007). In CLI, the passive pressure-dependent myogenic tone is also impaired possibly because of derangement of arteriolar wall architecture (decreased CSA, wall:lumen ratio, adventitial and medial thickness) and therefore failure in generating active myogenic tone (Coats, 2003, Coats *et al.*, 2003). The consequences of the incapability to control blood flow and blood pressure in resistance arteries results in increased blood hydrostatic pressure, impairment of transcapillary fluid exchange and oedema formation. Martinez-Lemus *et al.* characterized the wall of resistance arteries as being highly plastic, in which transition from tone to remodeling is a continuum event: from Ca^{2+}-dependent tone at seconds time scale to Ca^{2+} sensitization in minutes, cellular rearrangement in hours, matrix cross-linking in days and matrix turnover in weeks (Martinez-Lemus *et al.*, 2009).

Mechanical properties are closely associated with the structural and functional aspects of small arteries. In spite of that, the role of adventitial fibroblasts and how they affect the microvascular calibre in the presence of intramural pressure is still poorly understood, and such a gap in knowledge deserves our attention.

1.4 PRESSURE-DEPENDENT MYOGENIC TONE MECHANISMS

Myogenic tone shows an inverse relationship between pressure and diameter, where an increase of intraluminal pressure causes a decrease in diameter, and vice versa. Moreover, the strength of the myogenic response varies depending on the diameter and the particular vascular bed. In the hamster cheek pouch, relative myogenic responsiveness increased with decreasing vessel size in second- and third-order

arterioles, whereas fourth-order arterioles were substantially less responsive than third-order arterioles (Davis 1993). Relative myogenic tone varies between different vascular beds, with rat cerebral (Gokina *et al.*, 2005) and skeletal muscle vessels (Coats, 2010) exhibiting more prominent myogenic response than small mesenteric vessels (Chin *et al.*, 2007). Differences in the strength of the myogenic response between vessels with similar diameter have also been observed within the network of a vascular bed. For example, there was a weak myogenic response in subendocardial but a strong myogenic response in subepicardial porcine arteries (Kuo *et al.*, 1988).

According to the reviews by Hill *et al.* (2006) and Khavandi *et al.* (2009), myogenic behaviour can be divided into three phases. The first consists of myogenic or basal tone development, associated with a large increase in L-type VOCC-mediated membrane depolarization and $[Ca^{2+}]_i$. The second phase is known as myogenic reactivity, where further constriction happens in response to an increase in intraluminal pressure. The $[Ca^{2+}]_i$ concentration is maintained at this phase, but $[Ca^{2+}]_i$ sensitization of the mechanical apparatus is thought to occur. The third phase is called forced dilation, when the wall of the artery is unable to maintain a constriction against mounting pressure. There are a number of candidates that could be mediating myogenic response, however there is no agreement on whether it is the vessel wall tension (Davis *et al.*, 1992, Dunn and Gardiner, 1997, Brekke *et al.*, 2002), stretch-activated cation (SAC) channels (Davis *et al*. 1992), VOCC (McCarron *et al.* 1997), extracelullar matrix (ECM) (Davis *et al.*, 2001) or actin cytoskeleton (Cipolla *et al.*, 2002). Knowledge about the cellular mechanisms underlying myogenic tone is important and could be exploited for therapeutic intervention, as myogenic responsiveness is commonly altered in vascular diseases. Therefore, it is crucial to understand the stimuli, sensor, signal transduction pathways involving second messengers, regulation of contractile proteins and finally the adjustment for vasomotor tone. Figure 1.3 shows the overall postulated pathway for pressure-dependent myogenic tone, based on the review by Hill *et al.* (2006).

Increase in intraluminal pressure	Stimulus
↓	↓
Membrane/cytoskeletal stretch/increased tension	Sensed variable
↓	↓
Membrane/cytoskeletal detection systems	Detector
↓	↓
Signal transduction mechanisms Modulation of ion channels: (SAC, TRPC, ENaC, VOCC, BK_{Ca}, K_v) Membrane depolarization Ca^{2+} mobilization Kinase activation/inactivation (MLCK, PKC, SK, TK) Phosphatase inhibition (MLCP) Cytoskeletal reorganization	Transducers ↓
↓	
Regulation of contractile protein	Molecular proteins
↓	↓
Adjustment of vasomotor tone	Controlled variable

Figure 1.3 Overall scheme of putative signalling events mediating pressure-induced myogenic tone*. SAC (stretch-activated channel); TRPC (transient receptor potential channel); VOCC (voltage-operated calcium channel); MLCK (myosin light chain kinase); MLCP (myosin light chain phosphatise); PKC (protein kinase C); SK (sphingosine kinase); TK (tyrosine kinase); ENaC (epithelial sodium channel);* BK_{Ca} *(*Ca^{2+}*-activated* K^+ *channel);* K_v *(voltage-gated potassium channel) (Hill et al., 2006).*

1.4.1 Ion channels

Putative plasma membrane ion channels functioning as primary mechanosensors in mediating arteriolar myogenic vasoconstriction include VOCC (Kotecha and Hill 2005, Knot and Nelson 1998), SAC (Luchessi *et al.,* 2004), TRPC (Mederos y Schnitzler *et al.*, 2008), large conductance Ca^{2+}-activated K^+ channel (BK_{Ca}) (Dong *et al.,* 2009, Cheranov and Jaggar 2006), voltage-gated potassium channel (K_v)

(Sobey *et al.,* 1998) and Ca^{2+}-activated chloride channels (Cl_{Ca}) (Dimitropoulou *et al.*, 2001).

A plethora of evidence has shown that the pressure-dependent myogenic response is mediated by an increase of membrane depolarization and $[Ca^{2+}]_i$ in VSM, accompanied by the classical Ca^{2+}-calmodulin–induced myosin light chain (MLC) phosphorylation (Harder, 1984, Davis and Hill, 1999, Hill *et al.*, 2001, Schubert *et al.*, 2008). The pioneering study by Harder (1984) was the first to show that an increase in pressure caused depolarization and therefore an increase in Ca^{2+} influx and vasoconstriction, within the cerebral artery. A subsequent study showed that the increased Ca^{2+} influx occurred in parallel with the decrease in diameter (Knot and Nelson, 1998). Incubation in a Ca^{2+}-free solution or the administration of the Ca^{2+}-entry blocker diltiazem, led to a complete loss of myogenic tone (Bevan, 1982). The Ca^{2+} influx has been shown to depend primarily on L-type VOCC which can be inhibited by nifedipine (VanBavel *et al.*, 1998, Coats *et al.*, 2001, Scotland *et al.*, 2004, Kotecha and Hill, 2005).

The primary events that lead to an increase of $[Ca^{2+}]_i$ are the release of Ca^{2+} from intracellular stores and transmembrane influx. However, a study found the internal ryanodine-sensitive Ca^{2+} store to be insignificant in myogenic constriction, indicating that CICR is a minor contributor to the response (McCarron *et al.*, 1997). Recently, extracellular Ca^{2+} has been reviewed by Smajilovic and Tfelt-Hansen (2007) for eliciting the role as a first messenger through a G-protein coupled receptor (GPCR), namely the Ca^{2+}-sensing receptor (CaR). In subcutaneous arteries, the CaR was found to modulate pressure-dependent myogenic tone, while PKC was acting as its negative regulator (Ohanian *et al.*, 2005). However, the CaR paradigm is relatively new in the area of myogenic tone and more investigation is needed to clarify its function. Another recent study that supports GCPR as a mechanosensor is where $G_{q/11}$-coupled receptor, a GCPR, was activated and stimulated β-arrestin recruitment in response to increased pressure (Mederos y Schnitzler *et al.*, 2008). Subsequently, this process lead to TRPC-mediated membrane depolarization and enhanced myogenic constriction in renal and cerebral arteries.

Although Ca^{2+} has been shown as a necessary key signalling component in myogenic constriction, some studies have shown that only a minimal rise in $[Ca^{2+}]_i$ is required to elicit myogenic constriction (D'Angelo *et al.*, 1997, VanBavel *et al.*, 1998). Therefore, Ca^{2+} is not the only determinant of steady-state constriction and there are Ca^{2+}-independent regulatory systems involving protein kinase C (PKC), Rho/Rho kinase, protein tyrosine kinase and cytoskeleton, that accompany myogenic constriction (Jarajapu and Knot, 2002, Lagaud *et al.*, 2002, Massett *et al.*, 2002, Gokina *et al.*, 2005).

1.4.2 Intracellular second messengers

There has been a growing body of evidence that shows Ca^{2+} sensitivity regulation integrates with Ca^{2+}-independent mechanisms in the myogenic constriction, via intracellular second messengers signalling in VSM. Pressure or stretch acts as the stimulus for G proteins, which then stimulate the membrane enzyme phospholipase C (PLC) that specifically hydrolyzes phosphatidylinositol-4,5-biphosphate (PIP_2). PIP_2 is split into two second messengers, diacylglycerol (DAG) and inotisol-1,4,5-triphosphate (IP_3) (Narayanan *et al.*, 1994). Both IP_3 and DAG have been shown to increase with the level of intraluminal pressure and to remain elevated for the duration of the pressure increase (Narayanan *et al.*, 1994). The increase in the level of intracellular IP_3, induced by stretch, may be responsible for part of the pressure-induced increase of $[Ca^{2+}]_i$ (Jarajapu and Knot, 2002). The increase in DAG, which is an activator of protein kinase C (PKC), implicates the participation of PKC in the myogenic response (Gokina *et al.*, 1999, Wesselman *et al.*, 2001). Indeed, the PKC activator, phorbol-12,13-dibutyrate (PDBu) was found to increase the level of Ca^{2+}, and this effect was abolished by nifedipine, an L-type Ca^{2+} channel blocker (Lin *et al.* 1998; Ohanian *et al.* 2005). This suggests that the PKC-enhancing effect by PDBu was through the activation of L-type Ca^{2+} channels and this could increase Ca^{2+} sensitivity resulting in myogenic constriction (Lin *et al.*, 1998, Gokina *et al.*, 1999). Consistent with the fact that PKC phosphorylates mitogen-activated protein kinase (MAPK), it has been shown that inhibition of MAPK reduced the Ca^{2+} sensitivity and hence, attenuated the pressure-dependent myogenic tone (Lagaud *et al.*, 1999, Massett *et al.*, 2002). Another potential pathway regulating myogenic tone

is the RhoA/Rho kinase signaling pathway. Results have shown that RhoA/Rho kinase pathway to be activated by mechanical stretch, leading to an increase in intracellular [Ca^{2+}] sensitivity. This could potentially inhibit myosin phosphatase and/or activate actin cytoskeleton polymerization, followed by increased myogenic tone (Gokina *et al.*, 2005, Jarajapu and Knot, 2005). Another interesting key candidate in modulating myogenic tone is the epidermal growth factor receptor (EGFR). A study in mesenteric arteries has shown pressure/stretch to stimulate metalloproteinases 2/9 (MMP-2/9), leading to endogenous HB-EGF (heparin-binding EGF-like growth factor) release and EGFR transactivation (Lucchesi *et al.*, 2004). This mechanism was specific to myogenic tone as contractions to ANG II and KCl were independent of EGFR transactivation. The underlying mechanism within the VSM was not investigated, but it was speculated that MMP-2/9 activation may involve integrins (Belmadani *et al.*, 2008) or SACs (Scotland *et al.*, 2004), and the downstream signalling of EGFR activation may be PKC-dependent (Jarajapu and Knot, 2005) or through Nox/ROS (Csanyi *et al.*, 2009).

1.4.3 Cytochrome P-450

The cytochrome P-450 (CYP) enzymes metabolize endogenous arachidonic acid (AA) and are referred to as the third pathway of AA metabolism, the others being cyclooxygenases and lipooxygenases. The role of CYP has been reviewed as a candidate mediator in signaling events culminating in pressure-dependent myogenic tone in renal, skeletal muscle and pulmonary arteries (Kaley, 2000, Frisbee *et al.*, 2001, Parker *et al.*, 2005, Terashvili *et al.*, 2006). Phospholipase A_2 (PLA_2) is an enzyme which hydrolyzes phospholipids and produces AA. This AA can be further metabolized to produce autocrine vasoconstrictor 20-HETE (20-hydroxyeicosatetraenoic acid) and vasodilator 11,12-EET (11,12-epoxyeicosatrienoic acid), which could enhance ROS release. Stimulation of VSM cells by stretch, pressure and flow could trigger CYP to release 20-HETE, which inhibits the opening of Ca^{2+}-activated K^+ (K_{Ca}) channels in VSM, causing depolarization, and eventually increases Ca^{2+} entry and promotes myogenic constriction (Frisbee *et al.*, 2001). Another recent finding has found pressure-induced 20-HETE could activate the

neuronal vanilloid receptor TRPV1 on C-fibre nerve endings resulting in membrane depolarization, release of neuropeptide substance P and enhancement of myogenic tone (Scotland *et al.*, 2004). As for 11,12-EET, it exhibits biological activities opposite to 20-HETE; where it vasodilates blood vessels and stimulates hyperpolarization via K_{Ca} channels in VSM cells (Imig, 1999). Hence, the dual counterbalancing activity of these two AA metabolites may present a mechanism for balanced regulation of myogenic tone regulation.

1.4.4 RGD integrins

Another recent approach to understanding physical stimulus by intraluminal pressure is the mechanism of ECM coupling through the VSM plasma membrane, integrin-specific peptides and actin cytoskeleton (Hill *et al.*, 2006). The most common VSM integrin which has been studied is Arg-Gly-Asp (RGD), found in collagen and fibronectin (Glukhova and Koteliansky, 1995). RGD peptides, $\alpha_v\beta_3$-integrin, was found to cause a transient constriction followed by a sustained dilation through Ca^{2+} influx interference, and thus inhibit myogenic tone in isolated rat cremaster arterioles (Mogford *et al.*, 1996). An opposite effect was seen in isolated renal afferent arterioles, where RGD peptides caused constriction together with an increase in VSM $[Ca^{2+}]_i$ (Yip & Marsh 1997). The constriction produced by pressure and RGD peptide were additive, suggesting that different downstream signalling mechanisms are involved (Davis *et al.*, 2001). Alternatively, RGD-mediated vasodilation and vasoconstriction might be mediated by different integrins. Collectively, evidence suggests that integrins regulate L-type Ca^{2+} current in VSM and this is one of the key regulators of $[Ca^{2+}]_i$, and hence myogenic tone.

1.4.5 Emerging new candidates for mechanosensors in pressure-dependent myogenic tone: Reactive oxygen species and the actin cytoskeleton

Reactive oxygen species and oxidative stress have been synonymous in pathological conditions for decades. Recently, a growing body of evidence has shown that ROS could play a role in regulating pressure-dependent myogenic tone (Keller *et al.*, 2006, Lecarpentier, 2007). Besides ROS, another emerging new candidate is the actin cytoskeleton (Faraci, 2006). The effects of ROS and the actin cytoskeleton in pressure-dependent myogenic tone will both be reviewed comprehensively in Section 1.5 and 1.6, respectively, as they are the major interests of this thesis. Figure 1.4 summarizes the overall putative mechanotransduction pathways of pressure-dependent myogenic tone regulation, as have been discussed.

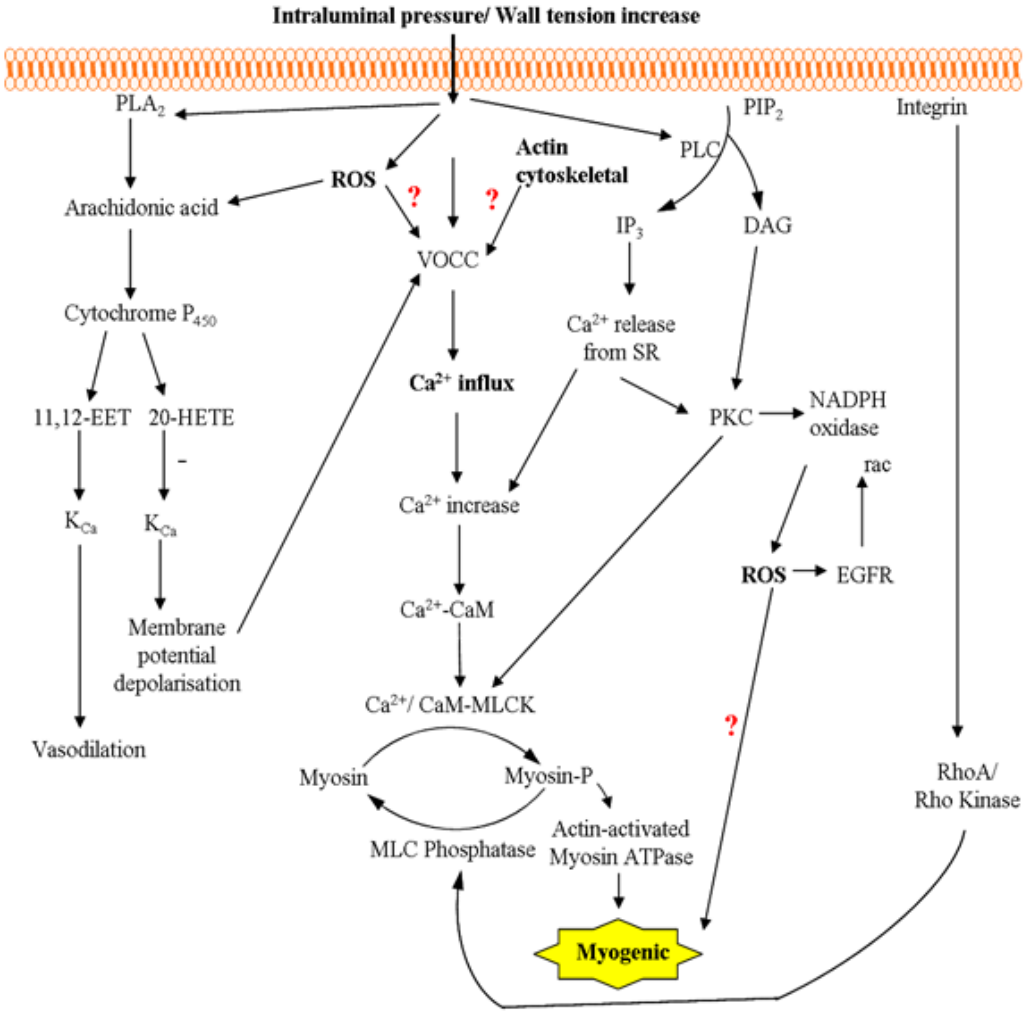

Figure 1.4 Overview of possible pathways involved in the myogenic response. *The possible pathways may involve ion channels, intracellular second messengers, cytochrome P450 and the newly arised new candidates, ROS and actin cytoskeleton. PIP_2 (phosphatidylinositol (4,5)-bisphosphate); PLC (phospholipase C); IP_3 (inositol trisphosphate); DAG (diacylglycerol); PKC (protein kinase C); VOCC (voltage-operated calcium channel); PLA_2 (phospholipase A_2); 20-HETE (20-hydroxyeicosatetraenoic acid); K_{Ca} (calcium-activated potassium channel); Ca^{2+} (calcium); CaM (calmodulin); MLCK (myosin light-chain kinase); myosin-P (myosin-phosphate); SR (sarcoplamic reticulum).*

1.5 REACTIVE OXYGEN SPECIES IN CARDIOVASCULAR HEALTH AND DISEASES

1.5.1 Reactive oxygen species and oxidative stress

ROS are classically considered as a toxic by-product of metabolism in oxidative stress (Taniyama & Griendling 2003; Dworakowski et al., 2006). When ROS is produced excessively, overwhelming of endogenous antioxidant systems and/or during downregulation of antioxidant systems, oxidative stress occurs (Griendling & Fitzgerald 2003; Taniyama & Griendling 2003; Dworakowski *et al.* 2006). Dysregulation due to oxidative stress has been shown to contribute substantially to the progression of cardiovascular diseases such as hypertension (Schiffrin 2004; Intengan *et al*. 1999), diabetes (Sachidanandam *et al.* 2007), hypercholesterolaemia (Ishikawa *et al.*, 2004), cardiac hypertrophy (Lang, 2002) and myocardial ischaemia (Ferrari *et al.*, 2004).

The term 'oxidative stress' may be an over-simplification as it is used to cover the diverse and complex role of ROS in physiological and pathophysiological conditions. Over the past decade, studies have shown that ROS at relatively low cellular levels may influence metabolism in physiological conditions (Keller *et al.*, 2006, Lecarpentier, 2007) and may be involved with the normal regulation of vascular tone and structure (Faraci, 2006). ROS may have direct and indirect effects on VSM, and there are studies suggesting that both relaxation and contraction of vascular muscle may occur, depending on the tissue model and the physiological circumstances.

1.5.5 Metabolism of ROS

ROS includes free radicals such as superoxide anion (O_2^-) and hydroxyl radical (OH^-), and nonradical species such as hydrogen peroxide (H_2O_2) (Hamilton *et al.* 2004). Superoxide dismutase (SOD) metabolizes O_2^- to H_2O_2. There are three isoforms for SOD: CuZn-containing cytosolic SOD1, Mn-containing SOD2 and CuZn-containing extracellular SOD3. Peroxidases such as catalase and glutathione

peroxidase further metabolize H_2O_2 to O_2 and water. H_2O_2 can also be transformed to OH^- and O_2^- to peroxynitrite ($ONOO^-$) (Hamilton *et al.*, 2004, Faraci, 2006, Miller *et al.*, 2006). Almost all types of vascular cell produce O_2^- and H_2O_2 (Lyle & Griendling 2005). Primarily, ROS within a blood vessel is produced by the membrane-bound enzyme Nox (Griendling *et al.*, 1994), but ROS has been shown to also be produced from adventitial fibroblasts (Pagano *et al.*, 1997), cyclooxygenase (Sobey *et al.*, 1998, Miller *et al.*, 2006) as well as eNOS (Matoba *et al.*, 2000). There are many stimuli which activate Nox, including ANG II (Mehta and Griendling, 2007), ET-1 (An *et al.* 2007), shear stress (Hwang *et al.* 2003), tumor necrosis factor-α (TNF-α) (Al-Mehdi and Fisher, 1998), metabolic factors including hyperglycaemia, insulin (Dworakowski *et al.*, 2006), hypercholesterolemia (Ishikawa *et al.* 2004), and vascular endothelial growth factor (VEGF) (Abid *et al.* 2007).

O_2^- is highly reactive, but it has a very short half-life and poor cell permeability. Therefore, the impact of O_2^- on vascular function could be instant but short-lasting. The reaction of O_2^- with EDNO is very rapid, 3 times faster than the dismutation of O_2^-, resulting in reduced NO bioavailability and increased $ONOO^-$. Conversely, H_2O_2 is relatively stable and highly diffusible between cells. Therefore, H_2O_2 is regarded as one of the most important ROS molecules for modulating vascular function. It has been reported as an EDHF in the mesenteric artery (Matoba *et al.*, 2000) and partially mediates flow-dependent vasodilatation in coronary arterioles (Miura *et al.*, 2003). Figure 1.5 shows the general metabolism of ROS and the associated complications in cardiovascular diseases.

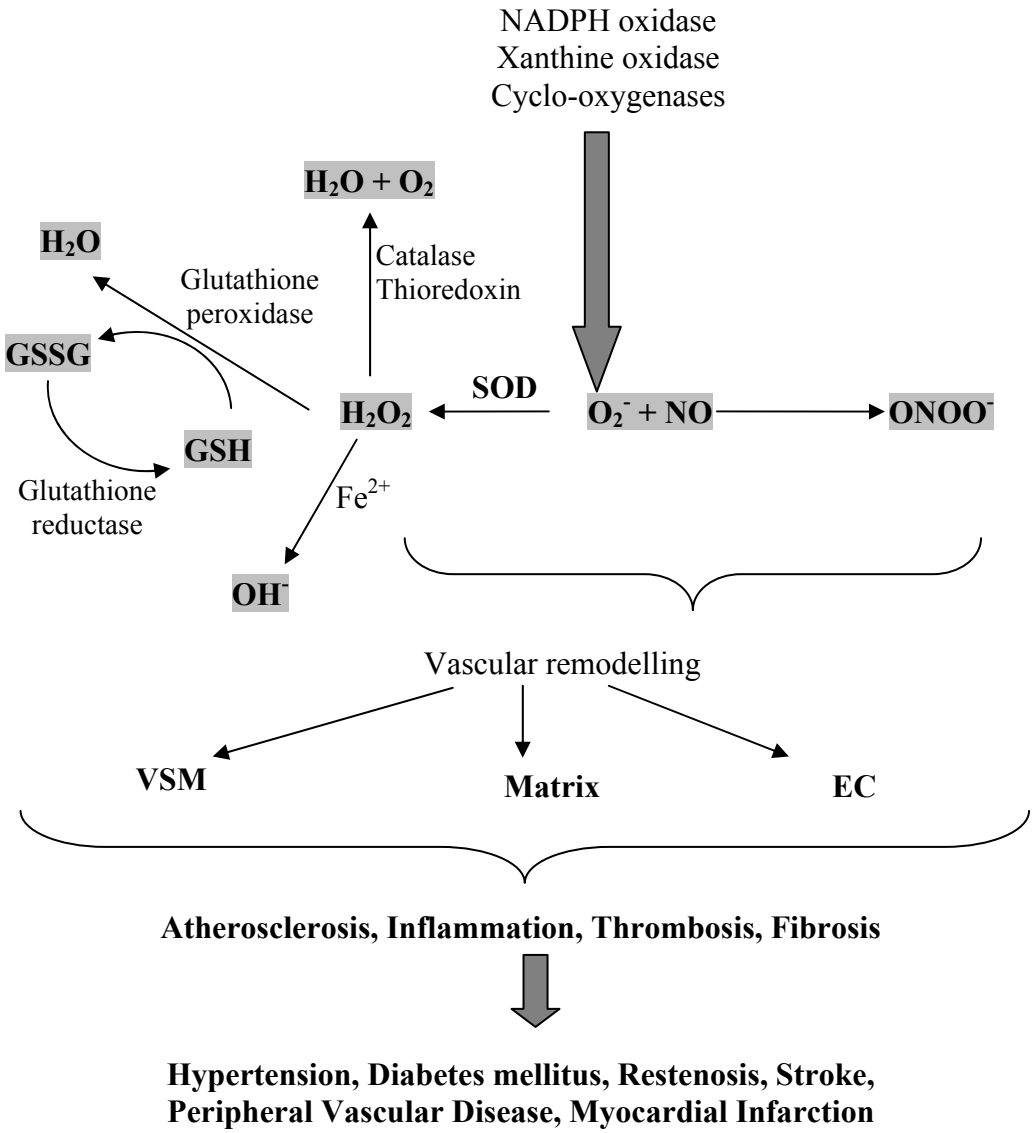

Figure 1.5 Generation of O_2^- and H_2O_2 from O_2 in vascular tissue and the associated complications in cardiovascular diseases. *GSSG, oxidized glutathione; GSH, reduced glutathione; SOD, superoxide dismutase; $ONOO^-$, peroxynitrite; NO, nitric oxide; VSM, vascular smooth muscle; EC, endothelial cells.*

1.5.3 NADPH oxidase subunits

The Nox in the vasculature consists of $p22^{phox}$, $p47^{phox}$ and novel homologues of $gp91^{phox}$, which are NOX1, NOX2 and NOX4 (Seshiah *et al.* 2002; Cave, 2008). These isoforms are different between cell types and they have separate locations within the cell. The evidence is becoming increasingly clear that the individual Nox isoforms have delineated roles within the cell and are linked with specific downstream effects (Cave *et al.,* 2005; Cave, 2008).

1.5.4 ANG II as an NADPH oxidase/ ROS activator

ANG II stimulates Nox and ROS activity in all cells within the vascular wall (Griendling and Ushio-Fukai, 2000, Pedruzzi *et al.*, 2004, Gonzalez *et al.*, 2008). ANG II not only stimulates Nox-dependent O_2^- formation in VSM cells but also in cardiac, endothelial, mesangial cells and adventitial fibroblasts (Zhang *et al.* 1999; Pedruzzi *et al.* 2004; Mehta & Griendling 2007). In rabbit aortic adventitial fibroblasts, induction of Nox subunit $p67^{phox}$ expression was caused by ANG II-induced O_2^- (Pagano *et al.*, 1998). In rat VSM, subunit $p22^{phox}$ has been shown to be a component in the ANG II-induced hypertrophy (Ushio-Fukai *et al.* 1996). A member of a new family of $gp91^{phox}$, NOX1, showed a role in mediating ANG II-induced O_2^- formation via redox signalling in VSM cells (Lassegue *et al.* 2001). Angiotensin AT_1 receptors (AT_1R) are believed to be mainly located in the VSM cells and to induce vasoconstriction (Maeso *et al.* 1996; Touyz & Schiffrin 2000), while angiotensin AT_2 receptors (AT_2R) mediate endothelium-dependent vasodilation (Carey *et al.*, 2000).

In addition to stimulating Nox to release ROS, ANG II has also been found to stimulate various downstream signalling pathways in relation to pressure-dependent myogenic tone. For instance, intraluminal pressure facilitated by ANG II may activate AT_1R which in turn causes transactivation of the platelet-derived growth factor (PDGF), then through the Ras-Raf pathway activates extracellular signal-regulated kinase 1/2 (ERK1/2) (Matrougui *et al.*, 2000, Eskildsen-Helmond and

Mulvany, 2003). However, how the mechanical loading can cause such acute and rapid activation is still unknown. Suggested pathways may include the PLC-IP_3 pathway resulting in increase of $[Ca^{2+}]_i$ and Ca^{2+}-dependent ERK1/2 stimulation, or the PLC-DAG pathway whereby PKC can activate ERK1/2 (Eskildsen-Helmond and Mulvany, 2003). Other interesting supporting findings were that AT_1R stimulation could initiate G-to-F actin and strengthen the cytoskeletal structure (Martinez-Lemus, 2008) or it could activate TRPC-mediated membrane depolarization and cause myogenic tone (Mederos y Schnitzler *et al.*, 2008).

1.5.5 ROS in the biology of vascular tone

The first direct evidence that endogenous ROS can act as a signalling molecule was found by Kontos *et al*. (1984). Their study found that dilation by topical sodium arachidonate and bradykinin was inhibited by catalase and SOD in cat cerebral artery. Thus, O_2^- and H_2O_2 or radical derivatives such as OH^- were likely to be the mediators from sodium arachidonate and bradykinin that caused vasodilation. Since then, a growing body of evidence has demonstrated ROS as potent intracellular and intercellular second messengers to modulate many downstream signalling molecules via $[Ca^{2+}]_i$-dependent and $[Ca^{2+}]_i$–independent pathways and eventually cause substantial interplay in myogenic response.

The major effect of O_2^- was thought to be peripheral vasocontraction by its reaction with EDNO, as shown widely in oxidative stress. It is now known that in cerebral arteries, O_2^- can cause both constriction and dilation (Wei *et al.* 1996; Didion & Faraci 2002). The K^+ channel blocker, tetraethylammonium (TEA), reduced cerebral relaxation to O_2^-, suggesting that K_{Ca} channels are involved (Wei *et al.*, 1996). H_2O_2 has also been shown to induce both vasorelaxation and vasoconstriction, depending on the vascular bed and the pre-constrictor agent. H_2O_2 from the endothelium may act as a vasodilatory EDHF in murine (Kimura *et al.,* 2002), human mesenteric arteries (Matoba *et al.* 2002) and human coronary arterioles (Miura *et al.* 2003). At higher concentration (>1 mM), H_2O_2 has been found to cause vasoconstriction followed by vasodilatation (Miller *et al.*, 2005). Dilatation of rat cerebral arterioles in

response to exogenous H_2O_2, or endogenous bradykinin-derived H_2O_2 is mediated by activation of K_{Ca} channels (Sobey *et al.*, 1997). In other studies, mitochondrial-derived ROS dilated cerebral arteries by increasing K_{Ca} channel activity via Ca^{2+} sparks (Xi *et al.*, 2005), whereas H_2O_2 dilated cerebral arterioles by activating ATP-sensitive K^+ channels (Wei *et al.*, 1996). Thus, activation of K^+ channels may be a major mechanism of dilatation in response to H_2O_2 in the microcirculation. In a study on canine basilar arteries, different types of exogenous ROS elicit different characteristics of contraction, whereby H_2O_2 showed the fast onset and a transient contraction, O_2^- showed slow onset and a transient contraction, and OH^- showed a sustained contraction (Tosaka *et al.*, 2002). This shows the importance of identifying the types of radical and nonradical species in the pathological mechanisms as each ROS could play a different role.

1.5.6 ROS as a signalling molecule in pressure-dependent myogenic tone

From the study of ROS in cultured cells to vascular tone, the interest of its role in modulating pressure-dependent myogenic tone has been growing. Exogenous H_2O_2 was found to increase myogenic tone in tail arterioles (Nowicki *et al.*, 2001) and mesenteric arteries (Lucchesi *et al.*, 2005). In addition, endogenous ROS (H_2O_2) was produced from Nox after dipheleneiodonium (DPI) and N-acetylcysteine (NAC) treatment, and mice lacking rac1 and $p47^{phox}$ showed inhibited myogenic tone (Nowicki *et al.*, 2001). Another supporting study showed myogenic tone was dependent on mitochondria-derived ROS (H_2O_2) during cold (28°C), which stimulated RhoA/Rho kinase signalling and smooth muscle α_{2C}-adrenoceptors, a mechanism that could be relevant to Raynaud's pathophysiology (Bailey *et al.*, 2005). Although H_2O_2 caused constriction in the study, other studies showed that it could also act as a vasodilator (EDHF) (Matoba *et al.*, 2002, Miura *et al.*, 2003, Drouin *et al.*, 2007). The dual effects of H_2O_2 were also observed in a study by Luchessi *et al.* (2005) where low concentrations of exogenous H_2O_2 caused vasodilation when the K^+ channel was compromised by KCl, and the opposite effect was seen when KCl was removed in pressurized mesenteric arteries. H_2O_2 also exhibits a biphasic effect, causing vasoconstriction at low concentrations and

vasodilation at high concentrations, also possibly mediated via K^+ channels (Cseko *et al.*, 2004). With these observations, it could be possible that in pathophysiological conditions where K^+ channel activity is altered, a transition from the physiological vasodilatory effect of H_2O_2 to a contractile effect may play an important role in increasing peripheral resistance and pathogenesis of hypertension (Cseko *et al.*, 2004). In hamster gracilis muscle, Sk1/S1P was shown to mediate pressure-dependent myogenic tone by stimulating the Rac/Nox/O_2^- pathway (Keller *et al.*, 2006). Inhibition of a specific Nox subunit was shown to reduce pressure-dependent myogenic tone, but it did not affect the $[Ca^{2+}]_i$, which suggested that ROS is playing a modulatory rather than obligatory role in regulation of Ca^{2+} sensitivity (Keller *et al.*, 2006). This observation is very important as Sk1/S1P could be a potential therapeutic target, although there should be a balance for the beneficial formation of O_2^- as a physiological signalling molecule.

Moving on from these physiological studies, the role of ROS has also been investigated in diseased animal models. NOX2-derived O_2^- may contribute to the enhanced myogenic response in renal afferent arterioles in spontaneously hypertensive rats (SHR), but not in normal rats (Ren *et al.*, 2010). According to this study, the role of ROS is complex, because on one hand, increased O_2^- in afferent arterioles could add to hypertension development. But on the other hand, after hypertension is established, O_2^--induced myogenic enhancement could provide protection from glomerular barotrauma and injury in SHRs. In streptozotocin-induced diabetic rats, cerebral myogenic tone was increased in parallel with decreased large conductance BK_{Ca} channel activity and increased H_2O_2 (Dong *et al.*, 2009). Rotenone, an inhibitor of the mitochondrial electron transport chain complex I, partially reversed the myogenic response, H_2O_2 levels and BK_{Ca} effect. This indicates that BK_{Ca} channels may be related to the inhibitory effects of rotenone on ROS (H_2O_2) production and the myogenic tone of diabetic rats (Dong *et al.*, 2009).

The important role of ROS as a signalling molecule in pressure-dependent myogenic tone is indisputable. However, there arises a significant dilemma in determining the borderline of the beneficial and the hazardous effect of ROS. Additionally, ROS

members are highly diverse and able to elicit multiple effects within the same tissue. Paravicini & Sobey (2003) have highlighted the importance of the delicate balance between O_2^- and H_2O_2 mediated by SOD when studying vascular oxidative stress. Therefore, it is essential to understand the exact mechanism categorized in order to determine how ROS can be 'good' or 'bad' signalling molecules.

1.5.7 The role of adventitial-derived ROS in vascular function

Traditionally, vascular wall inflammation has been considered as an 'inside-out' response, where cardiovascular risk factors promote leukocyte accumulation in the lumen, increase ROS production, and the intimal-to-adventitial outward progression of inflammation. Since the past decade, accumulating evidence now supports that the adventitia is a biological centre for various pathological stimuli. A new paradigm of 'outside-in' response became apparent when Pagano's group found that vascular wall inflammation and vascular remodelling was initiated in the adventitia and progressed through the media inward towards the intima (Pagano *et al.*, 1997, Rey and Pagano, 2002, Haurani and Pagano, 2007, Pagano and Gutterman, 2007).

As mentioned previously, the adventitia has been reported as a major source of O_2^- (Pagano *et al.*, 1997). Adventitial fibroblasts are exposed to the matrix protein environment and could be easily activated in response to a variety of potential stimuli such as ANG II, TNF-α, ET-1, hypoxia, stretch and injury (Haurani and Pagano, 2007). For example, ANG II was found to induce $p67^{phox}$ mRNA expression to generate O_2^- in aortic adventitial fibroblasts (Pagano *et al.*, 1998). Therefore, the adventitia has been suggested as the first-responder during early disease development such as hypertension, atherosclerosis, restenosis, and injury. The adventitial pathology is indicated by an increase in adventitial cell number (Arribas *et al.*, 1997, Jimenez-Altayo *et al.*, 2007), thickness (Chazova *et al.*, 1995), proliferation (Chazova *et al.*, 1995) and secretion of paracrine factors (Di Wang *et al.*, 1999), which in the latter lead to the widespread of vascular wall growth, remodelling and inflammation.

Numerous studies have shown that ROS, particularly O_2^- and H_2O_2, serve as second messengers activating a variety of signalling cascades such as in vascular proliferation and vascular remodelling (Chin *et al.,* 2007, Drouin *et al.,* 2007, Terashvili *et al.,* 2006, Miller *et al.,* 2006). Superoxide is not likely a paracrine mediator since its half-life (less than 50 ms) and radius of diffusion is extremely short (less than 40 microns) i.e. only the distance between a few cells (Saran and Bors, 1994). An abundance of evidence in cultured tissue studies have shown H_2O_2 serves as a better paracrine mediator due to its stability and cell permeability (Miura et al., 2003, Matoba et al., 2002). Figure 1.6 shows the signalling pathways in cultured VSM cells whereby Nox-derived H_2O_2 is the paracrine mediator during vascular inflammation.

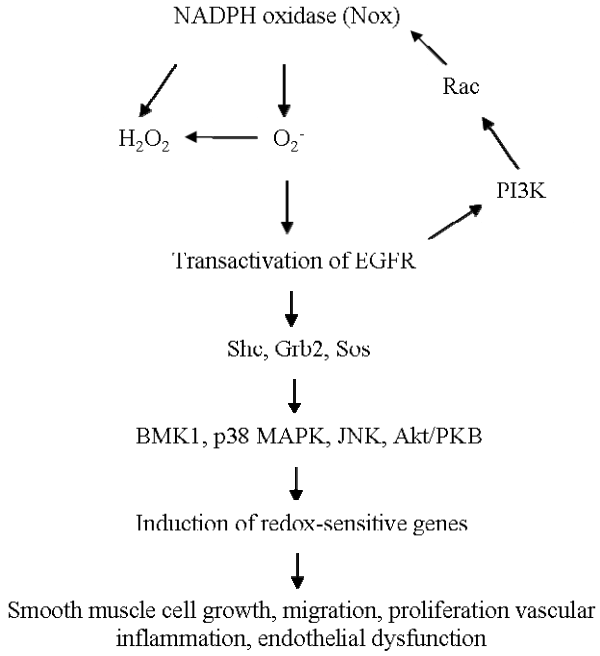

Figure 1.6 The signalling pathways activated by H_2O_2 in cultured vascular smooth muscle. *NADPH oxidase mediated H_20_2/ROS lead to a feed-forward propagation of signalling mechanism, increased ROS production and enhanced medial remodelling. Akt/PKB, Akt/protein kinase B; BMK1, big mitogen-activated protein kinase 1; EGFR, epidermal growth factor receptor; Grb2, growth factor receptor-bound protein 2; JNK, c-Jun n-terminal kinase; p38 MAPK, mitogen-activated protein kinase; PI3K, phosphatidylinositol-3 kinase; Shc, src homology complex; Sos, son-of-sevenless (Csanyi et al., 2009).*

Despite numerous studies suggesting adventitial fibroblast-derived H_2O_2 as a paracrine factor in cultured adventitial cells, little attention has been given to its effect on vascular tonic mechanisms. Di Wang's study suggested that O_2^- plays the paracrine role in ANG II-induced hypertension to mediate spontaneous aortic vascular tone (Di Wang *et al.*, 1999). The study found that enhanced adventitial O_2^- inactivated EDNO which promoted smooth muscle Ca^{2+} influx and dramatically increased spontaneous tone, via the adventitial-endothelium-medial pathway. Another interesting aspect was the finding that LPS-induced NO production from the adventitia was more than from the medial layer and that this adventitial-derived NO could activate guanylyl cyclase and vasodilatation in the rat aorta (Kleschyov *et al.*, 1998). Recently, the adventitia was reported to generate a NO-like compound that may produce paracrine effects and mediate VSM cells function in endothelium denuded rat aortas. Strikingly, removing the adventitia in the carotid artery was found to reduce the VSM cells contractile response to KCl and potentiate endothelium-dependent relaxation, but the reason for such effects was not investigated (Gonzalez *et al.*, 2001). One possible explanation for this result could be that the adventitial/ROS-dependent pathway was inhibited. Thus the lack of ROS increased EDRFs/NO bioavailability and increased endothelium-dependent relaxation (Di Wang *et al.*, 1998). A subsequent study by Gonzalez's group showed that ANG II enhanced NO release in the adventitia cells 10-fold more than the medial layer (Somoza *et al.*, 2005). The mechanism behind this was still unclear, but the authors have suggested a possible cross-talk between the endothelium and adventitia. These data have confirmed that the adventitia exerts a modulatory role on vascular function. There has not been any attempt to study specifically the effect of adventitia and adventitial removal to arterial myogenic tone, thus, this will become the main focus of this thesis.

1.6 PREVIOUS STUDIES ON ACTIN CYTOSKELETON POLYMERIZATION IN MYOGENIC MECHANISM

There are two distinct types of actin-based filamentous systems in contractile smooth muscle cells: the cytoskeleton, which comprises predominantly non-muscle actin (and intermediate filaments) and the actin filaments of the smooth muscle contractile apparatus that interact with smooth muscle myosin (Small and Gimona, 1998). The actin cytoskeleton has generally been considered a non-force generating structure in contractile smooth muscle cells. However, it has been demonstrated that alterations in actin polymerization can directly modulate the contraction of cerebral arteries (Cipolla *et al.*, 2002), tracheal smooth muscle (Mehta and Gunst, 1999) and the guinea pig ileum (Mauss *et al.*, 1989). Smooth muscle cells maintain a relatively large proportion (~30-40%) of total actin in an unpolymerized, globular (G) form. As a consequence, the F:G actin ratio in smooth muscle is on the order of 1:1 or 2:1 (Cipolla *et al.*, 2002). The polymerization/ depolymerization of actin filaments is a dynamic process which is also involved and/or mediates a variety of cell responses including cell survival, proliferation, apoptosis, motility and secretion (Papakonstanti & Stournaras 2008). Actin polymerization occurs at the barbed end of the actin filament, where G actin is added onto existing F actin. Actin depolymerization takes place at the point end of the actin filament (the opposite of barbed end) (Tang and Anfinogenova, 2008). In non-muscle cells, the actin cytoskeleton was shown to respond to mechanical stimuli such as tension with polymerization of G-to-F actin (Moldovan *et al.*, 2000).

1.6.1 Actin cytoskeleton in cultured cells

The trigger for actin cytoskeleton polymerization *in vivo* besides the apparent mechanosensitivity is not fully understood. However, cellular processes in regulating actin cytoskeleton polymerization in cultured non-muscle cells has been studied extensively according to reviews by Tang & Anfinogenova (2008), Gunst & Zhang (2008) and Martinez-Lemus *et al.* (2009). The tyrosine phosphorylation of CAS (Crk-associated substrate), an adhesion protein, is mediated by Abelson tyrosine kinase (Abl), a non receptor tyrosine kinase, following the activation of ANG II

receptors in VSM, which leads to actin filament organization (Takahashi *et al.*, 1998). Integrin-associated membranes such as FAK (focal adhesion kinase) and c-Src regulates actin cytoskeletal by the phosphorylation of a cytoskeletal protein, paxilin, through the Ca^{2+}-insensitive signalling pathway (Tang and Gunst, 2001). Transmembrane integrins, the cell surface receptors, are the key mechanical sensors that communicate with actin cytoskeleton, which can be regulated by FAK, c-Src, paxilin and heat-shock protein (HSP) (Gerthoffer and Gunst, 2001). The Rho family of small GTPases, Rho, Cdc42 and Rac, can also regulate the actin cytoskeleton. It has been shown that Rho mediated agonist-induced actin stress fibre formation in cultured smooth muscle cells via the Rho kinase/LIM kinase/cofilin pathway. Cdc42 together with Rac activates p21-activated kinase (PAK)/p38 MAPK/HSP and finally actin cytoskeleton modulation and cell migration (Gunst and Zhang, 2008). Also, these protein kinases and small GTPases regulate downstream mediators like actin-associated proteins, such as Wiskot-Aldrich Syndrome protein (N-WASP), actin-related protein (Arp2/3 complex), profilin, cofilin and paxilin (Tang and Anfinogenova, 2008).

1.6.2 The role of the actin cytoskeleton in pressure-dependent myogenic tone

Based on the wealth of knowledge from cultured cell studies, the role of the actin cytoskeleton has now become increasingly evident in vascular function, and recently, in pressure-dependent myogenic tone. Actin cytoskeletal disruption in cerebral arteries by cytochalasin D (Cyto D) was shown to inhibit myogenic tone, but not pressure-induced depolarization or the $[Ca^{2+}]_i$ (Gokina and Osol, 2002). Cipolla *et al.* (2002) hypothesized that the mechanism involved is likely via integrin-mediated activation of signalling pathways such as Rho-A, PKC, PLC and tyrosine phosphorylation. These activations will then lead to the stimulation of actin polymerization (increased F:G actin), formation of contractile stress fibres and eventually an increase in VSM force production and decrease in diameter (Cipolla *et al.*, 2002). Another supporting study showed that actin polymerization inhibition by Cyto D and latrunculin B has no effect on global $[Ca^{2+}]_i$ in pressurized rat mesenteric arteries (Shaw *et al.* 2003). This indicates that modulation of the dynamic

equilibrium between the F/G-actin may be an important mechanism, acting independently of global $[Ca^{2+}]_i$ homeostasis, to regulate the smooth muscle contractile state (Shaw *et al*. 2003). This was further confirmed by confocal microscopy where an increase in F-actin staining intensity and a decrease in G-actin staining intensity were observed in mouse tail VSM cells, when transmural pressure was elevated (Flavahan *et al.* 2005). A more recent study that involved genetic modification has found that *Notch3* is an upstream modulator of the RhoA/Rho kinase pathway activation in tail artery myogenic tone (Belin de Chantemele *et al.*, 2008). The study has suggested that FAK and actin filament bundles (stress fibres) are dependent on RhoA activation resulting in actin cytoskeletal organization and integrin complex assembly. Conclusively, *Notch3* is a key receptor in transforming pressure to myogenic tone. Martinez-Lemus's group has recently reviewed the nature of arteriolar remodelling events, which includes the aspects of intact arteriolar contraction and its relation with actin cytoskeletal remodelling, as shown in Figure 1.7 (Martinez-Lemus *et al.* 2009).

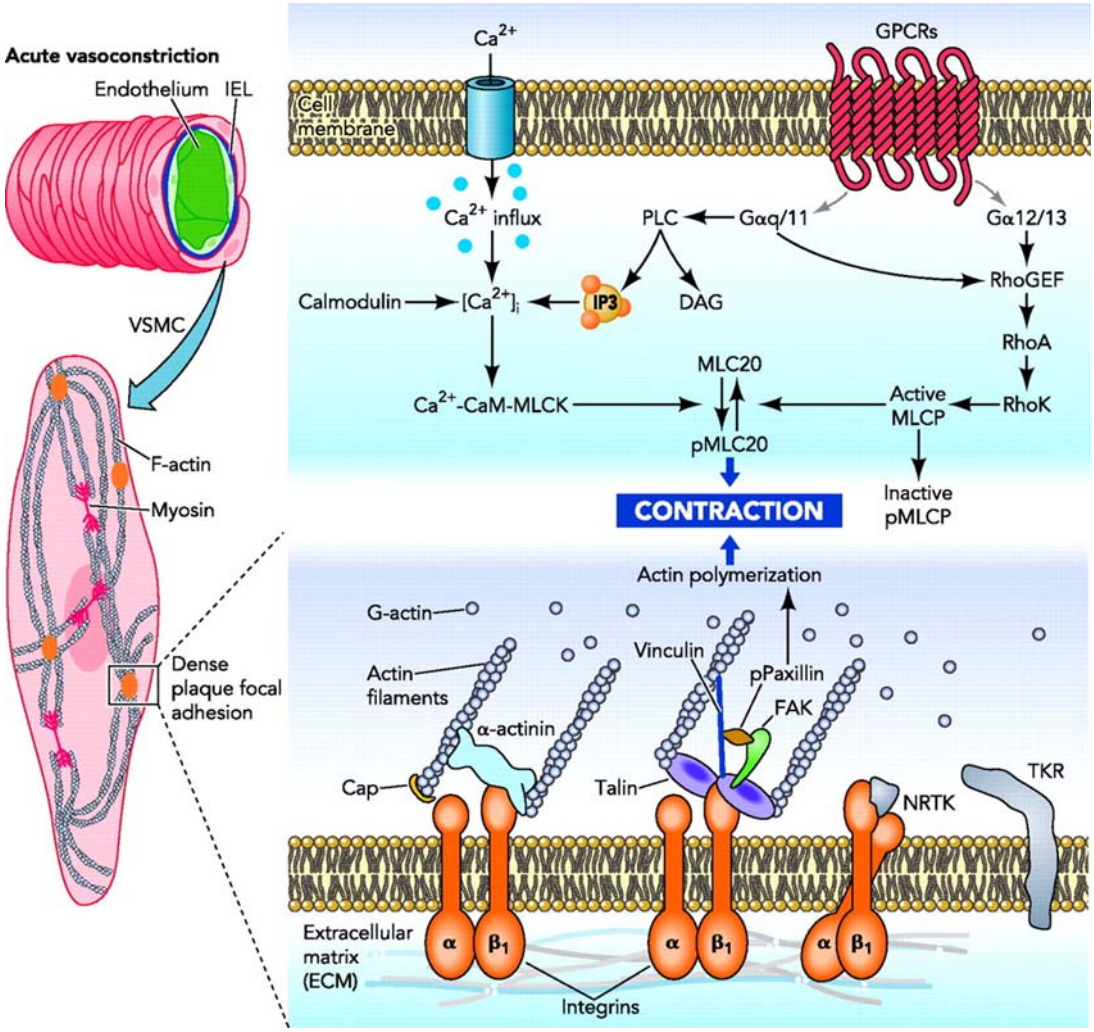

Figure 1.7 Schematic picture of acute vasoconstriction by two different pathways. *The classic pathway via the acto-myosin cross-bridge/$[Ca^{2+}]_i$ (above panel) and the new evolving pathway of actin polymerization within VSM (below panel). The classic Ca^{2+}-dependent myosin light chain (MLC) phosporylation starts as $[Ca^{2+}]i$ is elevated in response to extracellular Ca^{2+} or intracellular Ca^{2+} store depletion caused by IP_3 and PLC-dependent signalling. Cytosolic Ca^{2+} binds calmodulin (CaM) and activates MLC kinase which in turn phosphorylates MLC. The transmembrane protein, G-protein-coupled-receptor (GPCR) is activated by stimuli and trigger the increase of $[Ca^{2+}]i$ and also RhoA/Rho kinase signalling, a Ca^{2+}-independent pathway which inactivates MLCP. On the other hand, G-to-F actin incorporates and strengthens the cytoskeleton. This process requires paxillin, integrins, talin, focal adhesion kinase (FAK), non-receptor tyrosine kinases (NRTK) and tyrosine kinases (TKR) (Martinez-Lemus et al., 2009).*

1.6.3 The interaction between actin cytoskeleton and ROS in myogenic constriction

There has been new evolving evidence on the dynamic role of the actin cytoskeleton and ROS in vascular function, but most of the studies have been in cultured cells (Wesselman and De Mey, 2002, Hu *et al.*, 2005, Touyz *et al.*, 2005b, Moldovan *et al.*, 2006). In VSM cells, ANG II was found to mediate Nox/ROS formation and thus activate p38 MAP kinase and JNK, but not ERK 1/2 (Touyz *et al.*, 2005b). This process involved the actin cytoskeleton as ANG II was shown to promote actin and $p47^{phox}$ interaction (Touyz *et al.*, 2005b). The potential central point of cross-talk between the actin cytoskeleton and $p47^{phox}$ in the pathway was suggested to be via cortactin, a cytoskeletal protein (Touyz *et al.*, 2005a). However, the finding in human VSM cells was not in agreement with the finding in intact pressurized mesenteric arteries, where ANG II-induced contraction (model for vascular remodelling) enhanced ERK1/2 activity (Matrougui *et al.,* 2000). However, it was consistent in these two studies that ANG II-ERK1/2-contraction process required an intact actin cytoskeleton network. The difference in responses to stretch in cultured cell studies compared with intact vessels were discussed by Hill's group (Hill *et al.*, 2000). For instance, cultured cells lose their spindle shape, whereas in intact vessels they are arranged circumferentially and almost perpendicular to the long axis of the vessel. In addition, intact vessels contain a smooth muscle and an endothelial layer, whereas cultured cells contain only a similar type of cell. Nevertheless, these issues require further investigation when comparing the cell culture and intact vessel models. In another study, the stable oxidant $ONOO^-$ was found to result in maximal dilation and diminished myogenic response in cerebral ischaemia models (Maneen *et al.*, 2006). In addition, $ONOO^-$-induced dilation was caused by decreased G-to-F actin cytoskeletal polymerization, thought to be due to direct actin nitrosylation by $ONOO^-$ and eventually loss of myogenic tone (Maneen *et al.*, 2006). Taking this evidence together, more research should be undertaken to investigate whether or not adventitial-derived ROS interacts with the actin cytoskeleton during acute pressure-dependent myogenic tone, as this could help in our understanding of diseased conditions.

1.7 POTENTIAL THERAPEUTIC IMPLICATIONS OF ARTERIAL MYOGENIC TONE

Considering our current knowledge of myogenic tone regulation, an ability to adjust vascular resistance through specific modulation of myogenic mechanism would enable normal neurohormonal mechanisms to interact with the therapeutically treated tone. Therefore, identifying the primary mechanosensors in the initiation of pressure-dependent myogenic tone is essential as these components could be targets for drug development. For example, in situations in which the cardiovascular system is depressed in shock and low-flow states, a drug increasing myogenic tone would be beneficial. On the contrary, in hyperdynamic conditions, reduction of drug-induced myogenic tone would be needed.

The possibility of the adventitia, especially the adventitial fibroblast, being a potential platform for intravascular local drug delivery is very intriguing. Work in the future should focus on understanding ways to control adventitial fibroblast activation, to reduce unwanted changes in vascular structure. As the adventitial fibroblasts contain Nox subunits, the development of specific inhibitors of Nox would provide pharmacological tools to completely elucidate the roles of these isoforms in vascular physiology and pharmacology, particularly, in pressure-dependent myogenic tone. To date, there is only one such compound i.e. plumbagin that has been reported to inhibit Nox/O_2^- production by NOX4 in cultured kidney embryonic cells (Ding *et al.*, 2005). However, this compound was found to be carcinogenic and whether this compound selectively inhibits NOX4 activity or acts merely as a ROS scavenger was not investigated. Rey *et al.,* (2001) designed a Nox inhibitor known as gp91ds-*tat*, which competitively binds to $p47^{phox}$ and prevents the assembly of the enzyme. To date, this peptide has been said to be the most successful Nox inhibitor because of its selectivity. However, it is uncertain if gp91ds-*tat* inhibits other Nox-containing isoforms of Nox, such as NOX1 or NOX4. In conclusion, it is essential to understand the specific Nox subunit source of ROS within the adventitial fibroblasts as it may become a potential therapeutic target in treating vascular diseases.

1.8 STUDY AREA

A preliminary study was conducted in an attempt to confirm that adventitial fibroblasts are the sources of ROS by stripping the adventitia of human skeletal muscle arterioles with CLI (Coats, unpublished data, Gonzalez *et al.,* 2001). A significant amount of ROS was detected under confocal microscopy within the adventitial cells of normal compared to diseased skeletal muscle arterioles. Functional wise, the stripping process was a viable method as it showed no effect on the contractile response. In adventitia-stripped vessels, pressure-dependent myogenic tone was attenuated. Taking the literature review and the unpublished preliminary work together, the main hypothesis of this study was that adventitial-Nox-mediated ROS, facilitated by actin cytoskeleton polymerization, could be an alternative signalling pathway in pressure-dependent myogenic tone. Thus, the main aim of the current thesis was to adapt a successful technique for adventitial removal/ablation and thereafter investigate its effect on the physiology of pressure-dependent myogenic tone in resistance arteries. Specifically, this study will focus on a number of aims as described below:

1. Preliminary experiments on the effect of Nox-derived ROS and actin cytoskeleton polymerization on pressure-dependent myogenic tone. Following that, the possibility of ROS liberation modulating the G/F actin reorganisation within the smooth muscle cells will be investigated (Chapter 3).

2. In order to allow a more in-depth understanding of the adventitial function in pressure-dependent myogenic tone, a technique for adventitial removal will be attempted for the first time in resistance arteries. The success of the adventitial removal technique will be determined by a sufficiently diminished adventitial layer, but with intact smooth muscle, endothelial cells and structural integrity (Chapter 4).

3. Upon establishment of the technique, the direct effect of the adventitia on pressure-dependent myogenic tone and adventitia-derived ROS formation will be investigated. The correlation between non-adventitial-dependent responses and $[Ca^{2+}]_i$ signal during pressurization will also be studied (Chapter 5).

CHAPTER 2:
GENERAL METHODOLOGY

2.1 Tissue Isolation

2.1.1 Rat middle cerebral artery

Adult male Sprague-Dawley rats (12-14 weeks, 250-300g) were killed by cervical dislocation and the brain was removed. The middle cerebral arteries (MCA) originating from circle of Willis (Figure 2.1) were dissected from the surrounding connective tissue and immediately placed in ice-cold Krebs. Then, the arteries were carefully liberated from all adherent tissue under a dissection microscope (WPI Model SSZ 10x/22). Fresh artery segments were used on the same day.

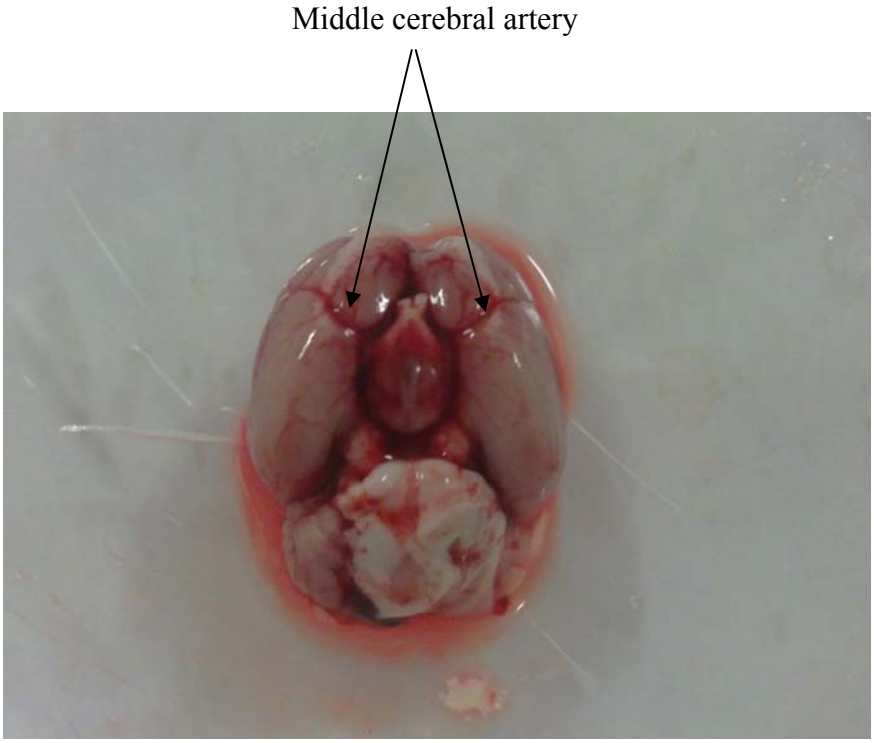

Figure 2.1 Middle cerebral arteries

2.1.2 Rat mesenteric resistance artery

Adult male Sprague-Dawley rats (12 weeks, 250-300g) were killed by cervical dislocation. A 1st-order mesenteric artery was identified from the main branch and followed to the 2nd-order branches, which further divided into the 3rd-order branches. The 2nd-order branches were dissected out and immediately placed in ice-cold Krebs and pinned down on a Sylgard coated block (Figure 2.2). The mesenteric resistance arteries (MRA) were carefully liberated from all adherent tissue and isolated from the mesentery under a dissection microscope (WPI Model SSZ 10x/22). Fresh artery segments were used on the same day.

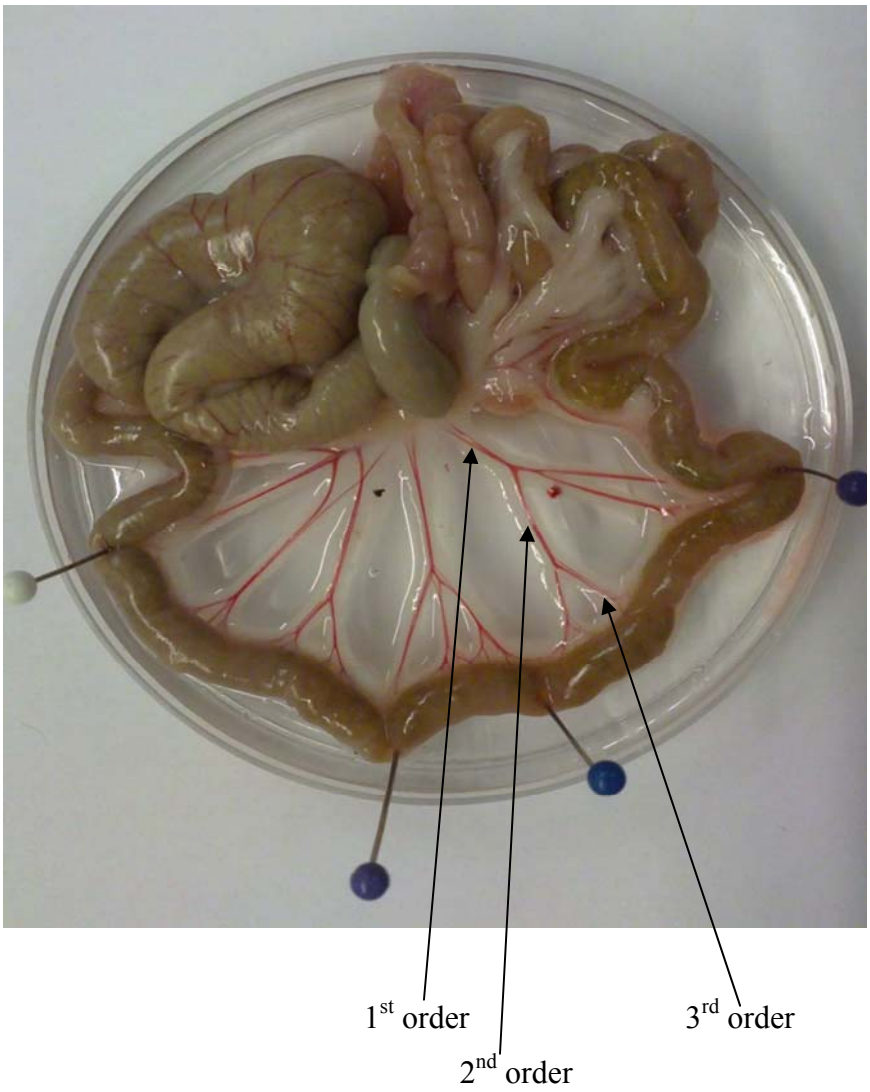

Figure 2.2 Mesenteric resistance arteries

2.2 Krebs solution

Krebs physiological saline solution (PSS) containing (in mM) sodium chloride (NaCl) 119, potassium chloride (KCl) 4.5, sodium bicarbonate ($NaHCO_3$) 25, potassium dihydrogen phosphate (KH_2PO_4) 1.0, magnesium sulphate ($MgSO_4.7H_2O$) 1.0, glucose 11.0 and calcium chloride ($CaCl_2$) 2.5 if needed. Krebs solution was prepared fresh daily.

2.3 Myography Techniques

2.3.1 Wire myography

Segments of 2 mm long arteries were mounted on a DMT Multimyograph model 610P, four-channel wire myograph chamber on two 40 μm diameter stainless steel wires. One jaw is fixed to a micrometer while another jaw is fixed to the force transducer for recording of isometric force generated by the arteries (Myo-Interface Model 410A; Intercept Chart Software). The myograph chamber was filled with 10 ml PSS. The PSS was maintained at 37°C and gassed with carbogen (95% O_2, 5% CO_2; BOC Gases) for the duration of the experiment.

Vessels were normalized to optimal resting tension for vasoconstrictor studies (internal circumference L_1= 0.8 L_{100}) (Mulvany & Halpern 1977). The vessels were stretched stepwise and the relationship between resting tension and internal circumference (L) was then determined. The internal circumference (L) under a transmural pressure of 100 mmHg (L_{100}) was established. The micrometer was adjusted to a circumference equal to 0.8×L_{100}. The isometric tension at this setting is termed as the 'resting force' in the absence of any constrictor tone. The choice of using a circumference of 0.8 L_{100} was used as previous experiments have shown that maximum active tension was generated when small arteries were stretched to a circumference of 0.8 L_{100} (Mulvany & Halpern 1977). This normalized resting tension was determined for each vessel from its own length–tension curve (Figure 2.3).

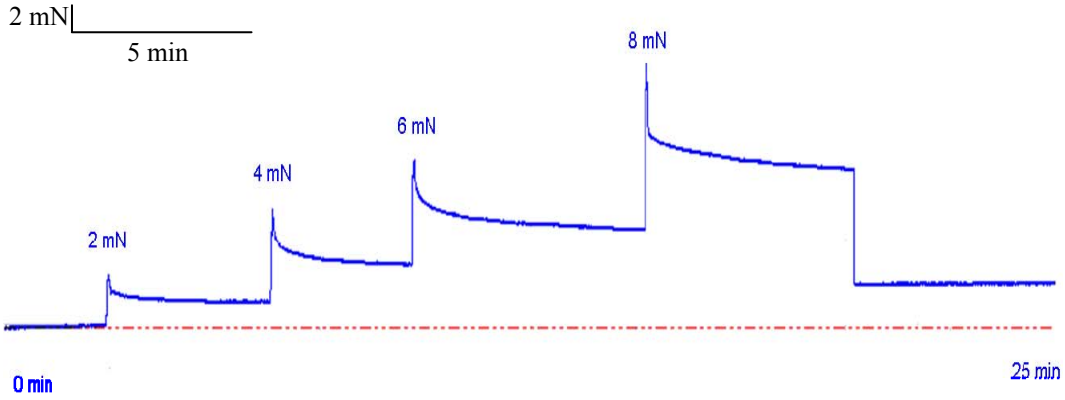

Figure 2.3 Normalization procedure. *A representative tracing of normalization step with four stretches performed at 2, 4, 6 and 8 mN, prior to the equilibrating period of half an hour.*

In attempt to ensure viability and reproducibility of contraction, each vessel was stimulated by 60 mM KPSS (potassium PSS; equimolar substitution of NaCl with KCl) which depolarizes the smooth muscle cells and induces contraction. This procedure was repeated twice at each beginning and conclusion of experiment. Subsequently after 60 mM KPSS stimulation, the arteries were washed and allowed to return to constant tone, dose–response concentration curves with constrictor agonist phenylephrine (PE) were performed. Vessels that achieved 40-50% of PE-induced contraction (10^{-7} M) of maximal KPSS-induced tone were accepted (Heitzer *et al.,* 1999). A time-control was carried out simultaneously within an experiment. Figure 2.4 shows an example of wire myography tracing of a PE's cumulative concentration response curve (CCRC) in a MRA.

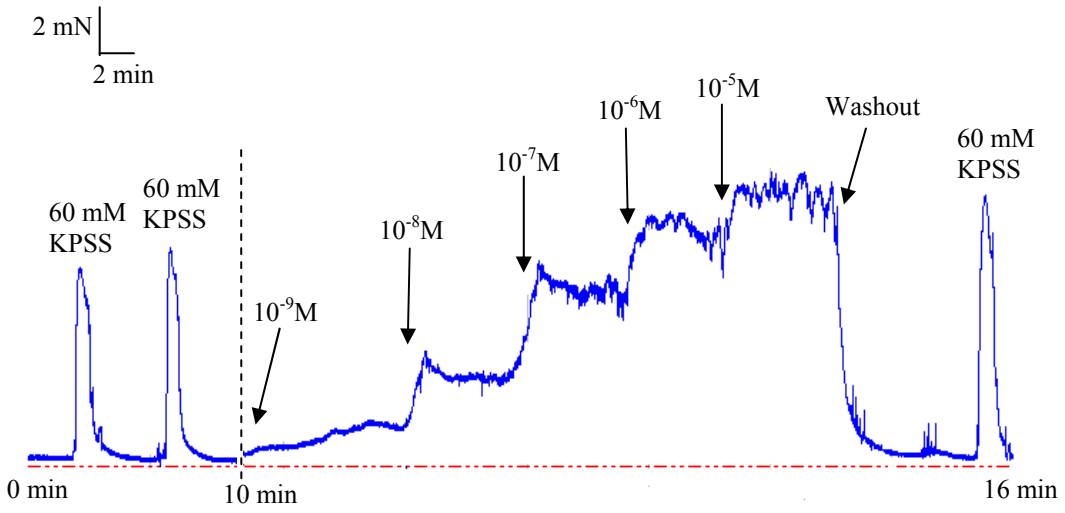

Figure 2.4: An original tracing of phenylephrine (PE) cumulative concentration response curve (CCRC) on a wire myograph. *60 mM high potassium-PSS (KPSS) wash is a standard protocol at the start and conclusion of each experiment to test the viability of a rat mesenteric resistance artery.*

2.3.2 Pressure myography

Isolated arteries were studied on a pressure myograph system (Danish MyoTech P110), cannulated and secured with two fine nylon sutures to hollow glass micro-cannulae (outside diameter ~75 μm) and pressurized with PSS (Figure 2.5 and Figure 2.6). PSS was maintained at 37°C and gassed with 16% O_2/ 5% CO_2 balance N_2 maintaining pH 7.2-7.4. Following mounting, any blood residue was flushed gently at ~5 mmHg through the lumen. Pressure-dependent increases in artery length are referred to as 'buckling' (Coats and Hillier, 1999). The artery was unbuckled by adjusting the cannula attached to a micrometer. All arteries were studied in the absence of flow. Prior to experimental protocols, arteries were equilibrated at an intraluminal pressure of 40 mmHg for one hour (Falloon *et al.,* 1995). Thereafter the artery's external diameter was monitored throughout the experiment. Criteria for viable vessels were (1) no side branches leak on the vessel (2) the development of spontaneous tone during equilibration period (3) an arbitrary level of contraction of >15% from basal diameter after challenged with 60 mM KPSS (4) contractions were reasonably uniform over the entire range of the vessel (Davis et al., 2009, Schofield et al., 2002). Vessels that did not meet these criteria were discarded. Arterial

pressure-dependent myogenic responses were studied at a stepped-pressure of 40 mmHg (below myogenic threshold), 80 mmHg (mid-point) and 120 mmHg (maximum pressure) for a period of 5 min at each pressure step. Any leaked vessel or vessel which failed to show a pressure-dependent myogenic constriction was discarded. At the conclusion of each experiment, Ca^{2+} free PSS (Ca_{free}) containing smooth muscle relaxant papaverine hydrochloride (10^{-4}M) was used to determine the maximum passive diameter. The passive diameter changes in response to changes to intraluminal pressure (40, 80 and 120 mmHg) were obtained. This diameter was used as a reference for other diameters measured during the experiments. Myogenic tone (%) was calculated using the equation:

$$\text{Myogenic tone (\%)} = \frac{(\text{Diameter}_{\text{Ca free}} - \text{Diameter}_{\text{Ca}})}{\text{Diameter}_{\text{Ca free}}} \times 100\ \%$$

Figure 2.7 shows the typical protocol in pressure myograph studies, starting with 60 mM KPSS, followed by pressure-steps in the presence of Ca^{2+} and then by pressure-steps in the absence of Ca^{2+}.

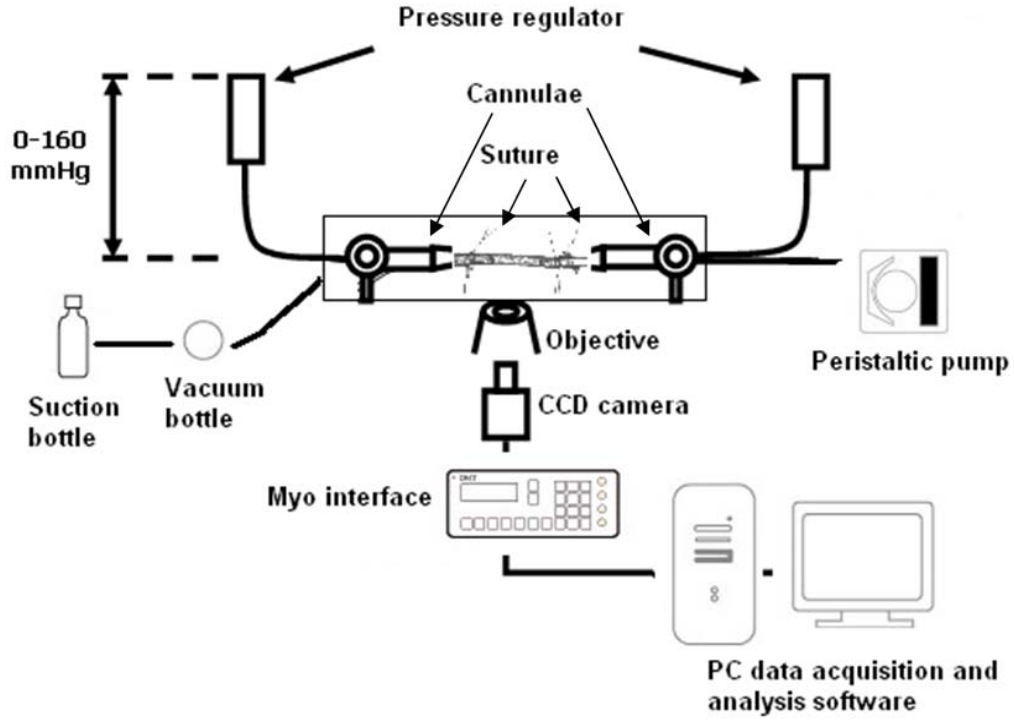

Figure 2.5 A schematic diagram of a pressure myograph set-up. *An intact small vessel is cannulated between two glass cannulae and pressurized to suitable transmural or intraluminal pressure. Pharmacological agents are added to the bath, and the external diameter changes can be readily measured via digital video camera and saved in the computer.*

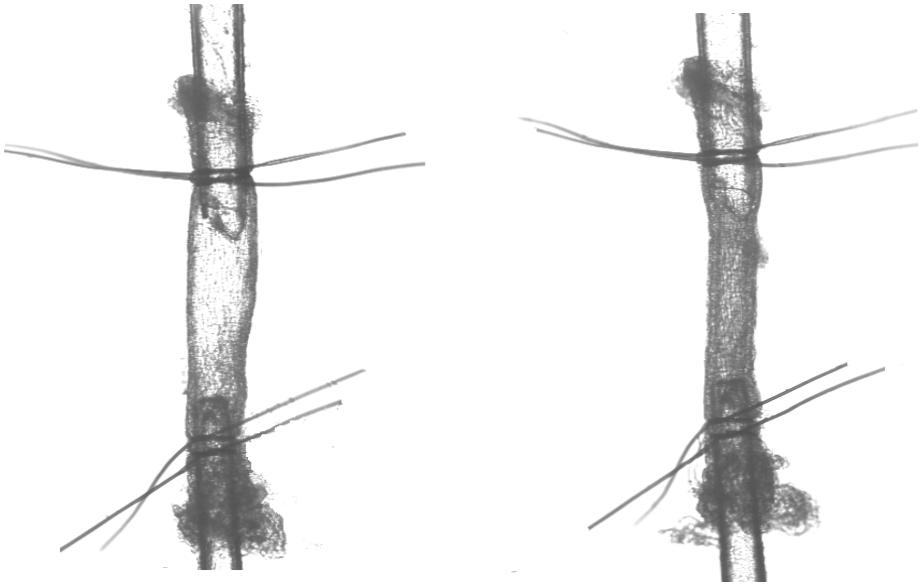

Figure 2.6 Snapshot of a cannulated rat middle cerebral artery (MCA). *The MCA is pressurized at an intraluminal pressure of 40 mmHg (left) and 120 mmHg (right).*

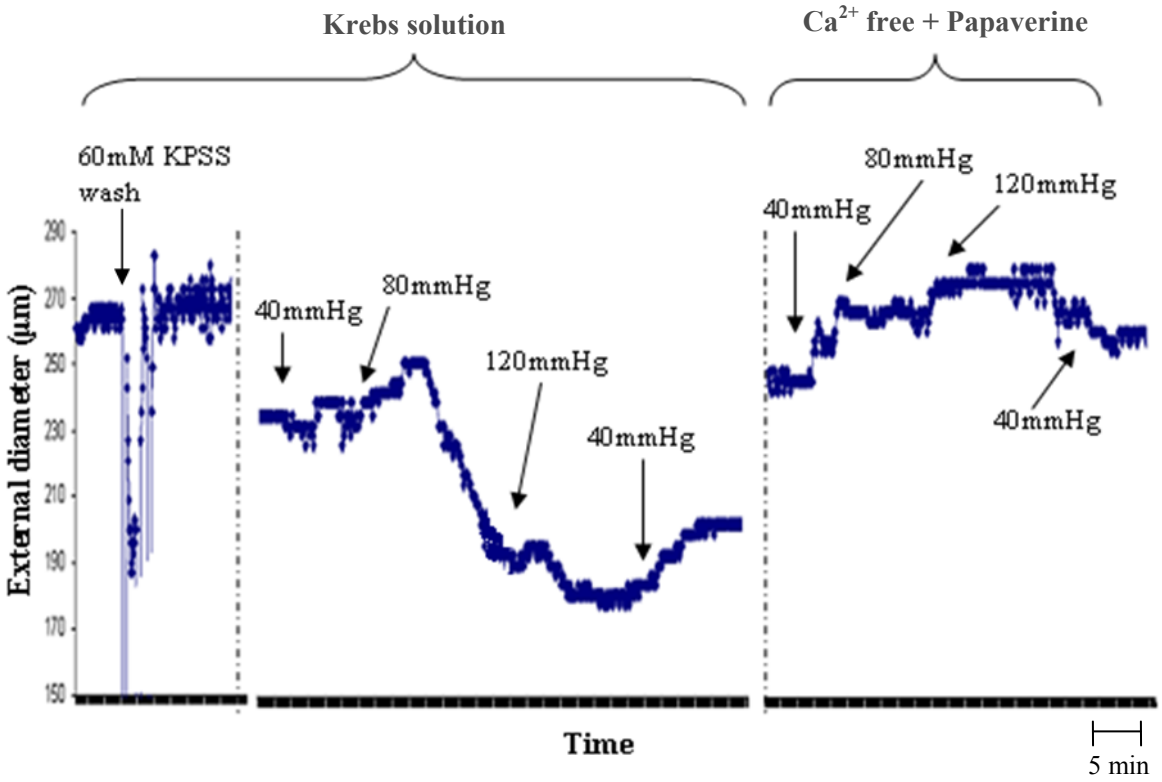

Figure 2.7 A typical representative of an original tracing of a myogenic study. *The study starts with 60 mM KPSS-induced contraction to confirm vessel viability. After equilibration of 45 min-1 hour, a pressure step is conducted (40-80-120-40 mmHg) in presence of Krebs PSS. At the conclusion of each experiment, the Ca^{2+}-containing PSS is replaced by Ca^{2+}-free PSS + papaverine and another set of similar pressure-step will be commenced.*

2.4 Confocal Laser Scanning Microscopy

Vessels were stained with dyes or fluorophores according to the aims of the respective studies before being mounted on a glass slide. The vessels were visualized by Leica True Confocal Scanner for the 5-SpectroPhotometer channels (TCS SP-5), coupled to an upright microscope (DM6000 Leica Microsystems, Germany). The microscope was attached to motorized XY-stage and Z-drive focus on the microscope stand. The setting was equipped with objectives of high-grade corrected Plan Apochromat lens (HC x PL APO, Leica), which were x20 air objective (numerical aperture 0.75) and x40 oil objective (numerical aperture 1.30).

Images were captured with Leica Application Suite Advanced Fluorescence (LAS AF) software (Leica Microsystems, Germany), at a digital optical zoom of 1-6. All images were obtained using a resolution of static image of 1024 x 1024 frame and line averaging of 3 scans. Laser power excitation was generally 25 % for the Argon 488-nm and HeNe 543-nm. Detector gain and amplifier offset were set to optimize the dynamic range of the instrument according to the objective magnification

When images were to be processed for quantification of fluorescence, two vessels from the same animal (control and intervention) were treated and measured at the same time under identical conditions using Volocity (Perkin Elmer, UK).

2.5 Chemiluminescence Study for ROS Measurement

Superoxide anion (O_2^-) production in the arteries was determined through the use of lucigenin-enhanced chemiluminescence (Nishiyama *et al.*, 2003, Miller *et al.*, 2009). Although a study indicated that lucigenin itself could act as a source of O_2^- through auto-oxidation of the lucigenin cation radical (Vasquez-Vivar *et al.*, 1997), however, such auto-oxidation did not occur at less than 100 μmol/L in the rat renal cortex (Attia *et al.*, 2001). Chemiluminescence study of intact vessels was adapted from previous studies (Miller *et al.*, 2007, Miller *et al.*, 2009). The vessel segments were pre-incubated with ANG II (0.1 μM), $NADH^+$ (substrate for NADPH oxidase, 100 μM) and the Cu^{2+}-chelating agent diethyldithiocarbamate DETCA (to inhibit endogenous Cu^{2+}/Zn^{2+} superoxide dismutase [SOD], 10 mM) for 30 min in 37°C Krebs. After incubation, the arteries were transferred into Krebs-HEPES buffer containing ANG II (0.1 μM), $NADH^+$ (100 μM) and lucigenin (5 μM) (Skatchkov *et al.*, 1999) in plastic cuvettes (#367 Chrono-Log Corporation, PA). Luminescence was measured by a luminometer (Sirius, Berthold Detection Systems, Germany) in relative light units per second (RLU/s) for every 20 s for a period of 10 min, with delay measurement for 5 s. Blank was the control, where it was a tissue-free sample containing all drugs as mentioned previously. Measurement of lucigenin was taken at room temperature, as suggested by a previous study (Hyrsl *et al.*, 2004). Figure 2.8 shows the theory underlying the methodology used in this study.

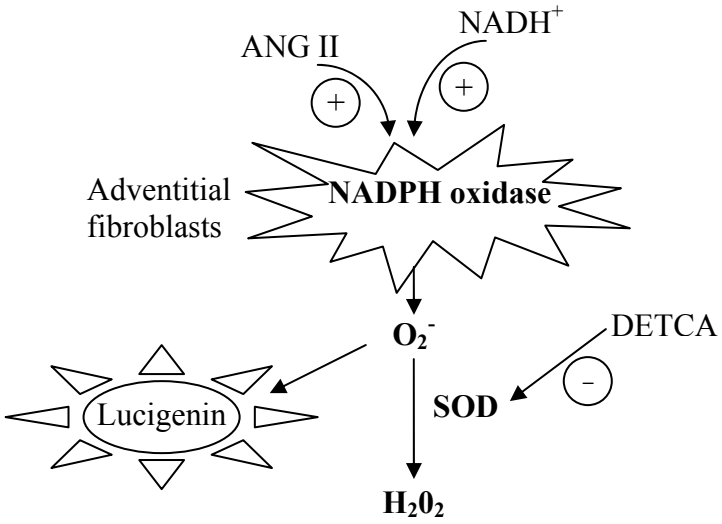

Figure 2.8 The scheme depicts the rationale of the experiment protocol. *Adventitial fibroblasts containing NADPH oxidase (Nox) are stimulated by Angiotensin II (ANG II). $NADH^+$ (NADPH oxidase substrate) drives the capacity for O_2^- production. The immediate reactive oxygen species (ROS) product of Nox is superoxide (O_2^-), which will be detected by lucigenin. However, due to spontaneous and enzymatic dismutation by superoxide dismutase (SOD), O_2^- can be rapidly converted to hydrogen peroxide (H_2O_2). To prevent this reaction, diethyldithiocarbamate (DETCA) was used to inhibit SOD activity so O_2^- level can be maintained for lucigenin-enhanced reading.*

CHAPTER 3:
THE ROLE OF NADPH OXIDASE/ ROS AND ACTIN CYTOSKELETON IN PRESSURE-DEPENDENT MYOGENIC FUNCTION

3.1 Introduction

Following review of pressure-dependent myogenic responses in resistance arteries, there has been considerable progress in our understanding of the sensory apparatus and cellular mechanisms (Hill *et al.*, 2006, Schubert *et al.*, 2008). However, the exact molecular identities of transmural pressure mechanosensors and the underlying mechanisms that lead to myogenic constriction have not been completely elucidated.

Metabolism of oxygen by cells generates potentially detrimental ROS. Under normal conditions the rate and magnitude of oxidant formation and elimination is tightly balanced. However, an imbalance in redox-signalling results in oxidative stress, which is the pathogenic outcome of ROS overproduction. ROS was found to be mainly produced from adventitial Nox (Pagano *et al.*, 1997, Di Wang *et al.*, 1998, Rey and Pagano, 2002), and one of its well-known activators is ANG II (Seshiah *et al.*, 2002, Somoza *et al.*, 2005, Shen *et al.*, 2006, An *et al.*, 2007). The increasing role of ANG II-induced ROS in modulating VSM signalling diseases has been reviewed by many researchers (Harrison *et al.*, 2003, Touyz, 2005, Lyle and Griendling, 2006, Mehta and Griendling, 2007), but its role in the physiology of myogenic tone in resistance arteries is still unclear. Previously, ANG II was shown to induce remodelling with the presence of myogenic tone in cremaster and mesenteric arteries by increasing Nox activity by 356% (Zhou *et al.*, 2005, Martinez-Lemus, 2008). The potential initiation of the ANG II effect is primarily via AT_1R activation, as blockade by the specific AT_1R inhibitor losartan was shown to reduce myogenic tone in cerebral and renal arteries (Mederos y Schnitzler *et al.*, 2008). The mechanism is not fully understood yet, but ANG II has been shown to elicit activation of platelet-derived growth factor β-receptor (PDGF-R) and also ERK1/2, followed by remodelling in pressurized mesenteric artery (Eskildsen-Helmond and Mulvany, 2003). ANG II-induced ROS production was shown to be biphasic in the thoracic aorta, whereby the first phase (30 s) involved stimulation of AT_1R, followed by PKC upregulation and increased Nox-mediated ROS release (Seshiah *et al.*, 2002). During the second phase (30 min), the initial ROS stimulated Src, leading to EGFR transactivation and produced PI3K followed by PIP_3. This PIP_3 in turn

activated rac which would bind to the GTP, producing GTP-bound rac, which then could bind to Nox and lead to a higher amounts of ROS (Seshiah *et al.*, 2002). Taking this evidence together, ANG II will be used as an activator of Nox-mediated ROS. Based on the lack of knowledge of the direct effect of pressure-induced ROS liberated from ANG II/Nox in resistance arteries, this study aims to investigate this matter.

Besides ROS, several lines of studies have implicated that actin cytoskeleton polymerization is a potential regulator in pressure-dependent myogenic tone (Gokina and Osol, 2002, Shaw *et al.*, 2003, Flavahan *et al.*, 2005, Belin de Chantemele *et al.*, 2008). Previous reports suggest that the cytoskeletal processes that occur during the contractile activation of smooth muscle cells may have much in common with the cytoskeletal mechanisms that regulate cell motility and migration (Cipolla *et al.*, 2002, Gunst and Zhang, 2008). A more in-depth mechanistic insight has shown the RhoA-Rho kinase signalling pathway to be a key regulator of dynamic remodelling of the actin cytoskeleton, where RhoA translocation to the plasma membrane within the caveolae activated myogenic tone in mesenteric arteries (Dubroca *et al.*, 2007). Another more recent study by the same group has shown that *Notch3*, expressed in VSM, is required for RhoA activity during pressure-dependent myogenic tone in tail and cerebral arteries (Belin de Chantemele *et al.*, 2008). Also, based on previous reports that actin cytoskeleton polymerization inhibition disrupted the structural organization and reduced the contractile activity (Cipolla *et al.*, 2002, Gokina and Osol, 2002, Shaw *et al.*, 2003, Flavahan *et al.*, 2005), this thesis looked at the role of the actin cytoskeleton in the process of pressure-dependent myogenic tone in resistance arteries.

An interesting relationship between ANG II, ROS and the actin cytoskeleton was reviewed by Touyz *et al.* (2005). In human VSM cells, they found that ANG II stimulated $p47^{phox}$-actin cytoskeleton polymerization and hence VSM contraction (Touyz *et al.*, 2005). This increased ROS activated p38 MAPK and *c*-Jun *n*-terminal kinase (JNK). ANG II has been shown to induce contraction of rat aorta via HSP-27 phosphorylation, an important regulator of actin polymerization. This response was

dependent on activation of p38 MAPK by AT_1R and production of ROS (Meloche *et al.*, 2000). This has clearly shown that the cytoskeleton may be the central point of crosstalk in growth and redox signalling by ANG II, which may be important in VSM function. However, no study has been undertaken on intact arteries to prove the acute interaction of Nox/ ROS and actin cytoskeleton in the regulation of pressure-dependent myogenic tone, which has now become the interest of study in this thesis.

3.2 Aims

1. To investigate the potential role of Nox-derived ROS in the mechanism of pressure-dependent myogenic tone
2. To investigate the possibility of ROS modulation of G-F actin as part of the mechanisms recruited during pressure-dependent myogenic tone

3.3. Methods

3.3.1 Tissue isolation

(a) Rat middle cerebral artery

The basic methodology used has been described in detail in Section 2.1.1. Briefly, adult Sprague-Dawley rats were humanely killed and the middle cerebral arteries (MCA) were dissected. Criteria of the Sprague-Dawley rat specifics were noted in Table 3.1.

(b) Rat mesenteric artery

The basic methodology used has been described in detail in Section 2.1.2. Briefly, adult Sprague-Dawley rats were humanely killed and the 2nd-order branches (from the main mesenteric artery branch, MRA) were dissected. Criteria of the Sprague-Dawley rat specifics were noted as in Table 3.1.

	MCA	MRA
Sex	Male	Male
Weight	270-300g	270-300g
Age	12-14 weeks	12-14 weeks
External diameter	170 ± 2.81 μm	256 ± 8.74 μm
N	46	8

Table 3.1 Animal study details. *The sex, weight, age of rats and external diameter specifics of rat middle cerebral arteries (MCA) and mesenteric resistance arteries (MRA) used in the experiments.*

3.3.2 The effect of NADPH oxidase (Nox)-derived ROS and the actin cytoskeleton on pressure-dependent myogenic tone

The protocol for setting up a pressure myography experiment has been described in detail in Section 2.3.2. In brief, the isolated arteries were cannulated on a pressure myograph system (Danish MyoTech P110) and filled with PSS (37°C, gassed with 16% O_2/ 5% CO_2 balance N_2, pH 7.2-7.4, no flow). After equilibration (1 hour), a control was determined at stepped increases in pressure (e.g. 40 to 80 to 120 mmHg) for a period of 5 min each, followed by an intervention experiment. The vessel's external diameter changes were measured throughout the experiment.

For time-control studies, different cycles of pressure curves for each experiment were conducted on the same segment of artery. A study with DMSO as vehicle control was also carried out.

Powerful antioxidant NAC (10 mM) or Nox inhibitor DPI (10 μM) or actin polymerization inhibitor Cyto D (5 μM) was incubated in the bath for one hour before another pressure-step response was commenced. These artery segments with different interventions were from different animals.

Angiotensin II (ANG II, 10^{-9} M), a Nox activator, was incubated for 2 hours in attempt to increase Nox-mediated ROS and the effect on pressure-induced myogenic tone was measured. Following this, treatment with NAC 10 mM for one hour in the presence of ANG II was completed to scavenge the free radicals before another repeat of the pressure steps (40-80-120 mmHg).

Ca^{2+} free PSS (Ca_{free}) containing smooth muscle relaxant papaverine hydrochloride (10^{-4} M) was replaced with PSS at the end of each experiment, in order to determine the total of myogenic tone based on the formula shown in Section 2.3.2.

3.3.3 Chemiluminescence study for ROS measurement

Firstly, confirmation of the superoxide (O_2^-) signal being detected by lucigenin-enhanced chemiluminescence was established. Xanthine (10^{-5} M)/ xanthine oxidase (2.5 mU) reaction was used to generate O_2^- signal, which was then quenched by superoxide dismutase (SOD).

Chemiluminescence method was described in Section 2.5. In brief, the O_2^- produced from the MCA and MRA was measured by lucigenin-enhanced chemiluminescence. The vessel segments were pre-incubated with ANG II (0.1 μM), $NADH^+$ (substrate for Nox, 100 μM) and diethyldithiocarbamate DETCA (SOD inhibitor, 10 mM) and also SOD (200 U/ml) for 30 min in 37°C Krebs. Then, the arteries were transferred into Krebs-HEPES buffer containing ANG II (0.1 μM), $NADH^+$ (100 μM) and lucigenin (5 μM) in plastic cuvettes. Luminescence was measured in relative light unit per second (RLU/s) for every 20 s for a period of 10 min (delay measurement = 5 s) by a luminometer (Sirius, Germany).

3.3.4 Actin cytoskeletal polymerization imaging by confocal microscopy

MCAs were mounted in the pressure myograph (Danish MyoTech P110). Individual vessels were pressurized to 40 and 120 mmHg. Intervention study was by adding Cyto D (5 μM), an actin polymerization inhibitor, for 1 hour in the bath. Then, the MCA segments were fixed in phosphate buffered formaldehyde (10 %, 1 hour), rinsed with PSS, followed by permeabilization with 0.5 % Triton X-100 (15 min) and rinsed again with PSS. Following which MCAs were removed from the cannulae and incubated with 1 μM phalloidin-FITC in a 1.5 ml eppendorf tube for 2 hours in the dark. After rinsing with PSS, the vessels were counterstained with propidium iodide (PI) (1 mg/ml, 1 hour, dark) before mounting on a glass slide. The now stained MCAs were visualized using a Leica TCS SP-5 laser scanning confocal system with x20 air objective (N/A 0.75, Leica) and x40 oil objective (N/A 1.30, Leica), as described in Section 2.4. Optical slices for the *z* stacks were at 147.5 μm in depth, 5.46 μm in stepsize and 28 in *z* steps. The volumetric pixel (voxel) width was 756.8nm. The emission spectral range was 480-549 nm for phalloidin-FITC and 602-679 nm for PI.

The F-actin green fluorescence intensity for individual VSM cell was analyzed quantitatively (Maneen *et al.,* 2006, Touyz *et al.,* 2005). Tissue samples were visualized through the *z stack* slices, and the VSM cells with the most complete and widest transverse profile was selected. Once a profile was selected, the region of interest (ROI) was highlighted and quantified by Volocity software (Perkin Elmer, UK). One profile was selected for each sample, where 20-25 VSM cells were examined for each profile. At this point, the red fluorescence channel for nuclei staining was turned off to avoid overlapped quantification. The F-actin fluorescence pixel intensity per square micrometer (μm^2) was measured for each profile. Data was expressed in total fluorescence intensity (arbitrary unit) from the mean of pixel intensity per μm^2 in each profile from different animals. To achieve consistency in sampling technique, paired samples were taken from the same *n* animal (control vs. intervention) and given similar simultaneous treatment.

3.3.5 Drugs and chemicals

Angiotensin II (ANG II), diphenyleneiodonium (DPI), N-acetyl-l-cysteine (NAC), cytochalasin D (Cyto D), β-nicotinamide adenine dinucleotide (NADH), N,N′-dimethyl-9,9′-biacridinium dinitrate (lucigenin), diethyldithiocarbamate (DETCA), propidium iodide (PI), papaverine hydrochloride were purchased from Sigma, UK. Potassium chloride (KCl) was purchased from BDH, Poole, England and phalloidin-FITC was from Invitrogen. All the drugs were dissolved in distilled water (dH_2O), except for DPI, Cyto D and lucigenin which were in dimethyl sulfoxide (DMSO) (final bath concentration ≤ 0.1 %) and $NADH^+$ in 0.01 M NaOH. All of the drugs were stored in aliquots at -20°C in 10^{-2} M stocks. Only $NADH^+$, lucigenin and papaverine were prepared fresh before each experiment. Aliquots were thawed before use and diluted with Krebs physiological saline solution (PSS) which was prepared fresh daily. For the chemiluminescence study, modified Krebs-HEPES buffer was used with the following composition (in mM): 118 NaCl, 5 KCl, 1.1 $MgSO_4$, 2.5 $CaCl_2$, 1.2 KH_2PO_4, 25 $NaHCO_3$, 10 HEPES, 10 glucose, also prepared freshly.

3.3.6 Statistical analysis

Contraction data to vasoconstrictor agonists is represented as percentage contraction relative to the maximum contraction evoked by 60 mM KPSS. Statistical analysis of the data was performed using Microsoft Excel 2003 and GraphPad Prism version 4. Statistical analyses were performed by two-way ANOVA for repeated measure or paired Student's t-test. Significance was assumed if $p<0.05$. Data are expressed as means ± standard error of the mean (SEM). *n* is the number of animals studied.

3.4 Results

3.4.1 Control experiments for pressure-dependent myogenic tone

Before starting any intervention experiments, a number of control experiments were conducted for the purpose of validition. The MCA had an outer diameter of 170 ± 3 μm (*n*=44) when placed under transmural pressure of 40 mmHg. After a 60-min period of equilibration at 40 mmHg, MCA spontaneously reduced their diameter by 25.6 ± 2.3% when compared with the initial diameter during the equilibration period.

Figure 3.1a shows the typical pressure-diameter pattern in response to stepwise increases from 40-80-120 mmHg. Removal of Ca^{2+} from the PSS revealed the degree of active pressure-dependent tone (Figure 3.1a), the net difference of the diameter change response in Ca^{2+} and Ca^{2+}-free PSS was defined as pressure-dependent myogenic tone (Figure 3.1b).

For time control experiments, a sustained pressure-dependent myogenic tone was shown even after 3 cycles of pressure-steps (Figure 3.2). Therefore, it is valid to assume that any effects seen in further experiments are due to the presence of agonists or inhibitors.

DMSO as a vehicle control was tested to see if it had any effect on myogenic tone. Figure 3.3a shows the relations of diameter-pressure of MCA in PSS, PSS + DMSO and Ca^{2+}-free PSS. Although the results showed that DMSO slightly increased myogenic tone in Figure 3.3b, it was not significant. In fact, the increased tone which was similar to the second cycle pattern in the time control (Figure 3.2) confirming that DMSO has no effect and can be used as a vehicle.

(a)

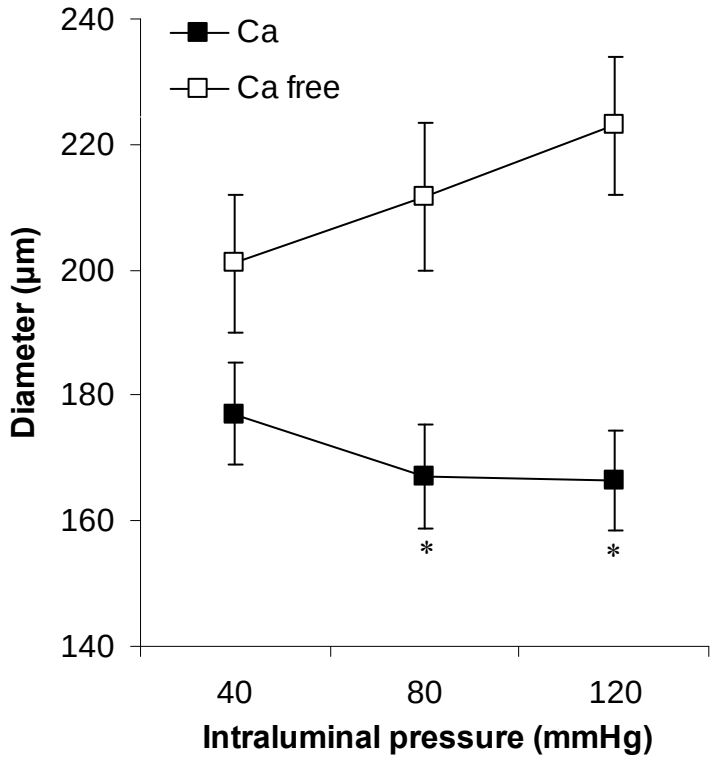

(b)

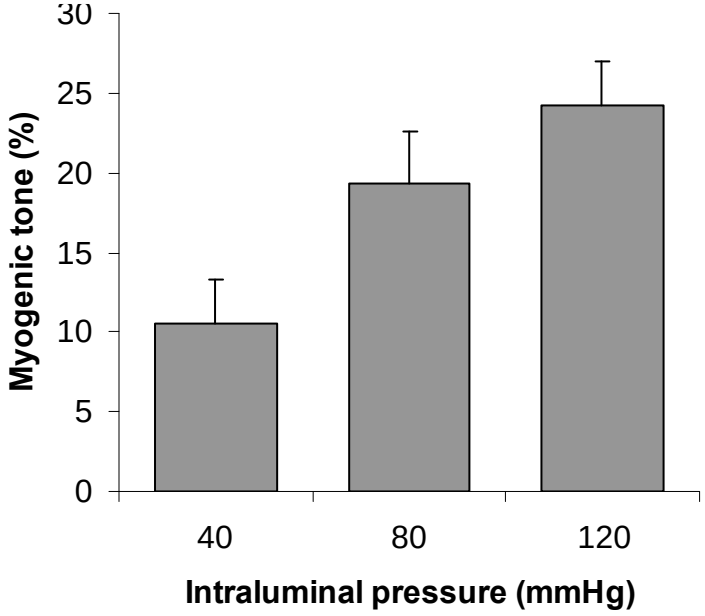

Figure 3.1 Pressure-dependent myogenic tone. ***(a)*** *Responses to increasing pressure-step in MCA in Ca^{2+}-containing and Ca^{2+}-free PSS in presence of papaverine (10^{-4} M) (*p<0.05 vs. Ca^{2+} free).* ***(b)*** *The myogenic tone responses at each pressure-step in Ca^{2+}-containing and Ca^{2+}-free PSS. Statistical evaluation was by ANOVA for repeated measure and Bonferroni post hoc. Values are means ± SEM (n=16).*

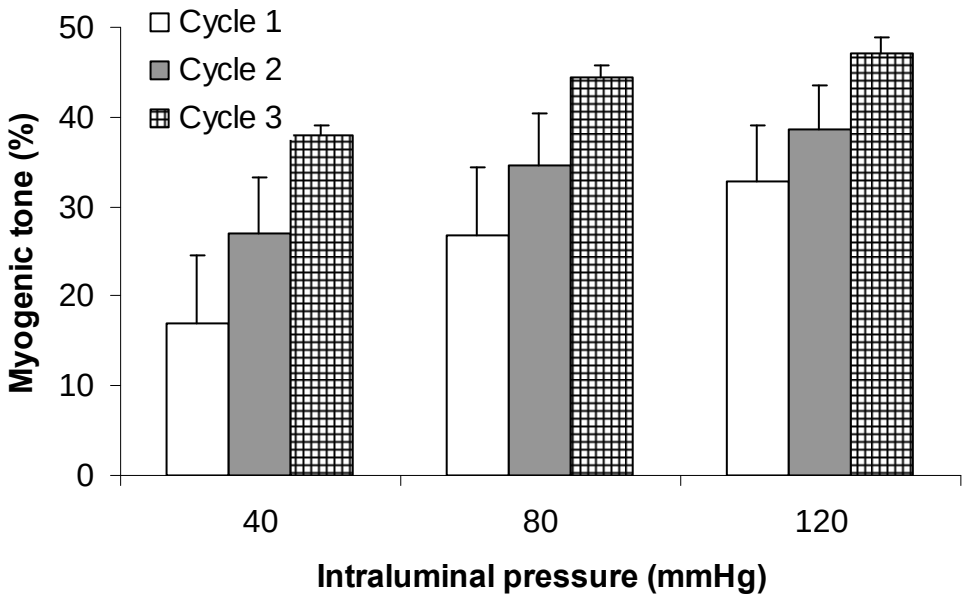

Figure 3.2 Time-control experiment. *Three cycles of pressure steps of 40-80-120 mmHg with one hour gap between each cycle in MCA. Results were expressed as percentage of the maximum dilatation in Ca^{2+}-free PSS plus papaverine (10^{-4} M). Values are means ± SEM (n=3).*

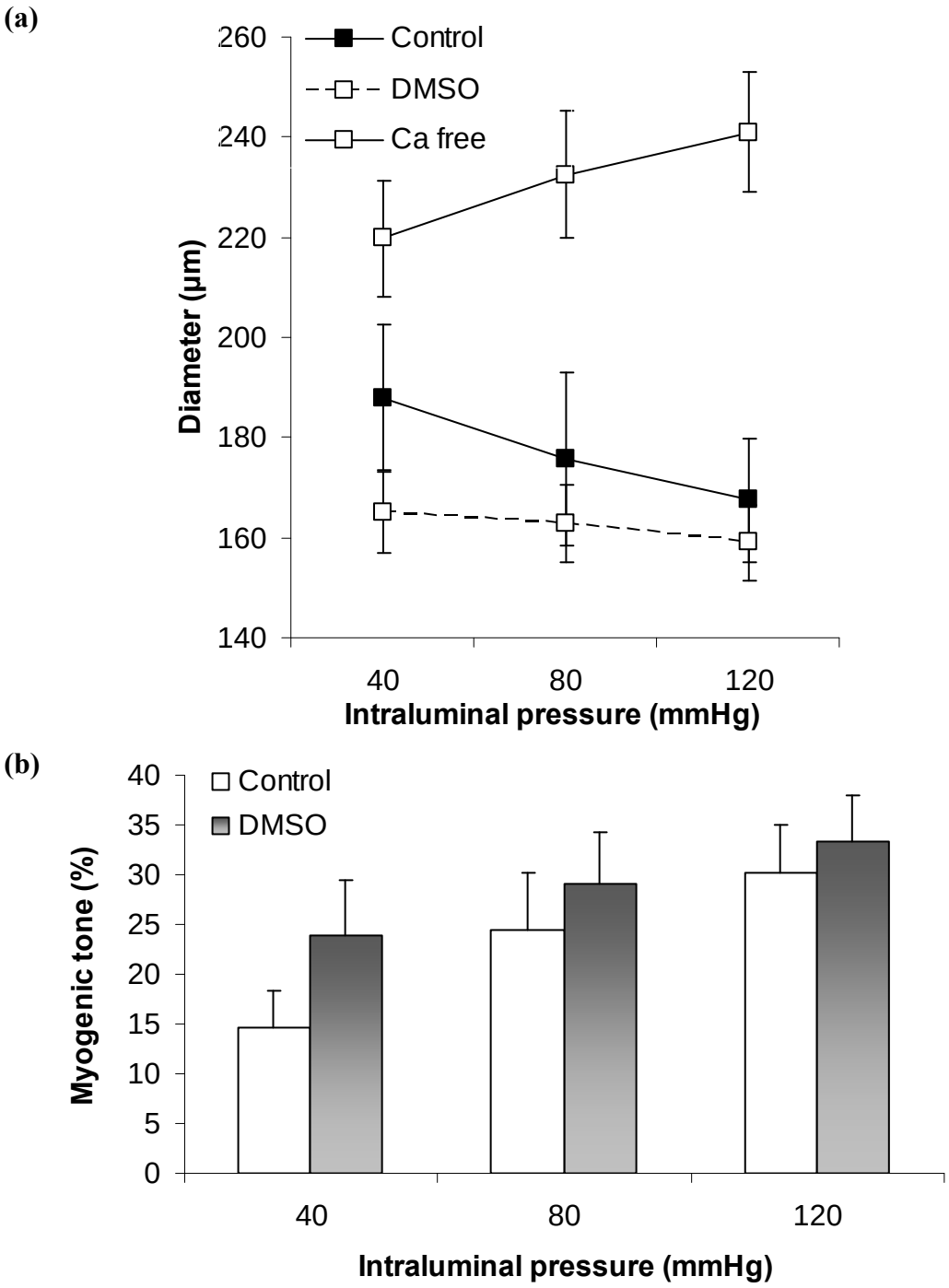

Figure 3.3 Vehicle control experiment (a) *Effect of DMSO as a vehicle control on the MCA's pressure-diameter relationship* ***(b)*** *Myogenic tone of control and DMSO at every pressure-step. Results were expressed as percentage of the maximum dilatation in Ca^{2+}-free PSS plus papaverine (10^{-4} M). Statistical evaluation was by ANOVA for repeated measure and Bonferroni post hoc. Values are means ± SEM (n=4).*

3.4.2 Effect of the antioxidant NAC and the Nox inhibitor DPI on pressure-dependent myogenic tone

NAC (10 mM), an antioxidant, was incubated in the bath to investigate the effect of ROS-scavenging on pressure-dependent myogenic tone. NAC significantly inhibited pressure-dependent tone from 21.8 ± 5.3% to 7.2 ± 5.3% (at 80 mmHg) and from 25.7 % to 7.6 ± 5.2% (at 120 mmHg) ($p<0.05$) (Figure 3.4a and b).

Considering the effect of NAC and the potential source of ROS being Nox, the effect of the Nox inhibitor diphenyleneiodonium, DPI, was measured. Pressure-dependent myogenic responses in the presence of DPI were significantly reduced ($p<0.05$) and completely abolished at 120 mmHg (1.0 ± 2.3 %) compared to the control (Figure 3.5a and b).

Both NAC and DPI showed no difference to 60 mM KPSS-induced contraction compared to control (Figure 3.6a and b).

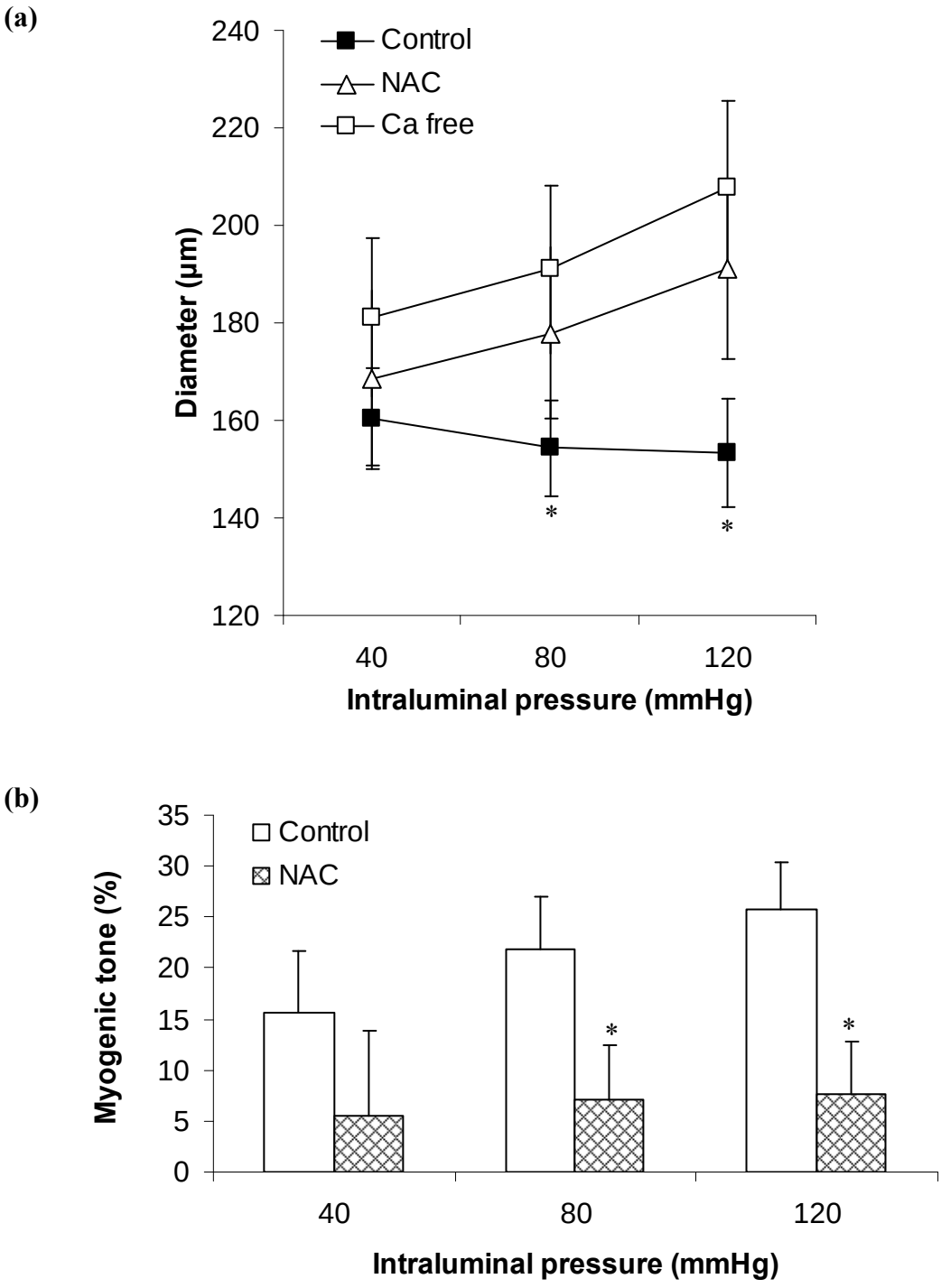

Figure 3.4 The effect of antioxidant NAC (a) *The relation of control, NAC (10 mM) and Ca^{2+} free on pressure-diameter relationship (*p<0.05 vs. Ca^{2+} free) and* ***(b)*** *myogenic tone (*p<0.05 vs. control at 80 and 120 mmHg) in MCA. Statistical evaluation was by ANOVA for repeated measure and Bonferroni post hoc. Values are means ± SEM (n=5).*

(a)

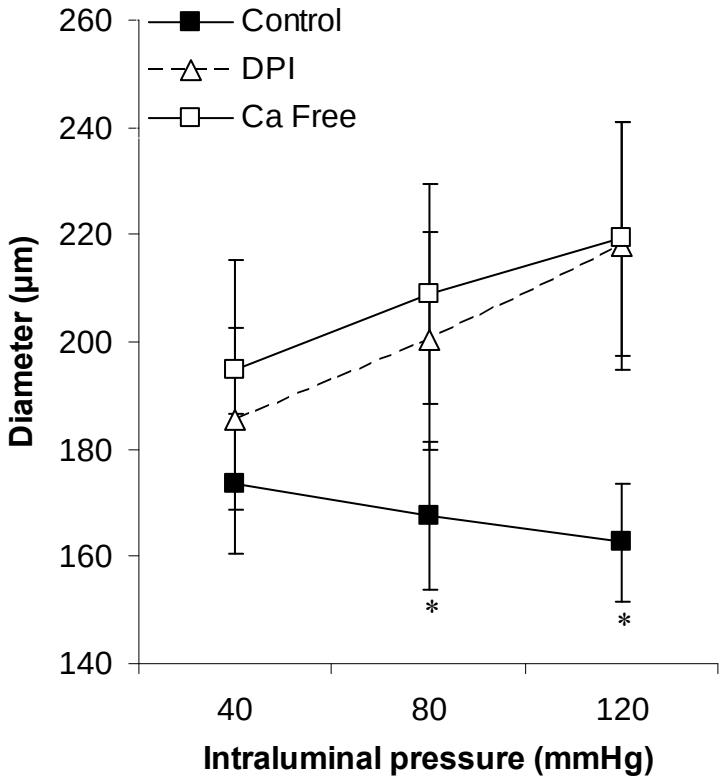

(b)

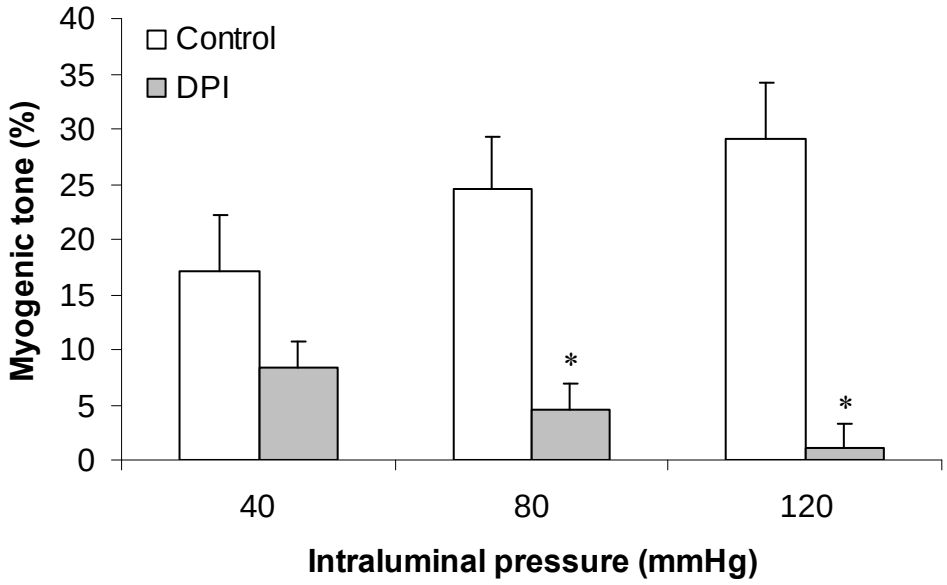

Figure 3.5 The effect of Nox inhibitor DPI (a) *The relation of control, DPI (10 µM) and Ca^{2+} free on pressure-diameter relationship ($p<0.05$ vs. Ca^{2+} free) and* ***(b)*** *myogenic tone (*$p<0.05$ vs. control at 80 and 120 mmHg) in MCA. Statistical evaluation was by ANOVA for repeated measure and Bonferroni post hoc. Values are means ± SEM (n=6).*

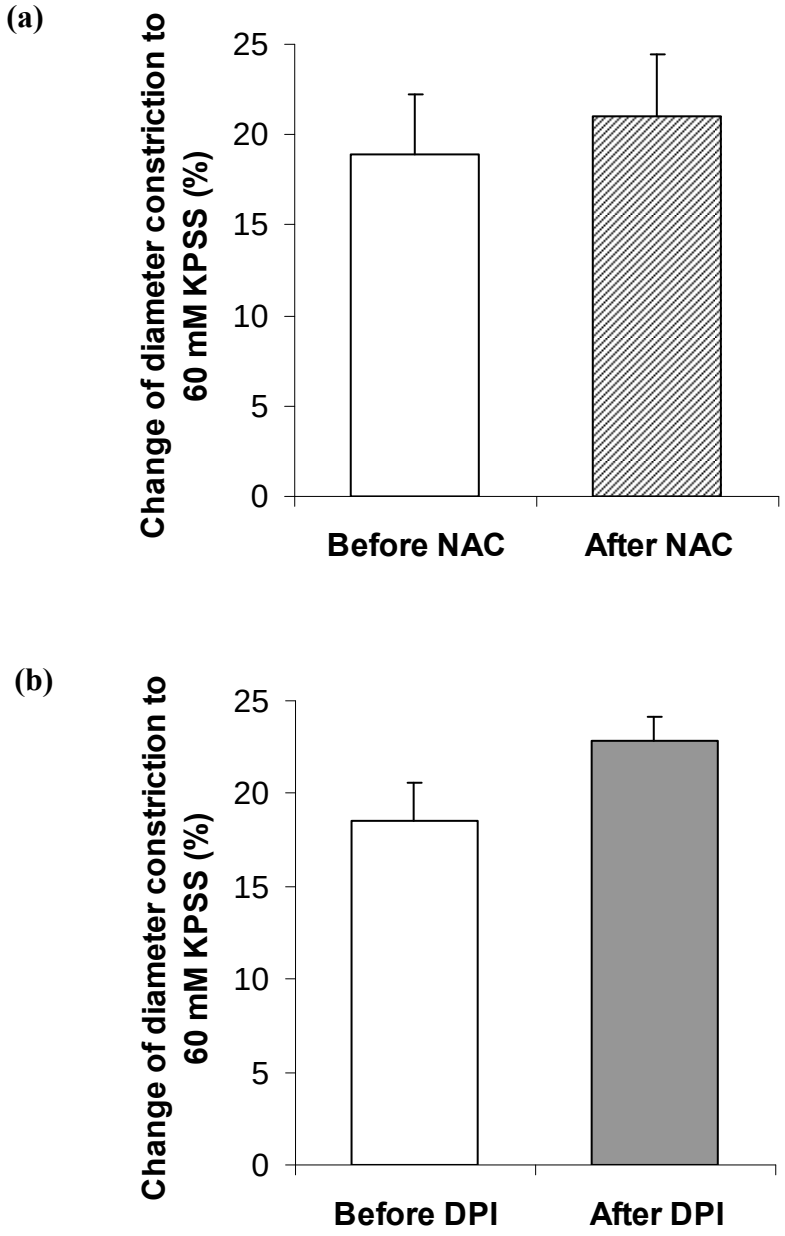

Figure 3.6 Diameter changes to 60 mM KPSS before and after treatment with NAC or DPI (a) *NAC (n=5) and* ***(b)*** *DPI (n=6) showed no effect on 60 mM KPSS wash in MCA.*

3.4.3 The role of the Nox activator ANG II in pressure-dependent myogenic tone response

Concentration curve response (CRC) to ANG II (10^{-12}-10^{-7} M) was carried out (Figure 3.7). ANG II at 10^{-9} M (producing ~20% increase in tone) was chosen as the concentration for incubation experiments (Smith *et al.,* 1999; Ballew *et al.* 2001; Hsu *et el.,* 2004). ANG II has been demonstrated to stimulate Nox to produce ROS (Griendling and Ushio-Fukai, 2000). Therefore, the effect of ANG II-induced ROS scavenging by NAC (10 mM) on pressure-dependent myogenic tone was investigated. The results showed that ANG II caused a sustained pressure-dependent myogenic tone similar to the control (Figure 3.8a). ANG II + NAC treatment had significantly reduced the pressure-dependent myogenic tone at 80 and 120 mmHg (Figure 3.8b), as shown in previous study (Coats and Wadsworth, 2004).

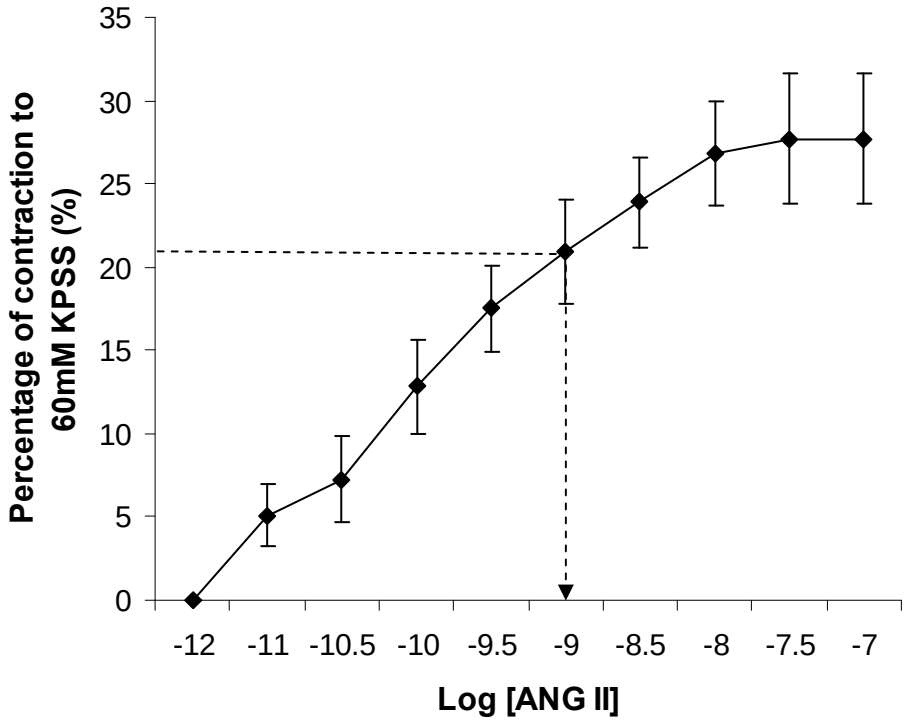

Figure 3.7 Concentration response curve to ANG II *(10^{-12}-10^{-7} M) was commenced in pressurized MCA (40 mmHg) Values are means ± SEM (n=3).*

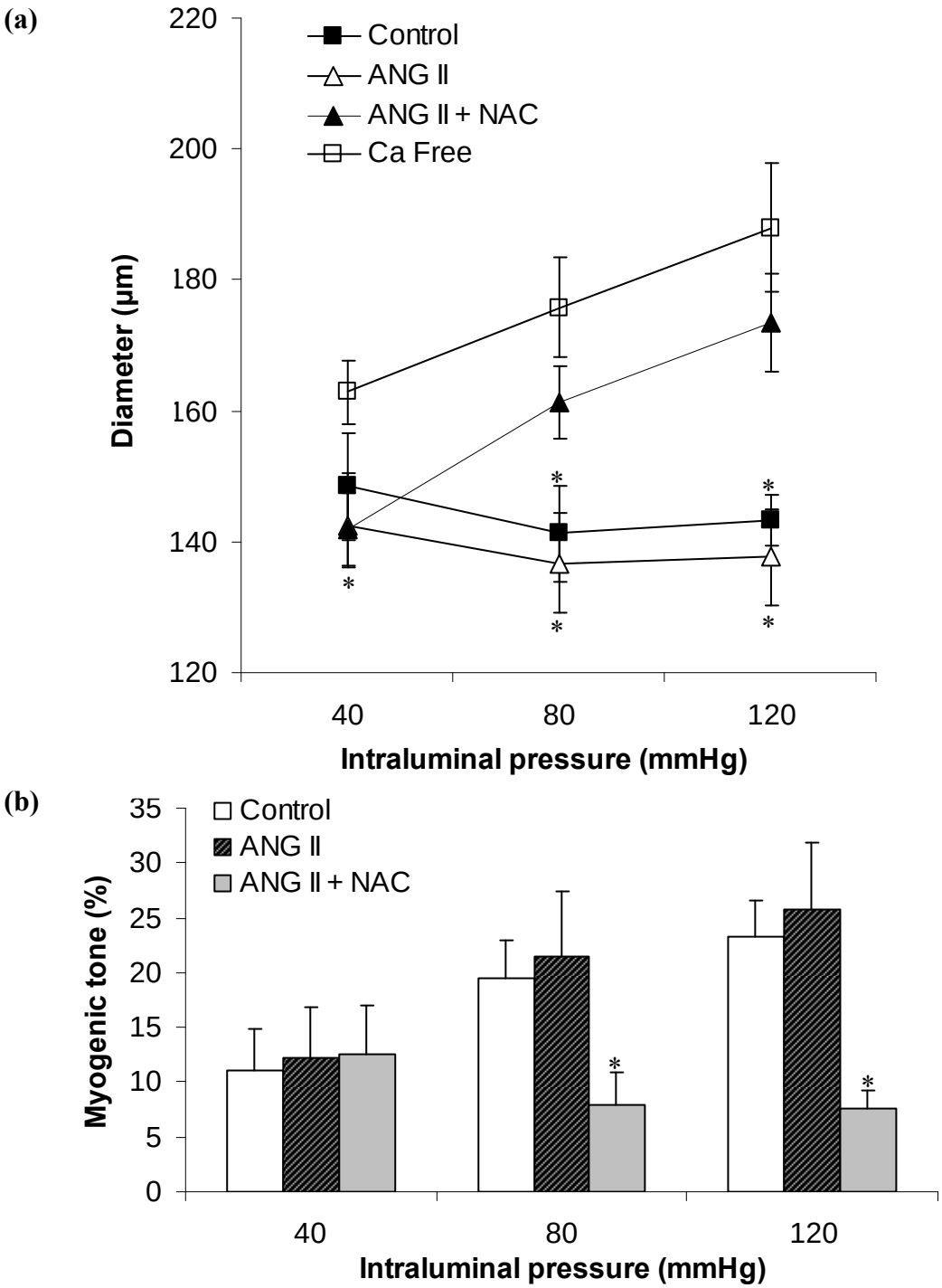

Figure 3.8 The effect of ANG II-upregulated ROS (a) *The relation of control, Nox/ ROS upregulator ANG II (10^{-9} M), antioxidant NAC (10 mM) and Ca^{2+} free on pressure-diameter relationship (*p<0.05 vs. Ca^{2+} free) and* ***(b)*** *myogenic tone in MCA (*p<0.05 vs. control at 80 and 120 mmHg). Statistical evaluation was by ANOVA for repeated measure and Bonferroni post hoc. Values are means ± SEM. (n=4, respectively).*

3.4.4 Effect of inhibitors of actin polymerization on pressurized constriction

The MCA showed a typical myogenic constriction with elevation of intraluminal pressure from 40 to 80 to 120 mmHg. Actin polymerization inhibition with Cyto D (5 μM) abolished pressure-dependent myogenic tone significantly at 40 mmHg (9.5 ± 4.3 %), 80 mmHg (3.8 ± 0.7 %) and to near complete abolishment at 120 mmHg (1.8 ± 0.5 %) (Figure 3.9). However, Cyto D was shown to abolish the 60 mM KPSS contraction response significantly, suggesting that its effect was not specific (Figure 3.10).

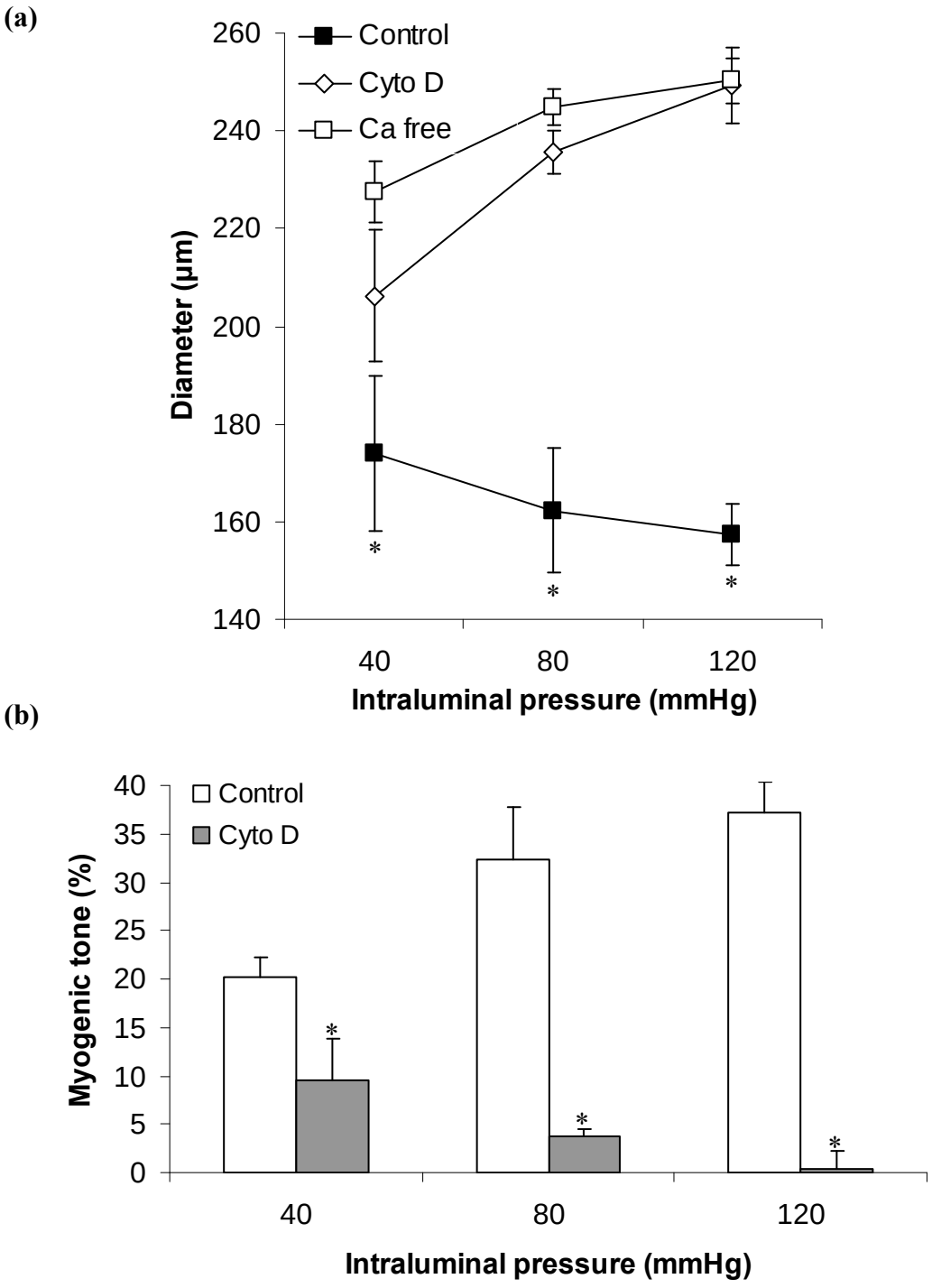

Figure 3.9 The effect of actin polymerization inhibitor Cyto D (a) *The relation of control, Cyto D (5 µM) and Ca^{2+} free on pressure-diameter relationship (*p<0.05 vs. Ca^{2+} free)* ***(b)*** *and myogenic tone in MCA (*p<0.05 vs. control at 40, 80 and 120 mmHg). Statistical evaluation was by ANOVA for repeated measure and Bonferroni post hoc. Values are means ± SEM (n=4, respectively).*

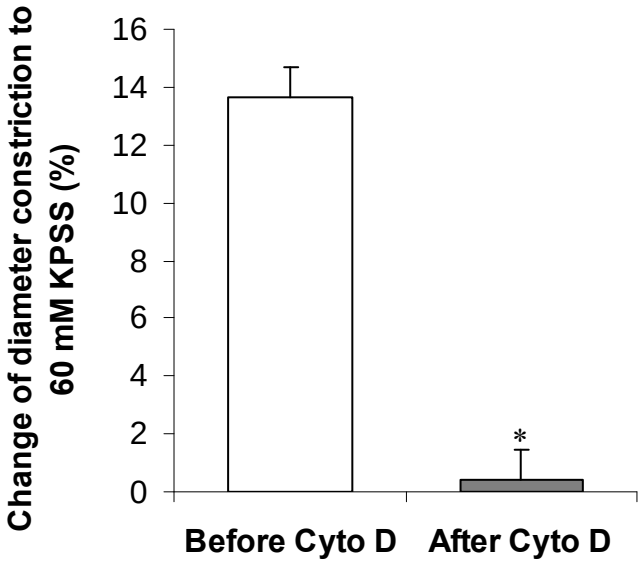

Figure 3.10 External diameter changes to 60 mM KPSS before and after treatment with Cyto D. *Cyto D treatment in MCA affected the contraction induced by 60 mM KPSS. Statistical evaluations was by paired Student t-test (*p<0.05 vs. before treatment). Values are mean ± SEM (n=4).*

3.4.5 Measurement of superoxide release from resistance arteries

Lucigenin-enhanced chemiluminescence was used to detect O_2^- production. As a control preliminary study, the generation of O_2^- was confirmed with xanthine and xanthine oxidase, and the O_2^- signal was quenched by SOD (Figure 3.11).

Two types of resistance arteries were used here, MCA and MRA. The O_2^- production was stimulated by ANG II and further enhanced by $NADH^+$, a substrate for Nox, and DETCA, a SOD inhibitor. For control experiment, SOD was replaced with DETCA. A preliminary study with ANG II at 10^{-9} M to match the pressure myograph studies was undertaken. However, the total obliteration of O_2^- signal for 600 s showed no significant difference between the blank (60.1 ± 4.5 RLU/s) and MCA (74.8 ± 11.1 RLU/s). Therefore in attempt to enhance the O_2^- signal, the ANG II's concentration was increased to 0.1 μM (Miller *et al.,* 2005).

In both the MRA and MCA, SOD quenched the total O_2^- level significantly over a 10-min period (Figure 3.12 & 3.13). In the real time measurement, O_2^- production in the arteries was significantly higher than the control. The plateau level of O_2^- signal in the MCA and MRA was maintained ~4-fold higher compared to the control (Figure 3.14).

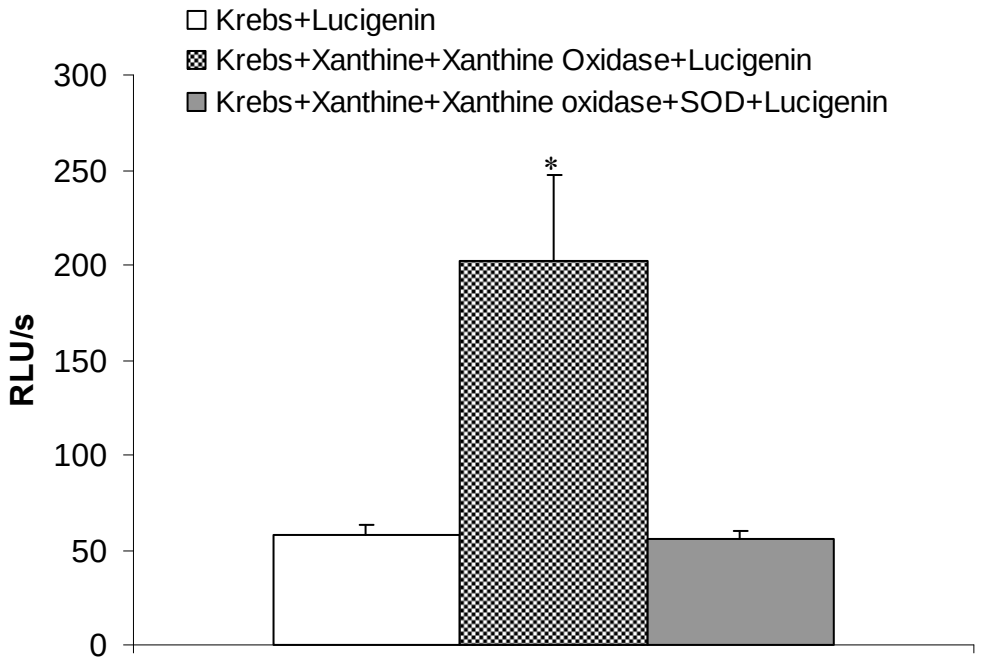

Figure 3.11 The total obliteration of superoxide (O_2^-) signal detected by chemiluminescence. *O_2^- was generated by xanthine (10^{-5} M)/ xanthine oxidase (2.5 mU) and quenched by 200 U/ml superoxide dismutase (SOD) (n=5).*

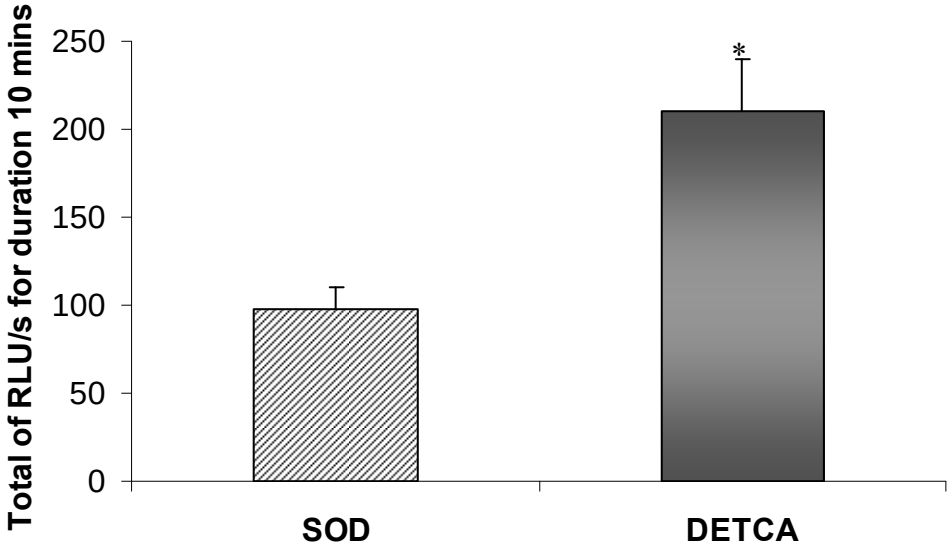

Figure 3.12 The total obliteration of superoxide (O_2^-) signal in mesenteric resistance arteries (MRA). *O_2^- release in MRA was induced by ANG II (10^{-7} M) and Nox substrate, $NADH^+$ (100 μM), facilitated by either SOD (200 U/ml) (n=5) or SOD inhibitor, DETCA (10 mM) (n=6). Values are means ± SEM. *p<0.05 vs. SOD (paired Student t-test).*

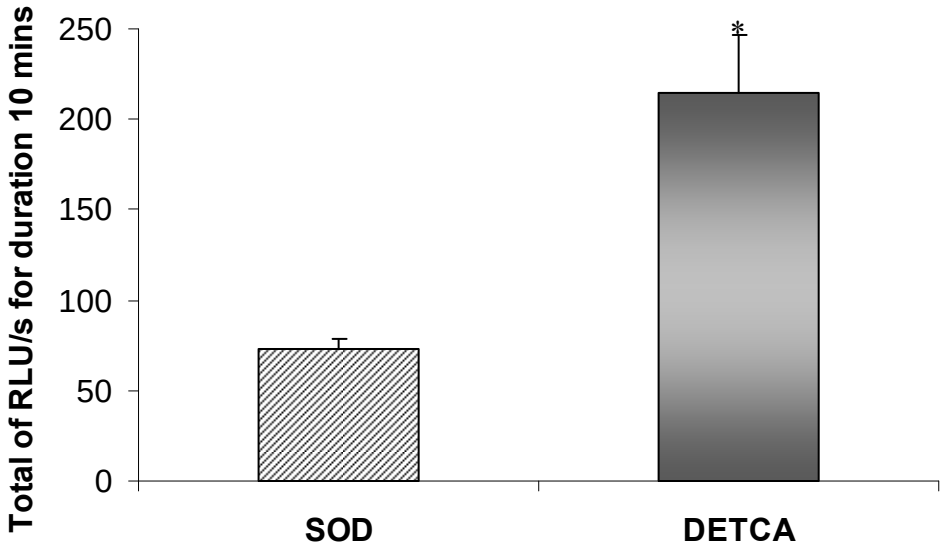

Figure 3.13 The total obliteration of superoxide (O_2^-) signal in middle cerebral arteries (MCA). *The total of superoxide (O_2^-) release in MCA induced by angiotensin II (ANG II, 10^{-7}M) and Nox substrate, $NADH^+$ (100 μM), was facilitated by either SOD (200 U/ml) (n=5) or SOD inhibitor, DETCA (10 mM) (n=7). Values are means ± SEM. *p<0.05 vs. SOD (paired Student t-test).*

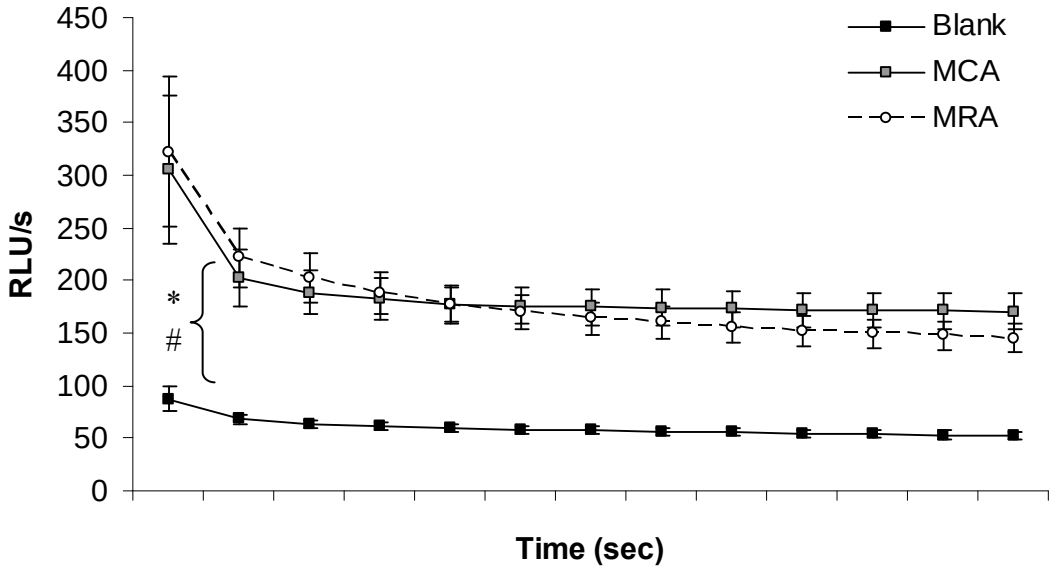

Figure 3.14 Vascular superoxide (O_2^-) production assessed by lucigenin-enhanced chemiluminescence. *MCA and MRA were incubated with ANG II (10^{-7} M) for 30 min to increase O_2^- generation, facilitated by the Nox substrate $NADH^+$ and the SOD inhibitor DETCA. Control reading was without any vessels. ANG II, $NADH^+$ and DETCA increased O_2^- production over time significantly in MCA and MRA compared to the blanks. Values are means ± SEM. * and # $p<0.05$ MCA and MRA vs. control (ANOVA for repeated measures, n=8).*

3.4.6 Confocal imaging of actin polymerization

Confocal laser scanning microscopy was used to visualize F-actin stained by phalloidin-FITC in pressurized and fixed vessels, counterstained with PI to indicate the nucleus. The vessels were studied in pairs and they were processed and analyzed at the same time under identical conditions. Figure 3.12a shows the F-actin as the most prominent in VSM layer of a fixed artery at 40 mmHg. The endothelial cells were aligned with blood flow and delineated along the lumen. Adventitial cells, likely representing adventitial fibroblasts, were scattered loosely on the outer vessel wall (Figure 3.15b).

An optical slice through the *z stack* that showed the most complete transverse profile of VSM layer was selected for F-actin fluorescence intensity. Results showed that F-actin staining showed more significant fluorescence intensity at high pressure (120 mmHg; 171.2 ± 6.4 unit) compared to low pressure (40 mmHg; 76.3 ± 8.2 unit) (Figure 3.16 and. 3.15b), indicating increase of the G-to-F actin polymerization.

(a)

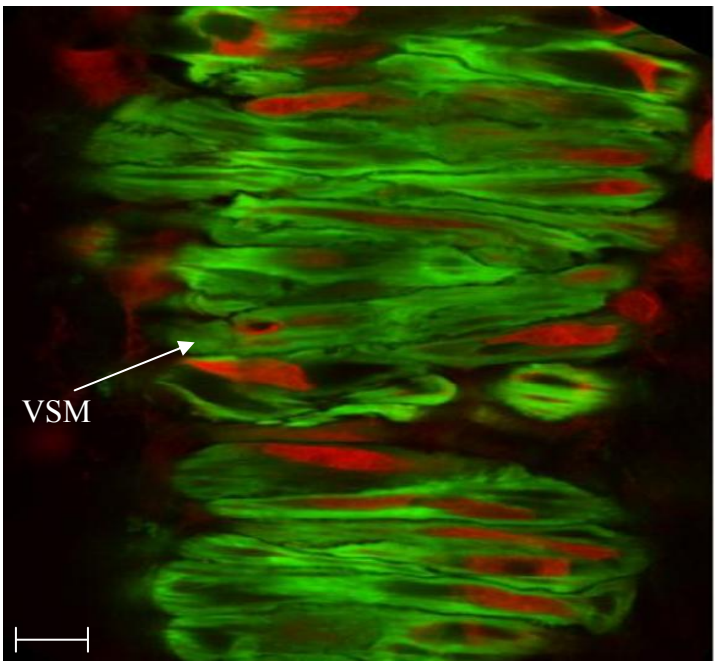

(b)

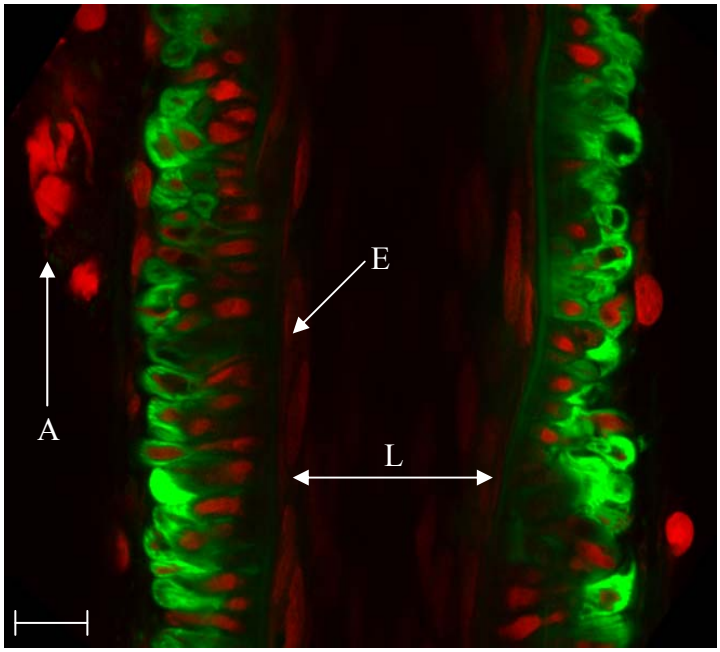

Figure 3.15 Representative confocal laser scanning microscopy images of a control vessel (40 mmHg). *The images demonstrate the* ***(a)*** *vascular smooth muscle (VSM) (x120) and* ***(b)*** *lumen (L) (x120) of a MCA fixed at 40 mmHg. Green staining is phalloidin-FITC for F-actin and red staining is propidium iodide for nucleus. The endothelial cells (E) line the lumen and are oriented in the direction of flow. Actin fibres are abundant within the VSM cells. Adventitial cells (A) are easily distinguished from VSMs by their lack of actin-staining and loose structure. Scale bar represents 20 µm One representative of four experiments.*

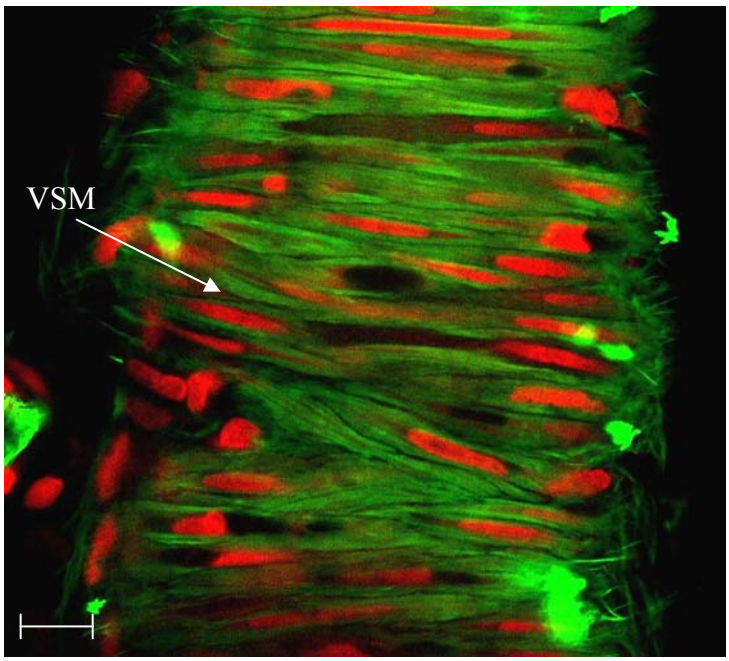

Figure 3.16 Representative confocal laser scanning microscopy image of a control vessel (120 mmHg). *The image demonstrates the vascular smooth muscle layer (VSM) of a MCA fixed at 120 mmHg. The vessel showed an increase of F-actin (green) fluorescence intensity during contraction at high pressure (120 mmHg). The occasional bright areas are the autofluorescence. Propidium iodide (red) used for staining the nucleus. Bar represents 20 μm. One representative of four experiments.*

3.4.7 Effect of cytochalasin D in fixed pressurized vessel

The fluorescence intensity in the MCA treated with Cyto D (5 μM) was significantly decreased at 120 mmHg (44.6 ± 9.0 unit) compared to untreated vessel at 120 mmHg (171.2 ± 6.4 unit) ($p<0.05$) (Figure 3.17b and Figure 3.16). In contrast, Cyto D did not show significant difference to the F-actin staining at 40 mmHg (77.4 ± 1.5 unit) compared to untreated vessels fixed at the same pressure (76.3 ± 8.2 unit) (Figure 3.15a and 3.17a). In spite of these results that could suggest Cyto D as inhibiting G-to-F actin cytoskeleton polymerization at 120 mmHg, however, its specific effect could not be justified as it also affected 60 mM KPSS-induced contraction (Figure 3.10). Thus, the exact action of Cyto D to actin cytoskeleton polymerization is still unclear at this moment.

(a)

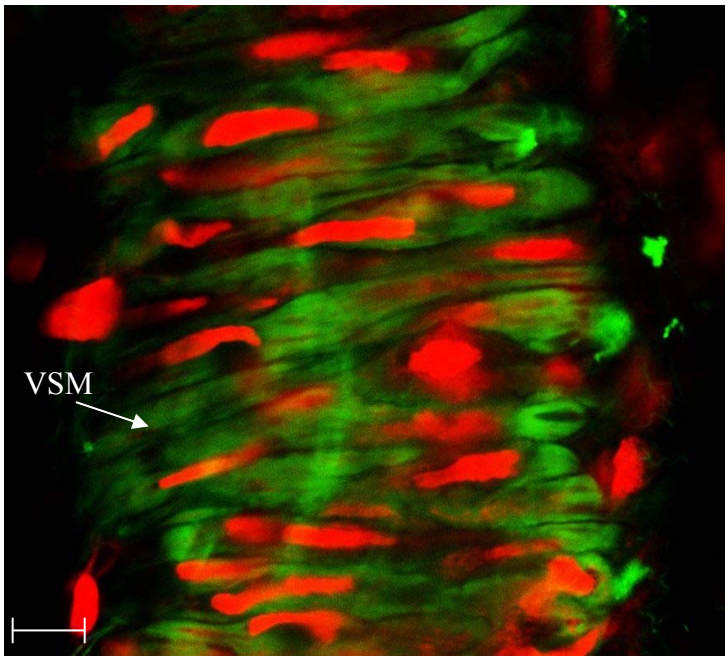

(b)

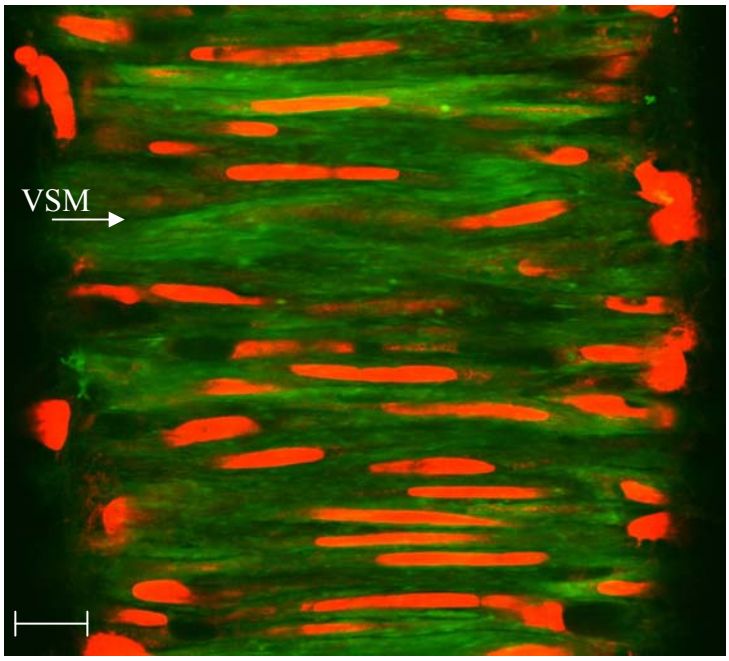

Figure 3.17 Representative confocal laser scanning microscopy images of vessel with actin polymerization inhibition. *The images demonstrate the vascular smooth muscle layer (VSM) of MCA after actin polymerization inhibitor, Cyto D, incubation and fixed at* ***(a)*** *40 and* ***(b)*** *120 mmHg. The vessel fixed at higher pressure showed less F-actin fluorescence intensity compared to the lower pressure. Green staining is phalloidin-FITC for F-actin and red staining is propidium iodide for nucleus. Bar represents 20 µm. One representative of four experiments.*

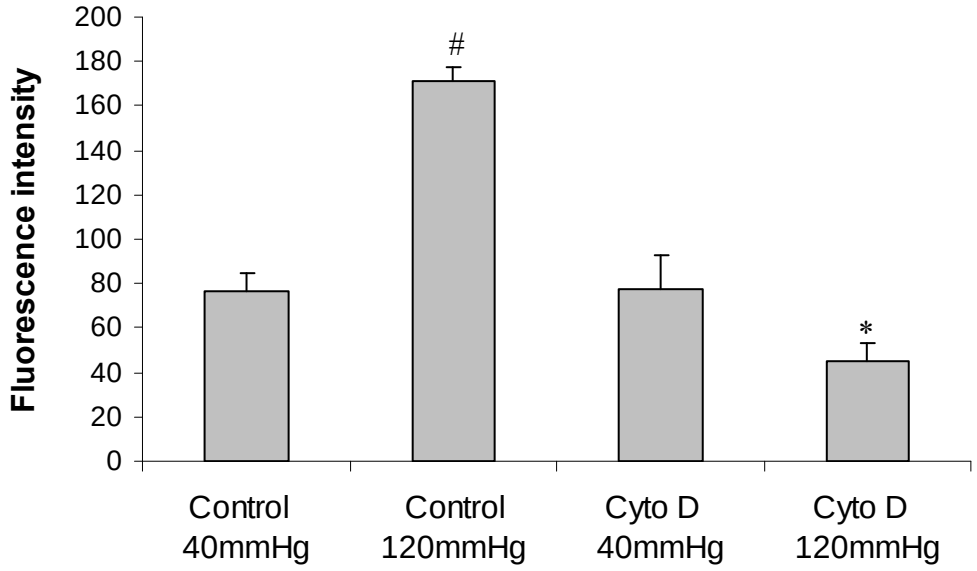

Figure 3.18 The F-actin fluorescence intensity at different pressure. *The fluorescence intensity was the sum of F-actin-stained regions in a VSM plane of each paired MCA sample. All of the samples were commenced under the same conditions to allow valid intensity quantitation. Values are means ± SEM (n=3-4). # p<0.05 vs. control at 40 mmHg, and *p<0.05 vs control at 120 mmHg (paired Student t-test analysis).*

3.5 Discussion

This study provided a number of important observations, which were, (1) Nox-mediated ROS is essential in myogenic constriction (2) ROS is liberated when induced by ANG II (3) actin cytoskeleton polymerization is important in pressure-dependent myogenic constriction in resistance arteries.

In the control pressure-dependent myogenic response result, the MCA control showed a typical myogenic constriction with transmural pressure increment in the presence of Ca^{2+}, as typically shown in many other pressure myography studies (Gokina *et al.*, 2005, Keller *et al.*, 2006, Dubroca *et al.*, 2007, Coats, 2010). The time control study with three cycles of pressure-steps showed a consistent pressure-dependent myogenic tone, confirming the viability of the vessels throughout the

duration of the experiments. A vehicle control with DMSO (<0.01% dilution) vs. non-vehicle control in myogenic tone was carried out. There was no difference with DMSO or without, as both experiments showed an active pressure-dependent myogenic tone with distending pressure. This was also supported by another study where DMSO (diluted 1/500 in PSS) was carried out as vehicle control in rat MRA and showed no effect on the myogenic response (Earley *et al.*, 2004). These control experiments confirmed the active pressure-dependent myogenic tone in resistance arteries and that any changes in the effect will be due to drug intervention.

3.5.1 Effect of reactive oxygen species inhibition to pressure-dependent myogenic tone

The antioxidant NAC has been used extensively as an inhibitor of ROS-dependent activity (Nowicki *et al.*, 2001, Wu *et al.*, 2009) and DPI as a Nox inhibitor (Di Wang *et al.*, 1998, Nowicki *et al.*, 2001, Keller *et al.*, 2006, Shen *et al.*, 2006). In this study, NAC and DPI incubation significantly reduced the pressure-dependent myogenic tone. This is in agreement with previous findings where NAC and DPI were found to abolish the pressure-dependent myogenic tone in resistance arteries (Nowicki *et al.*, 2001, Coats and Wadsworth, 2004). NAC and DPI showed no effect on the high-K^+ PSS (60 mM) constriction, indicating that the abolishment of myogenic tone was specific by Nox/ROS inhibition. A previous similar study has shown that pressure-induced ROS generation in hamster gracilis muscle was rapid with the steepest increase within the first 2 min (Keller *et al.*, 2006). In that study, although Nox inhibition by DPI eliminated the initial ROS increase, an augmentation in ROS was detected after 10 min of pressurization, which could be caused by non-Nox sources (Keller *et al.*, 2006). Superoxide could be the ROS responsible as it is known to be produced rapidly and it has a very short life. Also discovered in the same study, increasing the intraluminal pressure activated a stretch-sensing mechanism that stimulated the release of sphingosine-1-phosphate (S1P), which in turn could act as a receptor ligand. S1P then stimulated the Rac/Nox-induced ROS pathway, which increased Ca^{2+} sensitivity by inhibiting myosin light chain phosphatase (MLCP) and result in enhanced myogenic contraction (Keller *et al.*, 2006). Hence, based on this

study's result and previous studies, it could be plausible that Nox is responsible for the acute rapid increase in ROS following an increase in the transmural pressure.

ANG II was used in attempt to increase endogenous ROS. Although it was not proven in this study that NAC was directly inhibiting ANG II-induced ROS, however, this hypothesis is plausible considering the fact that ANG II (10^{-9} M) has been shown to release a low level of ROS in VSM cells (Touyz *et al.,* 2005a). Also supporting evidence was shown in cultured adventitial fibroblasts, where ANG II-induced ROS rapidly stimulated phosphorylation of p38 MAPK and JNK, both of which were inhibited by NAC, DPI and transfection of antisense $gp91^{phox}$ (Shen *et al.*, 2006, An *et al.*, 2007). A 4-hour incubation with ANG II was also shown to increase O_2^- in internal mammary arteries via AT_1 receptor (Berry *et al.*, 2000). In the same study, Nox was found as the source for O_2^- as DPI abolished the ANG II-induced O_2^-. Therefore, based on previous relevant studies, this thesis finding suggests that NAC could be inhibiting ROS induced from ANG II. Although O_2^- was shown to be generated from Nox in this study, the location of the source was unknown since Nox is present within the endothelium, VSM and adventitia (Shen *et al.*, 2006, Belmadani *et al.*, 2008, Di Wang *et al.*, 2008).

The use of DPI, as a specific Nox flavoprotein inhibitor, has been controversial as it is not absolutely specific for Nox. It was found to inhibit mitochondrial NADH dehydrogenase, NOS, xanthine oxidase and cytochrome P450 reductase as well (O'Donnell *et al.*, 1993). Therefore, it would inhibit most sources of ROS and potentially signalling pathways unrelated to ROS production. Another inhibitor of Nox that could have been used is apocynin, but also, it is not specific as it affects transmembrane Ca^{2+} flux (Keller *et al.*, 2006). DPI has been shown to inhibit spontaneous tone in pulmonary artery smooth muscle, in part by its ability to inhibit L-type Ca^{2+} channels (Weir *et al.*, 1994), but in this study, DPI maintained myogenic contraction in response to 60 mM KPSS. Thus, the use of DPI for inhibiting Nox specifically could be justified in this study.

3.5.2 Quantification of reactive oxygen species stimulated by ANG II

In this study, ANG II was used to initiate endogenous ROS as this method would be more physiological instead of adding exogenous ROS. ANG II-stimulated ROS were increased significantly and sustained in both MCA and MRA. ANG II in addition to $NADH^+$ and DETCA enhanced the O_2^- production in MCA and MRA. There have been numerous reports that are in agreement with this current finding, where ANG II was shown to increase the amount of ROS released from cerebral artery (Miller *et al.*, 2007), aorta (Cifuentes *et al.*, 2000, Landmesser *et al.*, 2002, Nishiyama *et al.*, 2003, An *et al.*, 2007), mammary artery (Berry *et al.*, 2000) and human endothelial cells (Zhang *et al.*, 1999). There was some controversy over whether NADPH or $NADH^+$ is the main substrate for Nox (Bedard and Krause, 2007). In cultured VSM cells, the $NADH^+$/NADPH oxidase preferentially utilizes $NADH^+$ as opposed to NADPH as substrate, which was in contrast to the phagocytic enzymes (Ushio-Fukai *et al.*, 1996). Rat aortic segments were found to produce higher O_2^- in response to $NADH^+$ by ~1.6-fold than that generated by NADPH (Rajagopalan *et al.*, 1996). So for these reasons, $NADH^+$ was chosen as the Nox substrate in this chemiluminescence study.

ANG II was used at 10^{-9} M as a submaximal concentration to activate Nox in pressure myography, however, in chemiluminescence preliminary study; this concentration did not show any significant difference in O_2^- signal between blank and MCA. It could be that the ANG II concentration might be too low, as it was previously shown ANG II at 10^{-7} M released amount of ROS three times more than ANG II at 10^{-9} M (Touyz *et al.,* 2005a). Another reason for failing to find significant difference in O_2^- signal could be the luminometer's lack of sensitivity (Miller *et al.,* 2009). However, since the aim of chemiluminescence was to compare the ANG II-induced O_2^- release in MCA and MRA, it was acceptable to increase the concentration to 10^{-7} M as was used by the Miller's group (Miller *et al.,* 2009, Miller *et al.,* 2007).

3.5.3 Actin cytoskeletal role in pressure-dependent myogenic tone

Cytochalasins are membrane-permeable fungal metabolites that have been used to inhibit the actin cytoskeleton in cell motility, growth and development. The act of mechanism is irreversible and it binds to the rapidly growing end (barbed-ends) of actin filament and compete with actin-binding proteins, therefore preventing further actin polymerization (Cooper, 1987). There is limited information on the Cyto D concentration that should be used in the vascular studies, from the range of 50 nM to 50 μM (Mehta and Gunst, 1999, Moldovan *et al.*, 2000, Cipolla *et al.*, 2002, Gokina and Osol, 2002, Shaw *et al.*, 2003). However in this thesis, Cyto D was used at 5 μM based on previous myogenic tone studies (Gokina and Osol, 2002). Surprisingly, this study has found that Cyto D treatment affected high-K^+ PSS contraction, probably due to excessively high concentration. However, previous studies have shown that cytochalasin at lower concentration was specific to actin cytoskeleton polymerization inhibition, where it did not affect the $[Ca^{2+}]_i$, MLC phosphorylation and myosin ATPase activity in smooth muscle (Saito *et al.*, 1996, Gokina and Osol, 2002, Shaw *et al.*, 2003) and also the phenylephrine-induced contraction (Flavahan et al., 2005). Hence, based on this result, the specific effect of Cyto D at 5 μM to pressure-dependent myogenic tone is still unclear.

This study was the first attempt to visualize rat MCA actin cytoskeleton within VSM in response to transmural pressure changes. At low pressure, the F-actin intensity showed intense staining at the cell periphery and less staining in the centre of the cell. It is typical that the smooth muscle cells are spindle-shaped, situated centrally and longitudal to the cell axis. This study has not proven directly that the transition of G-to-F actin had increased during myogenic tone enhancement; however, this hypothesis is plausible based on previous work by the Flavahan's group. They have found that under actin cytoskeleton 3D-imaging of myogenic tone in tail arterioles, the F-actin staining by Alexa 568-phalloidin was augmented and G-staining by Alexa 488 DNAse I was decreased (Flavahan *et al.*, 2005). In addition, the transmural elevation with presence of Cyto D caused fragmentation or ruptured structure of the actin fibres (Flavahan *et al.*, 2005), as similarly found in this study.

The effect of actin polymerization inhibitor Cyto D to the F-actin intensity was further investigated in pressurized MCA under confocal laser scanning microscopy. The sub-myogenic threshold pressure (40 mmHg) vessel showed less F-actin staining intensity compared to high pressure (120 mmHg). When Cyto D was added, it significantly disrupted the actin cytoskeletal structure underlying VSM in high pressurized vessel. The dramatic effect of Cyto D to reduce pressure-induced actin polymerization was also found in previous confocal study where Cyto D destroyed the actin cytoskeleton in mouse tail arterioles pressurized at 90 mmHg (Flavahan *et al.* 2005). Based on previous literature, Cyto D might inhibit actin polymerization exclusively without affecting the VSM contraction. However, considering the fact that Cyto D (5 μM) treatment also inhibited 60 mM KPSS-induced contraction in this study, its specific effect to actin cytoskeleton is not known at this point. Further study should be undertaken at lower concentration of Cyto D to determine the exact effect of actin polymerization inhibition without affecting pressure-independent contraction.

3.5.4 Conclusion

The current study has shown that Nox-mediated ROS could be the mechanosensor in pressure-dependent myogenic tone, either in physiological or ANG II-stimulated conditions. However, the role of actin cytoskeleton during pressure-dependent myogenic tone in rat MCA is still unclear.

CHAPTER 4:
TECHNIQUE DEVELOPMENT FOR FUNCTIONAL ISOLATION OF ADVENTITIAL-DEPENDENT CONTRIBUTION TO ACUTE VASCULAR CONTRACTILE RESPONSES IN RESISTANCE ARTERIES

4.1 Introduction

There has been growing evidence on the role of adventitia-dependent regulation in arterial smooth muscle tone. Ever since the adventitia was reported as a major source of O_2^- in the rabbit and rat aorta (Pagano *et al.*, 1997), there has been accumulating evidence reported on the physiological and pathophysiological functions of the adventitia (Rey and Pagano, 2002, Laflamme *et al.*, 2006, Haurani and Pagano, 2007, Pagano and Gutterman, 2007, Di Wang *et al.*, 2010). Adventitial O_2^- was found to be increased dramatically in an ANG II-infused hypertensive model (Di Wang *et al.*, 1999). Also from the same study, the enhanced O_2^- production gave rise to spontaneous myogenic contraction in the aorta. The authors suggested that O_2^- originating from the adventitia inactivates endothelium-derived nitric oxide (NO), promoting Ca^{2+} influx in VSM and hence spontaneous tone (Di Wang *et al.*, 1998, Di Wang *et al.*, 1999). In short, the authors have proposed an adventitial-endothelial-medial paracrine pathway, which suggests an active role for adventitia in regulating vascular tone. Alternatively, another study reported that O_2^- can constrict endothelium-denuded canine basilar arteries, indicating that O_2^- can directly constrict cerebral arteries independent of its effect on NO bioavailability (Tosaka *et al.*, 2002). Therefore, it is now evident that adventitia, as the source of O_2^- can be a great influence on vascular tone, but its direct effect in regulating pressure-dependent myogenic tone in small resistance arteries is still unclear.

There have been many attempts to understand the physiological role of adventitia in the laboratory. Recently, vascular engineering has emerged with a method for producing three independent vascular constructs comprising of only adventitia, only media, and adventitia plus media (Laflamme *et al.*, 2006, Auger *et al.*, 2007). These studies were the first direct evidence that the adventitia has the capacity to contract and relax in response to vasoactive factors. A major advantage of adventitial engineering as an experimental tool is the ability to directly test the effect of exogenous or paracrine factors on adventitial function, separate from the effects on the tunica media or intima. This prevents the need to mechanically strip the adventitia, a procedure that is either incomplete or causes accidental trauma to the

vessel wall. On the other hand, the disadvantage of tissue-engineering is that it cannot replicate all of the complexities of the adventitial wall like the vasa vasorum, external elastic lamina and innervation.

There have been many attempts to remove the adventitia layer without damaging the vessel wall, in order to allow a more in-depth understanding about adventitial function. However, Kemler *et al.,* (1997) demonstrated histologically that stripping the adventitia did not remove the layer completely. Arribas group proposed an enzymatic treatment with collagenase type II prior to mechanical stripping in rat carotid and iliac arteries (Gonzalez *et al.*, 2001b, Somoza *et al.*, 2005). This method allowed complete adventitial removal as confirmed by optical and confocal microscopy, where VSM was proven undamaged. The abolishment of electrical field stimulation-induced frequency-dependent contraction also proved that the adventitia was successfully removed. However, the KCl-induced contraction was found to be significantly reduced in adventitia-removed arteries (Gonzalez *et al.*, 2001a), which means, the adventitial removal technique still has its limitation. Di Wang's group has attempted to study the role of adventitial aortic rings in releasing O_2^- by mounting the adventitia facing outward and inward (inverted) in organ baths (Di Wang *et al.*, 1998). This technique might suit conduit vessels like aorta, but it is not suitable for small resistance arteries as it may cause vessel damage by stretching the VSM during the inverting process.

In larger arteries, the adherence of adventitia to the medial layer is weak, so the adventitia of ovine brachiocephalic trunk (Cabrera Fischer *et al.*, 2006) and ovine femoral arteries (Fischer *et al.*, 2010) was directly dissected by forceps and scissors. This method however, modified the arterial stiffness and decreased the lumen diameter (Cabrera Fischer *et al.*, 2006, Fischer *et al.*, 2010). According to the authors, adventitial removal would remove perivascular adipose tissue and also nerve terminals that may release vasoactive factors. Therefore the limitation of this stripping technique is that, the geometric and biomechanical changes could be due to the removal of the adventitia, perivascular adipose tissue and/or nerve endings. Besides mechanical stripping, another approach has been made, which was via

chemical treatment to abolish the adventitial functional layer. In an attempt to characterize the effects of recombinant eNOS gene expression in adventitia on vasomotor responses, canine cerebral arteries were dipped in 100% EtOH for 2-3 s (Onoue *et al.*, 1998) or in 4 % paraformaldehyde for 15 s (Onoue *et al.*, 1999, Tsutsui *et al.*, 1999). They have proven that the adventitial layer was ablated based from the reduced relaxation response by perivascular-relaxant, nicotine (Chiba and Tsuji, 1985, Tsuji and Chiba, 1986). Although these previous methods were commenced in cerebral arteries, the arteries were of large resistance artery models (1-1.5 mm diameter), and the focus of this thesis is resistance arteries. This study will attempt to remove or at least ablate its function in resistance models of the cerebral arteries and mesenteric arteries. The external diameter sizes that have been used in previous resistance studies can vary from 100 to 230 μm for MCA (Jimenez-Altayo *et al.,* 2007, Coulson *et al.,* 2002, Lagaud *et al.,* 2002), and from 150 to 390 μm for MRA (Gschwend *et al.,* 2003, Looft-Wilson and Gisolfi, 2000).

In our attempt to confirm the removal of the adventitia, this study will use the adventitial-innervation as a marker for adventitial function. Figure 4.1 shows the summarized schematic interaction between adrenergic, cholinergic and nitrergic nerves to the VSM. Nicotine's mechanism of action is still unclear as it has been shown to elicit reciprocal nitrergic and noradrenergic innervation, depending on the tissue type and species as reviewed by Toda and Okamura (2003). However, an abundance of research has agreed that nicotine's mechanism of action is based on the adventitial innervation system. Nicotine releases NO (vasodilatation) from nerves of canine (Toda 1975) cerebral arteries and activates adrenergic nerves (vasoconstriction) in guinea pig aorta (Ikushima *et al*. 1982) and canine mesenteric artery (Toda & Okumura 2003). In addition, nicotine has been shown to activate nicotinic cholinoceptors on adrenergic nerves to release adrenergic neurotransmitters in rat mesenteric arteries (Shiraki *et al.*, 2000, Eguchi *et al.*, 2007). After treatment with guanethidine (adrenergic blocker) or phentolamine (alpha-adrenergic antagonist), the contraction response was reversed to relaxation (Toda & Okumura 2003). This concept of nicotine-induced relaxation will be used in this study to indicate adventitial function abolishment.

Based on these previous limited techniques for removing adventitia, this current study would attempt for the first time to adapt a successful adventitial removal technique in resistance arteries that preserves VSM and endothelial function, as well as its vascular integrity and mechanical properties.

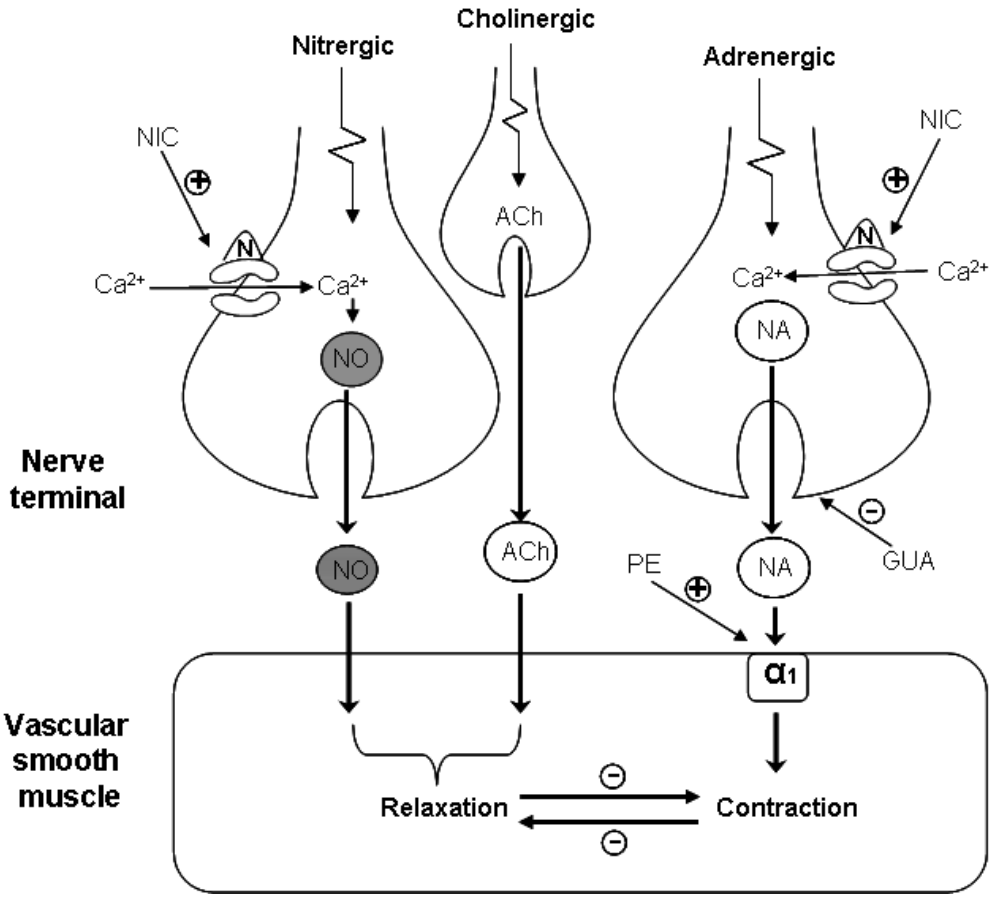

Figure 4.1 Hypothetical schematic interaction between nitrergic, adrenergic and cholinergic nerves to the vascular smooth muscle (VSM) relaxation or contraction. *Primarily, the innervation is mediated by sympathetic adrenergic nerves. Nicotine has been shown to elicit reciprocal nitrergic and noradrenergic innervation, depending on the tissue type and species. Minus denotes inhibition, plus denotes activation. ACh, acetylcholine; GUA, guanethidine; N, nicotinic receptor; NIC, nicotine; NO, nitric oxide; PE, phenylephrine (Toda and Okamura, 2003).*

4.2 Aim

1. To develop a method that successfully eradicates adventitial-dependent function and maintains functionally and structurally intact underlying smooth muscle and endothelium in small resistance arteries.

2. To investigate the influence of adventitial ablation on the passive mechanical properties of resistance arteries.

4.3. Methods

4.3.1 Tissue isolation

(a) Rat middle cerebral artery

The basic methodology has been described in detail in Section 2.1.1. Briefly, adult male Sprague-Dawley rats (270-300g, 12-14 weeks) were humanely killed and the middle cerebral arteries (MCA) (194 ± 10 μm, *n*=40) were dissected.

(b) Rat mesenteric artery

The basic methodology has been described in detail in Section 2.1.2. Briefly, adult male Sprague-Dawley rats (270-300g, 12-14 weeks) were humanely killed and the mesenteric resistance arteries (MRA) from the 3rd-order branches (from the main branch) (345 ± 2 μm, *n*=40) were dissected.

4.3.2 Adventitial removal by collagenase treatment

Adventitial removal by collagenase was based on a previous study (Gonzalez *et al.,* 2001) and the MRA was used for this method. After isolation, MRA segments were cut into 4 mm long rings, secured with sutures at both ends and divided into 4 different groups (Figure 4.2). Two controls were used here, i.e. control 1 (C1) and control 2 (C2). C1 was a control to C2, to ensure that the procedure of putting the vessel in a 37°C shaking water bath (15 min) did not affect the vessel viability. Then

vessel 1 (V1) and vessel 2 (V2) were placed in eppendorf tubes filled with Krebs solution containing 2 mg/ml collagenase type II, in a shaking water bath (37°C) for 15 min. The vessels were immediately rinsed and placed for 10 min in cold Krebs (4°C). For V1, the vessels were mounted straight away on the wire myography, whereas for V2, arteries were pinned at both ends to a Sylgard-based dissecting dish, and the adventitia was carefully removed by gentle stripping with fine forceps under a dissecting microscope.

The above protocol was repeated with different incubation times (7.5 and 10 min) and collagenase concentration (1.5 mg/ml) in MRA. Also, it was repeated for conduit vessel i.e. aorta at the concentration of 2, 2.5 and 3 mg/ml collagenase type II.

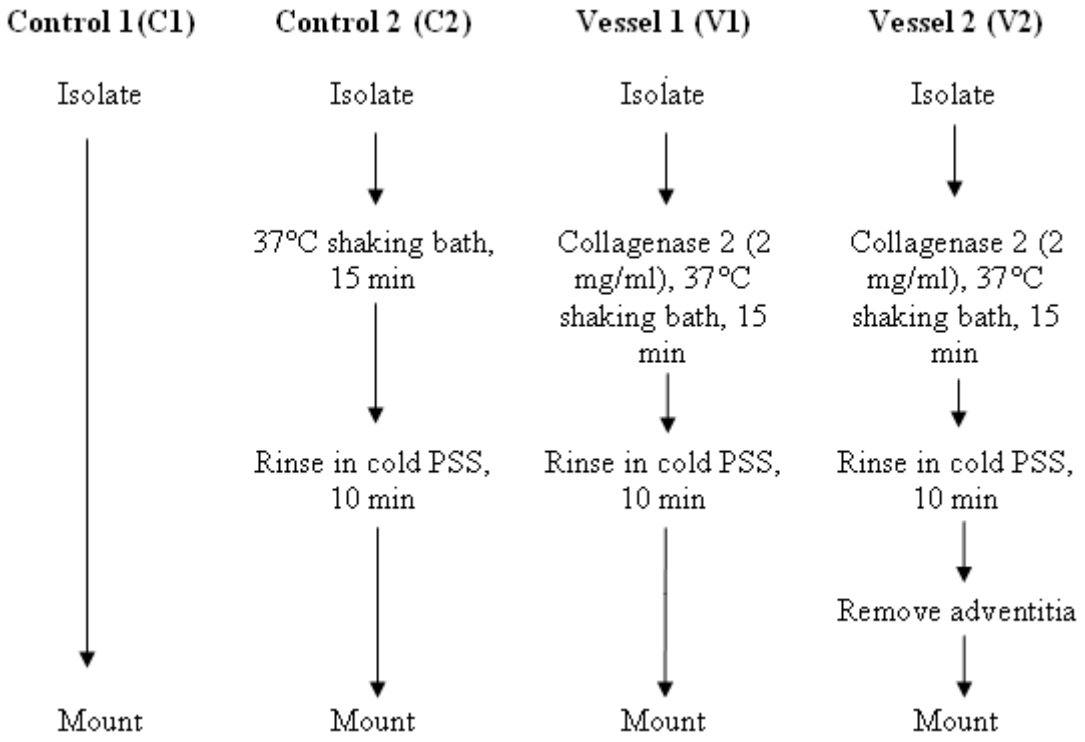

Figure 4.2 The diagram for adventitial removal method by collagenase type II treatment in mesenteric resistance arteries (MRA).

4.3.3 Adventitial removal by paraformaldehyde treatment

A pair of vessel segment with identical size was taken from the same animal. The control (+Adv) was untreated vessels. To disrupt the function of the adventitial layer, the outer surface of the arterial rings was treated with 4 % paraformaldehyde for 15 s (-Adv). Both ends of each vessel were tied beforehand with sutures to avoid damage from the chemical to the endothelium. Then immediately the vessels were rinsed in cold PSS (4°C) before mounting on the wire myography. Each pair of +Adv and –Adv segments were treated identically and simultaneously during the experiment. For this adventitial removal method, MRA and MCA were used to test the methodology's reproducibility.

4.3.4 Confocal microscopy

The degree of damage to the vessel wall following paraformaldehyde dipping was tested with laser-scanning confocal microscopy (Leica TCS SP-5), as described in Section 2.4. In brief, the confocal was coupled to an upright microscope (DM6000 Leica Microsystems, Germany) with x20 air objective (N/A 0.75, Leica) and x40 oil objective (N/A 1.3, Leica). Images were captured with LAS AF (Leica Microsystems, Germany).

MRAs were isolated and divided into a pair of matched groups; +Adv and -Adv. For these groups, unfixed arteries were stained with propidium iodide (PI: 1 mg/ml, 1 hour, dark). Propidium iodide is a nonpermeable fluorescent nuclear dye. Staining unfixed arteries with PI-containing PSS was used to determine the degree of damage to smooth muscle cells (SMC) after dipping into 4 % paraformaldehyde. The vessel wall was visualized under elastin autoflorescence wavelength (excitation 488 nm and emission 500-560 nm). The images were observed under magnification of x20 air objective and x40 oil objective.

For PI-staining, the artery was fixed in phosphate buffered formaldehyde (10 % for 1 hour) and then rinsed with PSS. The artery was permeabilized with 0.5 % Triton X-100 (15 min) and rinsed with PSS. Following which the artery was removed from the cannulae and incubated with PI (1 mg/ml, 1 hour, dark). The emission spectral range

was 488/615-nm for PI and the confocal images were processed using Volocity software (Perkin Elmer, UK).

4.3.5 Functional tests by wire myography

The wire myograph has been described in Section 2.3.1. Briefly, isometric tension was recorded from vessels mounted on 40 μm tungsten wires (DMT Multimyograph model 610P, Denmark) in continuously bubbled PSS. Length-tension curves were constructed and normalized, as previously described (Section 2.4.1). 60 mM KPSS-induced contractions were tested.

The adventitial function ablation experiment was confirmed by significant reduced relaxation by the perivascular nerve relaxant, nicotine (10^{-5} M). The vessels were preconstricted with either phenylephrine PE (10^{-7} M) for MRA or serotonin 5HT (10^{-7} M) for MCA. Previous studies found that low concentration of nicotine (5 x 10^{-5} and 10^{-4} M) activated capsaicin-sensitive sensory C nerves via an action on nicotinic receptors and higher concentration (3 x 10^{-4} and 10^{-3} M) directly activated VSM to dilate (independent of sensory nerves) (Li and Duckles, 1993). Therefore, attenuation of nicotine-induced relaxation at 10^{-5} M was chosen in this study as a marker for the degree of adventitial layer disruption (Tsutsui *et al.*, 1999). Since nicotine elicits reciprocal effects, where it can cause contraction (Kurahashi *et al.*, 2001) and also relaxation (Eguchi *et al.*, 2007), the adrenergic neuron blocker guanethidine, Gua (10^{-5} M) was used throughout the experiment so that nicotine could only give a relaxation response. Nicotine-induced relaxation between +Adv and -Adv was compared to determine the damage to the adventitial layer.

For endothelium-dependent and endothelium-independent relaxation, acetylcholine (ACh) and sodium nitroprusside (SNP) were used, respectively. All vessels were pre-constricted with PE (10^{-6} M) for MRA and 5HT (10^{-6} M) for MCA.

All of the pharmacological experiments between +Adv and –Adv were paired experiments, as explained in Section 4.3.3.

4.3.6 Transmural nerve stimulation

Transmural nerve stimulation (TNS), also known as electric field stimulation (EFS) is a method to selectively and maximally activate nerves without stimulating the VSM directly (Duckles & Silverman 1980). Tissues were electrically and transmurally stimulated by a pair of parallel platinum electrodes, which were placed on either side of the tissue, 1 cm apart. TNS was applied with a Grass stimulator (S44D, USA) using the following parameters: 40-130 V, 0.3-0.5 msec pulse duration, increasing frequency (1, 2, 4, 8 & 16 Hz) for 10 s each with 4 min between trains (Urabe *et al.*, 1991, Laflamme *et al.*, 2006, Auger *et al.*, 2007). The +Adv should exhibit a frequency-dependent contraction response. The neurogenic nature of the TNS response in +Adv will be confirmed by the attenuated vasoconstrictor response in the presence of the adrenergic neuron blocker Gua (10^{-5} M, 30 min) (Sullivan and Davison, 2001, Akiyama *et al.*, 2005). The TNS response in +Adv is expected to be either attenuated or abolished by Gua. TNS was conducted in the MRA only, as the MCA is not fully-innervated and hence not suitable for field stimulation studies.

4.3.7 Assessment of vascular mechanics by pressure myography

The basic methodology has been described in detail in Section 2.3.2. In brief, isolated arteries were studied on a pressure myograph system (Danish MyoTech P110), cannulated and secured with fine nylon sutures to glass micro-cannula and pressurized with oxygenated PSS. In keeping with the standard protocol all MCA (+Adv and –Adv) were studied in the absence of flow.

Vascular mechanics of the rat MCA (+Adv and –Adv) were assessed in a Ca^{2+}-free PSS containing 2 mM EGTA and papaverine (10^{-4} M). After equilibration for 15 min at 37°C at an intraluminal pressure of 40 mmHg, Ca^{2+}-free PSS containing 20 mM caffeine was replaced for 2 min to exhaust intracellular sarcoplasmic reticulum Ca^{2+} stores. Then the vessels were washed three times with Ca^{2+}-free PSS + EGTA and allowed to equilibrate for another 15 min before a pressure curve was constructed.

Intraluminal pressure was raised from 5 to 10 mmHg, and thereafter in increments of 10 mmHg until 140 mmHg. For each pressure step, the external diameter, internal diameter (ID) and wall thickness (WT) were measured.

Calculations of vascular mechanics

To understand mechanical properties in resistance arteries, it is important to study the arteries in their natural myogenic state rather than drug-induced states. Mechanical properties might be altered if the vessel structure is damaged or diseased (Coulson *et al.*, 2002, Coats, 2010). The diameter of blood vessels at full dilation is believed to depend on the arrangement of extracellular matrix protein, notably elastin and collagen. With this concept, this study has used mechanical properties as another method to determine the viability of the vessel for establishing adventitial ablation technique in our lab. The following mechanical parameters were calculated based on Baumbach *et al.* 1988:

$$\text{Incremental distensibility} = \Delta ID / (ID \times \Delta IP) \times 100$$

Incremental distensibility represents the percentage change of the internal diameter, ΔID for each change of increase in intraluminal pressure ΔIP. The units of incremental distensibility are percent per millimetre mercury pressure (%/ mmHg).

$$\text{Circumferential stress } (\sigma) = (IP \times ID)/ (2WT)$$

Circumferential stress (σ) is the total force (active and passive) developed per unit area of the arterial wall as a result from intraluminal pressure. The pressure was converted from millimetres mercury to dynes per centimeter squared (1 mmHg = 1.334×10^3 dynes/cm^2).

$$\text{Circumferential strain } (\varepsilon) = (ID\text{-}D_0)/ D_0$$

Circumferential strain (ε) is fractional change in internal diameter from the original diameter D_0 as a result from intraluminal pressure changes. Internal diameter

measured at 5 mm Hg was used for original diameter in the calculation of circumferential strain, because reliable measurements of the internal diameter of artery could not be obtained at an intraluminal pressure of 0 mmHg (Baumbach *et al.* 1988). Strain is a unitless ratio.

To determine the intrinsic elastic properties of the artery, the stress-strain ratio data for individual arteries were obtained according to Young's elastic modulus (*E*).

$$E = \frac{\sigma}{\varepsilon}$$

Since the arterial stress-strain curve is nonlinear, it is more appropriate to obtain a 'tangent' or 'incremental modulus' by determining the slope of an exponential stress-strain curve using the equation:

$$\sigma = \sigma_{orig} e^{\beta\varepsilon}$$

where σ is the stress, σ_{orig} is the stress at the original diameter at 5 mmHg, ε is the strain and β is the tangential elastic modulus (Baumbauch *et al.,* 1988).

4.3.8 Materials

Phenylephrine (PE), nicotine (Nic), acetylcholine (ACh), sodium nitroprusside (SNP), serotonin (5HT), caffeine, papaverine hydrochloride, ethylene glycol tetraacetic acid (EGTA), propidium iodide (PI), guanethidine (Gua) were purchased from Sigma, UK. KCl was purchased from BDH, Poole, England. Collagenase type II enzyme (4176; CLS2; 323 U/mg) was purchased from Worthington, USA. All drugs were dissolved in distilled water (dH_2O). The drugs were stored in aliquots at -20°C, except for collagenase which was made freshly before each experiment. Aliquots were thawed before use and diluted with Krebs physiological saline solution (PSS), containing (in mM) 119 NaCl, 4.5 KCl, 25 $NaHCO_3$, 1.0 KH_2PO_4, 1.0 $MgSO_4.7H_2O$, 11.0 glucose and 2.5 $CaCl_2$ if needed. Krebs solution was prepared fresh daily.

4.3.9 Statistical analysis

Values are presented as mean ± standard error of the mean (SEM). Statistical analysis of the data was performed using Microsoft Excel 2003 and GraphPad Prism version 4.03. Statistical analyses were performed by two-way ANOVA for repeated measure or one-way ANOVA (paired Student t-test) for the paired studies. Significance was assumed if $p<0.05$. *n* is the number of animals studied.

4.4 Results

4.4.1 Preliminary study on adventitial removal by collagenase type II in intact small arteries

Vascular viability by wire myography

Figure 4.3 shows the effect of 60 mM KPSS on control 1 (C1), control 2 (C2), unstripped vessel 1 (V1) and stripped vessel (V2). The results showed that collagenase (2 mg/ml) significantly reduced the vascular contractility ($p<0.05$) to 60 mM KPSS in both unstripped and stripped vessels compared to C1 and C2.

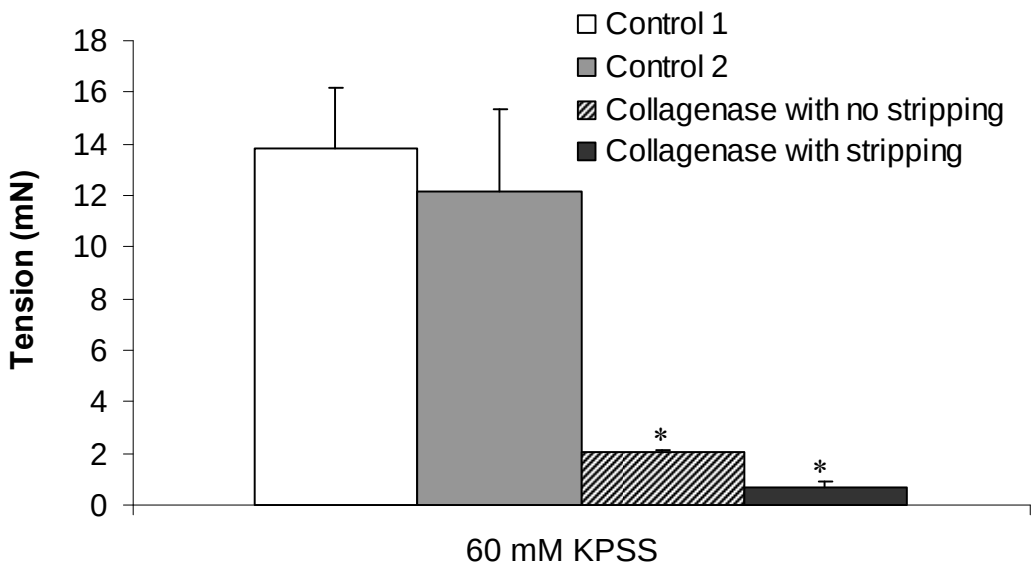

Figure 4.3 The 60 mM KPSS-induced contraction. *Bar graph showing the tension produced by mesenteric resistance arteries (MRA) following addition of 60 mM KPSS in +Adv and -Adv. Control 1 is control vessel which was mounted on the wire after isolation, and Control 2 is control vessel which undergoes warm bath (37°C, 15 min, shaking) without collagenase treatment. Values are means ± SEM. *p<0.05 vs Control 2, One-way ANOVA (n=6).*

Different collagenase type II concentrations (2 and 1.5 mg/ml) and incubation periods (7.5, 10 and 15 min) were tested. The results still showed poor response to 60 mM KPSS contraction in unstripped (V1) and also stripped vessels (V2) (Table 4.1).

Collagenase (mg/ml)	Time (min)	Contraction to 60 mM KPSS (mN)				*n*
		C1	C2	V1	V2	
2	10	15.2 ± 2.2	15.6 ± 2.2	7.7 ± 0.7*	2.4 ± 0.6*	5
2	7.5	15.8 ± 0.9	16.4 ± 1.8	8.6 ± 1.2*	1.7 ± 0.5*	4
1.5	15	11.6 ± 3.0	15.6 ± 3.6	2.1 ± 0.6*	0.7 ± 0.5*	3
1.5	10	17.1	19.8	8.4	1.7	1

Table 4.1 Preliminary tests of collagenase treatment with different concentrations (mg/ml) and incubation times (min) in mesenteric resistance arteries (MRA) *C1: Control 1, C2: Control 2, V1: Vessel 1, V2: Vessel 2. Values are means ± SEM. *p<0.05 vs Control 2, One-way ANOVA.*

The aorta was used (*n*=3) to confirm the reproducibility of the technique in our lab based on previous methods (Gonzalez *et al.*, 2001b). The 60 mM KPSS wash caused contractile tension in control of 15.6 ± 1.6 mN, collagenase 2 mg/ml of 11.5 ± 4.9 mN, collagenase 2.5 mg/ml of 12.5 ± 2.9 mN and collagenase 3 mg/ml of 14.4 ± 2.2 mN. As there was no significant difference between groups, it was concluded that the collagenase method was successful in big conduit arteries.

Vascular structure integrity by confocal microscopy

Confocal microscopy was used to investigate the level of cellular trauma across the vessel. Initially, images of unfixed vessels were obtained with the confocal. The non-permeant cell dye, PI, was used as an indicator for compromised cells. Figure 4.4 shows a control vessel (+Adv) with viable integrity with no significant PI-positive stained cells within the vessel wall. Elastin autoflourescence wavelength (green) was set to observe the inside of the vascular wall. Figure 4.5 shows images of arteries after collagenase treatment with and without mechanical stripping. The stripped vessel was PI-positive stained throughout and this indicated that all of the cells were dead and the vessel was damaged (Figure 4.5a). The outmost layer and cells within the VSM layer were dead in the unstripped vessel, indicating that collagenase had damaged the vessel and allowed PI to penetrate through the wall (Figure 4.5b).

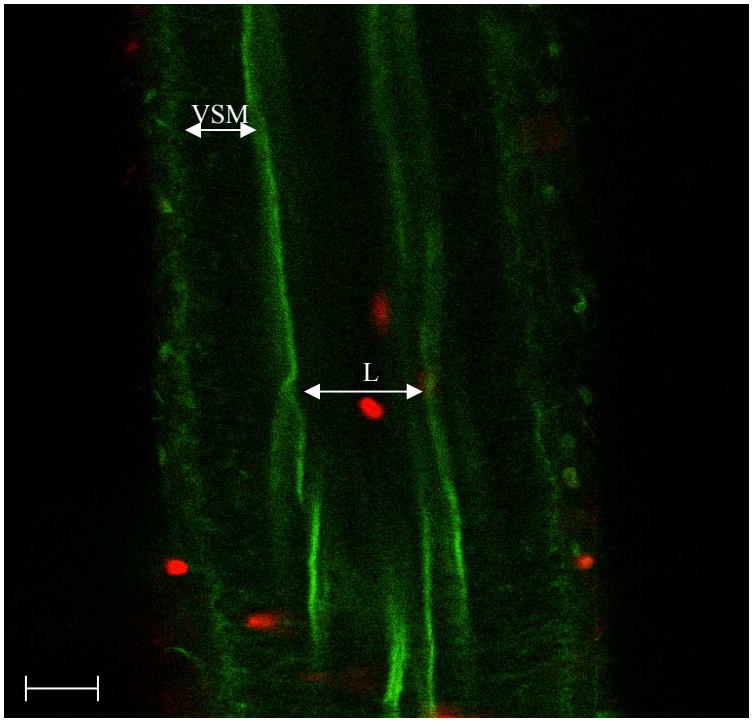

Figure 4.4 Representative confocal image demonstrating a control unfixed mesenteric resistance artery (MRA). *Green is the elastin autofluorescence and red is propidium iodide-stained nucleus (dead cells). Magnification was taken at x40 oil objective. Scale bar represents 20 μm. L, lumen; VSM, vascular smooth muscle. One representative from three experiments.*

(a)

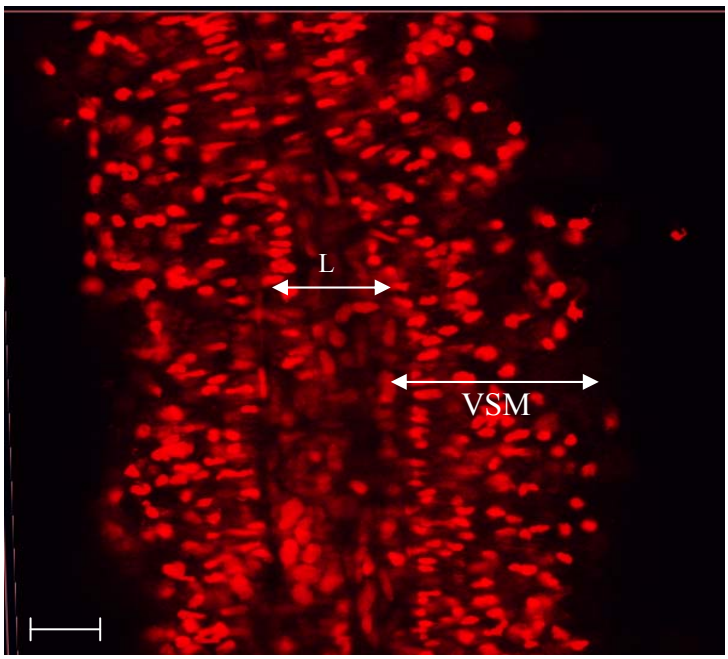

(b)

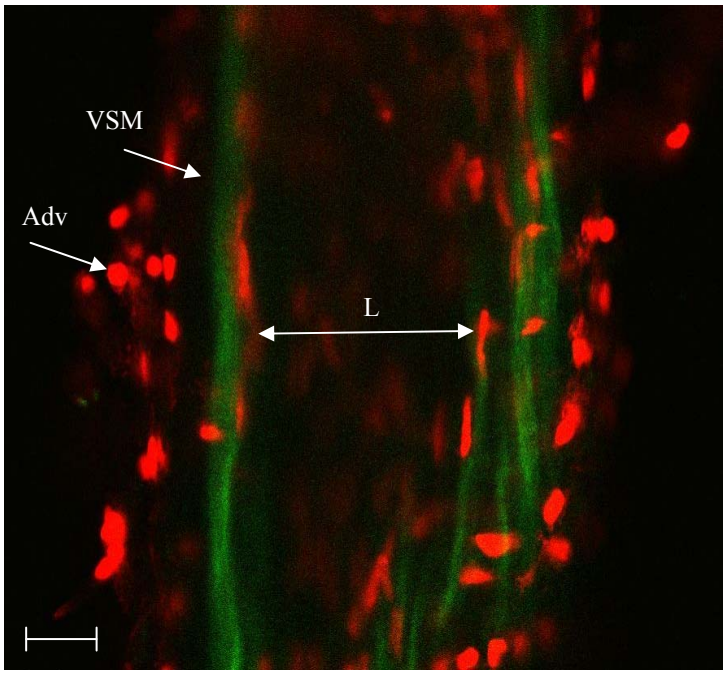

Figure 4.5 Representative confocal images demonstrating the effect of collagenase type II treatment in rat mesenteric resistance artery (MRA). *The images show the adventitia (Adv), VSM and lumen (L) after collagenase type II treatment (2 mg/ml, 15 min)* ***(a)*** *with stripping and* ***(b)*** *without stripping. Green is the elastin autofluorescence and red is propidium iodide-stained nucleus (dead cells). Magnification was taken at x40 oil objective. Bar represents 20 µm. One representative from* ***(a)*** *two experiments and* ***(b)*** *three experiments.*

4.4.2 Developing a technique of adventitial-ablation by paraformaldehyde-buffered solution

Following collagenase exposure which damaged the vascular integrity, a chemical treatment approach with 4 % paraformaldehyde was considered based on a previous study to ablate the adventitial function.

(a) Rat mesenteric artery

Vascular integrity by confocal microscopy

Figure 4.6 is showing the image of a vessel after being dipped in paraformaldehyde for 15 s (-Adv). Only the outmost layer (the adventitia) is dead as it was exposed to the chemical. This has proven that the 4 % paraformaldehyde dipping for 15 s did not penetrate through the vessel wall and damage the cells. Thus, this chemical dipping was not detrimental to the vascular integrity.

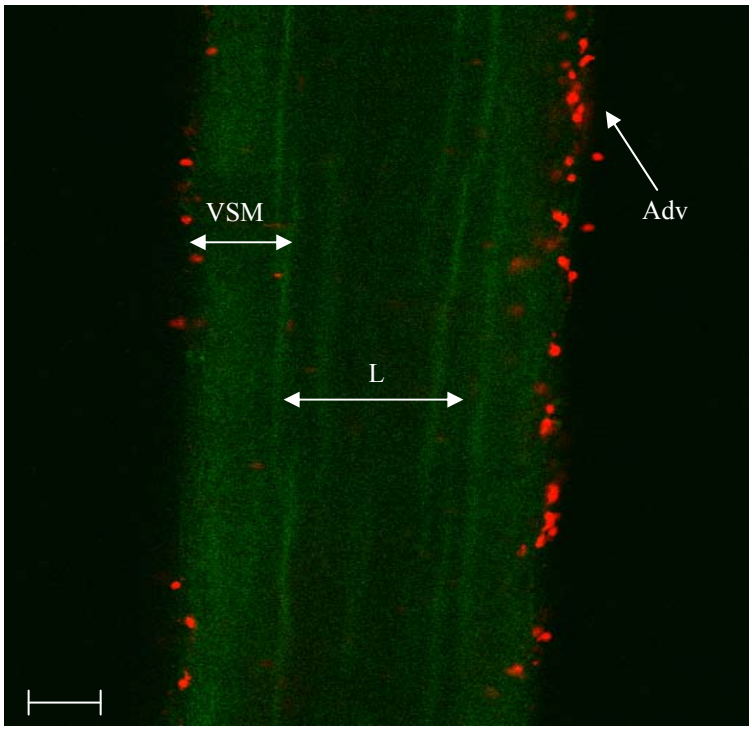

Figure 4.6 Representative confocal image demonstrating the effect of 4 % paraformadehyde (15 s) on the mesenteric resistance artery (MRA). *The image shows the adventitia (Adv), VSM and lumen (L) after being dipped in 4 % paraformadehyde for 15 s (-Adv). Green is the elastin autofluorescence and red is propidium iodide-stained nucleus (dead cells). Only the outmost layer (the adventitia) is dead as it was exposed to the chemical treatment. The vessel showed no significant red staining of dead cells within the vascular wall, proving that the 4 % paraformaldehyde dipping did not penetrate through the vessel wall. Magnification was taken at x40 oil objective. Bar represents 20 μm. One representative from three experiments.*

Vascular functional tests by wire myography

Figure 4.7 shows the 60 mM KPSS response in +Adv and –Adv being consistent at the beginning and the end of the experiment. There was no significant difference between the groups of MRA.

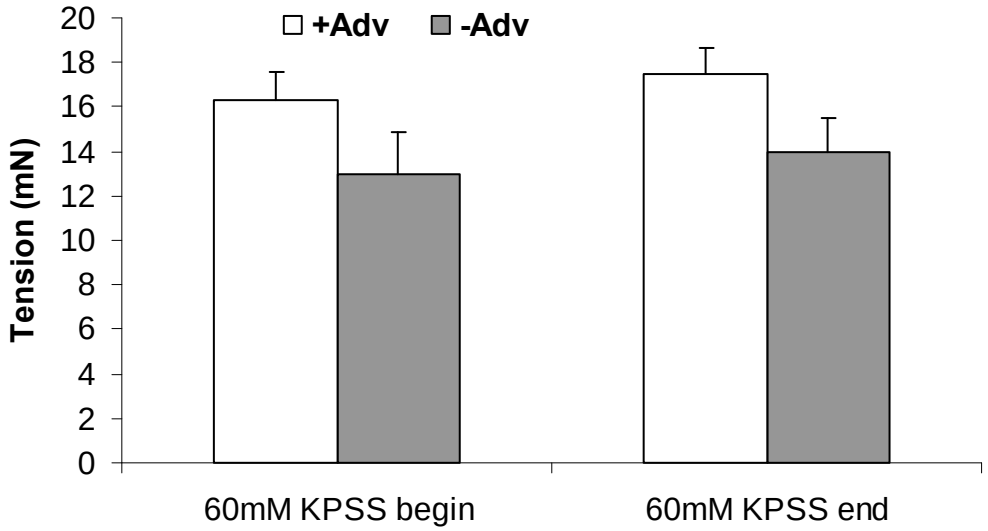

Figure 4.7 Comparison of the effect of 60 mM KPSS on rat mesenteric resistance arteries (MRA) (+Adv and –Adv) at the start and conclusion of the experiment*. There was no significant difference between the groups in response to 60 mM KPSS-induced contraction ($p>0.05$ vs control, paired Student t-test). Values are means ± SEM (n=8).*

The functionality of the endothelium was tested by the use of the endothelium-dependent relaxant ACh to ensure that the chemical dipping did not damage the endothelium. ACh causes relaxation with presence of endothelium and constriction without endothelium. ACh (10^{-7} M) caused vasodilatation in +Adv and –Adv by 92.9 ± 5.0 % and 77.3 ± 7.4 %, respectively (Figure 4.8). Both of the groups showed complete relaxation with 10^{-6} M. The endothelium was considered intact in –Adv as there was no significant difference compared to the control.

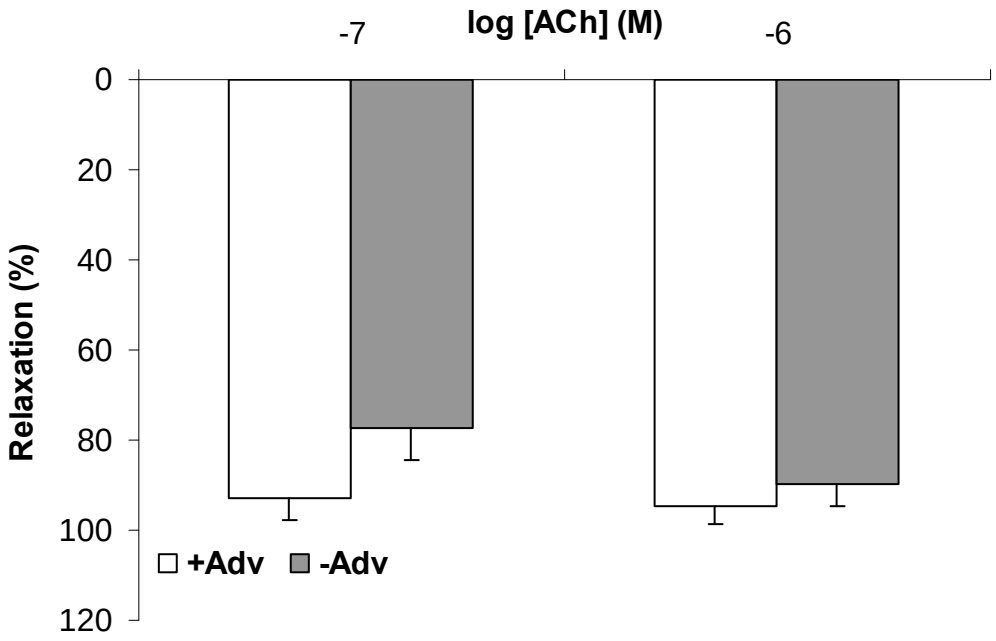

Figure 4.8 The effect of endothelium-dependent relaxant, acetylcholine (ACh) (10^{-7} and 10^{-6} M) on vasodilator response of +Adv and –Adv mesenteric resistance arteries (MRA). *The relaxation response of -Adv showed no difference with +Adv's relaxation ($p>0.05$, paired Student t-test). Values are means ± SEM (n=6).*

Sodium nitroprusside (SNP) is a nitric oxide (NO) donor (nitrovasodilator). It was used in this study as an endothelium-independent relaxant as relaxation mechanisms have been found to be mediated in the VSM (Gunduz *et al.*, 2009). Therefore, SNP can be used as a marker for VSM viability. At 10^{-7} and 10^{-6} M, SNP caused almost complete relaxation in +Adv and –Adv (Figure 4.9), confirming the VSM functional viability in –Adv.

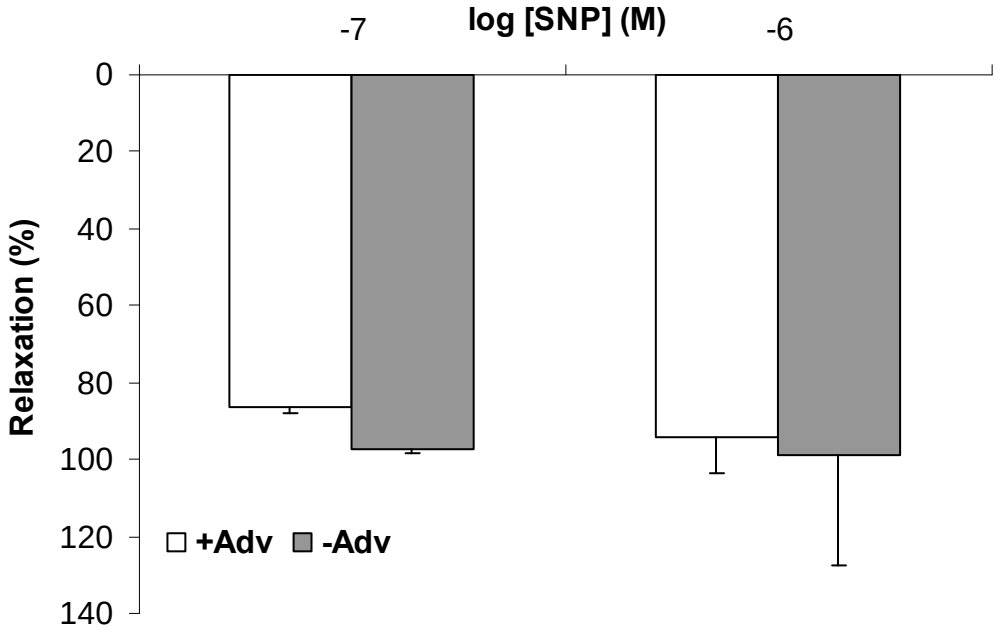

Figure 4.9 The effect of endothelium-independent relaxant, sodium nitroprusside (SNP) (10^{-7} and 10^{-6} M) on vasodilator response of the +Adv and –Adv mesenteric resistance arteries (MRA). *The relaxation response of -Adv showed no difference with +Adv's relaxation. ($p>0.05$, paired Student t-test). Values are means ± SEM ($n=6$).*

Nicotine at 10^{-5} M was chosen as the marker for adventitial-dependent function based on a previous study (Tsutsui *et al.*, 1999). The nicotine response was conducted in the presence of Gua. The +Adv showed relaxation of 52.8 ± 2.8 %, and in the –Adv maximum relaxation response was reduced to 14.1 ± 2.9 % significantly ($p<0.05$, paired Student t-test) as compared to control (+Adv) (Figure 4.10).

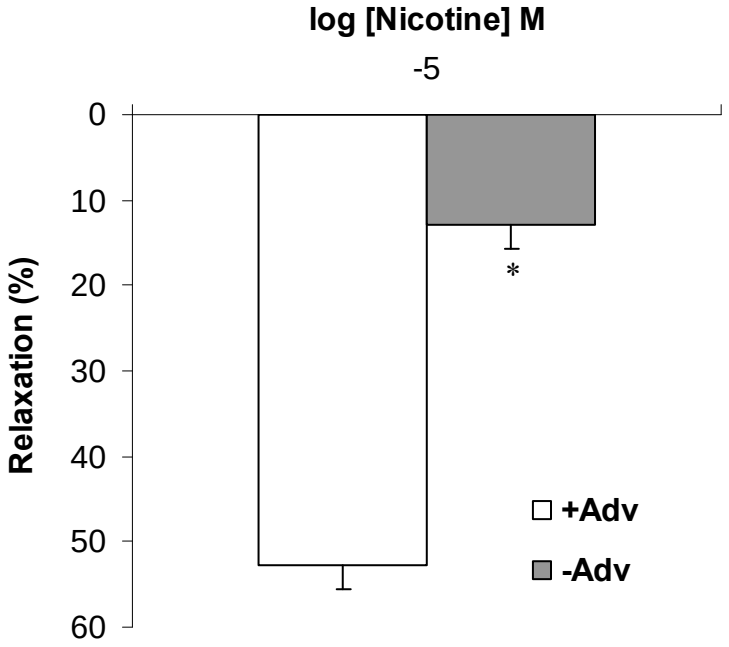

Figure 4.10 The effect of perivascular nerve relaxant, nicotine (10^{-5} M), on vasodilator response of +Adv and –Adv mesenteric resistance arteries (MRA). *A significant attenuation ($p<0.05$) of relaxation by nicotine in –Adv vs. +Adv. (*$p<0.05$ vs control, paired Student t-test). Values are means ± SEM (n=5).*

Transmural nerve stimulation

Figure 4.11 shows the real-time tracing of the TNS experiment. The 60 mM KPSS wash was conducted at the start and end of each experiment to ensure reproducible tissue viability. In Figure 4.12, the control vessels (+Adv) showed increasing contraction to frequency (1-16 Hz) in a frequency-dependent manner. The frequency-dependent contractile response was significantly attenuated after adrenergic blocker Gua incubation (30 min), indicating that the contractile response was neurogenic.

A complete abolishment of the neurogenic contraction was observed in –Adv when stimulated at 16 Hz (Table 4.2). Increasing the voltage with constant frequency (16 Hz) also failed to initiate any neurogenic contraction. The neurogenic contraction between control and intervention was compared at 16 Hz. The data was expressed in percentage of constriction to 60 mM KPSS-induced contraction. The control with adventitia intact (+Adv) showed 59.3 ± 3.4 % of contraction, and was significantly reduced to 10.7 ± 4.1 % after Gua treatment. When the adventitial function was ablated by paraformaldehyde (-Adv), the contraction was abolished significantly at 0.1 ± 0.1 %. The tissues were viable throughout the experiment shown by consistent 60 mM KPSS contraction.

TNS experiment was attempted in +Adv MCA segments. The real-time tracing in Figure 4.13 showed a neurogenic contractile response with the first stimulation at 16 Hz, confirming presence of nerve fibres. However, after a few more stimulations, the contractile response did not last probably due to lack of innervation. Therefore, TNS was not further conducted in MCA.

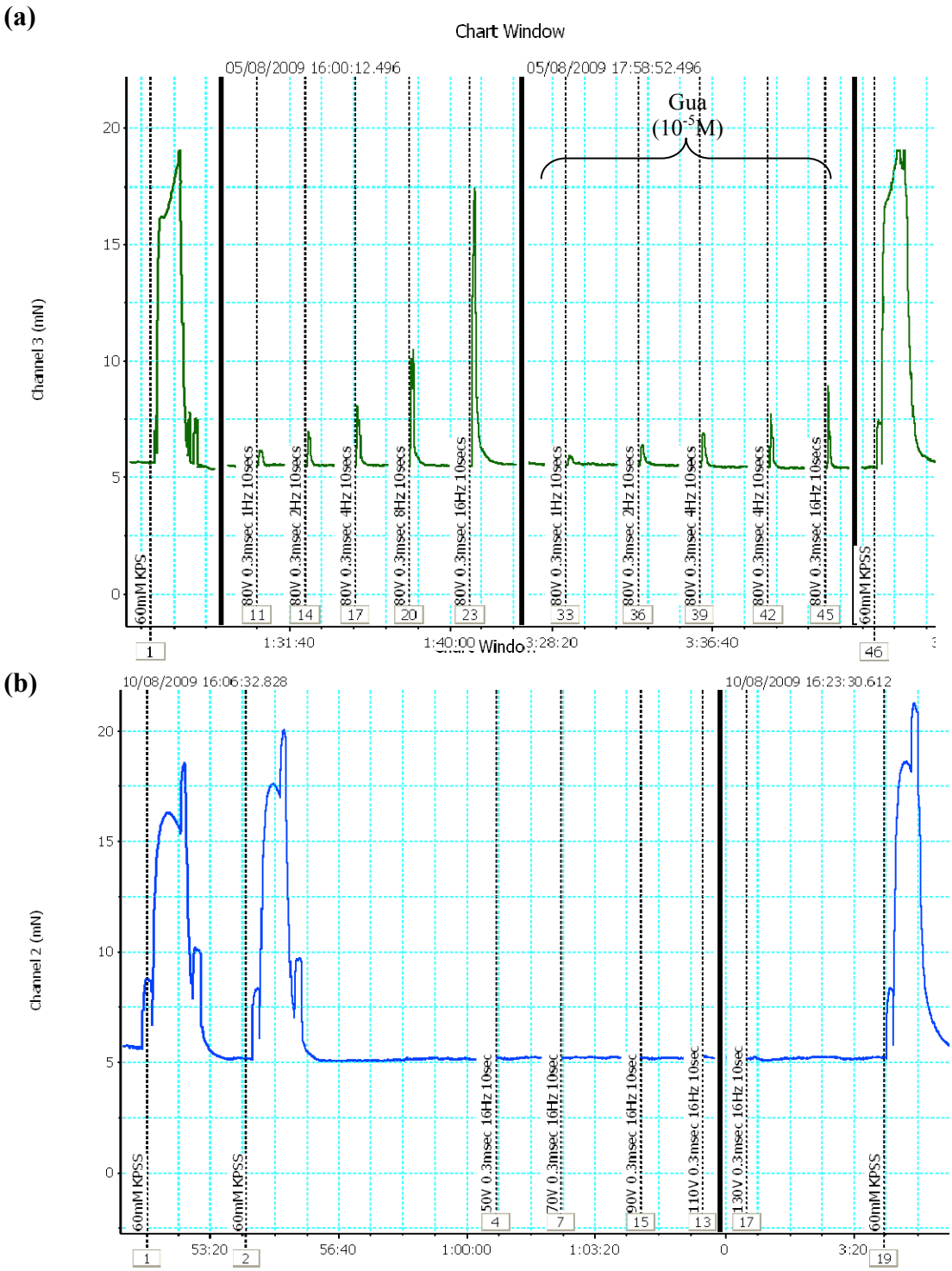

Figure 4.11 Typical real-time tracing of TNS. (a) *Frequency-dependent contractile response (1-16 Hz) in +Adv mesenteric resistance arteries (MRA). The response was attenuated by the adrenergic neuron blocker, guanethidine (Gua) in +Adv* ***(b)*** *The neurogenic contraction was abolished in –Adv at 16 Hz, even at an increasing voltage.*

Table 4.2 Neurogenic contractile response in mesenteric resistance arteries (MRA). *Neurogenic contractile response at 16 Hz in control (+Adv), guanethidine (Gua)-treated (+Adv) and chemically dipped (-Adv). Results are expressed as percentage of constriction to 60 mM KPSS wash (*p<0.05 vs. +Adv and #p<0.05 vs. +Adv, paired Student t-test respectively). Values are means ± SEM (n=6).*

Frequency	Control (+Adv)	+ Gua (+Adv)	Chemically dipped vessel (-Adv)
16 Hz	59.3 ± 3.4 %	10.7 ± 4.1 % *	0.1 ± 0.1 % #

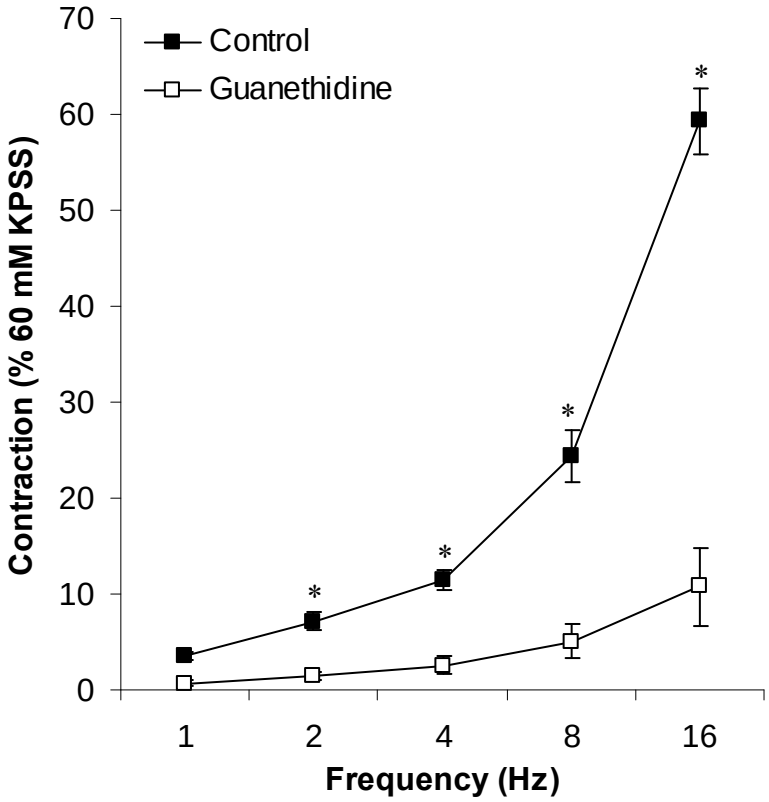

Figure 4.12 Neurogenic contractile response (1-16 Hz) in control (+Adv) and guanethidine (Gua)-treated mesenteric resistance arteries (MRA). **p<0.05 vs control, ANOVA for repeated measure and Bonferroni post hoc. Values are means ± SEM (n=6).*

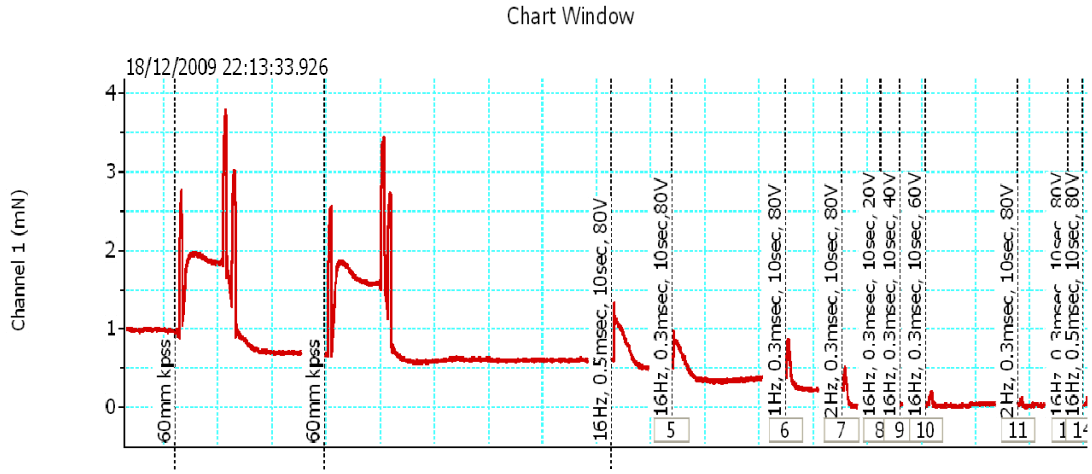

Figure 4.13 A representative of a real-time transmural nerve stimulation (TNS) tracing in a rat middle cerebral artery (MCA). *The beginning of the experiment was started off with standard 60 mM KPSS washes. Electric stimulations were conducted at different frequencies and voltages. The initial neurogenic contractile response faded with time.*

(b) Rat middle cerebral artery

Vascular integrity by confocal microscopy

Confocal microscopy was again used to investigate the level of cellular trauma across the MCA, from the adventitia layer to the endothelium, after the adventitial ablation technique. Figure 4.14 shows the image of a MCA after being dipped with paraformaldehyde for 15 s (-Adv). Green is the autofluorescence and red is PI-positive stained nucleus. Only the outmost layer (the adventitia) was compromised as it was exposed to the chemical treatment. This has proven that the 4 % paraformaldehyde dipping did not penetrate through the vessel wall and damage the cells.

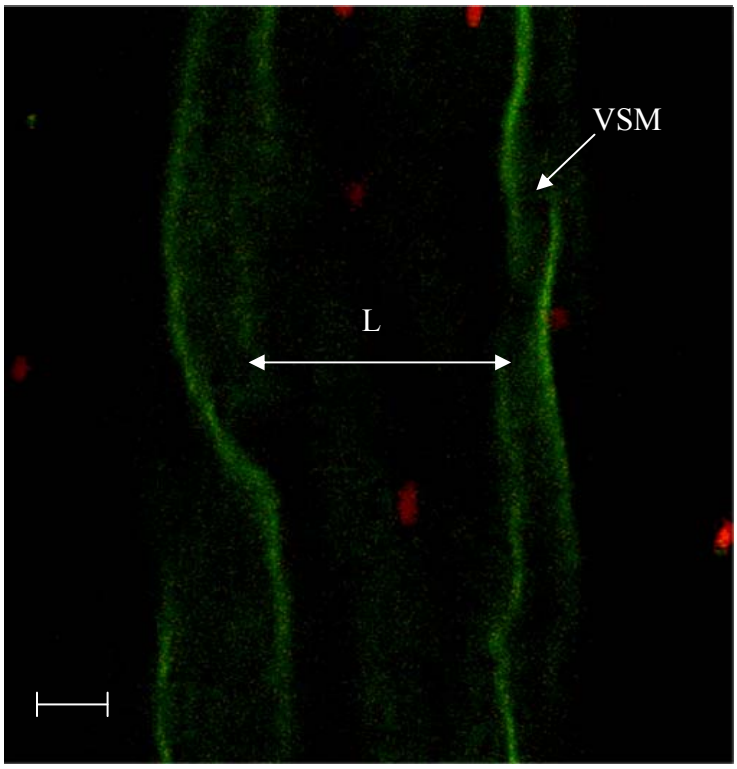

Figure 4.14 Representative confocal image demonstrating the effect of 4 % paraformaldehyde (15 s) on the middle cerebral artery (MCA). *The image shows the VSM and lumen (L) of MCA after being dipped in 4 % paraformaldehyde (-Adv). Green is the elastin autofluorescence and red is propidium iodide-stained nucleus. Only the outmost layer (the adventitia) was compromised as it was exposed to the chemical treatment. The confocal images have proven that the 4 % paraformaldehyde dipping did not penetrate through the vessel wall and damage the cells because there was no red staining of dead cells within the vessel. Magnification was taken at x40 oil objective. Bar represents 20 µm. One representative of three experiments.*

Vascular functional tests by wire myography

Figure 4.15 shows that the 60 mM KPSS-induced contraction resulted in no significant difference between +Adv and –Adv.

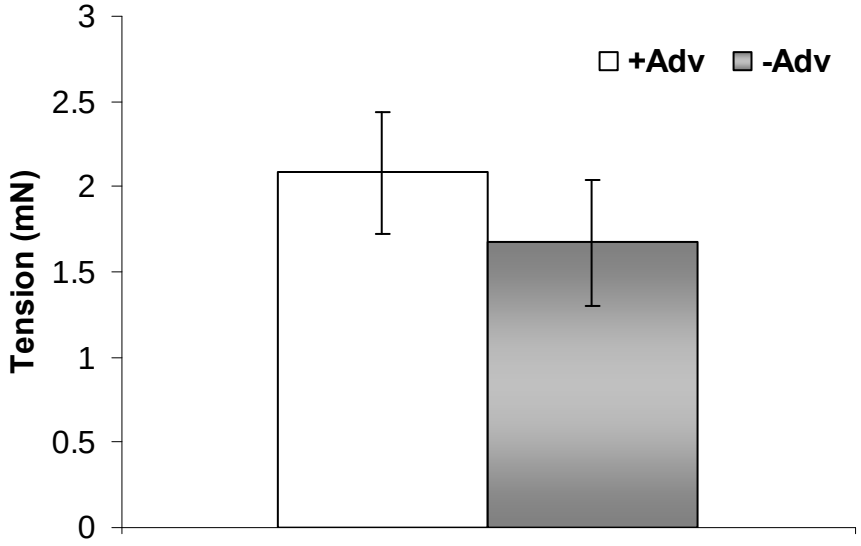

Figure 4.15 Comparison of the effect of 60 mM KPSS in +Adv and –Adv rat middle cerebral arteries (MCA). *There is no significant difference in both of the groups ($p>0.05$ vs control, paired Student t-test). Values are means ± SEM (n=8).*

Figure 4.16 shows the contraction to the vasoconstrictor 5HT at 10^{-7} and 10^{-6} M in +Adv and –Adv. There was no significant difference between both groups, indicating that the VSM in -Adv is still intact.

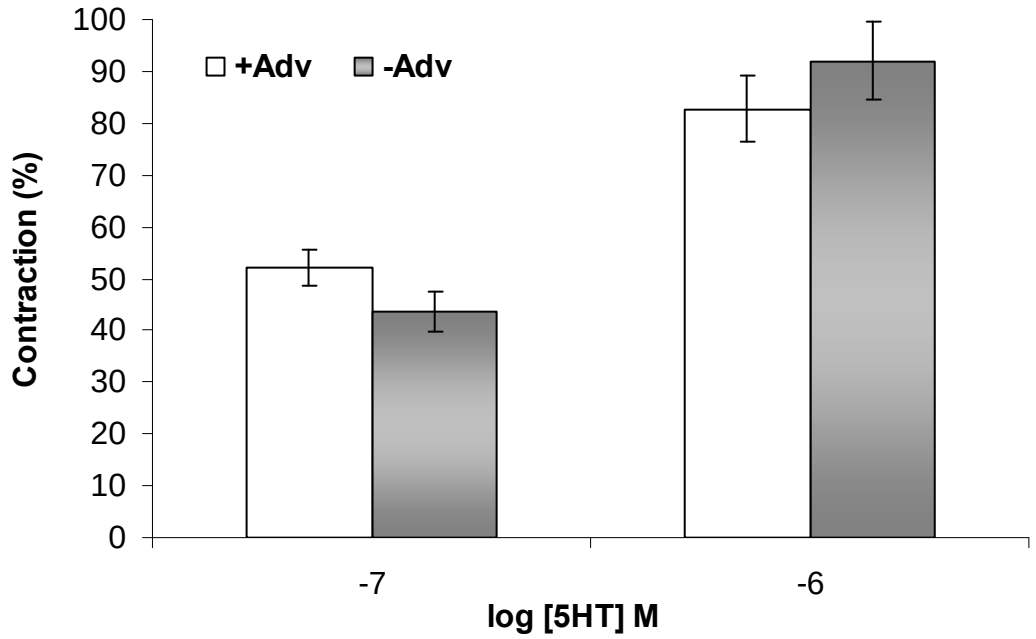

Figure 4.16 The effect of constrictor agonist, serotonin (5HT) (10^{-7} and 10^{-6} M) in +Adv and –Adv middle cerebral arteries (MCA). *The result has shown that the receptor-dependent contraction was still viable after chemical treatment as there was no significant difference ($p>0.05$, paired Student t-test) compared to +Adv contraction. Values are means ± SEM (n=9-10).*

Endothelium-dependent relaxant ACh caused vasodilatation at 10^{-7} M and 10^{-6} M with no significant difference in +Adv and –Adv (Figure 4.17). These data showed that the endothelium in –Adv was still intact.

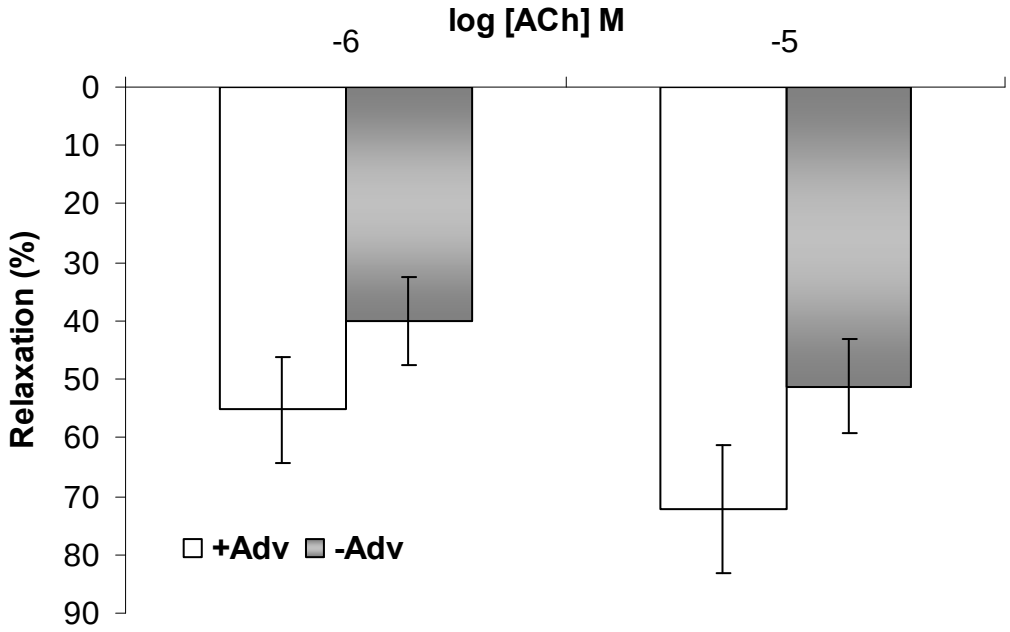

Figure 4.17 The effect of endothelium-dependent relaxant, ACh (10^{-7} and 10^{-6} M) in +Adv and –Adv middle cerebral arteries (MCA). *The relaxation response of –Adv showed no difference to +Adv ($p>0.05$, paired Student t-test). Values are means ± SEM (n=7).*

As for endothelium-independent relaxation, a NO donor, SNP, was used. At 10^{-6} M, SNP caused almost complete relaxation in -Adv, similar to +Adv (Figure 4.18). This shows that although the adventitial function was damaged, the VSM in –Adv remained viable.

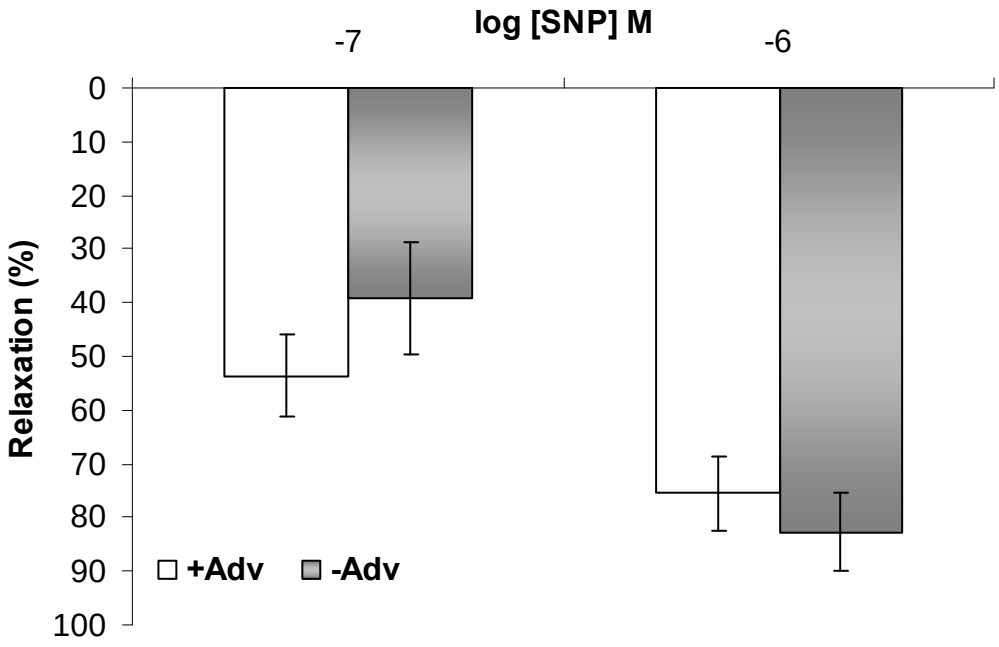

Figure 4.18 The effect of endothelium-independent relaxant, SNP (10^{-7} and 10^{-6} M) in +Adv and –Adv middle cerebral arteries (MCA). *There were no significant difference between +Adv and –Adv. ($p>0.05$, paired Student t-test). Values are means ± SEM (n=9-10).*

Nicotine at 10^{-5} M was chosen as the marker for adventitial-dependent function. The nicotine response was conducted with the presence of Gua to ensure nicotine gives only a relaxation effect, as explained previously in the methods section. The control vessel (+Adv) showed a relaxation of 65.2 ± 6.9 %. The 15-sec dipping (-Adv) significantly reduced the maximum relaxation response to 18.8 ± 8.9 % ($p<0.05$, paired Student t-test) compared to +Adv (Figure 4.19).

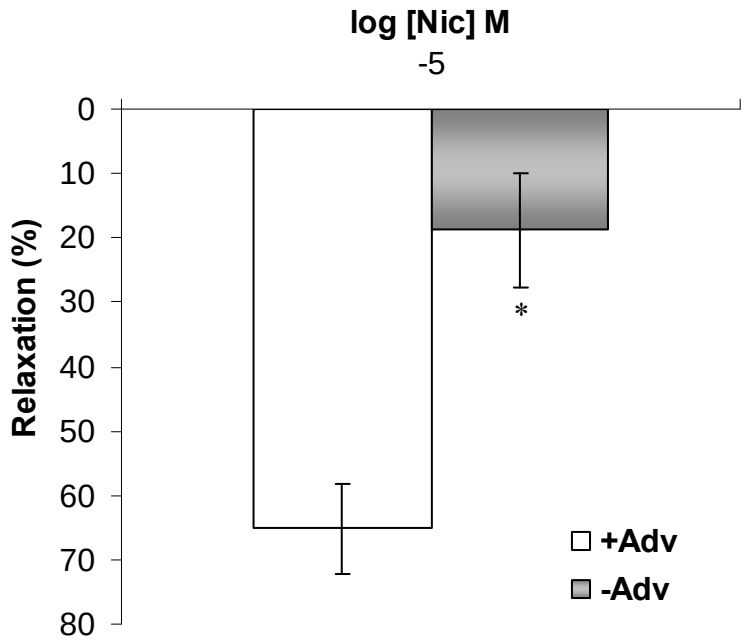

Figure 4.19 The effect of perivascular nerve stimulant, nicotine (10^{-5} M) in +Adv and –Adv middle cerebral arteries (MCA). *–Adv vessel showed significant reduction in relaxation response compared to +Adv. *p<0.05 vs control (paired Student t-test). Values are means ± SEM (n=7-8).*

Vascular passive mechanical properties

Figure 4.20 to Figure 4.25 show the passive mechanical properties of +Adv and –Adv MCA under fully relaxed conditions (Ca^{2+}-free extracellular conditions). There were no significant differences between +Adv and –Adv in the change of external-diameter (Figure 4.20), wall/lumen ratio (Figure 4.21a) and cross-sectional area (CSA) (Figure 4.22b) to increasing intraluminal pressure (5-140 mmHg). Incremental distensibility, a direct measure of circumferential compliance, showed no significant difference in either +Adv or –Adv (Figure 4.22). Circumferential stress and circumferential strain were plotted over the pressure curve (Figure 4.23). The exponential fit gave a good R^2 value ($R^2 > 0.900$) and the 'J'-shaped curve which is typically seen in passive-state arteries (Figure 4.24). The R^2 value for +Adv and –Adv were 0.971 and 0.991, respectively. The overall stiffness (β) calculated for passive-state vessels again showed no difference between +Adv and –Adv (Figure 4.25). These data have confirmed that the adventitial ablation technique did not change any of the passive mechanical properties of the small artery.

(a)

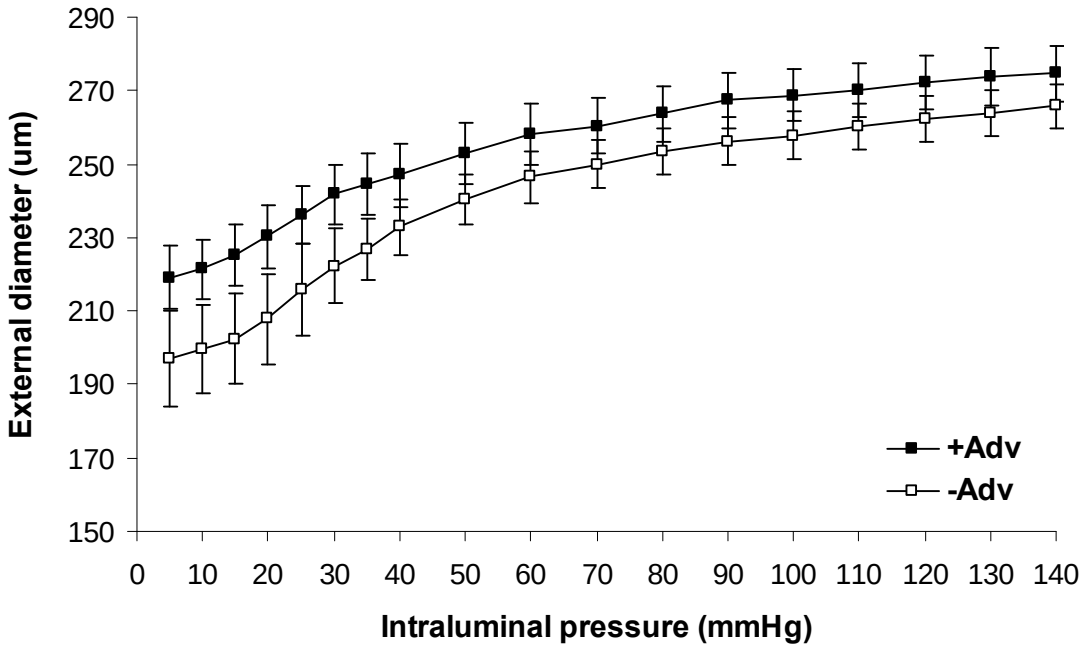

(b)

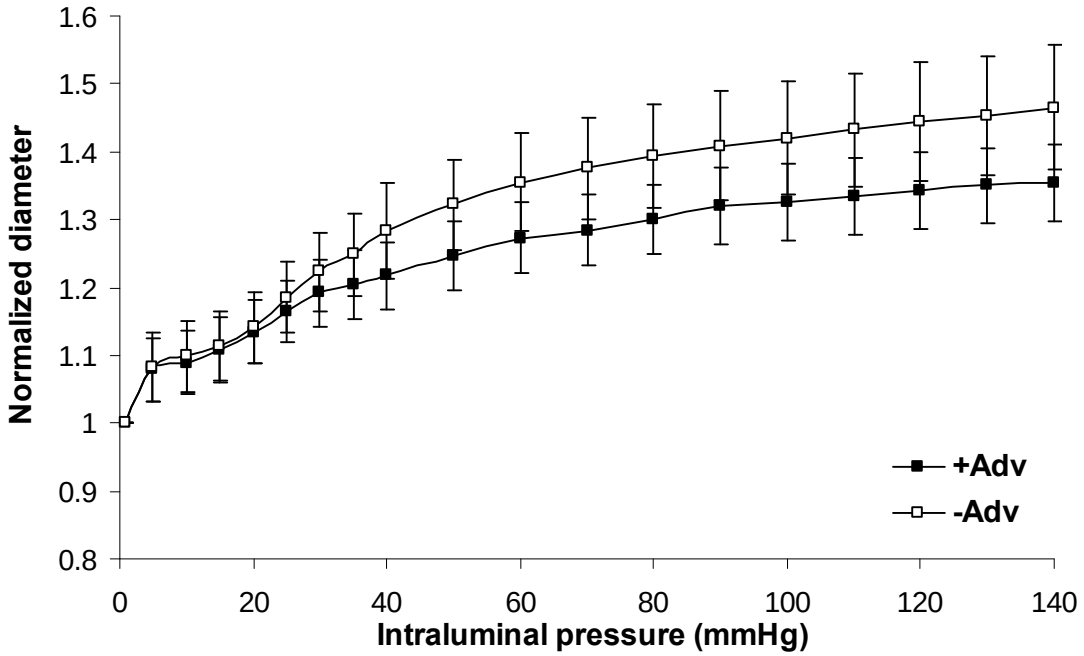

Figure 4.20 Passive external diameter and normalized diameter in relation to intraluminal pressure in +Adv and -Adv middle cerebral arteries (MCA) (a) *The passive external diameter and* ***(b)*** *normalized diameter (compared to initial diameter at 5 mmHg) in fully relaxed MCA. Each point represents mean ± SEM (n=7-8).*

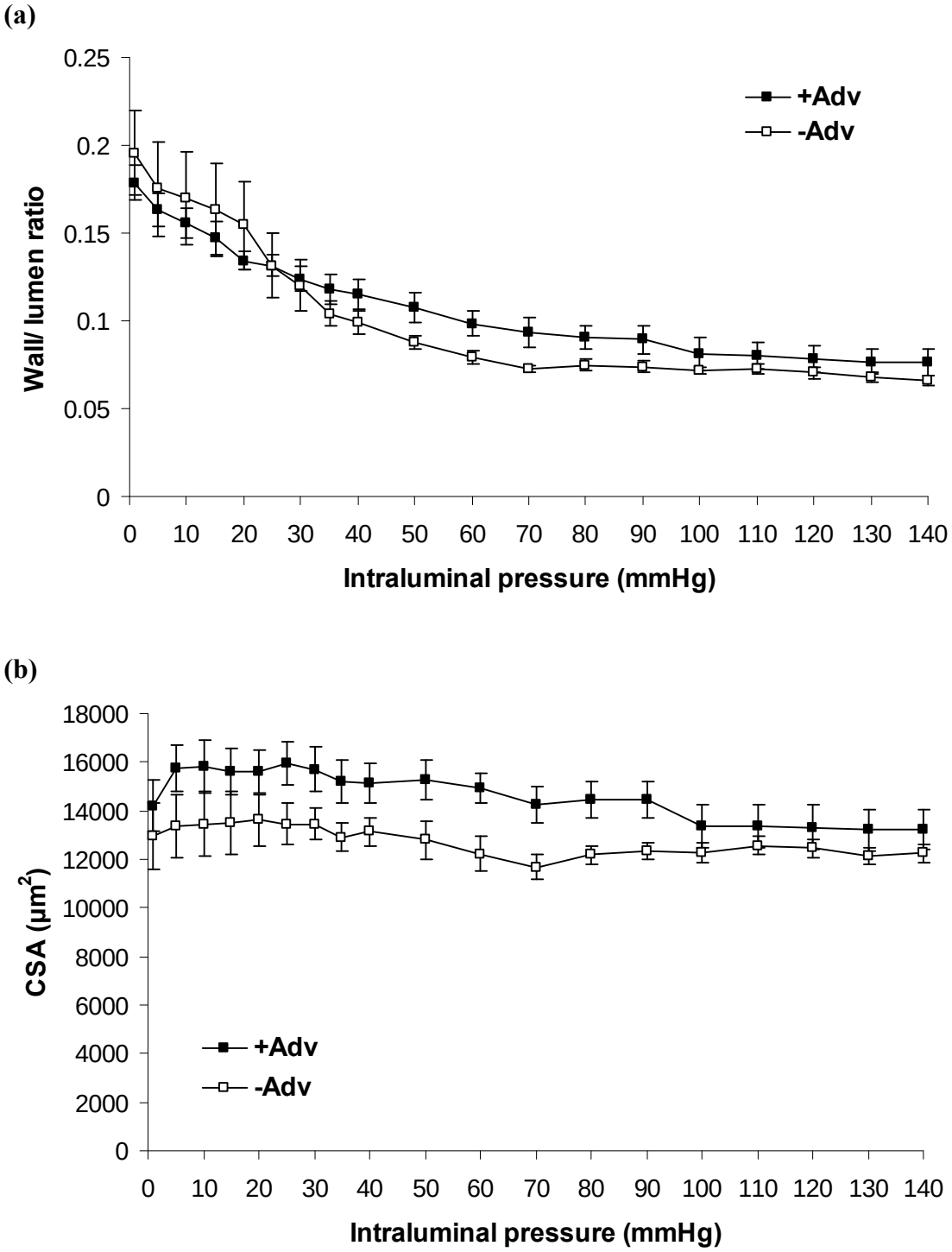

Figure 4.21 Wall:lumen ratio and cross-sectional area in +Adv and –Adv middle cerebral arteries (MCA) (a) *The relations of wall:lumen ratio-intraluminal pressure and* ***(b)*** *cross-sectional area (CSA)-intraluminal pressure in fully relaxed MCA. Each point represents mean ± SEM (n=6-8).*

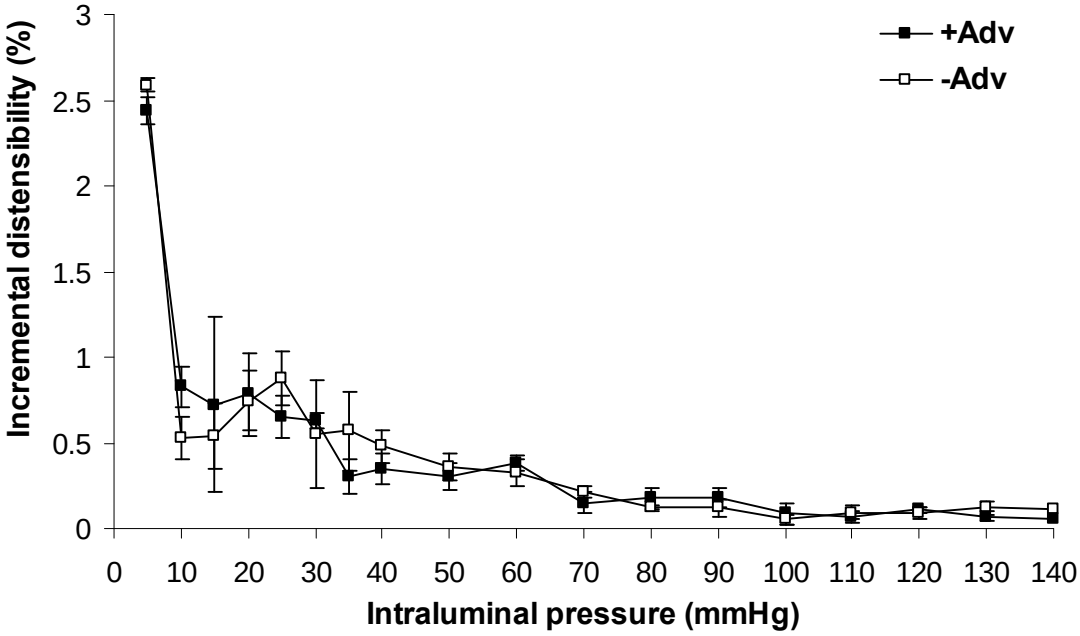

Figure 4.22 The relationship of incremental distensibility-intraluminal pressure in fully relaxed middle cerebral arteries (MCA) +Adv and -Adv*. Each point represents mean ± SEM (n=7-8).*

(a)

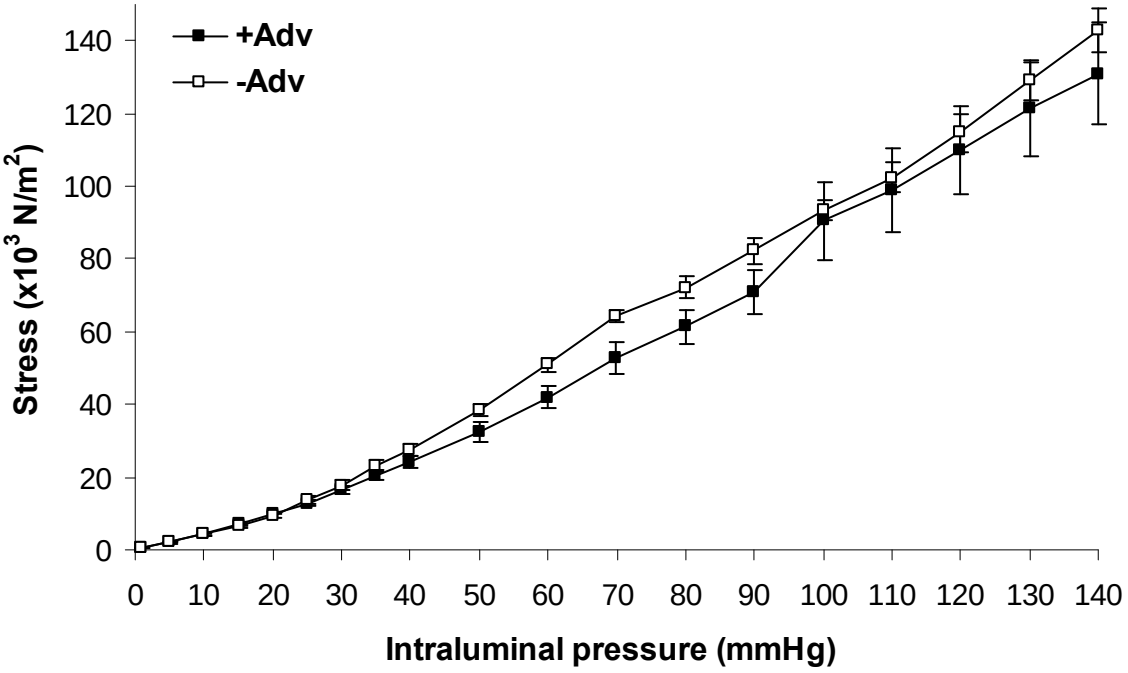

(b)

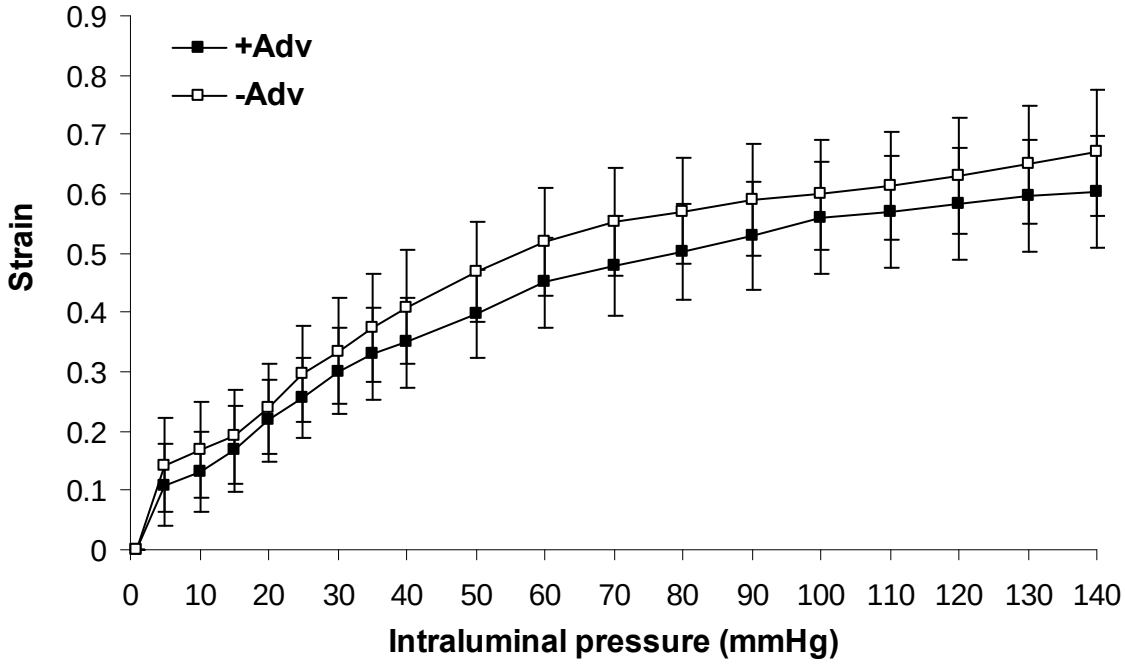

Figure 4.23 Stress and strain relations in +Adv and –Adv middle cerebral arteries (MCA) (a) *Passive relations of stress-intraluminal pressure and* ***(b)*** *strain-intraluminal pressure in fully relaxed MCA. Each point represents mean ± SEM (n=6-8).*

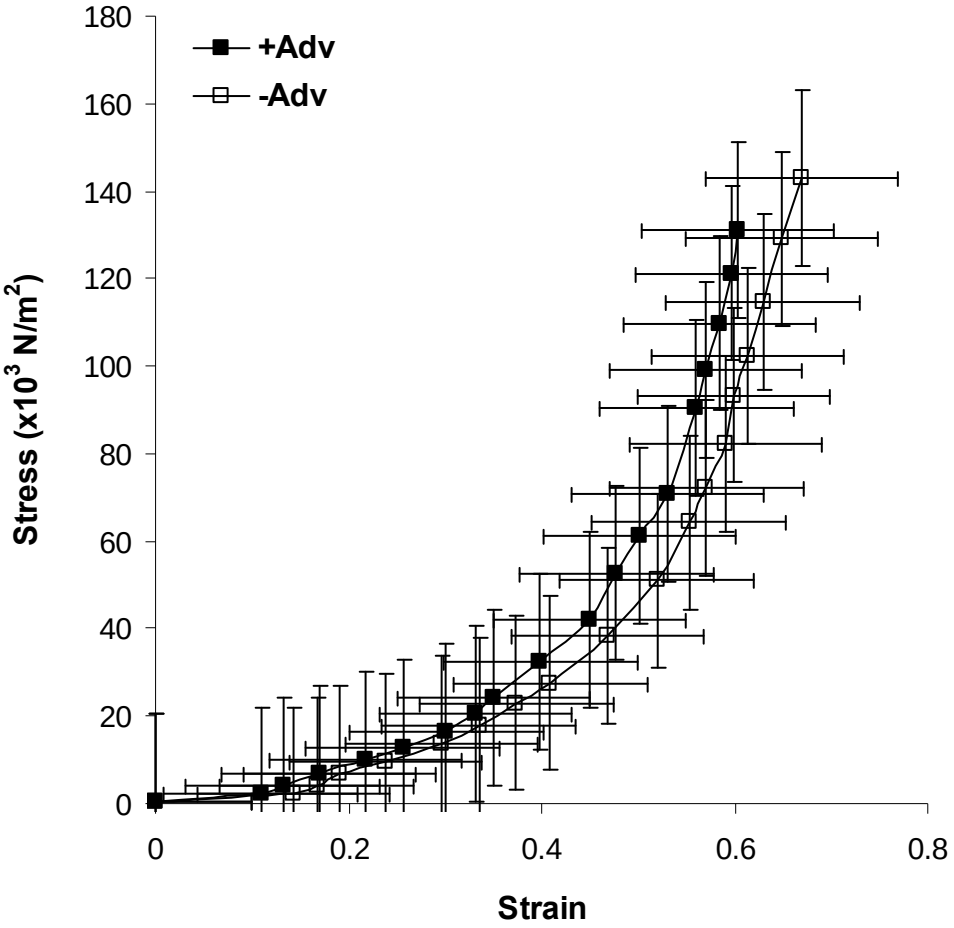

Figure 4.24 The stress-strain relation in +Adv and –Adv middle cerebral arteries (MCA). *Each point represents mean ± SEM (n=6-7).*

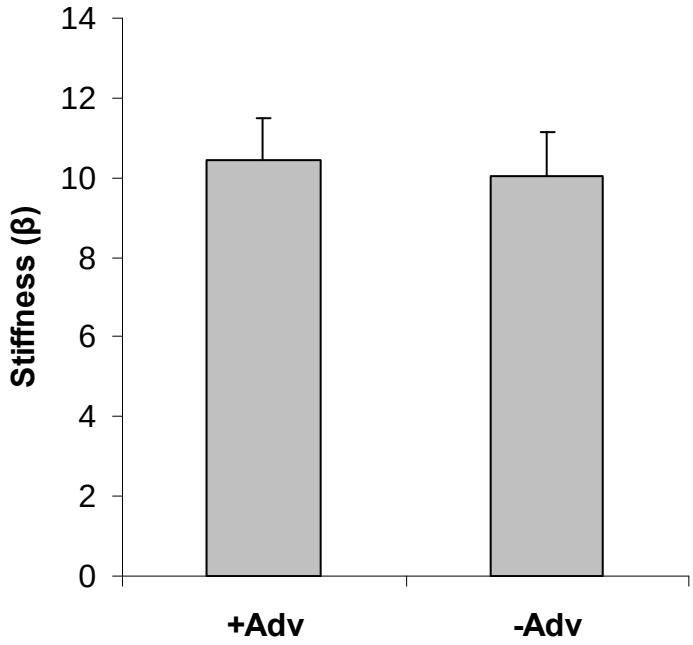

Figure 4.25 Average values of the stiffness parameter (β) for passive +Adv and –Adv middle cerebral arteries (MCA). *Each bar represents mean ± SEM (n=6-7).*

4.5 Discussion

For the first time, this study has adapted a simple, nontraumatic chemical method for ablating the adventitial function in resistance arteries that, 1) allows complete adventitial dysfunction, 2) preserves medial and intimal function, 3) maintains the passive mechanical properties, and 4) is reproducible in different types of vessels.

4.5.1 Preliminary study on adventitial removal by collagenase type II enzyme

The physiological function of the adventitial layer has been well-known to be the site of nerves that innervate underlying tissues (Lee *et al.,* 1983). To study vascular reactivity devoid of adventitia, it is crucial to establish a method that does not damage the medial and endothelial layers. Enzymatic methods for removing the adventitia have been proven to be successful in the rat iliac and carotid arteries (Gonzalez *et al.*, 2001b). However, this enzymatic method was proven to be unsuccessful in the preliminary study with rat small mesenteric arteries and cerebral arteries. The damage to the stripped vessel wall was confirmed using confocal

microscopy where dead cells within the vessel wall were apparent. The contractile response in –Adv was also affected. In conclusion of the preliminary study, this suggests that mechanical removal of the adventitia without damaging the vessel wall is not feasible. Rat mesenteric arteries consists of only two to three layers of smooth muscle cells (Walker-Caprioglio *et al.* 1991) and the cerebral artery is lacking an external elastic laminae (Lee, 1995), thus it may not be possible to remove the adventitia by stripping mechanically without damaging the medial layer. However, when the collagenase method was repeated in aorta, VSM contraction to 60 mM KPSS was viable. The aorta is a relatively thick elastic structure which is extremely dense with elastin and collagen (Wheater *et al.* 1979). Therefore, the aorta is not as fragile as resistance arteries in response to enzymes and mechanical stripping.

4.5.2 Adapting adventitial ablation technique by paraformaldehyde treatment

The focus of this study was then diverted from enzyme treatment to chemical treatment as it may serve as a better method for adventitia removal in small arteries. The two tissue models, i.e. rat MCA and MRA, both showed similar results. For this reason, the MCA and MRA will be discussed collectively. The degree of VSM and external elastic laminae damage was tested by confocal microscopy with unfixed treated-vessel (-Adv) stained with PI. The confocal results have shown that the chemical treated vessel was still viable. Contraction to 60 mM KPSS in+Adv and -Adv showed no significant difference. The 60 mM KPSS is widely known to increase VSM depolarization leading to the opening of VOCC with subsequent Ca^{2+} influx and finally vascular contraction (Wang *et al.*, 2001). With this current result, it was confirmed that paraformaldehyde dipping did not affect the primary depolarization-contraction mechanism in –Adv.

Nicotine-induced relaxation in +Adv and –Adv were compared to determine the damage to the adventitial layer. An earlier study has shown that nicotine stimulated presynaptic nicotinic cholinoceptors release noradrenaline (NA) or related substances, which then stimulated NO release from neighbouring non-adrenergic non-cholinegic (NANC) nitrergic nerves (Shiraki *et al.*, 2000). Subsequent studies

have proven otherwise, whereby nicotine-induced vasodilatation was independent of the endothelium and dependent on adrenergic nerves. This could then activate vanilloid-1 receptors located in the adjacent calcitonin gene-related peptide CGRPergic nerves to release adrenergic related substances and vasodilator CGRP (Eguchi *et al.*, 2007, Kawasaki *et al.*, 2009). In spite of these arguments on the exact action of nicotine, the greatest interest was its vasodilatory effect which could be inhibited by the adrenergic blocker guanethidine (Zhang *et al.*, 1998, Toda and Okamura, 2003, Kawasaki *et al.*, 2009).

In this present study there was no difference with ACh and SNP response in +Adv and -Adv. ACh is an endothelium-dependent relaxant, whereas SNP is a potent NO donor in the VSM, independent of Ca^{2+} influx and the presence of endothelium. The relaxation mechanism has been found to be mediated by signalling in the VSM, such as increase of guanylate cyclase/cyclic guanosine monophosphate (cGMP) (Kagota *et al.*, 2001) and thromboxane A_2 (Iwatani *et al.*, 2008). Also, NO release from SNP stimulates cGMP/ protein kinase G (PKG) that activated the Ca^{2+} pump that removes Ca^{2+} out from the intracellular space and hence causes relaxation of VSM (Iwatani Y *et al.*, 2007). The results have shown that quick paraformaldehyde treatment did not affect the functions of the endothelium and VSM in –Adv compared to +Adv. This suggests that the method was successful to eradicate adventitial-dependent function and maintain functionally and structurally intact underlying smooth muscle and endothelium.

Transmural nerve stimulation (TNS) is an easy confirmation method of adventitial ablation in paraformaldehyde-treated vessels as the nerves are located mostly in adventitial-medial border (Kido *et al.*, 2001, Birch *et al.*, 2008). This method has been widely used in various types of tissues, such as mesenteric arteries (Klinge and Sjostrand, 1977, Jayasundar and Vohra, 1978, Sanchez-Fernandez *et al.*, 2004), vas deferens (Klukovits *et al.*, 2002) and uterus (Itoh *et al.*, 1995). As the mesenteric arteries are well-innervated, the +Adv vessels showed an increasing neurogenic frequency-dependent contractile response. To confirm the contractions were neurogenic, Gua was used and the contractile response was attenuated significantly.

In –Adv, complete abolishment of the neurogenic contraction was observed at the highest frequency (16 Hz). This is additional confirmation that the innervation of the –Adv MRA was completely damaged by paraformaldehyde treatment. The TNS method did not work in the lab with MCA. According to a review by Lee (1995), myelienated and unmyelienated nerves are found in proximal basilar arteries and only one or two myelienated nerves are found in the MCA. Therefore, TNS is not a suitable experiment for vessels, which are not well-innervated like the MCA.

The major components in resistance arteries that determine the mechanical properties and thereby the calibre of the vessels are elastin and collagen, these being the passive elements and smooth muscle being the active element (Dobrin, 1978, van den Akker *et al.*, 2010). In the study of vascular remodelling for instance, passive mechanical properties are typically investigated rather than maximally active VSM because these two main passive elements are the major contributors to the vascular wall stiffness. Dobrin (1978) and van den Akker *et al.* (2010) have given in-depth reviews on the mechanical properties of small arteries. According to the reviews, the adventitia is especially rich in collagen and it can provide stiffness and tensile strength when sufficiently loaded with transmural pressure. Elastin is an important element in vascular wall structures likewise collagen also found in the media and adventitia (Briones *et al.*, 2005).. The passive stress-strain relationship of arteries is nonlinear due to the composite action of collagen and elastin found in both the internal elastic lamina and media (Coulson *et al.*, 2002). The dense focal adhesions at the membrane and actin cytoskeleton have been considered to form the mechanical base in VSM (van den Akker *et al.*, 2010). Polymerization of G-actin to F-actin was required for tension generation in VSM, providing membrane rigidity and adaptation to local forces (Gunst and Zhang, 2008). However, it is still unclear whether actin polymerization is independent of actomyosin contraction. In normal circumstances, the incremental elastic modulus (the slope of the stress-strain relationship) is constant over a large part of autoregulatory range due to the distensibility of elastic fibres (van den Akker *et al.*, 2010). However, in pathological conditions like CLI (Coats, 2010), hypertension (Briones *et al.*, 2005) and metabolic syndrome (Phillips *et al.*, 2005), the stress-strain relationship can be altered. Therefore, investigation into the stress-

strain and stiffness in –Adv vessels as in this study could determine whether or not the adventitial ablation technique is detrimental. Results have shown that the wall/lumen ratio, cross-surface area, incremental distensibility were not altered in –Adv vessels. Therefore, the derived stress-strain relationship and stiffness calculations showed no difference between –Adv and the normal vessel. The initial shallow slope in the stress-strain relationship is due to the deformation of the highly extensible elastin fibres, and the steepest portion is due to the recruitment of the stiffer collagen fibres (Coulson *et al.*, 2002, Briones *et al.*, 2005, van den Akker *et al.*, 2010). This is a promising result because this showed that paraformaldehyde treatment did not affect the passive mechanical properties which comprised mainly extracellular collagen and elastin.

4.5.3 Conclusion

In conclusion, this chapter has demonstrated a chemical method for producing resistance arteries lacking adventitial function. This adventitial-ablation method was proven reproducible as it was successful in models of rat mesenteric and rat middle cerebral arteries. Although the adventitial function was ablated, the medial and intimal functions were still intact in –Adv. The mechanical properties were maintained in –Adv like a normal vessel. Therefore, transient paraformaldehyde dipping has proven to be a successful technique for ablating adventitial function. Application of this technique has the potential to aid study of adventitial-dependent and adventitial-independent contribution to vascular function in small resistance arteries.

CHAPTER 5:
MODULATING PRESSURE-DEPENDENT MYOGENIC TONE: ROLE OF ADVENTITIAL-DERIVED REACTIVE OXYGEN SPECIES

5.1 Introduction

An increasing body of evidence has shown the direct participation of the adventitia in vascular function (An *et al.*, 2007, Haurani and Pagano, 2007, Pagano and Gutterman, 2007, Di Wang *et al.*, 2010). The main limitation for further study of the adventitia within an intact tissue is the difficulty in separating the vascular layers, despite many previous attempts (Kemler *et al.*, 1997, Gonzalez *et al.*, 2001). This current study (Chapter 4) has developed a technique to ablate the adventitial function in small arteries that preserves medial and intimal function as well as vascular integrity, which could be applicable for future investigation of adventitial and non-adventitial myogenic responses.

The initial indication that ROS enhanced or sustained myogenic responses physiologically was found in tail arterioles (Nowicki *et al.*, 2001, Bailey *et al.*, 2005), mesenteric arteries (Veerareddy *et al.*, 2004) and skeletal muscle arterioles (Coats and Wadsworth, 2004). The involvement of ROS in VSM Ca^{2+} signalling is a relatively new area of interest (Miura *et al.*, 2003, Cheranov and Jaggar, 2006, Resta *et al.*, 2010, Shimoda and Undem, 2010, Trebak *et al.*, 2010). A growing body of evidence suggests that Ca^{2+} sensitivity in VSM, mediated by ROS, RhoA/Rho kinase and PKC, is underlying the mechanism of pressure-dependent myogenic tone (Gokina *et al.*, 2005, Schubert *et al.*, 2008, Resta *et al.*, 2010). Ca^{2+} sensitivity is a condition where GCPR stimulation leads to inactivation of MLCP, allowing accumulation of phosphorylated MLC and enhanced contraction (Schubert *et al.* 2008) have proposed that pressure-dependent myogenic constriction is mediated via two-phases, i.e. a predominant Ca^{2+}-dependent 'initiation/trigger' phase followed by a Ca^{2+}-independent 'maintenance' phase. Both phases are critical to the myogenic response because inhibition of either has the potential to abolish it.

A recent study on the interaction of ROS and Ca^{2+} in the development of myogenic tone demonstrated that the inflammatory cytokine TNF-α can activate intact cerebral Nox to produce acute H_2O_2, which then increased SR release. This leads to the opening of large-conductance Ca^{2+}-activated K^+ (K_{Ca}) channels, membrane

hyperpolarization and eventually to a reduced global $[Ca^{2+}]_i$ and cerebral vasodilatation (Cheranov and Jaggar, 2006). In contrast, a previous study has shown that internal RyR-sensitive Ca^{2+} stores are insignificant during the genesis of myogenic tone (McCarron *et al.*, 1997), which could possibly be due to the different conditions during inflammation (Cheranov and Jaggar, 2006) and normal physiology (McCarron *et al.*, 1997). In the study of pulmonary hypoxia, substantial evidence has shown that ROS can influence VSM $[Ca^{2+}]_i$. Exogenous and also endogenous ROS were found to mediate Rho/RhoA kinase-dependent VSM contraction in the lung by increasing the myofilament Ca^{2+} sensitivity in chronic pulmonary hypoxia (Resta *et al.*, 2010, Shimoda and Undem, 2010). While many studies provide evidence that ROS alters $[Ca^{2+}]_i$, in vitro studies have also shown that $[Ca^{2+}]_i$ may impact O_2^- formation, in particular via subunit NOX5 which contains a binding site for Ca^{2+} calmodulin and is involved in endothelial growth and inflammatory responses (Fulton, 2009, Montezano *et al.*, 2010).

To date, there have been no studies that have investigated the effect of intact non-adventitial arteries to pressure-dependent myogenic tone. This study hypothesized that adventitial-ablation directly attenuates ROS release and inhibits pressure-dependent myogenic response. In addition, this study will investigate the mechanistic relation of $[Ca^{2+}]_i$ changes during the process of adventitial or non-adventitial/Nox/ROS/myogenic tone.

5.2 Aims

1. To measure the effect of adventitial ablation on pressure-dependent myogenic tone.
2. To measure the release of ROS from the adventitia layer.
3. To identify adventititial-dependent influence on mechanisms underlying pressure-dependent myogenic tone.

5.3 Method

5.3.1 Tissue isolation

(a) Rat middle cerebral artery

Adult male Sprague-Dawley rats (12 weeks, 250-300g) were killed by cervical dislocation. The middle cerebral arteries (MCA) (177 ± 8 μm, *n*=15) were dissected from adherent tissue and immediately placed in ice-cold Krebs, as described in Section 2.1.1.

(b) ***Rat mesenteric artery***

Adult male Sprague-Dawley rats (12 weeks, 250-300g) were killed by cervical dislocation. The 2nd-order mesenteric resistance arteries (MRA) (345 ± 2 μm, *n*=17) from the main proximal branch were dissected and immediately placed in ice-cold Krebs, as described in Section 2.1.2.

5.3.2 Adventitial ablation technique

To disrupt the function of the adventitial layer, the outer surface of arterial rings was treated with 4 % paraformaldehyde (-Adv) for 15 s (Section 4.3.3). Then immediately the vessels were rinsed in cold PSS (4°C) before commencing an experiment. Control rings (+Adv) were not treated with 4 % paraformaldehyde. This method was conducted in two types of vessels for reproducibility purpose, i.e. MRA and MCA.

5.3.3 Pressure-dependent myogenic tone experiment with pressure myography

Isolated arteries were studied on a pressure myograph system (Danish MyoTech P110), cannulated and secured with fine nylon sutures to glass micro-cannulae and pressurized with oxygenated PSS (Section 2.4.2). In keeping with the standard

protocol all arteries (+Adv and –Adv) were studied in the absence of flow and pressure-dependent myogenic tone at 40-80-120-40 mmHg was measured by the changes of the vessel's external diameter. For MRA, a submaximal preconstriction with phenylephrine (PE) at 10^{-7} M was used to enhance the myogenic tone (Ramirez *et al.,* 2006, VanBavel *et al.,* 1998). At the end of each experiment, Ca^{2+}-containing PSS was replaced with a Ca^{2+}-free PSS (Ca_{free}) plus papaverine (10^{-4} M) to determine the maximal diameter and thereafter the total myogenic tone.

5.3.4 Chemiluminescence measurements of ROS

A segment of ~4 mm for each type of vessel (+Adv and –Adv) was pre-incubated (30 min, 37°C Krebs) with ANG II (0.1 μM), $NADH^+$ (substrate for Nox, 100 μM), and superoxide dismutase (SOD) (for quenching O_2^-, 200 U/ml) or SOD Cu^{2+}-chelating agent diethyldithiocarbamate DETCA (SOD Cu^{2+}-chelating inhibitor, 10 mM). After incubation, the arteries were transferred into Krebs-HEPES buffer containing ANG II (0.1 μM), $NADH^+$ (100 μM) and lucigenin (5 μM) (Skatchkov *et al.*, 1999) in plastic cuvettes and measured by a luminometer (Sirius, Berthold Detection Systems, Germany). One segment per cuvette was used. Luminescence was measured in relative light units per second (RLU/s) and measured every 20 s for a period of 10 min (Section 3.3.4).

5.3.5 Intracellular calcium measurement

The MCAs were loaded with the Ca^{2+}-sensitive fluorescent indicator dye, Fura-2 AM (Invitrogen; UK) (10 μl of 1 mM stock solution premixed with equal volume of 25 % pluronic acid in DMSO solution), and then diluted in 5 ml PSS to yield final bath concentration of 2 μM (Lagaud *et al.,* 2002). The arteries were incubated in Fura-2AM-PSS in a tin foil-covered eppendorf in the upright position for one hour. The eppendorf was placed in a platform shaker (Stuart Scientific, UK) at 30 rev/ min within a 37°C bath to ensure homogenous staining. This was followed by a washout period of 30 min at 37°C PSS. At each time of experiment both +Adv and -Adv were prepared. Both arteries were mounted in two separate pressure myograph chambers

with offset micro-cannulae adjusted to the bottom of the window base. The arteries were allowed to equilibrate for 45 min at 20 mmHg at 37°C in Ca^{2+}-containing PSS, as previously described (Section 2.3.2).

The myograph chamber was placed on the stage of an inverted microscope (Nikon Diaphot) with a Nikon Fluor x40 (N/A 1.30) oil objective. A 75-W xenon light source (Photon Technology International) was used to achieve the required excitation. Felix quantitative ratio fluorescence software (version 1.4 Photon Technology International) was used to collect, convert and store Fura-2 signals. The emission was recorded at 510 nm, whereas the excitation wavelength was alternated between 340 and 380 nm, and the respective 510 nm emissions were collected with a photomultiplier tube. Background-subtracted 340/380 ratios were calculated automatically and recorded continuously throughout the experiment. The VSM intracellular Ca^{2+} concentration ($[Ca^{2+}]_i$) is expressed as the mean 340-to-380 nm ratio [$R(F_{340}/F_{380})$] fluorescence ratio Fura-2.

After equilibration, a steep pressure-step from 20 to 80 mmHg was performed to ensure full dye loading, then the pressure was brought back down to 20 mmHg. After a plateau was reached, an increasing pressure-step from 20, 40, 80, 120 and return to 40 mmHg was conducted. The arteries were then washed out with 60 mM KCl. Finally at the conclusion of each experiment, the PSS was changed to a Ca^{2+} free-PSS containing 2 mM EGTA and the pressure-step repeated. The same experimental protocol was carried out in both +Adv and –Adv. The measurement in each artery was normalized to the maximum recorded in response to 60 mM KCl.

5.3.6 Drugs and chemicals

Angiotensin II (ANG II), β-nicotinamide adenine dinucleotide ($NADH^+$), N,N′-dimethyl-9,9′-biacridinium dinitrate (lucigenin), diethyldithiocarbamate (DETCA), and papaverine hydrochloride were purchased from Sigma, UK. KCl was purchased from BDH, Poole, England. Fura-2AM and 25 % pluronic acid were from Invitrogen. All other drugs were dissolved in distilled water (dH_2O), except for lucigenin dissolved in final DMSO (bath concentration ≤ 0.1 %) and $NADH^+$ in 0.01 M NaOH. All of the drugs were stored in aliquots at -20°C in 10^{-2} M stocks, except for KCl in 1 M stock. 4 % paraformaldehyde was made up and kept in 4°C refrigerator. Only NADH, lucigenin and papaverine were prepared fresh before each experiment. Aliquots were thawed before use and diluted with Krebs physiological saline solution (PSS) which was prepared fresh daily. For the chemiluminescence study, modified Krebs-HEPES buffer was used with the following composition (in mM):118 NaCl, 5 KCl, 1.1 $MgSO_4$, 2.5 $CaCl_2$, 1.2 KH_2PO_4, 25 $NaHCO_3$, 10 HEPES, 10 glucose, also prepared freshly.

5.3.7 Statistical analysis

Values are presented as mean ± standard error of the mean (SEM). Statistical analysis of the data was performed using Microsoft Excel 2003 and GraphPad Prism version 4.03. Statistical analyses were performed by two-way ANOVA for repeated measure or paired Student t-test for two groups of matched tests. Significance was assumed if $p<0.05$ (control vs. Ca^{2+} free). Data are expressed as means ± SEM. *n* is the number of animals studied.

5.4 RESULTS

5.4.1 Rat middle cerebral artery

Pressure-dependent myogenic tone

Figure 5.1 shows the response of +Adv and –Adv MCA to 60 mM KPSS wash. There was no significant difference in the contractions. In pressure-dependent myogenic tone response, +Adv showed the typical tone increase with pressure-steps (Figure 5.2a and b). Whereas for –Adv, myogenic tone was reduced significantly ($p<0.05$) at 80 and 120 mmHg compared to +Adv at respective pressure.

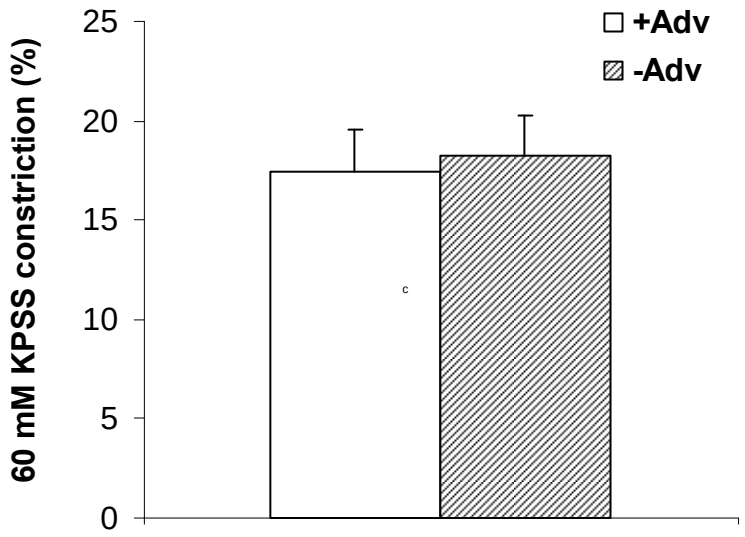

Figure 5.1 Percentage change of diameter in response to 60 mM KPSS in +Adv and –Adv middle cerebral arteries (MCA) *($p>0.05$, paired Student t-test). Values are means ± SEM (n=8).*

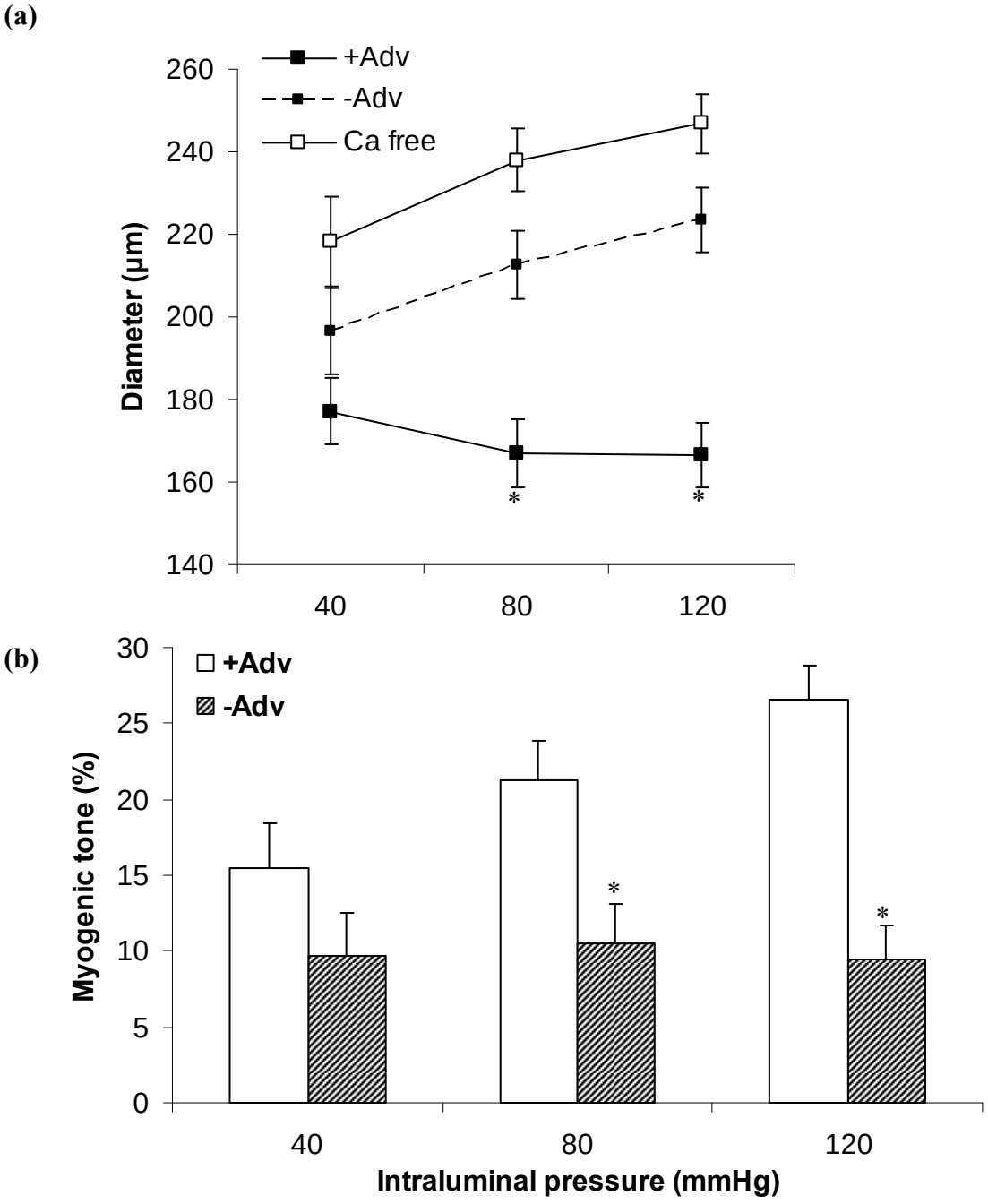

Figure 5.2 Pressure-dependent myogenic tone in +Adv and –Adv middle cerebral arteries (MCA) (a) *Comparison of +Adv and –Adv MCA on pressure-diameter relationship (*p<0.05 vs. Ca^{2+} free) and* ***(b)*** *myogenic tone (*p<0.05 vs. control at 80 and 120 mmHg). Statistical evaluations were by ANOVA for repeated measure and Bonferroni post hoc. Values are means ± SEM (n=8).*

Chemiluminescence measurements

Lucigenin-enhanced chemiluminescence was used to detect superoxide (O_2^-) production. In the presence of ANG II (an activator of Nox), $NADH^+$ (substrate for Nox) and DETCA (SOD inhibitor), O_2^- production in +Adv was significantly higher ($p<0.05$) than –Adv throughout the 4 min measurement (Figure 5.3). O_2^- release was initially high and started to reach a plateau after 2 min.

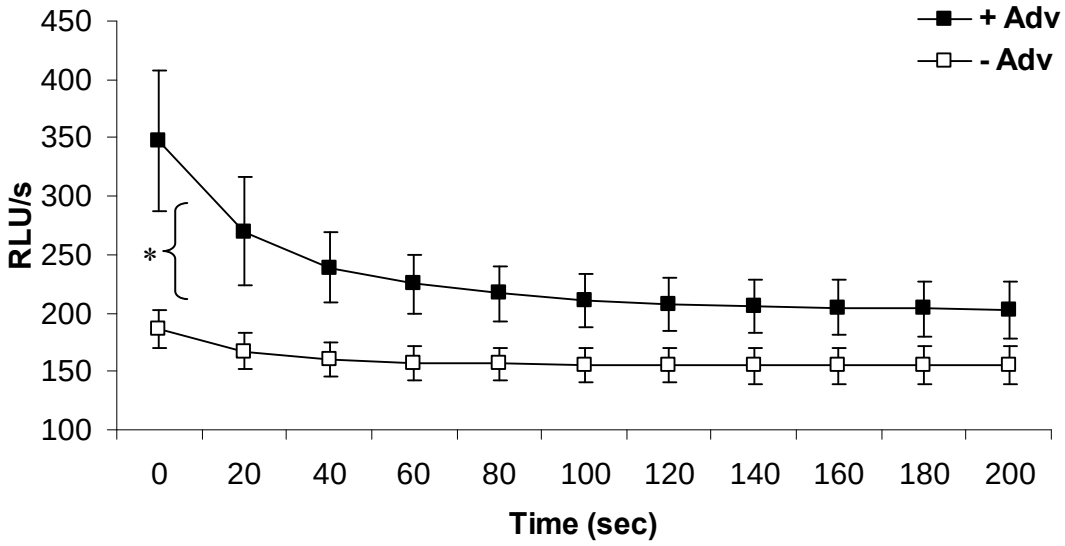

Figure 5.3 Vascular superoxide (O_2^-) production assessed by lucigenin-enhanced chemiluminescence in middle cerebral arteries (MCA). *+Adv and –Adv were incubated with ANG II (10^{-7} M) for 30 min to increase O_2^- generation, facilitated by the Nox substrate $NADH^+$ and the SOD inhibitor DETCA. O_2^- production over time was significantly reduced in -Adv compared to +Adv. Values are means ± SEM.*
** $p<0.05$ vs +Adv throughout the measurement time (ANOVA for repeated measure) (+Adv n=7, -Adv n=6).*

5.4.2 Rat mesenteric artery

Pressure-dependent myogenic tone

Figure 5.4 shows the response of +Adv and –Adv mesenteric resistance arteries to 60 mM KPSS. There was no significant difference in the contraction to 60 mM KPSS. In pressure-dependent myogenic tone response, +Adv showed the typical tone increase with pressure-steps. Whereas for –Adv, myogenic tone was reduced significantly ($p<0.05$) at 80 and 120 mmHg compared to +Adv at respective pressure (Figure 5.5).

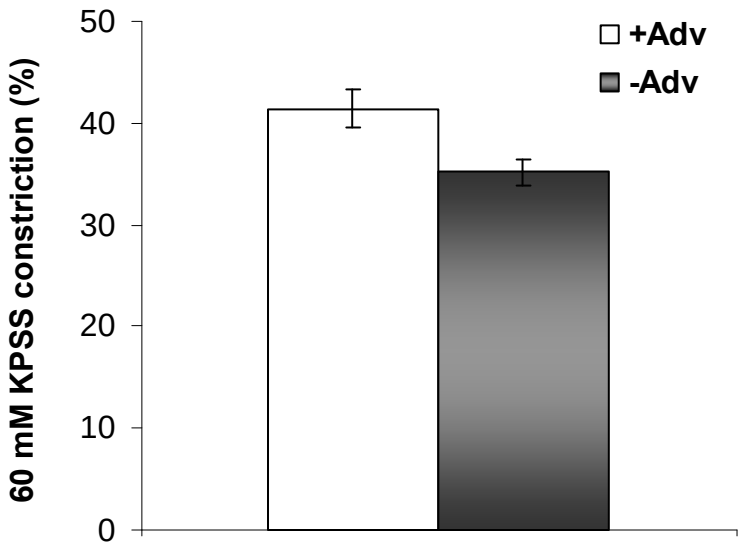

Figure 5.4 Percentage change of diameter in response to 60 mM KPSS in +Adv and –Adv of mesenteric resistance arteries (MRA). *($p>0.05$, paired Student t-test). Values are means ± SEM (n=6).*

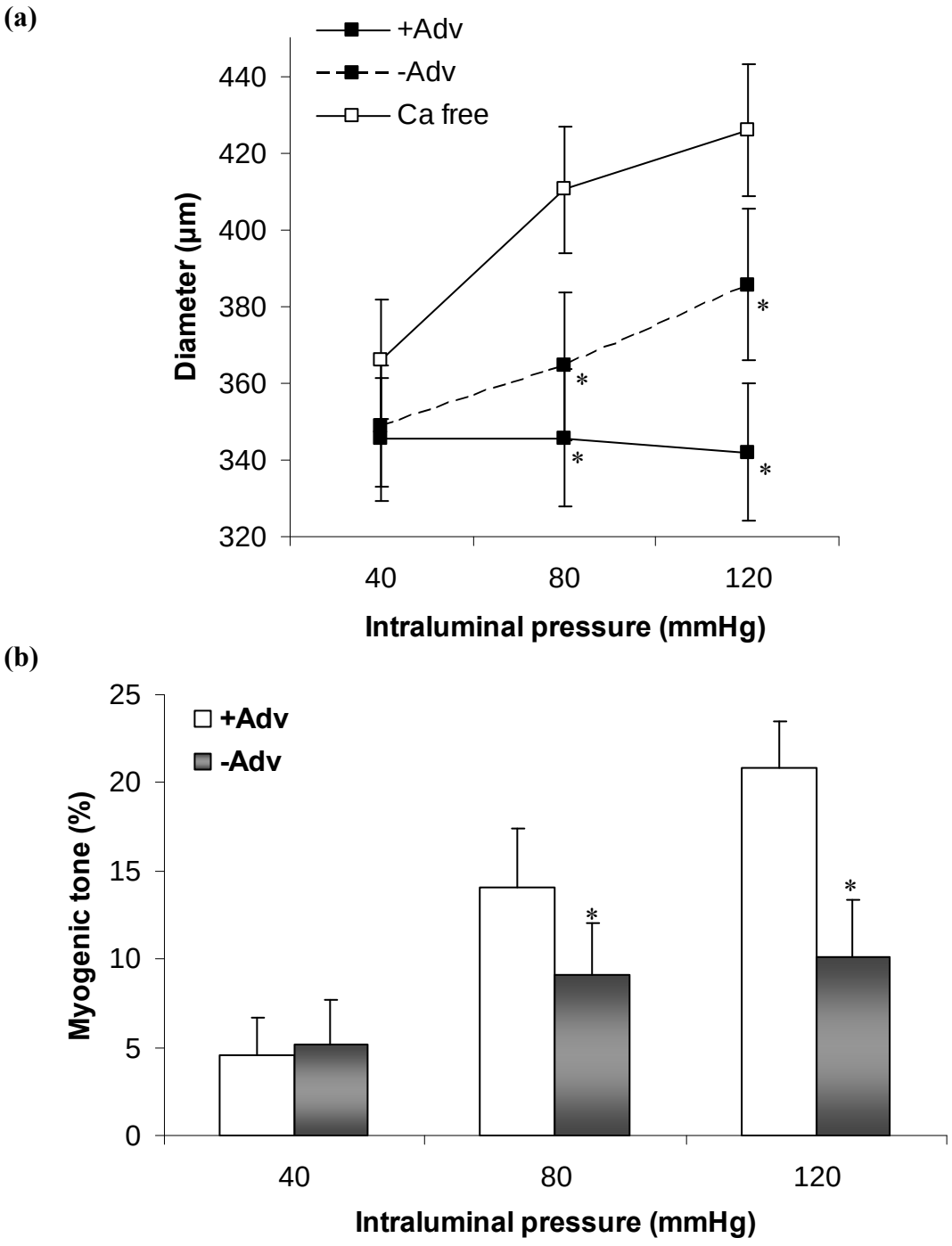

Figure 5.5 Pressure-dependent myogenic tone in mesenteric resistance arteries (MRA) (a) *The effect of +Adv and –Adv on pressure-diameter relationship (*p<0.05 vs. Ca^{2+} free) and* ***(b)*** *myogenic tone (*p<0.05 vs. control at 80 and 120 mmHg). –Adv abolished the myogenic tone at high pressure. Statistical evaluations were by ANOVA for repeated measure and Bonferroni post hoc test. Values are means ± SEM (n=6).*

Chemiluminescence measurements

Lucigenin-enhanced chemiluminescence showed a similar pattern in the MRA whereby O_2^- production in +Adv was significantly higher ($p<0.05$) than -Adv (Figure 5.6). The O_2^- showed an initial peak and gradually reached a plateau after 380 s.

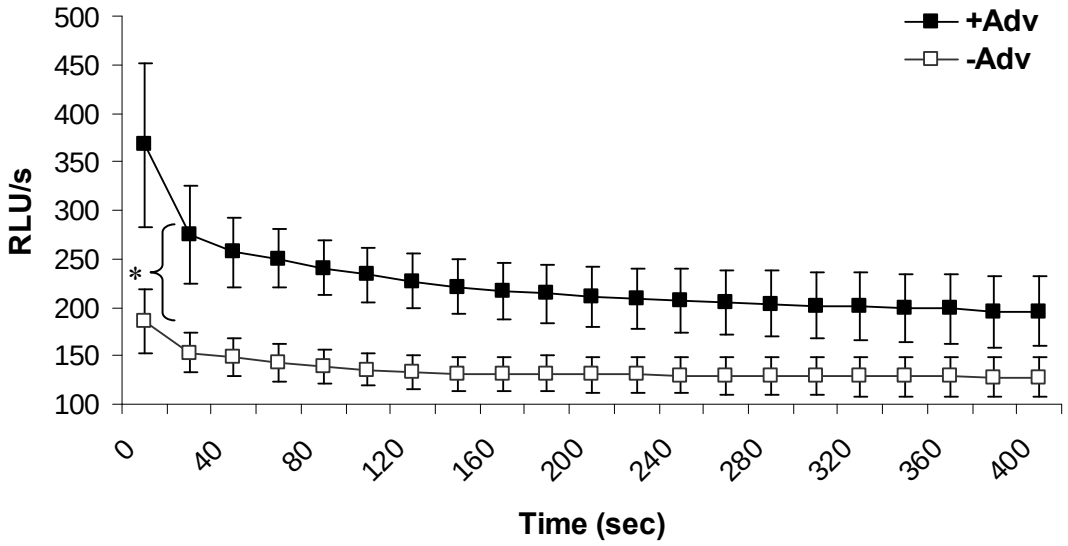

Figure 5.6 Vascular superoxide (O_2^-) production assessed by lucigenin-enhanced chemiluminescence in mesenteric resistance arteries (MRA). *+Adv and –Adv were incubated with ANG II (10^{-7} M) for 30 min to increase O_2^- generation, facilitated by the Nox substrate $NADH^+$ and the SOD inhibitor DETCA. O_2^- production over time was significantly reduced in -Adv compared to +Adv. Values are means ± SEM.*
** $p<0.05$ vs +Adv throughout the measurement time (ANOVA for repeated measure) (+Adv and -Adv n=6).*

5.4.3 Intracellular calcium measurement

To look at the effect of adventitial-ablation on Ca^{2+} influx, a preceding event underlying the mechanism of myogenic tone, the changes in fluorescence of the Ca^{2+}-sensitive dye Fura-2 were observed. Figure 5.7 shows a raw tracing of the Fura-2 ratio in a pressurized MCA (+Adv) on Felix software. The reading shows the changes in the 340-to-380 nm Fura-2 ratio [$R(F_{340}/F_{380})$] over the time course of an experiment. Initially, the pressure was increased from 20 to 80 mmHg to test the vessel's viability, then followed by pressure-step from 40 to 80 to 120 mmHg and finally back to 40 mmHg. This tracing has shown that pressure-dependent myogenic tone is dependent on the increase of intracellular Ca^{2+} ($[Ca^{2+}]_i$) in VSM.

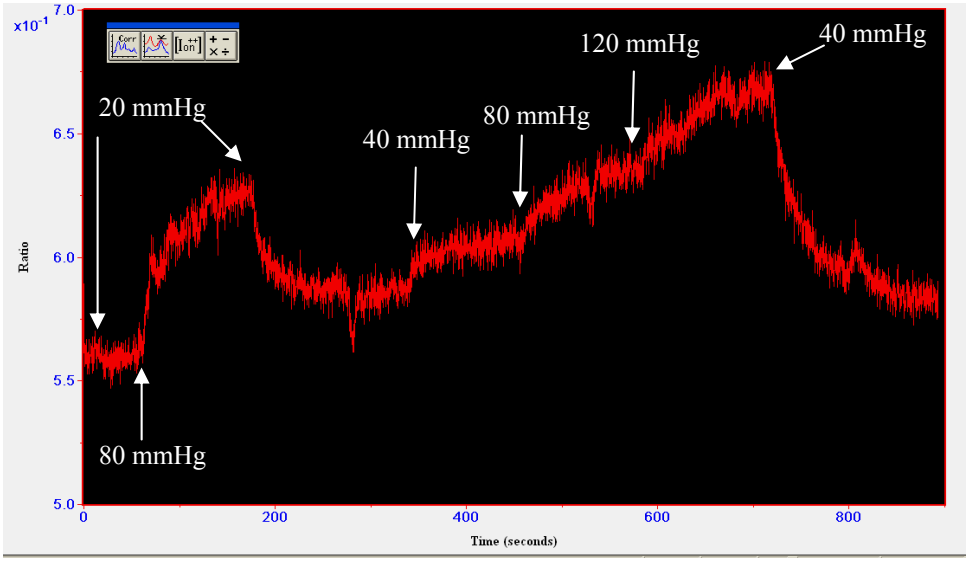

Figure 5.7 Representative raw tracing of Fura-2 fluorescence signal in a control pressurized middle cerebral artery (MCA, +Adv). *The reading shows 340/380 Fura-2 fluorescence ratio [$R(F_{340}/F_{380})$] in a time course. Initially, the pressure was increased from 20 to 80 mmHg to test the vessel's viability, then followed by pressure-steps from 40 to 80 to 120 and finally back to 40 mmHg.*

Figure 5.8 shows a series of real-time tracings from a MCA subjected to pressurization. The pressure-steps subjected to the vessel (20-40-80-120 mmHg and back to 40 mmHg) caused a pressure-dependent increase in the 340-to-380-nm (340/380) fluorescence ratio of Fura-2. The diameter showed vasoconstriction in response to elevating intraluminal pressure as typically seen in pressure-dependent myogenic tone. In Figure 5.9, a similar experiment protocol was conducted for –Adv vessels. The tracing showed an abolished myogenic tone with vasodilation in response to the pressure-step. Strikingly, the Fura-2 (340/380) fluorescence ratio increased with the pressure-steps, indicating adventitial ablation had no effect on the changes in $[Ca^{2+}]_i$ in spite of myogenic loss.

The influence of pressure-induced adventitial-derived ROS to the $[Ca^{2+}]_i$, indicated by 340/380 Fura-2 ratio, was investigated in the MCA. Data was expressed in the value of normalized Fura-2 ratio to 60 mM KCl contraction. In +Adv vessels, significant changes occurred at 80 mmHg (37.1 ± 9.0) and 120 mmHg (71.0 ± 21.2), as compared to basal pressure at 40 mmHg (20.1 ± 5.1) (Figure 5.10). However, surprisingly, the normalized ratio for –Adv showed no significant difference of magnitude compared to +Adv at each pressure step, indicating that adventitial-ablation did not affect the changes of $[Ca^{2+}]_i$ in response to pressure.

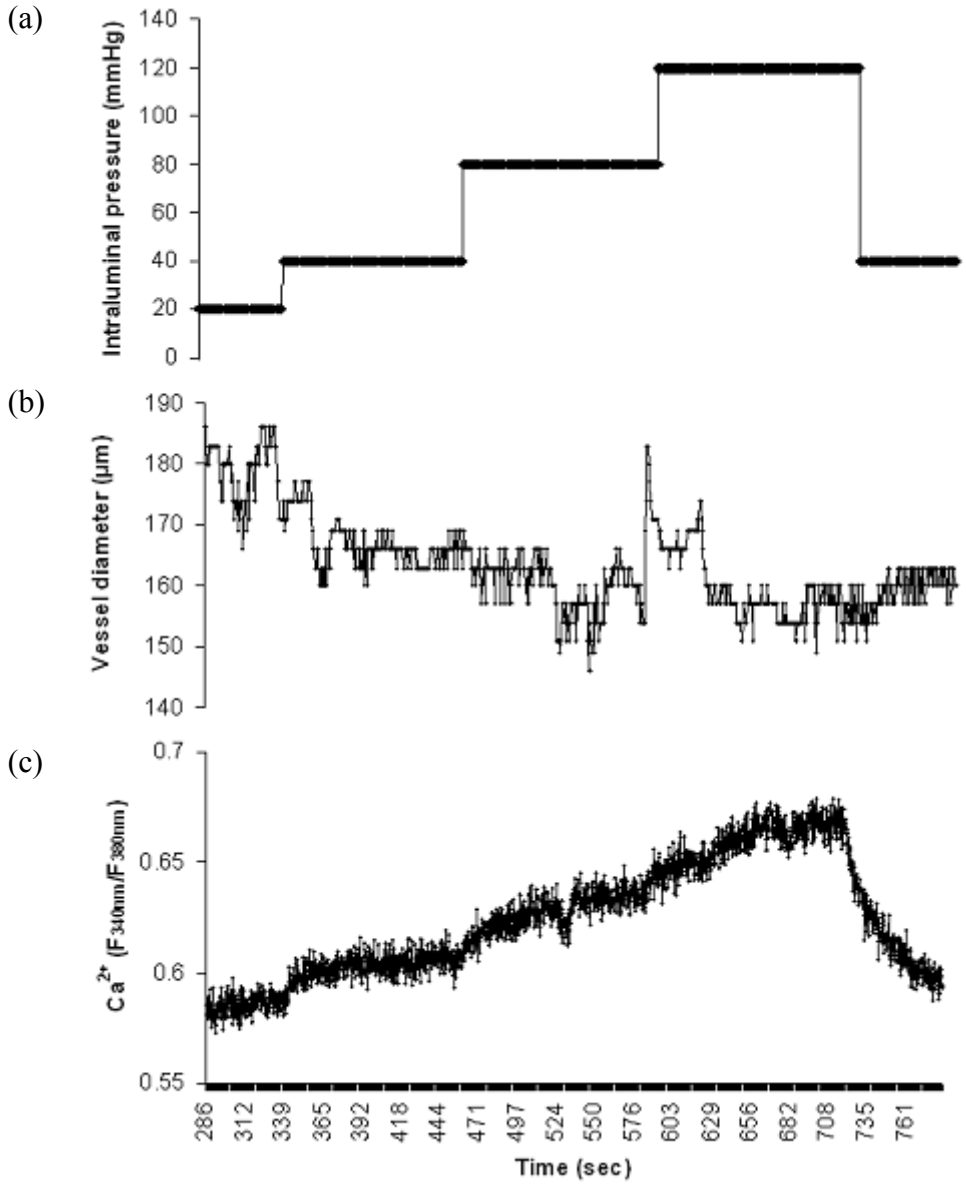

Figure 5.8 Example of pressure-induced changes in smooth muscle Ca^{2+} and vascular diameter in control (+Adv) rat middle cerebral artery (MCA). *A stepwise change in intraluminal pressure from 20, 40, 80 to 120 mmHg (panel a) induced a rapid increase in smooth muscle intracellular Ca^{2+}, determined by the Ca^{2+}-sensitive dye Fura-2 (fluorescence ratio F_{340}/F_{380}) (panel c). For diameter, the passive distension of the vessel that immediately follows the pressure-step is typically changed into active vasoconstriction (panel b).*

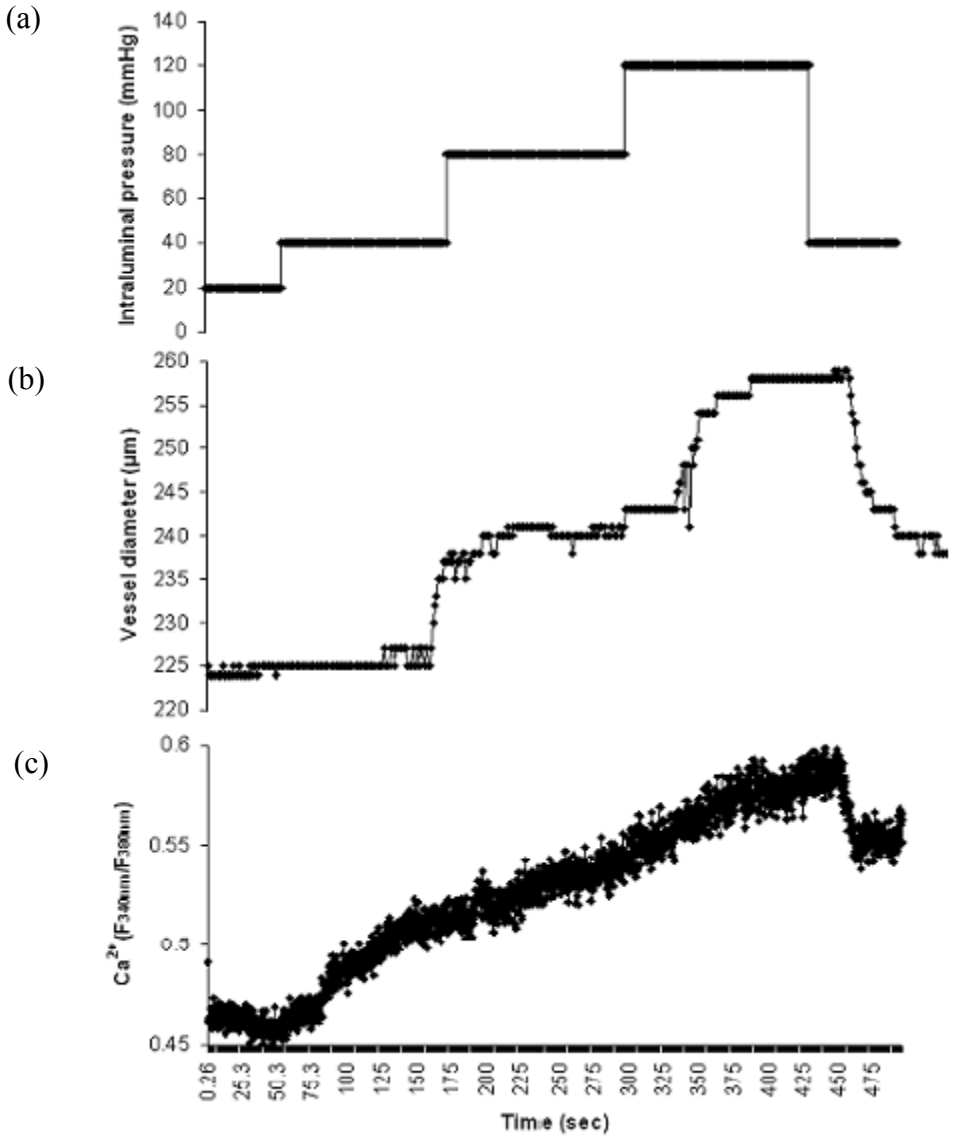

Figure 5.9 Example of pressure-induced changes in smooth muscle Ca^{2+} and vascular diameter in –Adv rat middle cerebral artery (MCA). *A stepwise change in intraluminal pressure from 20, 40, 80 to 120 mmHg (panel a) induced an increase in smooth muscle intracellular Ca^{2+}, determined by the Ca^{2+}-sensitive dye Fura-2 (fluorescence ratio F_{340}/F_{380}) (panel c). However, the distending intraluminal pressure caused passive distension of the vessel diameter (panel b).*

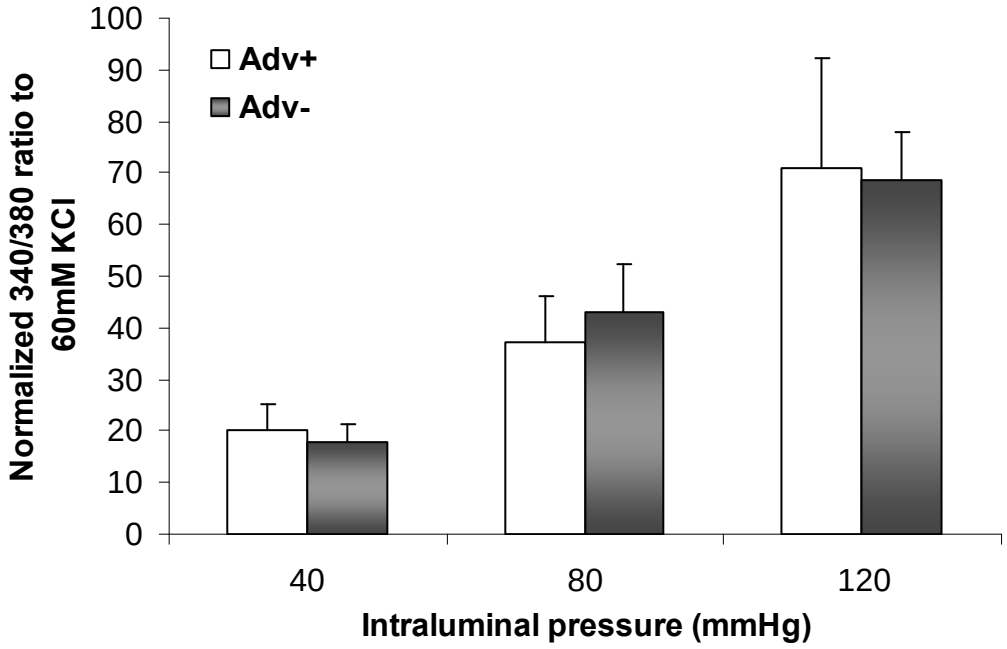

Figure 5.10 The averaged value of normalized Fura-2 ratio to 60 mM KCl in response to elevating intraluminal pressure in +Adv and –Adv middle cerebral arteries (MCA). *The ratio showed no significant difference in $[Ca^{2+}]_i$ between +Adv and –Adv. Statistical evaluations were by ANOVA for repeated measure and Bonferroni post hoc test. There was no significant difference between the groups. Values are means ± SEM (n=4-5)*

5.4 DISCUSSION

This current study presents the first evidence linking adventitia directly with elevated ROS and pressure-dependent myogenic tone by use of the adapted adventitial-ablation technique. This study has found that (1) adventitial ablation reduced pressure-dependent myogenic tone in resistance arteries (2) adventitial-derived O_2^- following ANG II stimulation was attenuated in adventitial-ablated vessels (-Adv) and (3) lack of adventitial-derived ROS did not affect $[Ca^{2+}]_i$ during increment of myogenic pressure-steps.

5.4.1 Role of adventitia in pressure-dependent myogenic tone

The results have shown that -Adv exhibited significant reduction in pressure-dependent myogenic tone in response to distending intraluminal pressure in the MCA and MRA. In agreement with published observations, the MRA showed less myogenic tone when compared to the MCA (Gonzalez *et al.*, 2005). The morphology of -Adv wall structure was proven intact by confocal microscopy in the previous chapter (Chapter 4), thus confirming the abolished response was due to adventitial function. Therefore, this study has shown the potential of adventitial-derived ROS mediating pressure-dependent myogenic response. However, there were traces of myogenic tone remaining with distending pressure in -Adv. Besides the adventitia, ROS can be produced in VSM (Bailey *et al.*, 2005, Lyle and Griendling, 2006) and endothelial cells (Drouin *et al.*, 2007), which may in turn contribute to signalling events leading to myogenic constriction. In addition, there are other potential factors influencing the mechanism of myogenic tone, such as increased membrane stretch/ wall tension, actin cytoskeleton stretch (Cipolla *et al.*, 2002), Ca^{2+} mobilization (Meininger *et al.*, 1991) and multiple intracellular signalling pathways such as increased PKC (Gokina *et al.*, 1999), p38 MAP kinases (Massett *et al.*, 2002), PLC (Jarajapu and Knot, 2002) and RhoA/Rho kinase (Jarajapu and Knot, 2005).

At normal resting membrane potential, voltage-gated K (K_v) channels seemed to be primarily in control, resulting in low $[Ca^{2+}]_i$ and basal tone. However, when K_v

channels are inhibited by 60 mM KPSS, the consequent depolarization activates VOCC and increases $[Ca^{2+}]_i$. At 60 mM KPSS, the membrane potential of VSM is near the equilibrium potential for K^+ (-21 mV), thereby resetting the steady-state $[Ca^{2+}]_i$ and contractility activity (Knot and Nelson, 1998, Lagaud *et al.*, 2002). Also, at this concentration, further changes in membrane potential are unlikely as the hyperpolarization is compromised (Knot and Nelson, 1998). From this study's result, 60 mM KPSS-induced contraction was not affected in –Adv despite the abolished myogenic tone. Therefore, this means that adventitial-derived ROS could be modulating pressure-dependent myogenic tone independent of membrane depolarization.

The exact mechanism regarding endogenous adventitial-derived ROS and myogenic tone is still unclear at this current time. However, this current finding is supported by other studies where the Nox inhibitor (DPI) and the antioxidant (NAC) showed reduced myogenic tone in the tail arteriole (Nowicki *et al.*, 2001). Similar attenuation in the myogenic response was observed in models of rac1 -/- mice and $p47^{phox}$ -/- mice (Nowicki *et al.*, 2001). Taking previous and current results together, this suggests that Nox-mediated ROS, which is known to be primarily located in the adventitial fibroblasts (Pagano *et al.*, 1997, Di Wang *et al.*, 1999), could be regulated by Rac to initiate myogenic constriction. Many previous cell motility studies have shown the underlying mechanisms underlying Nox-mediated ROS, for instance, Moldovon's group has demonstrated that ROS-regulated Nox and Rac1 caused endothelial cell motility via actin cytoskeleton polymerization (Moldovan *et al.*, 2006). The Nox-inhibitor (DPI) and SOD mimetic (MnTMPyP) were found to reduce G-to-F actin polymerization at the barbed (fast growing) ends and hence reduced endothelial cells motility, indicating that Nox and O_2^- regulate actin cytoskeletal dynamics. Surprisingly, although actin polymerization at barbed ends was inhibited by Cyto D, O_2^- dismutation by MnTMPyP, which resulted in H_2O_2 production, enhanced actin polymerization at the pointed ends (Moldovan *et al.*, 2000). Actin cytoskeletal dynamics has not only been shown in endothelial cells, but also in smooth muscle cells, according to Gunst and Zhang review (2008). Collectively, these cell studies have definitely raised the speculation that these

aforementioned events could be the possible mechanisms underlying pressure-dependent myogenic tone in this study, as the requirement of ROS is now established in biological processes.

5.4.2 Adventitial-derived ROS induced by ANG II

One aim of this study was to measure the release of ROS from the adventitia via lucigenin-enhanced chemiluminescence in MCA and MRA. The results have demonstrated that adventitial-derived O_2^- release was reduced in –Adv compared to +Adv. This finding is in keeping with our knowledge that ANG II induces Nox subunits to generate O_2^- as the primary product in the adventitia (Pagano *et al.*, 1998, Miller *et al.*, 2007). Luminometer sensitivity that was used to measure lucigenin-enhanced chemiluminescence is limited for measuring low levels of O_2^- and isolated MCA segments do not yield enough signal for detection (Gonzalez *et al.*, 2008). For these reasons, stimulators such as the Nox activator (ANG II), Nox substrate ($NADH^+$) and SOD inhibitor (DETCA) (Griendling *et al.*, 1994, Miller *et al.*, 2005) were used to enhance O_2^- signal detection. However, these variables were kept standardized between +Adv and –Adv so that the amount of ROS release from both types of vessels were comparable. Another limitation of chemiluminescence is that, lucigenin itself (250 μM) may undergo redox cycling and generate O_2^- in the presence of oxygen (Hyrsl *et al.*, 2004). However, this problem can be resolved by using a lower concentration of lucigenin with 5 μM, as being used in this study (Skatchkov *et al.*, 1999).

ANG II enhances Nox activity in the short-term (min) (Seshiah *et al.*, 2002, Chin *et al.*, 2007, Lu *et al.*, 2008, Miller *et al.*, 2009) and induces overexpression upon long-term incubation (hours or days) (Berry *et al.*, 2000, Weber *et al.*, 2005, Chen *et al.*, 2007). The half-life of O_2^- is less than 50 ms and the radius of diffusion is between a few cells (less than 40 μm) (Saran and Bors, 1994). However, DETCA was used to stop O_2^- dismutation in this study to maintain the level of O_2^-. Also, SOD was used in a tissue-free positive control experiment in the preliminary experiment to confirm the specificity of lucigenin's O_2^- detection (Chapter 3). Thus, it can be confirmed that O_2^-

was released from the adventitia of MCA and MRA models. In a previous study that attempted adventitial removal by collagenase digestion, the adventitia was found as the key layer in ANG II-induced contraction (Somoza *et al.*, 2005) and also enhanced endothelium-dependent relaxation in large arteries (Gonzalez *et al.*, 2001). These findings were consistent with the hypothesis that adventitial-O_2^- could inactivate EDNO and promote spontaneous tone, thus suggesting a paracrine adventitial-endothelial-medial signalling pathway (Di Wang *et al.*, 1998, Di Wang *et al.*, 1999). In spite of the current hypothesis that adventitial-Nox was the primary source for O_2^- production and that the adventitia influenced pressure-dependent myogenic tone, there is still a gap in knowledge regarding the mechanism.

5.4.3 Effect of adventitial ablation on intracellular calcium in pressure-dependent myogenic tone response

The mechanism underlying the effect of reduced pressure-dependent myogenic tone and also O_2^- production in –Adv vessels was investigated. The most important preceding determinant in pressure-dependent myogenic tone is the classic increase of $[Ca^{2+}]_i$ influx and also Ca^{2+} sensitivity (Moosmang *et al.*, 2003, Kotecha and Hill, 2005, Schubert *et al.*, 2008, Hill *et al.*, 2009), which led us to the question: how does non-adventitial pressurization (-Adv) affect $[Ca^{2+}]_i$? This study has demonstrated that pressure-dependent myogenic tone in +Adv MCA elicited typical increases in the 340/380 Fura-2 ratio according to elevating pressure-step. In –Adv vessel, surprisingly, there was no change compared to +Adv in $[Ca^{2+}]_i$. The amount of $[Ca^{2+}]_i$ in –Adv increased gradually with distending pressure, as seen in +Adv vessels. This result suggests that adventitial-derived ROS could be unrelated to the Ca^{2+}-dependent activation pathway and this can be supported by previous findings (Keller *et al.*, 2006). In addition, -Adv showed abolished pressure-dependent myogenic tone despite no change in the 60 mM KPSS-induced contraction. Previous studies have shown that under depolarized conditions (with 60 mM KPSS), normal arteries are still able to constrict according to increasing pressure-steps, but without any significant changes in $[Ca^{2+}]_i$ (Lagaud *et al.*, 2002, Lucchesi *et al.*, 2005). This current study has found that in –Adv vessels, the 60 mM KPSS-induced contraction

and $[Ca^{2+}]_i$ were not affected in spite of abolished myogenic tone. This evidence suggested that apart from membrane depolarization and $[Ca^{2+}]_i$ influx, another important early signalling event in the process of pressure-dependent myogenic tone could be the adventitial-derived ROS.

The mechanistic explanation underlying pressure-dependent myogenic tone could be via adventitia/Nox/ROS/$[Ca^{2+}]_i$-dependent mechanism. However, this could be nullified as the results have suggested that adventitia-derived ROS is independent of $[Ca^{2+}]_i$. Although this hypothesis was not proven directly in this study, there are many previous findings that could support it. A study by Keller *et al.* (2006) found that sphingosine kinase (Sk1)/sphingosine-1-phosphate (S1P) played a mandatory role in mediating Nox-derived ROS in pressure-dependent myogenic tone without affecting $[Ca^{2+}]_i$. The S1P could initiate a downstream of rac/Nox/O_2^- pathway resulting in increased apparent Ca^{2+} sensitivity; a mechanism in which running in parallel with RhoA/Rho kinase pathway within the VSM. It was suggested in the study that ROS production amplified an already initiated myogenic response based on the observation that the specific NOX2 inhibitor gp91ds-*tat* did not completely abolish the myogenic tone (Keller *et al.*, 2006). Based on this observation, the authors concluded that ROS signalling events are modulatory rather than obligatory in the process of regulating Ca^{2+} sensitivity during myogenic constriction. In the pulmonary circulation, myogenic tone does not typically exhibit in normotensive pulmonary arteries as the degree of VSM stretch is limited due to low arterial pressure. However, increased myogenic reactivity could contribute to elevated basal pulmonary tone in chronic hypoxia-induced pulmonary hypertension, and was found to be associated with increased RhoA/Rho kinase-dependent Ca^{2+} sensitivity, activated by ROS (Resta *et al.*, 2010). ET-1 and KCl were found to increase Nox/O_2^- leading to enhanced GTP-bound RhoA, myofilament Ca^{2+} sensitivity, and eventually vasoconstriction in models of chronic hypoxia, but not in control animals (Jernigan *et al.*, 2004, Fike *et al.*, 2008). Therefore, this highlights the divergent mechanisms that mediate pressure-induced tone in the systemic vs. pulmonary circulation, and in normal vs. hypertensive models.

A recent study by Narayanan *et al.* (2010) found that at the basal state in cerebral arteries, mitochondria contain Ca^{2+} and generate low levels of mitochondrial ROS (mitoROS). However, when stimulated by ET-1, IP_3R-mediated SR Ca^{2+} release occured, transcription activator NF-κB was elevated, followed by increased functional $Ca_v1.2$ protein expression and pressure-induced myogenic tone (Narayanan *et al.*, 2010). However, the finding was based on gene transcriptional events and the relevance to acute pressure-dependent myogenic tone has still yet to be confirmed.

5.4.4 Conclusion

In conclusion, this study has shown for the first time that the adventitia plays an important role in modulating acute pressure-dependent myogenic tone. Reactive oxygen species (O_2^-) could be the responsible molecule in mediating myogenic constriction. From a mechanistic basis, the adventitial-derived ROS effect in modulating myogenic tone is independent of $[Ca^{2+}]_i$.

CHAPTER 6:
SUMMARY OF PRIMARY EXPERIMENTAL FINDINGS

Classically, reactive oxygen species (ROS) and oxidative stress have been synonymous with pathological conditions (Hamilton *et al.*, 2004). Recently, evidence has shown that ROS may be acting as a signalling molecule within microcirculatory regulation, particularly in the genesis of pressure-dependent myogenic tone (Keller *et al.*, 2006, Gonzalez *et al.*, 2008, Ren *et al.*, 2010). Besides ROS, another new emerging candidate in mechanotransduction is the actin cytoskeleton, which has been recently shown to play an important role in the physiology of VSM contraction (Martinez-Lemus *et al.*, 2009). The main hypothesis was the adventitial-derived ROS could be a physiological modulator in pressure-dependent myogenic tone of resistance arteries. Preliminary data in this thesis has proven that Nox/ROS inhibition specifically abolished myogenic responses.

The potential role of adventitia in modulating vascular function has been widely shown in tissue culture studies (Shen *et al.*, 2006, Hu *et al.*, 2008), but little is known about the role of the adventitia in intact tissue vessels. In order to allow further understanding of its role in vascular function, this study has adapted an adventitial-ablation technique by quick dipping in 4 % paraformaldehyde-buffered saline. Following optimization and refinement, this method has subsequently been demonstrated to have no detrimental effect on medial and intimal function. The integrity of -Adv vascular wall based on confocal microscopy observation and the passive mechanical properties were still preserved in spite of the quick fixation with paraformaldehyde.

With the adventitial-ablation method now established, for the first time shown in resistance arteries, ANG II-induced O_2^- release was attenuated in –Adv. This finding is in agreement with previous reviews that Nox within the adventitia as the major production site for ROS (An *et al.*, 2007, Haurani and Pagano, 2007). Following that, the novel finding of adventitial ablation causing attenuation of pressure-dependent myogenic response in –Adv vessels with no effect on high-K^+ contraction was observed. Taken together, the primary finding of my work has demonstrated adventitial-derived ROS is likely to be a key signalling molecule in vascular physiology.

The classic Ca^{2+} influx pathway and Ca^{2+} sensitivity has been proven as a compulsory process in the pressure-dependent myogenic tone (Cheranov and Jaggar, 2006, Raina *et al.*, 2008, Schubert *et al.*, 2008), which led to the interest of its mechanistic relation with ROS. This study has shown for the first time that the abolished non-adventitial pressure-dependent myogenic tone has no effect on intracellular calcium ($[Ca^{2+}]_i$) changes.

In conclusion, this novel finding supports the main hypothesis, which is, adventitial-derived ROS (O_2^-) could be playing a role as a modulator in pressure-dependent myogenic tone, independent of the preceding events of $[Ca^{2+}]_i$ and membrane depolarization. The specific effect of actin cytoskeleton to pressure-dependent myogenic tone could not be justified at the moment as Cyto D was shown to affect high K^+-induced contraction. Therefore, there is still a gap as to whether there is a direct interaction linking adventitial-derived ROS and actin cytoskeletal polymerization, or whether they are of two separate events in parallel during pressurization. In order to answer this gap, future work with lower concentration of Cyto D could be done to verify actin cytoskeleton's role in modulating myogenic tone. In addition to that, future molecular work on the quantification of G-to-F actin cytoskeleton during pressurization could be investigated. It is also still unclear about the Ca^{2+}-independent downstream signalling events for adventitia-VSM-myogenic constriction events. Rac has been shown to be associated with Nox-mediated ROS in oxidative stress (Resta *et al.*, 2010), the possibility upon the Rac1/Nox/ROS signalling during pressure-dependent myogenic tone could be investigated in the future. Collectively, based on the current literature and findings from this thesis, the summary of postulated mechanisms involved in arterial pressure-dependent myogenic tone is shown in Figure 6.1.

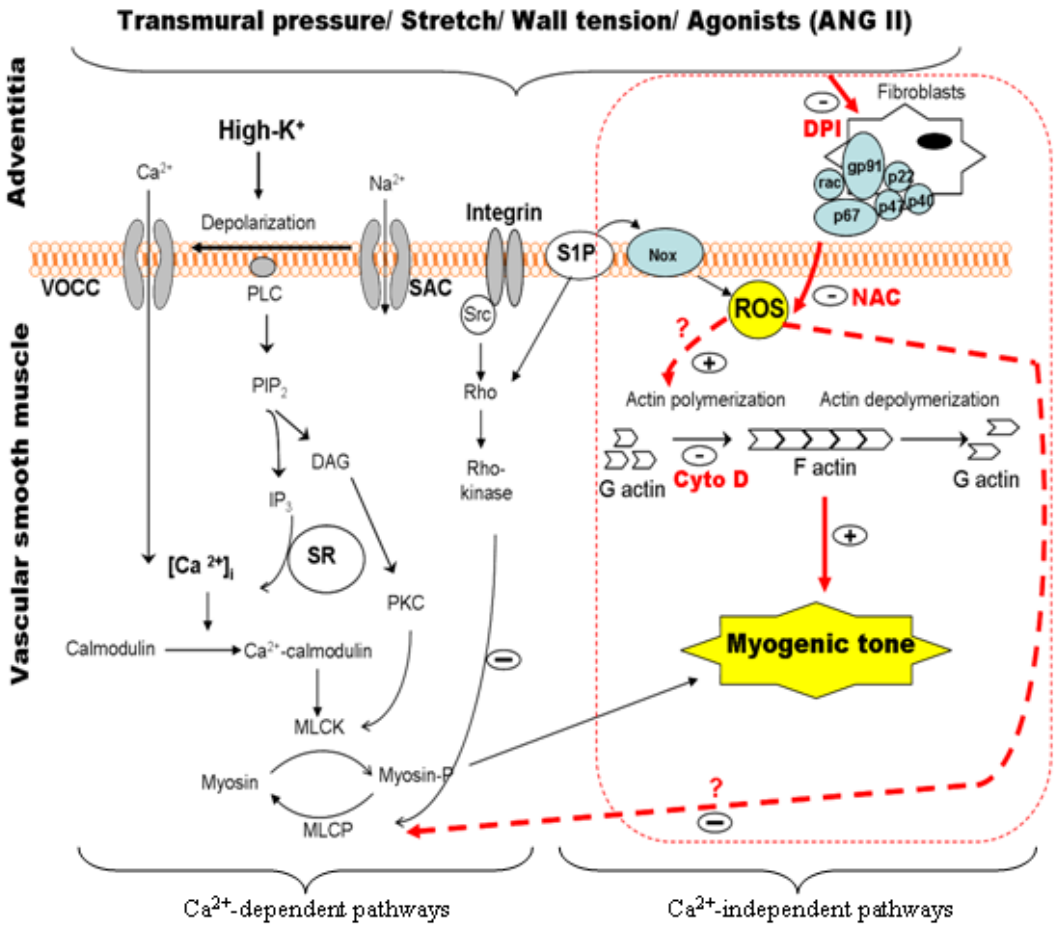

Figure 6.1 Schematic presentation of the proposed pathways *Increased transmural pressure or agonist activates stretch-sensing mechanisms that putatively lead to activation of Nox within the adventitial fibroblasts followed by release of ROS into VSM. Also, increase of transmural pressure activates actin cytoskeletal polymerization. The evidence shows that neither of these events has any effect on* $[Ca^{2+}]_i$ *and high-*K^+*, suggesting that ROS and actin may act as modulators in pressure-dependent myogenic tone. ANG II (angiotensin II);* Ca^{2+} *(calcium); CaM (calmodulin); Cyto D (Cytochalasin D); DAG (diacylglycerol); DPI (diphenyleneiodonium);* IP_3 *(inositol trisphosphate); MLCK (myosin light-chain kinase); MLCP (myosin light-chain phosphatase), myosin-P (myosin-phosphate);* Na^+ *(sodium), NAC (N-acetyl cysteine);* PIP_2 *(phosphatidylinositol (4,5)-bisphosphate); PLC (phospholipase C); PKC (protein kinase C); ROS (reactive oxygen species); S1P (sphingosine-1-phosphate); SAC (stretch-activated channel); SR (sarcoplamic reticulum), VOCC (voltage-operated calcium channel).*

The knowledge about cellular mechanisms underlying myogenic tone could be used as selective therapeutic targets in the future, as myogenic responsiveness is altered in vascular diseases (Chin *et al.*, 2007, Coats, 2010, Ren *et al.*, 2010). With more in-depth understanding of the mechanisms involved, new therapeutic approaches to modulate adventitia-derived ROS regulation in pathological conditions might arise. Such treatments could specifically interfere with pressure-dependent ROS release, yet potentially limit excess generation and preserve the role of ROS as a key signalling molecule for maintaining autoregulation in the microcirculation. Ultimately, it will be very important to put the pieces together, from cultured cells, intact vessels and animal trial studies to understand the physiological role and mechanism of pressure-dependent myogenic tone within a complex vascular network, so it could be applicable for the future clinical therapeutic implication.

REFERENCES

Abid, M. R., Spokes, K. C., Shih, S. C. & Aird, W. C. (2007) NADPH oxidase activity selectively modulates vascular endothelial growth factor signaling pathways. *J Biol Chem,* 282**,** 35373-85.

Ager, A., Gordon, J. L., Moncada, S., Pearson, J. D., Salmon, J. A. & Trevethick, M. A. (1982) Effects of isolation and culture on prostaglandin synthesis by porcine aortic endothelial and smooth muscle cells. *J Cell Physiol,* 110, 9-16.

Akiyama, S., Hobara, N., Maruo, N., Hashida, S., Kitamura, K., Eto, T. & Kawasaki, H. (2005) Adrenomedullin release in the rat mesenteric resistance artery. *Peptides,* 26, 2222-30.

Al-Mehdi, A. B. & Fisher, A. B. (1998) Invited editorial on "tumor necrosis factor-alpha in ischemia and reperfusion injury in rat lungs". *J Appl Physiol,* 85, 2003-4.

An, S. J., Boyd, R., Zhu, M., Chapman, A., Pimentel, D. R. & Wang, H. D. (2007) NADPH oxidase mediates angiotensin II-induced endothelin-1 expression in vascular adventitial fibroblasts. *Cardiovasc Res,* 75, 702-9.

Arribas, S. M., Gonzalez, C., Graham, D., Dominiczak, A. F. & McGrath, J. C. (1997) Cellular changes induced by chronic nitric oxide inhibition in intact rat basilar arteries revealed by confocal microscopy. *J Hypertens,* 15, 1685-93.

Attia, D. M., Verhagen, A. M., Stroes, E. S., van Faassen, E. E., Grone, H. J., De Kimpe, S. J., Koomans, H. A., Braam, B. & Joles, J. A. (2001) Vitamin E alleviates renal injury, but not hypertension, during chronic nitric oxide synthase inhibition in rats. *J Am Soc Nephrol,* 12, 2585-93.

Auger, F. A., D'Orleans-Juste, P. & Germain, L. (2007) Adventitia contribution to vascular contraction: hints provided by tissue-engineered substitutes. *Cardiovasc Res,* 75, 669-78.

Bailey, S. R., Mitra, S., Flavahan, S. & Flavahan, N. A. (2005) Reactive oxygen species from smooth muscle mitochondria initiate cold-induced constriction of cutaneous arteries. *Am J Physiol Heart Circ Physiol,* 289, H243-50.

Ballew, J. R., Watts, S. W. & Fink, G. D. (2001) Effects of salt intake and angiotensin II on vascular reactivity to endothelin-1. *J Pharmacol Exp Ther,* 296**,** 345-50.

Baumbach, G. L., Dobrin, P. B., Hart, M. N. & Heistad, D. D. (1988) Mechanics of cerebral arterioles in hypertensive rats. *Circ Res,* 62**,** 56-64.

Bayliss, W. M. (1902) On the local reactions of the arterial wall to changes of internal pressure. *J Physiol,* 28, 220-31.

Bedard, K. & Krause, K. H. (2007) The NOX family of ROS-generating NADPH oxidases: physiology and pathophysiology. *Physiol Rev,* 87, 245-313.

Belin de Chantemele, E. J., Retailleau, K., Pinaud, F., Vessieres, E., Bocquet, A., Guihot, A. L., Lemaire, B., Domenga, V., Baufreton, C., Loufrani, L., Joutel, A. & Henrion, D. (2008) Notch3 is a major regulator of vascular tone in cerebral and tail resistance arteries. *Arterioscler Thromb Vasc Biol,* 28, 2216-24.

Belmadani, S., Zerfaoui, M., Boulares, H. A., Palen, D. I. & Matrougui, K. (2008) Microvessel vascular smooth muscle cells contribute to collagen type I deposition through ERK1/2 MAP kinase, alphavbeta3-integrin, and TGF-beta1 in response to ANG II and high glucose. *Am J Physiol Heart Circ Physiol,* 295, H69-76.

Berry, C., Hamilton, C. A., Brosnan, M. J., Magill, F. G., Berg, G. A., McMurray, J. J. & Dominiczak, A. F. (2000) Investigation into the sources of superoxide in human blood vessels: angiotensin II increases superoxide production in human internal mammary arteries. *Circulation,* 101, 2206-12.

Bevan, J. A. (1982) Selective action of diltiazem on cerebral vascular smooth muscle in the rabbit: antagonism of extrinsic but not intrinsic maintained tone. *Am J Cardiol,* 49, 519-24.

Birch, D. J., Turmaine, M., Boulos, P. B. & Burnstock, G. (2008) Sympathetic innervation of human mesenteric artery and vein. *J Vasc Res,* 45, 323-32.

Brekke, J. F., Gokina, N. I. & Osol, G. (2002) Vascular smooth muscle cell stress as a determinant of cerebral artery myogenic tone. *Am J Physiol Heart Circ Physiol,* 283, H2210-6.

Briones, A. M., Gonzalez, J. M., Somoza, B., Giraldo, J., Daly, C. J., Vila, E., Gonzalez, M. C., McGrath, J. C. & Arribas, S. M. (2003) Role of elastin in spontaneously hypertensive rat small mesenteric artery remodelling. *J Physiol,* 552, 185-95.

Briones, A. M., Salaices, M. & Vila, E. (2005) Ageing alters the production of nitric oxide and prostanoids after IL-1beta exposure in mesenteric resistance arteries. *Mech Ageing Dev,* 126, 710-21.

Cabrera Fischer, E. I., Bia, D., Camus, J. M., Zocalo, Y., de Forteza, E. & Armentano, R. L. (2006) Adventitia-dependent mechanical properties of brachiocephalic ovine arteries in in vivo and in vitro studies. *Acta Physiol (Oxf),* 188, 103-11.

Carey, R. M., Wang, Z. Q. & Siragy, H. M. (2000) Update: role of the angiotensin type-2 (AT(2)) receptor in blood pressure regulation. *Curr Hypertens Rep,* 2, 198-201.

Cave, A. (2008) Selective targeting of NADPH oxidase for cardiovascular protection. *Curr Opin Pharmacol*., 9, 208-13.

Cave, A., Grieve, D., Johar, S., Zhang, M. & Shah, A. M. (2005) NADPH oxidase-derived reactive oxygen species in cardiac pathophysiology. *Philos Trans R Soc Lond B Biol Sci,* 360**,** 2327-34.

Chazova, I., Loyd, J. E., Zhdanov, V. S., Newman, J. H., Belenkov, Y. & Meyrick, B. (1995) Pulmonary artery adventitial changes and venous involvement in primary pulmonary hypertension. *Am J Pathol,* 146, 389-97.

Chen, M. F., Xie, X. M., Yang, T. L., Wang, Y. J., Zhang, X. H., Luo, B. L. & Li, Y. J. (2007) Role of asymmetric dimethylarginine in inflammatory reactions by angiotensin II. *J Vasc Res,* 44, 391-402.

Cheranov, S. Y. & Jaggar, J. H. (2006) TNF-alpha dilates cerebral arteries via NAD(P)H oxidase-dependent Ca2+ spark activation. *Am J Physiol Cell Physiol,* 290, C964-71.

Chiba, S. & Tsuji, T. (1985) Vascular responsiveness of isolated, perfused basilar arteries in dogs and monkeys. *Tohoku J Exp Med,* 146, 363-70.

Chin, L. C., Achike, F. I. & Mustafa, M. R. (2007) Hydrogen peroxide modulates angiotensin II-induced contraction of mesenteric arteries from streptozotocin-induced diabetic rats. *Vascul Pharmacol,* 46, 223-8.

Cifuentes, M. E., Rey, F. E., Carretero, O. A. & Pagano, P. J. (2000) Upregulation of p67(phox) and gp91(phox) in aortas from angiotensin II-infused mice. *Am J Physiol Heart Circ Physiol,* 279, H2234-40.

Cipolla, M. J., Gokina, N. I. & Osol, G. (2002) Pressure-induced actin polymerization in vascular smooth muscle as a mechanism underlying myogenic behavior. *FASEB J.,* 16, 72-76.

Coats, P. (2003) Myogenic, mechanical and structural characteristics of resistance arterioles from healthy and ischaemic subjects. *Clin Sci (Lond),* 105, 683-9.

Coats, P. (2010) The effect of peripheral vascular disease on structure and function of resistance arteries isolated from human skeletal muscle. *Clin Physiol Funct Imaging,* 30, 192-7.

Coats, P. & Hillier, C. (1999) Determination of an optimal axial-length tension for the study of isolated resistance arteries on a pressure myograph. *Exp Physiol,* 84, 1085-94.

Coats, P., Jarajapu, Y. P., Hillier, C., McGrath, J. C. & Daly, C. (2003) The use of fluorescent nuclear dyes and laser scanning confocal microscopy to study the cellular aspects of arterial remodelling in human subjects with critical limb ischaemia. *Exp Physiol,* 88, 547-554.

Coats, P., Johnston, F., MacDonald, J., McMurray, J. J. & Hillier, C. (2001a) Endothelium-derived hyperpolarizing factor : identification and mechanisms of action in human subcutaneous resistance arteries. *Circulation,* 103, 1702-8.

Coats, P., Johnston, F., MacDonald, J., McMurray, J. J. & Hillier, C. (2001b) Signalling mechanisms underlying the myogenic response in human subcutaneous resistance arteries. *Cardiovasc Res,* 49, 828-37.

Coats, P. & Wadsworth, R. (2004) Ros-Dependent Modulation of Myogenic Tone in Critical Limb Ischaemia. 8th International Symposium on Resistance Arteries *Journal of Vascular Research,* 1, Abstract 6-5.

Coats, P. & Wadsworth, R. (2005) Marriage of resistance and conduit arteries breeds critical limb ischemia. *Am J Physiol Heart Circ Physiol,* 288, H1044-50.

Cooper, J. A. (1987) Effects of cytochalasin and phalloidin on actin. *J Cell Biol,* 105, 1473-8.

Coulson, R. J., Chesler, N. C., Vitullo, L. & Cipolla, M. J. (2002) Effects of ischemia and myogenic activity on active and passive mechanical properties of rat cerebral arteries. *Am J Physiol Heart Circ Physiol,* 283, H2268-75.

Csanyi, G., Taylor, W. R. & Pagano, P. J. (2009) NOX and inflammation in the vascular adventitia. *Free Radic Biol Med,* 47, 1254-66.

Cseko, C., Bagi, Z. & Koller, A. (2004) Biphasic effect of hydrogen peroxide on skeletal muscle arteriolar tone via activation of endothelial and smooth muscle signaling pathways. *J Appl Physiol,* 97, 1130-7.

D'Angelo, G., Davis, M. J. & Meininger, G. A. (1997) Calcium and mechanotransduction of the myogenic response. *Am J Physiol,* 273, H175-82.

Davis, M. J. (1993) Myogenic response gradient in an arteriolar network. *Am J Physiol,* 264**,** H2168-79.

Davis, M. J., Davis, A. M., Ku, C. W. & Gashev, A. A. (2009) Myogenic constriction and dilation of isolated lymphatic vessels. *Am J Physiol Heart Circ Physiol,* 296**,** H293-302.

Davis, M. J., Donovitz, J. A. & Hood, J. D. (1992) Stretch-activated single-channel and whole cell currents in vascular smooth muscle cells. *Am J Physiol,* 262, C1083-8.

Davis, M. J. & Hill, M. A. (1999) Signaling mechanisms underlying the vascular myogenic response. *Physiol Rev,* 79, 387-423.

Davis, M. J., Wu, X., Nurkiewicz, T. R., Kawasaki, J., Davis, G. E., Hill, M. A. & Meininger, G. A. (2001) Integrins and mechanotransduction of the vascular myogenic response. *Am J Physiol Heart Circ Physiol,* 280, H1427-33.

De Vriese, A. S., Verbeuren, T. J., Van de Voorde, J., Lameire, N. H. & Vanhoutte, P. M. (2000) Endothelial dysfunction in diabetes. *Br J Pharmacol,* 130, 963-74.

Didion, S. P. & Faraci, F. M. (2002) Effects of NADH and NADPH on superoxide levels and cerebral vascular tone. *Am J Physiol Heart Circ Physiol,* 282**,** H688-95.

Dimitropoulou, C., White, R. E., Fuchs, L., Zhang, H., Catravas, J. D. & Carrier, G. O. (2001) Angiotensin II relaxes microvessels via the AT(2) receptor and Ca^{2+}-activated K^+ (BK_{Ca}) channels. *Hypertension,* 37**,** 301-7.

Di Wang, H., Boyd, R. & Forgione, A. (2008) Expression of ETA and ETB receptor in adventitial fibroblasts. *FASEB J.,* 22**,** 1148.8-.

Di Wang, H., Hope, S., Du, Y., Quinn, M. T., Cayatte, A., Pagano, P. J. & Cohen, R. A. (1999) Paracrine role of adventitial superoxide anion in mediating spontaneous tone of the isolated rat aorta in angiotensin II-induced hypertension. *Hypertension,* 33, 1225-32.

Di Wang, H., Pagano, P. J., Du, Y., Cayatte, A. J., Quinn, M. T., Brecher, P. & Cohen, R. A. (1998) Superoxide Anion From the Adventitia of the Rat Thoracic Aorta Inactivates Nitric Oxide. *Circ Res,* 82, 810-818.

Di Wang, H., Ratsep, M. T., Chapman, A. & Boyd, R. (2010) Adventitial fibroblasts in vascular structure and function: the role of oxidative stress and beyond. *Can J Physiol Pharmacol,* 88, 177-86.

Ding, Y., Chen, Z. J., Liu, S., Che, D., Vetter, M. & Chang, C. H. (2005) Inhibition of Nox-4 activity by plumbagin, a plant-derived bioactive naphthoquinone. *J Pharm Pharmacol,* 57, 111-6.

Dobrin, P. B. (1978) Mechanical properties of arteries. *Physiol Rev,* 58, 397-460.

Dong, L., Xie, M. J., Zhang, P., Ji, L. L., Liu, W. C., Dong, M. Q. & Gao, F. (2009) Rotenone partially reverses decreased BK Ca currents in cerebral artery smooth muscle cells from streptozotocin-induced diabetic mice. *Clin Exp Pharmacol Physiol,* 36, e57-64.

Drouin, A., Thorin-Trescases, N., Hamel, E., Falck, J. R. & Thorin, E. (2007) Endothelial nitric oxide synthase activation leads to dilatory H_2O_2 production in mouse cerebral arteries. *Cardiovasc Res,* 73, 73-81.

Dubroca, C., Loyer, X., Retailleau, K., Loirand, G., Pacaud, P., Feron, O., Balligand, J. L., Levy, B. I., Heymes, C. & Henrion, D. (2007) RhoA activation and interaction with Caveolin-1 are critical for pressure-induced myogenic tone in rat mesenteric resistance arteries. *Cardiovasc Res,* 73, 190-7.

Duckles, S. P. & Silverman, R. W. (1980) Transmural nerve stimulation of blood vessels in vitro: a critical examination. *Blood Vessels,* 17**,** 53-7.

Dunn, W. R. & Gardiner, S. M. (1997) Differential alteration in vascular structure of resistance arteries isolated from the cerebral and mesenteric vascular beds of transgenic [(mRen-2)27], hypertensive rats. *Hypertension,* 29, 1140-7.

Dworakowski, R., Anilkumar, N., Zhang, M. & Shah, A. M. (2006) Redox signalling involving NADPH oxidase-derived reactive oxygen species. *Biochem Soc Trans,* 34, 960-4.

Earley, S., Resta, T. C. & Walker, B. R. (2004) Disruption of smooth muscle gap junctions attenuates myogenic vasoconstriction of mesenteric resistance arteries. *Am J Physiol Heart Circ Physiol,* 287, H2677-86.

Eguchi, S., Miyashita, S., Kitamura, Y. & Kawasaki, H. (2007) Alpha3beta4-nicotinic receptors mediate adrenergic nerve- and peptidergic (CGRP) nerve-dependent vasodilation induced by nicotine in rat mesenteric arteries. *Br J Pharmacol,* 151, 1216-23.

Eskildsen-Helmond, Y. E. & Mulvany, M. J. (2003) Pressure-induced activation of extracellular signal-regulated kinase 1/2 in small arteries. *Hypertension,* 41, 891-7.

Falloon, B. J., Stephens, N., Tulip, J. R. & Heagerty, A. M. (1995) Comparison of small artery sensitivity and morphology in pressurized and wire-mounted preparations. *Am J Physiol,* 268**,** H670-8.

Faraci, F. M. (2006) Reactive oxygen species: influence on cerebral vascular tone. *J Appl Physiol,* 100, 739-43.

Feletou, M. & Vanhoutte, P. M. (1996) Endothelium-derived hyperpolarizing factor. *Clin Exp Pharmacol Physiol,* 23, 1082-90.

Ferrari, R., Guardigli, G., Mele, D., Percoco, G. F., Ceconi, C. & Curello, S. (2004) Oxidative stress during myocardial ischaemia and heart failure. *Curr Pharm Des,* 10, 1699-711.

Fischer, E. C., Santana, D. B., Zocalo, Y., Camus, J., de Forteza, E. & Armentano, R. (2010) Effects of removing the adventitia on the mechanical properties of ovine femoral arteries in vivo and in vitro. *Circ J,* 74, 1014-22.

Fike, C. D., Slaughter, J. C., Kaplowitz, M. R., Zhang, Y. & Aschner, J. L. (2008) Reactive oxygen species from NADPH oxidase contribute to altered pulmonary vascular responses in piglets with chronic hypoxia-induced pulmonary hypertension. *Am J Physiol Lung Cell Mol Physiol,* 295**,** L881-8.

Flavahan, N. A., Bailey, S. R., Flavahan, W. A., Mitra, S. & Flavahan, S. (2005) Imaging remodeling of the actin cytoskeleton in vascular smooth muscle cells after mechanosensitive arteriolar constriction. *Am J Physiol Heart Circ Physiol,* 288, H660-9.

Folkow, B. (1949) Intravascular pressure as a factor regulating the tone of the small vessels. *Acta Physiol Scand,* 17**,** 289-310.

Folkow, B. (2010) Cardiovascular "remodeling" in rat and human: time axis, extent, and in vivo relevance. *Physiology (Bethesda),* 25**,** 264-5.

Frisbee, J. C., Roman, R. J., Falck, J. R., Krishna, U. M. & Lombard, J. H. (2001) 20-HETE contributes to myogenic activation of skeletal muscle resistance arteries in Brown Norway and Sprague-Dawley rats. *Microcirculation,* 8, 45-55.

Furchgott, R. F. & Zawadzki, J. V. (1980) The obligatory role of endothelial cells in the relaxation of arterial smooth muscle by acetylcholine. *Nature,* 288, 373-6.

Fulton, D. J. (2009) Nox5 and the regulation of cellular function. *Antioxid Redox Signal,* 11**,** 2443-52.

Gerthoffer, W. T. & Gunst, S. J. (2001) Invited review: focal adhesion and small heat shock proteins in the regulation of actin remodeling and contractility in smooth muscle. *J Appl Physiol,* 91, 963-72.

Gibbons, G. H., Pratt, R. E. & Dzau, V. J. (1992) Vascular smooth muscle cell hypertrophy vs. hyperplasia. Autocrine transforming growth factor-beta 1 expression determines growth response to angiotensin II. *J Clin Invest,* 90, 456-61.

Glukhova, M. & Koteliansky, V. (1995) Integrins, Cytoskeletal and Extracellular Matrix Proteins in Developing Smooth Muscle Cells of Human Aorta. IN SM, S. & RP, M. (Eds.) *The Vascular Smooth Muscle Cell: Molecular and Biological Responses to the Extracellular Matrix.* San Diego, Academic.

Gokina, N. I., Knot, H. J., Nelson, M. T. & Osol, G. (1999) Increased Ca^{2+} sensitivity as a key mechanism of PKC-induced constriction in pressurized cerebral arteries. *Am J Physiol,* 277, H1178-88.

Gokina, N. I. & Osol, G. (2002) Actin cytoskeletal modulation of pressure-induced depolarization and Ca^{2+} influx in cerebral arteries. *Am J Physiol Heart Circ Physiol,* 282, H1410-1420.

Gokina, N. I., Park, K. M., McElroy-Yaggy, K. & Osol, G. (2005) Effects of Rho kinase inhibition on cerebral artery myogenic tone and reactivity. *J Appl Physiol,* 98, 1940-8.

Gonzalez, J. M., Briones, A. M., Starcher, B., Conde, M. V., Somoza, B., Daly, C., Vila, E., McGrath, I., Gonzalez, M. C. & Arribas, S. M. (2005) Influence of elastin on rat small artery mechanical properties. *Exp Physiol,* 90, 463-8.

Gonzalez, J. M., Somoza, B., Conde, M. V., Fernandez-Alfonso, M. S., Gonzalez, M. C. & Arribas, S. M. (2008) Hypertension increases middle cerebral artery resting tone in spontaneously hypertensive rats: role of tonic vasoactive factor availability. *Clin Sci (Lond),* 114, 651-9.

Gonzalez, M. C., Arribas, S. M., Molero, F. & Fernandez-Alfonso, M. S. (2001) Effect of removal of adventitia on vascular smooth muscle contraction and relaxation. *Am J Physiol Heart Circ Physiol,* 280, H2876-2881.

Griendling, K. K. & FitzGerald, G. A. (2003) Oxidative stress and cardiovascular injury: Part I: basic mechanisms and in vivo monitoring of ROS. *Circulation,* 108**,** 1912-6.

Griendling, K. K., Minieri, C. A., Ollerenshaw, J. D. & Alexander, R. W. (1994) Angiotensin II stimulates NADH and NADPH oxidase activity in cultured vascular smooth muscle cells. *Circ Res,* 74, 1141-8.

Griendling, K. K. & Ushio-Fukai, M. (2000) Reactive oxygen species as mediators of angiotensin II signaling. *Regul Pept,* 91, 21-7.

Gschwend, S., Henning, R. H., Pinto, Y. M., de Zeeuw, D., van Gilst, W. H. & Buikema, H. (2003) Myogenic constriction is increased in mesenteric resistance arteries from rats with chronic heart failure: instantaneous counteraction by acute AT1 receptor blockade. *Br J Pharmacol,* 139**,** 1317-25.

Gunduz, F., Baskurt, O. K. & Meiselman, H. J. (2009) Vascular dilation responses of rat small mesenteric arteries at high intravascular pressure in spontaneously hypertensive rats. *Circ J,* 73, 2091-7.

Gunst, S. J. & Zhang, W. (2008) Actin cytoskeletal dynamics in smooth muscle: a new paradigm for the regulation of smooth muscle contraction. *Am J Physiol Cell Physiol,* 295, C576-87.

Hamilton, C. A., Miller, W. H., Al-Benna, S., Brosnan, M. J., Drummond, R. D., McBride, M. W. & Dominiczak, A. F. (2004) Strategies to reduce oxidative stress in cardiovascular disease. *Clin Sci (Lond),* 106, 219-34.

Harder, D. R. (1984) Pressure-dependent membrane depolarization in cat middle cerebral artery. *Circ Res,* 55, 197-202.

Harrison, D. G., Cai, H., Landmesser, U. & Griendling, K. K. (2003) Interactions of angiotensin II with NAD(P)H oxidase, oxidant stress and cardiovascular disease. *J Renin Angiotensin Aldosterone Syst,* 4, 51-61.

Haurani, M. J. & Pagano, P. J. (2007) Adventitial fibroblast reactive oxygen species as autacrine and paracrine mediators of remodeling: Bellwether for vascular disease? *Cardiovasc Res,* 75, 679-689.

Hayashi, K., Ozawa, Y., Fujiwara, K., Wakino, S., Kumagai, H. & Saruta, T. (2003) Role of actions of calcium antagonists on efferent arterioles--with special references to glomerular hypertension. *Am J Nephrol,* 23, 229-44.

Heitzer, T., Wenzel, U., Hink, U., Krollner, D., Skatchkov, M., Stahl, R. A., MacHarzina, R., Brasen, J. H., Meinertz, T. & Munzel, T. (1999) Increased NAD(P)H oxidase-mediated superoxide production in renovascular hypertension: evidence for an involvement of protein kinase C. *Kidney Int,* 55**,** 252-60.

Henrion, D. (2005) Pressure and flow-dependent tone in resistance arteries. Role of myogenic tone. *Arch Mal Coeur Vaiss,* 98, 913-21.

Hill, M. A., Davis, M. J., Meininger, G. A., Potocnik, S. J. & Murphy, T. V. (2006) Arteriolar myogenic signalling mechanisms: Implications for local vascular function. *Clin Hemorheol Microcirc,* 34, 67-79.

Hill, M. A., Meininger, G. A., Davis, M. J. & Laher, I. (2009) Therapeutic potential of pharmacologically targeting arteriolar myogenic tone. *Trends Pharmacol Sci,* 30, 363-74.

Hill, M. A., Sun, Z., Martinez-Lemus, L. & Meininger, G. A. (2007) New technologies for dissecting the arteriolar myogenic response. *Trends Pharmacol Sci,* 28, 308-15.

Hill, M. A., Zou, H., Davis, M. J., Potocnik, S. J. & Price, S. (2000) Transient increases in diameter and $[Ca^{2+}]_i$ are not obligatory for myogenic constriction. *Am J Physiol Heart Circ Physiol,* 278, H345-52.

Hill, M. A., Zou, H., Potocnik, S. J., Meininger, G. A. & Davis, M. J. (2001) Invited review: arteriolar smooth muscle mechanotransduction: Ca^{2+} signaling pathways underlying myogenic reactivity. *J Appl Physiol,* 91, 973-83.

Hu, T., Ramachandrarao, S. P., Siva, S., Valancius, C., Zhu, Y., Mahadev, K., Toh, I., Goldstein, B. J., Woolkalis, M. & Sharma, K. (2005) Reactive oxygen species production via NADPH oxidase mediates TGF-beta-induced cytoskeletal alterations in endothelial cells. *Am J Physiol Renal Physiol,* 289, F816-25.

Hu, C. L., Xiang, J. Z. & Hu, F. F. (2008) Vanilloid receptor TRPV1, sensory C-fibers, and activation of adventitial mast cells. A novel mechanism involved in adventitial inflammation. *Med Hypotheses,* 71**,** 102-3.

Hsu, Y. H., Chen, J. J., Chang, N. C., Chen, C. H., Liu, J. C., Chen, T. H., Jeng, C. J., Chao, H. H. & Cheng, T. H. (2004) Role of reactive oxygen species-sensitive extracellular signal-regulated kinase pathway in angiotensin II-induced endothelin-1 gene expression in vascular endothelial cells. *J Vasc Res,* 41**,** 64-74.

Hwang, J., Saha, A., Boo, Y. C., Sorescu, G. P., McNally, J. S., Holland, S. M., Dikalov, S., Giddens, D. P., Griendling, K. K., Harrison, D. G. & Jo, H. (2003) Oscillatory shear stress stimulates endothelial production of O^{2-} from p47phox-dependent NAD(P)H oxidases, leading to monocyte adhesion. *J Biol Chem,* 278**,** 47291-8.

Hyrsl, P., Lojek, A., Ciz, M. & Kubala, L. (2004) Chemiluminescence of lucigenin is dependent on experimental conditions. *Luminescence,* 19, 61-3.

Ignarro, L. J., Buga, G. M., Wood, K. S., Byrns, R. E. & Chaudhuri, G. (1987) Endothelium-derived relaxing factor produced and released from artery and vein is nitric oxide. *Proc Natl Acad Sci U S A,* 84, 9265-9.

Ikushima, S., Muramatsu, I. & Fujiwara, M. (1982) Nicotine-induced response in guinea-pig aorta enhanced by goniopora toxin. *J Pharmacol Exp Ther,* 223**,** 790-4.

Imig, J. D. (1999) Epoxyeicosatrienoic acids. Biosynthesis, regulation, and actions. *Methods Mol Biol,* 120, 173-92.

Ishikawa, H., Uga, S., Mashimo, K., Yoshitomi, T., Kusanagi, M. & Shimizu, K. (2004) Pharmacological vascular reactivity in isolated hypercholesterolemic rabbit ciliary artery. *Exp Eye Res,* 78**,** 805-13.

Intengan, H. D., Deng, L. Y., Li, J. S. & Schiffrin, E. L. (1999) Mechanics and composition of human subcutaneous resistance arteries in essential hypertension. *Hypertension,* 33**,** 569-74.

Itoh, H., Sakai, J., Imoto, A. & Creed, K. E. (1995) The control of smooth muscle tissues by nonadrenergic noncholinergic (NANC) nerve fibres in the autonomic nervous system. *J Smooth Muscle Res,* 31, 67-78.

Iwatani Y, Numa H, Atagi S, Takayama F, Mio M & H., K. (2007) Mechanisms underlying enhanced vasodilator responses to various vasodilator agents following endothelium removal in rat mesenteric resistance arteries. *Yakugaku Zasshi,* 127, 729-33.

Iwatani, Y., Kosugi, K., Isobe-Oku, S., Atagi, S., Kitamura, Y. & Kawasaki, H. (2008) Endothelium removal augments endothelium-independent vasodilatation in rat mesenteric vascular bed. *Br J Pharmacol,* 154, 32-40.

Jarajapu, Y. P. & Knot, H. J. (2002) Role of phospholipase C in development of myogenic tone in rat posterior cerebral arteries. *Am J Physiol Heart Circ Physiol,* 283, H2234-8.

Jarajapu, Y. P. & Knot, H. J. (2005) Relative contribution of Rho kinase and protein kinase C to myogenic tone in rat cerebral arteries in hypertension. *Am J Physiol Heart Circ Physiol,* 289, H1917-22.

Jayasundar, S. & Vohra, M. M. (1978) An analysis of action of nicotinic agents on adrenergic nerve terminals in rat isolated vas deferens. *Arch Int Pharmacodyn Ther,* 232, 192-201.

Jernigan, N. L., Resta, T. C. & Walker, B. R. (2004) Contribution of oxygen radicals to altered NO-dependent pulmonary vasodilation in acute and chronic hypoxia. *Am J Physiol Lung Cell Mol Physiol,* 286**,** L947-55.

Jimenez-Altayo, F., Martin, A., Rojas, S., Justicia, C., Briones, A. M., Giraldo, J., Planas, A. M. & Vila, E. (2007) Transient middle cerebral artery occlusion causes different structural, mechanical, and myogenic alterations in normotensive and hypertensive rats. *Am J Physiol Heart Circ Physiol,* 293, H628-35.

Judkins, C. P., Diep, H., Broughton, B. R., Mast, A. E., Hooker, E. U., Miller, A. A., Selemidis, S., Dusting, G. J., Sobey, C. G. & Drummond, G. R. (2010) Direct evidence of a role for Nox2 in superoxide production, reduced nitric oxide bioavailability, and early atherosclerotic plaque formation in ApoE-/- mice. *Am J Physiol Heart Circ Physiol,* 298, H24-32.

Kagota, S., Tamashiro, A., Yamaguchi, Y., Sugiura, R., Kuno, T., Nakamura, K. & Kunitomo, M. (2001) Downregulation of vascular soluble guanylate cyclase induced by high salt intake in spontaneously hypertensive rats. *Br J Pharmacol,* 134, 737-44.

Kaley, G. (2000) Regulation of vascular tone: role of 20-HETE in the modulation of myogenic reactivity. *Circ Res,* 87, 4-5.

Kawasaki, H., Eguchi, S., Miyashita, S., Chan, S., Hirai, K., Hobara, N., Yokomizo, A., Fujiwara, H., Zamami, Y., Koyama, T., Jin, X. & Kitamura, Y. (2009) Proton acts as a neurotransmitter for nicotine-induced adrenergic and CGRPergic nerve-mediated vasodilation in the rat mesenteric artery. *J Pharmacol Exp Ther*., 330, 745-55.

Keller, M., Lidington, D., Vogel, L., Peter, B. F., Sohn, H.-Y., Pagano, P. J., Pitson, S., Spiegel, S., Pohl, U. & Bolz, S.-S. (2006) Sphingosine kinase functionally links elevated transmural pressure and increased reactive oxygen species formation in resistance arteries. *FASEB J.*, 05-4075fje.

Kemler, M. A., Kolkman, W. F., Slootweg, P. J. & Kon, M. (1997) Adventitial stripping does not strip the adventitia. *Plast Reconstr Surg,* 99**,** 1626-31.

Khavandi, K., Greenstein, A. S., Sonoyama, K., Withers, S., Price, A., Malik, R. A. & Heagerty, A. M. (2009) Myogenic tone and small artery remodelling: insight into diabetic nephropathy. *Nephrol Dial Transplant,* 24**,** 361-9.

Kido, M. A., Zhang, J. Q., Muroya, H., Yamaza, T., Terada, Y. & Tanaka, T. (2001) Topography and distribution of sympathetic nerve fibers in the rat temporomandibular joint: immunocytochemistry and ultrastructure. *Anat Embryol (Berl),* 203, 357-66.

Kimura, K., Tsuda, K., Moriwaki, C., Kawabe, T., Hamada, M., Obana, M., Baba, A., Hano, T. & Nishio, I. (2002) Leukemia inhibitory factor relaxes arteries through endothelium-dependent mechanism. *Biochem Biophys Res Commun,* 294**,** 359-62.

Kleschyov, A. L., Muller, B., Schott, C. & Stoclet, J. C. (1998) Role of adventitial nitric oxide in vascular hyporeactivity induced by lipopolysaccharide in rat aorta. *Br J Pharmacol,* 124, 623-6.

Klinge, E. & Sjostrand, N. O. (1977) Suppression of the excitatory adrenergic neurotransmission; a possible role of cholinergic nerves in the retractor penis muscle. *Acta Physiol Scand,* 100, 368-76.

Klukovits A, Gáspár R, Sántha P, Jancsó G, Falkay G. (2002) Functional and Histochemical Characterization of a Uterine Adrenergic Denervation Process in Pregnant Rats. *Biol Reprod*. 67, 1013-7.

Knot, H. J. & Nelson, M. T. (1998) Regulation of arterial diameter and wall [Ca^{2+}] in cerebral arteries of rat by membrane potential and intravascular pressure. *J Physiol,* 508 (Pt 1), 199-209.

Kontos, H. A., Wei, E. P., Povlishock, J. T. & Christman, C. W. (1984) Oxygen radicals mediate the cerebral arteriolar dilation from arachidonate and bradykinin in cats. *Circ Res,* 55**,** 295-303.

Kotecha, N. & Hill, M. A. (2005) Myogenic contraction in rat skeletal muscle arterioles: smooth muscle membrane potential and Ca^{2+} signaling. *Am J Physiol Heart Circ Physiol,* 289, H1326-34.

Kramer, B. K., Ittner, K. P., Beyer, M. E., Hoffmeister, H. M. & Riegger, G. A. (1997) Circulatory and myocardial effects of endothelin. *J Mol Med,* 75, 886-90.

Kuo, L., Davis, M. J. & Chilian, W. M. (1988) Myogenic activity in isolated subepicardial and subendocardial coronary arterioles. *Am J Physiol,* 255, H1558-62.

Kurahashi, K., Shirahase, H., Nakamura, S., Tarumi, T., Koshino, Y., Wang, A. M., Nishihashi, T. & Shimizu, Y. (2001) Nicotine-induced contraction in the rat coronary artery: possible involvement of the endothelium, reactive oxygen species and COX-1 metabolites. *J Cardiovasc Pharmacol,* 38 Suppl 1, S21-5.

Laflamme, K., Roberge, C. J., Grenier, G., Remy-Zolghadri, M., Pouliot, S., Baker, K., Labbe, R., D'Orleans-Juste, P., Auger, F. A. & Germain, L. (2006) Adventitia contribution in vascular tone: insights from adventitia-derived cells in a tissue-engineered human blood vessel. *FASEB J,* 20, 1245-7.

Lagaud, G., Gaudreault, N., Moore, E. D., Van Breemen, C. & Laher, I. (2002) Pressure-dependent myogenic constriction of cerebral arteries occurs independently of voltage-dependent activation. *Am J Physiol Heart Circ Physiol,* 283, H2187-95.

Lagaud, G. J., Lam, E., Lui, A., van Breemen, C. & Laher, I. (1999) Nonspecific inhibition of myogenic tone by PD98059, a MEK1 inhibitor, in rat middle cerebral arteries. *Biochem Biophys Res Commun,* 257, 523-7.

Landmesser, U., Cai, H., Dikalov, S., McCann, L., Hwang, J., Jo, H., Holland, S. M. & Harrison, D. G. (2002) Role of p47(phox) in vascular oxidative stress and hypertension caused by angiotensin II. *Hypertension,* 40, 511-5.

Lassegue, B., Sorescu, D., Szocs, K., Yin, Q., Akers, M., Zhang, Y., Grant, S. L., Lambeth, J. D. & Griendling, K. K. (2001) Novel gp91(phox) homologues in vascular smooth muscle cells : nox1 mediates angiotensin II-induced superoxide formation and redox-sensitive signaling pathways. *Circ Res,* 88**,** 888-94.

Lang, D. (2002) Cardiac hypertrophy and oxidative stress: a leap of faith or stark reality? *Heart,* 87, 316-7.

Lecarpentier, Y. (2007) Physiological role of free radicals in skeletal muscles. *J Appl Physiol,* 103, 1917-8.

Lee, R. M. (1995) Morphology of cerebral arteries. *Pharmacol Ther,* 66, 149-73.

Lee, R. M., Forrest, J. B., Garfield, R. E. & Daniel, E. E. (1983) Ultrastructural changes in mesenteric arteries from spontaneously hypertensive rats. A morphometric study. *Blood Vessels,* 20**,** 72-91.

Li, Z. & Duckles, S. P. (1993) Acute effects of nicotine on rat mesenteric vasculature and tail artery. *J Pharmacol Exp Ther,* 264, 1305-10.

Lin, M. J., Liu, S. H. & Lin-Shiau, S. Y. (1998) Phorbol ester-induced contractions of mouse detrusor muscle are inhibited by nifedipine. *Naunyn Schmiedebergs Arch Pharmacol,* 357, 553-7.

Lin, P. J., Pearson, P. J. & Chang, C. H. (1993) Endothelium-derived relaxing factors. *Changgeng Yi Xue Za Zhi,* 16, 1-13.

Liu, Y., Harder, D. R. & Lombard, J. H. (2002) Interaction of myogenic mechanisms and hypoxic dilation in rat middle cerebral arteries. *Am J Physiol Heart Circ Physiol,* 283**,** H2276-81.

Looft-Wilson, R. C. & Gisolfi, C. V. (2000) Rat small mesenteric artery function after hindlimb suspension. *J Appl Physiol,* 88**,** 1199-206.

Lu, C., Su, L. Y., Lee, R. M. & Gao, Y. J. (2008) Superoxide anion mediates angiotensin II-induced potentiation of contractile response to sympathetic stimulation. *Eur J Pharmacol,* 589, 188-93.

Lucchesi, P. A., Belmadani, S. & Matrougui, K. (2005) Hydrogen peroxide acts as both vasodilator and vasoconstrictor in the control of perfused mouse mesenteric resistance arteries. *J Hypertens,* 23, 571-9.

Lucchesi, P. A., Sabri, A., Belmadani, S. & Matrougui, K. (2004) Involvement of metalloproteinases 2/9 in epidermal growth factor receptor transactivation in pressure-induced myogenic tone in mouse mesenteric resistance arteries. *Circulation,* 110, 3587-93.

Lyle, A. N. & Griendling, K. K. (2006) Modulation of vascular smooth muscle signaling by reactive oxygen species. *Physiology (Bethesda),* 21, 269-80.

Maeso, R., Navarro-Cid, J., Munoz-Garcia, R., Rodrigo, E., Ruilope, L. M., Lahera, V. & Cachofeiro, V. (1996) Losartan reduces phenylephrine constrictor response in aortic rings from spontaneously hypertensive rats. Role of nitric oxide and angiotensin II type 2 receptors. *Hypertension,* 28**,** 967-72.

Maneen, M. J., Hannah, R., Vitullo, L., DeLance, N. & Cipolla, M. J. (2006) Peroxynitrite diminishes myogenic activity and is associated with decreased vascular smooth muscle F-actin in rat posterior cerebral arteries. *Stroke,* 37, 894-9.

Martinez-Lemus, L. A. (2008) Persistent agonist-induced vasoconstriction is not required for angiotensin II to mediate inward remodeling of isolated arterioles with myogenic tone. *J Vasc Res,* 45, 211-21.

Martinez-Lemus, L. A., Hill, M. A., Bolz, S. S., Pohl, U. & Meininger, G. A. (2004) Acute mechanoadaptation of vascular smooth muscle cells in response to continuous arteriolar vasoconstriction: implications for functional remodeling. *Faseb J,* 18, 708-10.

Martinez-Lemus, L. A., Hill, M. A. & Meininger, G. A. (2009) The plastic nature of the vascular wall: a continuum of remodeling events contributing to control of arteriolar diameter and structure. *Physiology (Bethesda),* 24, 45-57.

Massett, M. P., Ungvari, Z., Csiszar, A., Kaley, G. & Koller, A. (2002) Different roles of PKC and MAP kinases in arteriolar constrictions to pressure and agonists. *Am J Physiol Heart Circ Physiol,* 283, H2282-7.

Matchkov, V. V., Tarasova, O. S., Mulvany, M. J. & Nilsson, H. (2002) Myogenic response of rat femoral small arteries in relation to wall structure and $[Ca^{2+}]_i$. *Am J Physiol Heart Circ Physiol,* 283, H118-25.

Matoba, T., Shimokawa, H., Kubota, H., Morikawa, K., Fujiki, T., Kunihiro, I., Mukai, Y., Hirakawa, Y. & Takeshita, A. (2002) Hydrogen peroxide is an endothelium-derived hyperpolarizing factor in human mesenteric arteries. *Biochem Biophys Res Commun,* 290, 909-13.

Matoba, T., Shimokawa, H., Nakashima, M., Hirakawa, Y., Mukai, Y., Hirano, K., Kanaide, H. & Takeshita, A. (2000) Hydrogen peroxide is an endothelium-derived hyperpolarizing factor in mice. *J Clin Invest,* 106, 1521-30.

Matrougui, K., Eskildsen-Helmond, Y. E., Fiebeler, A., Henrion, D., Levy, B. I., Tedgui, A. & Mulvany, M. J. (2000) Angiotensin II stimulates extracellular signal-regulated kinase activity in intact pressurized rat mesenteric resistance arteries. *Hypertension,* 36, 617-21.

Mauss, S., Koch, G., Kreye, V. A. & Aktories, K. (1989) Inhibition of the contraction of the isolated longitudinal muscle of the guinea-pig ileum by botulinum C2 toxin: evidence for a role of G/F-actin transition in smooth muscle contraction. *Naunyn Schmiedebergs Arch Pharmacol,* 340, 345-51.

McCarron, J. G., Crichton, C. A., Langton, P. D., MacKenzie, A. & Smith, G. L. (1997) Myogenic contraction by modulation of voltage-dependent calcium currents in isolated rat cerebral arteries. *J Physiol,* 498 (Pt 2), 371-9.

Mederos y Schnitzler, M., Storch, U., Meibers, S., Nurwakagari, P., Breit, A., Essin, K., Gollasch, M. & Gudermann, T. (2008) Gq-coupled receptors as mechanosensors mediating myogenic vasoconstriction. *EMBO J,* 27, 3092-103.

Mehta, D. & Gunst, S. J. (1999) Actin polymerization stimulated by contractile activation regulates force development in canine tracheal smooth muscle. *J Physiol,* 519 Pt 3, 829-40.

Mehta, P. K. & Griendling, K. K. (2007) Angiotensin II cell signaling: physiological and pathological effects in the cardiovascular system. *Am J Physiol Cell Physiol,* 292, C82-97.

Meininger, G. A., Zawieja, D. C., Falcone, J. C., Hill, M. A. & Davey, J. P. (1991) Calcium measurement in isolated arterioles during myogenic and agonist stimulation. *Am J Physiol,* 261, H950-9.

Meloche, S., Landry, J., Huot, J., Houle, F., Marceau, F. & Giasson, E. (2000) p38 MAP kinase pathway regulates angiotensin II-induced contraction of rat vascular smooth muscle. *Am J Physiol Heart Circ Physiol,* 279, H741-51.

Miller, A. A., Drummond, G. R., De Silva, T. M., Mast, A. E., Hickey, H., Williams, J. P., Broughton, B. R. & Sobey, C. G. (2009) NADPH oxidase activity is higher in cerebral versus systemic arteries of four animal species: role of Nox2. *Am J Physiol Heart Circ Physiol,* 296, H220-5.

Miller, A. A., Drummond, G. R., Mast, A. E., Schmidt, H. H. & Sobey, C. G. (2007) Effect of gender on NADPH-oxidase activity, expression, and function in the cerebral circulation: role of estrogen. *Stroke,* 38, 2142-9.

Miller, A. A., Drummond, G. R., Schmidt, H. H. & Sobey, C. G. (2005) NADPH oxidase activity and function are profoundly greater in cerebral versus systemic arteries. *Circ Res,* 97, 1055-62.

Miller, A. A., Drummond, G. R. & Sobey, C. G. (2006) Reactive oxygen species in the cerebral circulation: are they all bad? *Antioxid Redox Signal,* 8, 1113-20.

Miura, H., Bosnjak, J. J., Ning, G., Saito, T., Miura, M. & Gutterman, D. D. (2003) Role for hydrogen peroxide in flow-induced dilation of human coronary arterioles. *Circ Res,* 92, e31-40.

Mogford, J. E., Davis, G. E., Platts, S. H. & Meininger, G. A. (1996) Vascular smooth muscle alpha v beta 3 integrin mediates arteriolar vasodilation in response to RGD peptides. *Circ Res,* 79, 821-6.

Moldovan, L., Moldovan, N. I., Sohn, R. H., Parikh, S. A. & Goldschmidt-Clermont, P. J. (2000) Redox changes of cultured endothelial cells and actin dynamics. *Circ Res,* 86, 549-57.

Moldovan, L., Mythreye, K., Goldschmidt-Clermont, P. J. & Satterwhite, L. L. (2006) Reactive oxygen species in vascular endothelial cell motility. Roles of NAD(P)H oxidase and Rac1. *Cardiovasc Res,* 71, 236-46.

Montezano, A. C., Burger, D., Paravicini, T. M., Chignalia, A. Z., Yusuf, H., Almasri, M., He, Y., Callera, G. E., He, G., Krause, K. H., Lambeth, D., Quinn, M. T. & Touyz, R. M. (2010) Nicotinamide adenine dinucleotide phosphate reduced oxidase 5 (Nox5) regulation by angiotensin II and endothelin-1 is mediated via calcium/calmodulin-dependent, rac-1-independent pathways in human endothelial cells. *Circ Res,* 106**,** 1363-73.

Moosmang, S., Schulla, V., Welling, A., Feil, R., Feil, S., Wegener, J. W., Hofmann, F. & Klugbauer, N. (2003) Dominant role of smooth muscle L-type calcium channel Cav1.2 for blood pressure regulation. *EMBO J,* 22, 6027-34.

Mulvany, M. J. & Aalkjaer, C. (1990) Structure and function of small arteries. *Physiol Rev,* 70, 921-61.

Mulvany, M. J. & Halpern, W. (1977) Contractile properties of small arterial resistance vessels in spontaneously hypertensive and normotensive rats. *Circ Res,* 41**,** 19-26.

Mulvany, M. J., Hansen, O. K. & Aalkjaer, C. (1978) Direct evidence that the greater contractility of resistance vessels in spontaneously hypertensive rats is associated with a narrowed lumen, a thickened media, and an increased number of smooth muscle cell layers. *Circ Res,* 43**,** 854-64.

Mulvany, M. J., Baumbach, G. L., Aalkjaer, C., Heagerty, A. M., Korsgaard, N., Schiffrin, E. L. & Heistad, D. D. (1996) Vascular remodeling. *Hypertension,* 28, 505-6.

Nakayama, K., Obara, K., Ishikawa, H. & Nishizizawa (2010) Specific mechanotransduction signalling involved in myogenic responses of the cerebral arteries *Kamkin, A. & Kiseleva, I. Mechanosensitivity in Cells and Tissues* 453-475, Springer Science+Business Media.

Narayanan, D., Xi, Q., Pfeffer, L. M. & Jaggar, J. H. (2010) Mitochondria Control Functional CaV1.2 Expression in Smooth Muscle Cells of Cerebral Arteries. *Circ Res*.

Narayanan, J., Imig, M., Roman, R. J. & Harder, D. R. (1994) Pressurization of isolated renal arteries increases inositol trisphosphate and diacylglycerol. *Am J Physiol,* 266, H1840-5.

Nishiyama, A., Kobori, H., Fukui, T., Zhang, G. X., Yao, L., Rahman, M., Hitomi, H., Kiyomoto, H., Shokoji, T., Kimura, S., Kohno, M. & Abe, Y. (2003) Role of angiotensin II and reactive oxygen species in cyclosporine A-dependent hypertension. *Hypertension,* 42, 754-60.

Nowicki, P. T., Flavahan, S., Hassanain, H., Mitra, S., Holland, S., Goldschmidt-Clermont, P. J. & Flavahan, N. A. (2001) Redox signaling of the arteriolar myogenic response. *Circ Res,* 89, 114-6.

O'Donnell, B. V., Tew, D. G., Jones, O. T. & England, P. J. (1993) Studies on the inhibitory mechanism of iodonium compounds with special reference to neutrophil NADPH oxidase. *Biochem J,* 290 (Pt 1), 41-9.

Ohanian, J., Gatfield, K. M., Ward, D. T. & Ohanian, V. (2005) Evidence for a functional calcium-sensing receptor that modulates myogenic tone in rat subcutaneous small arteries. *Am J Physiol Heart Circ Physiol,* 288, H1756-62.

Onoue, H., Tsutsui, M., Smith, L., O'Brien, T. & Katusic, Z. S. (1999) Adventitial expression of recombinant endothelial nitric oxide synthase gene reverses vasoconstrictor effect of endothelin-1. *J Cereb Blood Flow Metab,* 19, 1029-37.

Onoue, H., Tsutsui, M., Smith, L., Stelter, A., O'Brien, T. & Katusic, Z. S. (1998) Expression and function of recombinant endothelial nitric oxide synthase gene in canine basilar artery after experimental subarachnoid hemorrhage. *Stroke,* 29, 1959-65; discussion 1965-6.

Pagano, P. J., Chanock, S. J., Siwik, D. A., Colucci, W. S. & Clark, J. K. (1998) Angiotensin II induces p67phox mRNA expression and NADPH oxidase superoxide generation in rabbit aortic adventitial fibroblasts. *Hypertension,* 32, 331-7.

Pagano, P. J., Clark, J. K., Cifuentes-Pagano, M. E., Clark, S. M., Callis, G. M. & Quinn, M. T. (1997) Localization of a constitutively active, phagocyte-like NADPH oxidase in rabbit aortic adventitia: enhancement by angiotensin II. *Proc Natl Acad Sci U S A,* 94, 14483-8.

Pagano, P. J. & Gutterman, D. D. (2007) The adventitia: The outs and ins of vascular disease. *Cardiovasc Res,* 75, 636-639.

Papakonstanti, E. A. & Stournaras, C. (2008) Cell responses regulated by early reorganization of actin cytoskeleton. *FEBS Lett,* 582**,** 2120-7.

Paravicini, T. M. & Sobey, C. G. (2003) Cerebral vascular effects of reactive oxygen species: recent evidence for a role of NADPH-oxidase. *Clin Exp Pharmacol Physiol,* 30**,** 855-9.

Parker, T. A., Grover, T. R., Kinsella, J. P., Falck, J. R. & Abman, S. H. (2005) Inhibition of 20-HETE abolishes the myogenic response during NOS antagonism in the ovine fetal pulmonary circulation. *Am J Physiol Lung Cell Mol Physiol,* 289, L261-7.

Pedruzzi, E., Guichard, C., Ollivier, V., Driss, F., Fay, M., Prunet, C., Marie, J. C., Pouzet, C., Samadi, M., Elbim, C., O'Dowd, Y., Bens, M., Vandewalle, A., Gougerot-Pocidalo, M. A., Lizard, G. & Ogier-Denis, E. (2004) NAD(P)H oxidase Nox-4 mediates 7-ketocholesterol-induced endoplasmic reticulum stress and apoptosis in human aortic smooth muscle cells. *Mol Cell Biol,* 24, 10703-17.

Phillips, S. A., Sylvester, F. A. & Frisbee, J. C. (2005) Oxidant stress and constrictor reactivity impair cerebral artery dilation in obese Zucker rats. *Am J Physiol Regul Integr Comp Physiol,* 288, R522-30.

Raina, H., Ella, S. R. & Hill, M. A. (2008) Decreased activity of the smooth muscle Na^{+}/Ca^{2+} exchanger impairs arteriolar myogenic reactivity. *J Physiol,* 586, 1669-81.

Rajagopalan, S., Kurz, S., Munzel, T., Tarpey, M., Freeman, B. A., Griendling, K. K. & Harrison, D. G. (1996) Angiotensin II-mediated hypertension in the rat increases vascular superoxide production via membrane NADH/NADPH oxidase activation. Contribution to alterations of vasomotor tone. *J Clin Invest,* 97, 1916-23.

Ramirez, R. J., Hubel, C. A., Novak, J., DiCianno, J. R., Kagan, V. E. & Gandley, R. E. (2006) Moderate ascorbate deficiency increases myogenic tone of arteries from pregnant but not virgin ascorbate-dependent rats. *Hypertension,* 47**,** 454-60.

Ren, Y., D'Ambrosio, M. A., Liu, R., Pagano, P. J., Garvin, J. L. & Carretero, O. A. (2010) Enhanced myogenic response in the afferent arteriole of spontaneously hypertensive rats. *Am J Physiol Heart Circ Physiol,* 298, H1769-75.

Resta, T. C., Broughton, B. R. & Jernigan, N. L. (2010) Reactive oxygen species and RhoA signaling in vascular smooth muscle: role in chronic hypoxia-induced pulmonary hypertension. *Adv Exp Med Biol,* 661, 355-73.

Rey, F. E., Cifuentes, M. E., Kiarash, A., Quinn, M. T. & Pagano, P. J. (2001) Novel competitive inhibitor of NAD(P)H oxidase assembly attenuates vascular O_2^- and systolic blood pressure in mice. *Circ Res,* 89**,** 408-14.

Rey, F. E. & Pagano, P. J. (2002) The reactive adventitia: fibroblast oxidase in vascular function. *Arterioscler Thromb Vasc Biol,* 22, 1962-71.

Rizzoni, D., Muiesan, M. L., Porteri, E., de Ciuceis, C., Boari, G. E. M., Salvetti, M., Paini, A. & Rosei, E. A. (2009) Vascular remodelling, macro- and microvessels: Therapeutic implications. *Blood Pressure,* 18, 242-46.

Sachidanandam, K., Portik-Dobos, V., Harris, A. K., Hutchinson, J. R., Muller, E., Johnson, M. H. & Ergul, A. (2007) Evidence for vasculoprotective effects of ETB receptors in resistance artery remodeling in diabetes. *Diabetes,* 56**,** 2753-8.

Saito, S. Y., Hori, M., Ozaki, H. & Karaki, H. (1996) Cytochalasin D inhibits smooth muscle contraction by directly inhibiting contractile apparatus. *J Smooth Muscle Res,* 32, 51-60.

Sanchez-Fernandez, C., Gonzalez, M. C., Beart, P. M., Mercer, L. D., Ruiz-Gayo, M. & Fernandez-Alfonso, M. S. (2004) A novel role for cholecystokinin: regulation of mesenteric vascular resistance. *Regul Pept,* 121, 145-53.

Saran, M. & Bors, W. (1994) Signalling by O_2^-. and NO: how far can either radical, or any specific reaction product, transmit a message under in vivo conditions? *Chem Biol Interact,* 90, 35-45.

Schiffrin, E. L. (2004) Remodeling of resistance arteries in essential hypertension and effects of antihypertensive treatment. *Am J Hypertens,* 17, 1192-200.

Schmid-Schonbein, G. W. & Murakami, H. (1985) Blood flow in contracting arterioles. *Int J Microcirc Clin Exp,* 4**,** 311-28.

Schofield, I., Malik, R., Izzard, A., Austin, C. & Heagerty, A. (2002) Vascular structural and functional changes in type 2 diabetes mellitus: evidence for the roles of abnormal myogenic responsiveness and dyslipidemia. *Circulation,* 106, 3037-43.

Schubert, R., Lidington, D. & Bolz, S. S. (2008) The emerging role of Ca^{2+} sensitivity regulation in promoting myogenic vasoconstriction. *Cardiovasc Res,* 77, 8-18.

Scotland, R. S., Chauhan, S., Davis, C., De Felipe, C., Hunt, S., Kabir, J., Kotsonis, P., Oh, U. & Ahluwalia, A. (2004) Vanilloid receptor TRPV1, sensory C-fibers, and vascular autoregulation: a novel mechanism involved in myogenic constriction. *Circ Res,* 95, 1027-34.

Seshiah, P. N., Weber, D. S., Rocic, P., Valppu, L., Taniyama, Y. & Griendling, K. K. (2002) Angiotensin II stimulation of NAD(P)H oxidase activity: upstream mediators. *Circ Res,* 91, 406-13.

Shaw, L., Ahmed, S., Austin, C. & Taggart, M. J. (2003) Inhibitors of actin filament polymerisation attenuate force but not global intracellular calcium in isolated pressurised resistance arteries. *J Vasc Res,* 40, 1-10; discussion 10.

Shen, W. L., Gao, P. J., Che, Z. Q., Ji, K. D., Yin, M., Yan, C., Berk, B. C. & Zhu, D. L. (2006) NAD(P)H oxidase-derived reactive oxygen species regulate angiotensin-II induced adventitial fibroblast phenotypic differentiation. *Biochem Biophys Res Commun,* 339, 337-43.

Shimoda, L. A. & Undem, C. (2010) Interactions between calcium and reactive oxygen species in pulmonary arterial smooth muscle responses to hypoxia. *Respir Physiol Neurobiol*.

Shiraki, H., Kawasaki, H., Tezuka, S., Nakatsuma, A. & Kurosaki, Y. (2000) Endogenous calcitonin gene-related peptide (CGRP) mediates adrenergic-dependent vasodilation induced by nicotine in mesenteric resistance arteries of the rat. *Br J Pharmacol,* 130, 1083-91.

Siow, R. C. & Churchman, A. T. (2007) Adventitial growth factor signalling and vascular remodelling: potential of perivascular gene transfer from the outside-in. *Cardiovasc Res,* 75, 659-68.

Skatchkov, M. P., Sperling, D., Hink, U., Mulsch, A., Harrison, D. G., Sindermann, I., Meinertz, T. & Munzel, T. (1999) Validation of lucigenin as a chemiluminescent probe to monitor vascular superoxide as well as basal vascular nitric oxide production. *Biochem Biophys Res Commun,* 254, 319-24.

Small, J. V. & Gimona, M. (1998) The cytoskeleton of the vertebrate smooth muscle cell. *Acta Physiol Scand,* 164, 341-8.

Smajilovic, S. & Tfelt-Hansen, J. (2007) Calcium acts as a first messenger through the calcium-sensing receptor in the cardiovascular system. *Cardiovasc Res,* 75**,** 457-67.

Smith, R. D., Baukal, A. J., Dent, P. & Catt, K. J. (1999) Raf-1 kinase activation by angiotensin II in adrenal glomerulosa cells: roles of Gi, phosphatidylinositol 3-kinase, and Ca2+ influx. *Endocrinology,* 140**,** 1385-91.

Sobey, C. G., Heistad, D. D. & Faraci, F. M. (1997) Mechanisms of bradykinin-induced cerebral vasodilatation in rats. Evidence that reactive oxygen species activate K^+ channels. *Stroke,* 28, 2290-4; discussion 2295.

Sobey, C. G., Heistad, D. D. & Faraci, F. M. (1998) Potassium channels mediate dilatation of cerebral arterioles in response to arachidonate. *Am J Physiol,* 275, H1606-12.

Somoza, B., Gonzalez, M. C., Gonzalez, J. M., Abderrahim, F., Arribas, S. M. & Fernandez-Alfonso, M. S. (2005) Modulatory role of the adventitia on noradrenaline and angiotensin II responses role of endothelium and AT2 receptors. *Cardiovasc Res,* 65, 478-86.

Sun, D., Messina, E. J., Kaley, G. & Koller, A. (1992) Characteristics and origin of myogenic response in isolated mesenteric arterioles. *Am J Physiol,* 263**,** H1486-91.

Sullivan, J. C. & Davison, C. A. (2001) Gender Differences in the Effect of Age on Electrical Field Stimulation (EFS)-Induced Adrenergic Vasoconstriction in Rat Mesenteric Resistance Arteries. *J Pharmacol Exp Ther.* 296,782-8.

Takahashi, T., Kawahara, Y., Taniguchi, T. & Yokoyama, M. (1998) Tyrosine phosphorylation and association of p130Cas and c-Crk II by ANG II in vascular smooth muscle cells. *Am J Physiol,* 274, H1059-65.

Tang, D. D. & Anfinogenova, Y. (2008) Physiologic properties and regulation of the actin cytoskeleton in vascular smooth muscle. *J Cardiovasc Pharmacol Ther,* 13, 130-40.

Tang, D. D. & Gunst, S. J. (2001) Selected contribution: roles of focal adhesion kinase and paxillin in the mechanosensitive regulation of myosin phosphorylation in smooth muscle. *J Appl Physiol,* 91, 1452-9.

Taniyama, Y. & Griendling, K. K. (2003) Reactive oxygen species in the vasculature: molecular and cellular mechanisms. *Hypertension,* 42**,** 1075-81.

Terashvili, M., Pratt, P. F., Gebremedhin, D., Narayanan, J. & Harder, D. R. (2006) Reactive oxygen species cerebral autoregulation in health and disease. *Pediatr Clin North Am,* 53, 1029-37.

Toda, N. (1975) Nicotine-induced relaxation in isolated canine cerebral arteries. *J Pharmacol Exp Ther,* 193**,** 376-84.

Toda, N. & Okamura, T. (2003) The pharmacology of nitric oxide in the peripheral nervous system of blood vessels. *Pharmacol Rev,* 55, 271-324.

Tosaka, M., Hashiba, Y., Saito, N., Imai, H., Shimizu, T. & Sasaki, T. (2002) Contractile responses to reactive oxygen species in the canine basilar artery in vitro: selective inhibitory effect of MCI-186, a new hydroxyl radical scavenger. *Acta Neurochir (Wien),* 144, 1305-10; discussion 1310.

Touyz, R. M. & Schiffrin, E. L. (2000) Signal transduction mechanisms mediating the physiological and pathophysiological actions of angiotensin II in vascular smooth muscle cells. *Pharmacol Rev,* 52**,** 639-72.

Touyz, R. M. (2005) Intracellular mechanisms involved in vascular remodelling of resistance arteries in hypertension: role of angiotensin II. *Exp Physiol,* 90, 449-55.

Touyz, R. M., Yao, G., Quinn, M. T., Pagano, P. J. & Schiffrin, E. L. (2005a) p47phox associates with the cytoskeleton through cortactin in human vascular smooth muscle cells: role in NAD(P)H oxidase regulation by angiotensin II. *Arterioscler Thromb Vasc Biol,* 25, 512-8.

Touyz, R. M., Yao, G. & Schiffrin, E. L. (2005b) Role of the actin cytoskeleton in angiotensin II signaling in human vascular smooth muscle cells. *Can J Physiol Pharmacol,* 83, 91-7.

Trebak, M., Ginnan, R., Singer, H. A. & Jourd'heuil, D. (2010) Interplay between calcium and reactive oxygen/nitrogen species: an essential paradigm for vascular smooth muscle signaling. *Antioxid Redox Signal,* 12**,** 657-74.

Tschudi, M. R., Mesaros, S., Luscher, T. F. & Malinski, T. (1996) Direct in situ measurement of nitric oxide in mesenteric resistance arteries. Increased decomposition by superoxide in hypertension. *Hypertension,* 27, 32-5.

Tsuji, T. & Chiba, S. (1986) Responses of isolated canine and simian basilar arteries to thiopentone by a newly designed pharmacological method for measuring vascular responsiveness. *Acta Neurochir (Wien),* 80, 57-61.

Tsutsui, M., Onoue, H., Iida, Y., Smith, L., O'Brien, T. & Katusic, Z. S. (1999) Adventitia-dependent relaxations of canine basilar arteries transduced with recombinant eNOS gene. *Am J Physiol,* 276, H1846-52.

Urabe, M., Kawasaki, H. & Takasaki, K. (1991) Effect of endothelium removal on the vasoconstrictor response to neuronally released 5-hydroxytryptamine and noradrenaline in the rat isolated mesenteric and femoral arteries. *Br J Pharmacol,* 102, 85-90.

Ushio-Fukai, M., Zafari, A. M., Fukui, T., Ishizaka, N. & Griendling, K. K. (1996) p22phox is a critical component of the superoxide-generating NADH/NADPH oxidase system and regulates angiotensin II-induced hypertrophy in vascular smooth muscle cells. *J Biol Chem,* 271, 23317-21.

Van den Akker, J., Schoorl, M. J., Bakker, E. N. & Vanbavel, E. (2010) Small artery remodeling: current concepts and questions. *J Vasc Res,* 47, 183-202.

VanBavel, E., Bakker, E. N., Pistea, A., Sorop, O. & Spaan, J. A. (2006) Mechanics of microvascular remodeling. *Clin Hemorheol Microcirc,* 34, 35-41.

VanBavel, E., Wesselman, J. P. & Spaan, J. A. (1998) Myogenic activation and calcium sensitivity of cannulated rat mesenteric small arteries. *Circ Res,* 82, 210-20.

Vasquez-Vivar, J., Hogg, N., Pritchard, K. A., Jr., Martasek, P. & Kalyanaraman, B. (1997) Superoxide anion formation from lucigenin: an electron spin resonance spin-trapping study. *FEBS Lett,* 403, 127-30.

Veerareddy, S., Cooke, C. L., Baker, P. N. & Davidge, S. T. (2004) Gender differences in myogenic tone in superoxide dismutase knockout mouse: animal model of oxidative stress. *Am J Physiol Heart Circ Physiol,* 287, H40-5.

Walker-Caprioglio, H. M., Trotter, J. A., Mercure, J., Little, S. A. & McGuffee, L. J. (1991) Organization of rat mesenteric artery after removal of cells of extracellular matrix components. *Cell Tissue Res,* 264, 63-77.

Wang, G. J., Shum, A. Y., Lin, Y. L., Liao, J. F., Wu, X. C., Ren, J. & Chen, C. F. (2001) Calcium channel blockade in vascular smooth muscle cells: major hypotensive mechanism of S-petasin, a hypotensive sesquiterpene from Petasites formosanus. *J Pharmacol Exp Ther,* 297, 240-6.

Weber, D. S., Rocic, P., Mellis, A. M., Laude, K., Lyle, A. N., Harrison, D. G. & Griendling, K. K. (2005) Angiotensin II-induced hypertrophy is potentiated in mice overexpressing p22phox in vascular smooth muscle. *Am J Physiol Heart Circ Physiol,* 288, H37-42.

Wei, E. P., Kontos, H. A. & Beckman, J. S. (1996) Mechanisms of cerebral vasodilation by superoxide, hydrogen peroxide, and peroxynitrite. *Am J Physiol,* 271, H1262-6.

Weir, E. K., Wyatt, C. N., Reeve, H. L., Huang, J., Archer, S. L. & Peers, C. (1994) Diphenyleneiodonium inhibits both potassium and calcium currents in isolated pulmonary artery smooth muscle cells. *J Appl Physiol,* 76, 2611-5.

Wesselman, J. P. & De Mey, J. G. (2002) Angiotensin and cytoskeletal proteins: role in vascular remodeling. *Curr Hypertens Rep,* 4, 63-70.

Wesselman, J. P., Spaan, J. A., van der Meulen, E. T. & VanBavel, E. (2001) Role of protein kinase C in myogenic calcium-contraction coupling of rat cannulated mesenteric small arteries. *Clin Exp Pharmacol Physiol,* 28, 848-55.

Wheater, P. R. & Wilson, R. A. (1979) Schistosoma mansoni: a histological study of migration in the laboratory mouse. *Parasitology,* 79**,** 49-62.

Wu, J. R., Liou, S. F., Lin, S. W., Chai, C. Y., Dai, Z. K., Liang, J. C., Chen, I. J. & Yeh, J. L. (2009) Lercanidipine inhibits vascular smooth muscle cell proliferation and neointimal formation via reducing intracellular reactive oxygen species and inactivating Ras-ERK1/2 signaling. *Pharmacol Res,* 59, 48-56.

Xi, Q., Cheranov, S. Y. & Jaggar, J. H. (2005) Mitochondria-derived reactive oxygen species dilate cerebral arteries by activating Ca^{2+} sparks. *Circ Res,* 97, 354-62.

Yip, K. P. & Marsh, D. J. (1997) An Arg-Gly-Asp peptide stimulates constriction in rat afferent arteriole. *Am J Physiol,* 273**,** F768-76.

Yoshibayashi, M., Nishioka, K., Nakao, K., Saito, Y., Matsumura, M., Ueda, T., Temma, S., Shirakami, G., Imura, H. & Mikawa, H. (1991) Plasma endothelin concentrations in patients with pulmonary hypertension associated with congenital heart defects. Evidence for increased production of endothelin in pulmonary circulation. *Circulation,* 84, 2280-5.

Zhang, H., Schmeisser, A., Garlichs, C. D., Plotze, K., Damme, U., Mugge, A. & Daniel, W. G. (1999) Angiotensin II-induced superoxide anion generation in human vascular endothelial cells: role of membrane-bound NADH-/NADPH-oxidases. *Cardiovasc Res,* 44, 215-22.

Zhang, W., Edvinsson, L. & Lee, T. J. (1998) Mechanism of nicotine-induced relaxation in the porcine basilar artery. *J Pharmacol Exp Ther,* 284, 790-7.

Zhang, Z., Rhinehart, K., Kwon, W., Weinman, E. & Pallone, T. L. (2004) ANG II signaling in vasa recta pericytes by PKC and reactive oxygen species. *Am J Physiol Heart Circ Physiol,* 287, H773-81.

Zhao, G., Zhao, Y., Pan, B., Liu, J., Huang, X., Zhang, X., Cao, C., Hou, N., Wu, C., Zhao, K. S. & Cheng, H. (2007) Hypersensitivity of BKCa to Ca^{2+} sparks underlies hyporeactivity of arterial smooth muscle in shock. *Circ Res,* 101, 493-502.

Zhou, M., Jaimes, E. & Raij, L. (2005) Vascular but not cardiac remodeling is associated with superoxide production in angiotensin II hypertension. *J Hypertens. ,* 23, 1737-43.

Zweifach, B. W. (1991) Vascular Resistance: Structural vs functional basis. In Bevan, J. A, Halpern, W, Mulvany, M. J (Eds), *The Resistance Vasculature*. New Jersey: Humana Pres.

APPENDIX

RESEARCH OUTPUTS

Zainalabidin S, Wadsworth R.M. & Coats P. *Reactive Oxygen Species Modulates Pressure-dependent Myogenic Tone in Resistance Arteries.* Scottish Cardiovascular Forum (SCF), University of Inverness, Scotland. 23rd Jan 2009

Zainalabidin S, Wadsworth R.M. & Coats P. *Reactive Oxygen Species Mediates Acute Vascular Contraction Responses in Rat Mid Cerebral Artery* Physiology Society, Dublin, Ireland 7-10th July 2009

Zainalabidin S., Wadsworth R.M. & Coats P. *Adventitial Reactive Oxygen Species Modulates Myogenic Tone in Resistance Arteries* Scottish Cardiovascular Forum (SCF), University of Glasgow, Scotland. 5th Feb 2010.